Universidad del País Vasco/Euskal Herriko Unibersitatea
Facultad de Medicina y Enfermería
Departamento de Neurociencias

Autophagy and phagocytosis: functional relationship in microglia

Tesis doctoral para optar al grado de Doctor presentada por:

Virginia Sierra de la Torre
2022

Directoras de Tesis:

Amanda Sierra Saavedra
Ainhoa Plaza Zabala

Esta tesis doctoral ha sido realizada gracias al disfrute de una beca del Programa Predoctoral de Formación de Personal Investigador No Doctor del Departamento de Educación, Política Lingüística y Cultura del Gobierno Vasco durante el periodo 2018-2022.

El trabajo experimental ha sido financiado con becas del ministerio de Economía y Competitividad (http://www.mineco.gob.es), fondos FEDER (BFU2015-66689, RYC-2013-12817, BFU2019-2022), Fundación BBVA para Investigadores y Creadores Culturales, Gobierno Vasco (PI_2016_1_0011) y Fundación Tatiana Pérez de Guzmán el Bueno (2019-2021).

Table of contents

Table of contents

Abbreviations

1. Abbreviations

3-MA	3-methlyadenine
AD	Alzheimer's disease
AIM	Atg8-interacting motif
AIM	Atg8-interacting motif
ALS	Amyotrophic lateral schlerosis
AMPK	AMP-activated protein kinase
APh	Autophagosome
APP	Amyloid-beta precursor protein
ASC	Apoptosis-associated Speck-like protein containing CARD
Atg	autophagy related protein
ATP	Adenosine triphosphate
BAF	Bafilomycin
BAMs	Border-associated macrophages
BBB	Blood brain barrier
BECN	Beclin-1
CBF	Cerebral blood flow
CCA	Common carotid artery
CMA	Chaperone mediated autophagy
CNS	Central nervous system
CR3	Complement receptor 3
CRT	Calreticulin
CSTB	Cystatin B
CTSs	Cysteine proteases
CX3CL1	C-X3-C Motif Chemokine Ligand 1
CX3CR1	C-X3-C Motif Chemokine Receptor 1
DAMPs	Danger-associated molecular patterns
DAP12	DNAX-activation protein of 12 kD
DCs	Dendritic cell
DG	Dentate gyrus
ECL	Enhanced chemiluminescence
EM	Electron microscopy
EPM1	Progressive Myoclonus Epilepsy 1
ER	Endoplasmic reticulum
EXP-	Control
EXP+	Experimental conditions

FIP200	Focal adhesion kinase family interacting protein of 200 kD
FITC	Fluorescein
Gal-3	Galectin-3
GAS6	Arrest-specific protein 6
GFP	Green fluorescent protein
GL	Granular layer
GM-SCF	Granulocyte monocyte colony stimulating factor
GPR34	G protein-coupled receptor 34
GSK-3β	Glycogen synthase kinase-3β
HD	Huntington´s disease
HRP	Horseradish Peroxidase
ICH	Intracerebral hemorrhage
IGF1	Insulin-like growth factor
IL-10	Interleukin 10
IL-18	Interleukin-18
IL-1β	Interleukin-1β
IL-4	Interleukin 4
IL-6	Interleukin 6
iPLA2	Calcium-independent phospholipase A2
iPSC	Induced pluripotent stem cells
KA	Kainic acid
KO	Knock-out
LAMP2A	Lysosomal associated membrane protein 2A
LAMPs	Lysosome-associated membrane proteins
LAP	LC3-associated phagocytosis
LC3	Microtubule-associated light chain protein 3
LGPs	Lysosomal membrane glycoproteins
LIMPS	Lysosomal integral membrane proteins
LPC	Lysophosphatidylcholine
LPS	Bacterial lipopolysaccharide
LRP or CD91	Low-density lipoprotein receptor
LTs	Leukotriens
M6P	Mannose-6-phosphate
MCA	Middle cerebral artery
MerTK	c-Mer tyrosine kinase
MFG-8	Milk fat globule EGF factor
MRP	Mannose-phosphate receptors
MRT	MRT68921
MS	Multiple schlerosis
MTLE	Mesial temporal lobe epilepsy
MTORC1	Mechanistic target of rapamycin complex 1
NF-kB	Nuclear factor kappa b

NGF	Nerve growth factor
NK	Natural killer
NN	Nearest neighbours
NO	Nitric oxide
OGD/R	Oxygen and glucose deprivation and reperfusion
OND	Oxygen and nutrient deprivation
PAMPs	Pathogen-associated molecular patterns
PAS	Pre-autophagosomal structure
PD	Parkinson´s disease
PE	Phosphatidylethanolamine
PGE_2	Prostaglandin E2
PGs	Prostaglandins
Ph capacity	Phagocytic capacity
Ph Index	Phagocytic Index
Ph/A coupling	Phagocytosis/Apoptosis coupling
PI3P	Phosphatidyl-inositol-3-phosphate
PLA	Phospholipases
pMCAo	Permanent MCA occlusion
PMEs	Permanent MCA occlusion
ProS	Protein S
PS	Phosphatidylserine
RFP	Red fluorescent protein
ROS	Reactive oxygen species
RNA-seq	RNA-sequencing
rt-PA	Recombinant tissue plasminogen activator
S1P	Sphingosine-1-phosphate
SAH	Subarachnoid hemorrhage
SGZ	Subgranular zone
SNARE	Soluble NSF attachment protein
SPF	Specific pathogen free
SQTSM1	Sequestosome-1
Stab-1	Stabilin- 1
SVZ	Subventricular zone
TEM	Transmission electron microscopy
TFEB	Transcription factor EB
TGF-β	Transforming growth factor β
TLR	Toll-like receptors
tMCAo	Transient MCA occlusion
TNF- α	Tumour necrosis factor α
TREM2	Triggering receptor expressed on myeloid cells
TRITC	Tetramethylrohadamine
TRPV1	Transient receptor potential vanilloid 1

ULK1	Unc-51 like autophagy activating kinase 1
UTP	Uridine-triphosphate
v3D	Virtual 3D
vATPases	Vacuole ATPases
VEGF	Vascular endothelial growth factor
VNR or αvβ3	Vitronectin receptor
VPS15	Vacuolar protein sorting 15
VPS34	Vacuolar protein sorting 34
WT	Wild type
YS	Yolk sac

Resumen/Summary

2. Resumen/Summary

2.1 RESUMEN

La **microglía** es el macrófago del cerebro, en constante vigilancia del parénquima cerebral para garantizar el mantenimiento de la homeostasis tisular. Entre sus múltiples funciones, la microglía modula activamente la neurogénesis, participa en procesos de mielinización y vasculogénsis, así como en el control de la permeabilidad de la barrera hematoencefálica (BHE). Además, la microglía es ampliamente conocida por su papel como mediadora de la inflamación y le eliminación de material extracelular a través de la **fagocitosis**.

La microglía es conocida es conocida también como los **macrófagos profesionales** del cerebro, dedicados a la eliminación de material extracelular, como restos axonales, proteínas agregadas y células muertas. Nuestro laboratorio esta interesado en la eliminación de **células apoptóticas**, tanto en fisiología como en patología. La eliminación de células apoptóticas es un proceso esencial para evitar el vertido del contenido citotóxico que resulta de la muerte celular y **limitar** así la **inflamación** debida a la fuga de moléculas tóxicas. Para fagocitar correctamente los cuerpos apoptóticos, la microglía cuenta con una gran variedad de **receptores** que reconocen moléculas específicas liberadas por las células apoptóticas, para reclutar fagocitos, y los ligandos expresados en su superficie. Una vez que la microglía ha reconocido a la célula apoptótica, la **englobará**, formando el **fagosoma**, y finalmente la degradará después de su fusión con en **lisosoma**. La fagocitosis microglial es un proceso esencial para el mantener la salud del tejido.

Además de la fagocitosis, otro proceso esencial orientado a la preservación de la homeostasis tisular a través del reciclaje de componentes propios es la **autofagia**. Se han descrito varios tipos de autofagia, incluyendo la microautofagia, la autofagia mediada por chaperonas y la macroautofagia, pero nuestro interés principal reside en la macroautofagia (autofagia de ahora en adelante). A través de la autofagia la célula puede reciclar múltiples **macromoléculas**, como proteínas, además de orgánulos dañados o envejecidos, como mitocondrias. La iniciación de la autofagia requiere la formación de una **doble membrana** que anclará y englobará los componentes propios a degradar, formando el **autofagosoma**, que madurará y finalmente se fusionará con el **lisosoma** para la degradación del material englobado. La autofagia esta activa de manera basal pero también puede potenciarse en respuesta a determinados estímulos, como

la privación de nutrientes, para preservar la homeostasis en condiciones restrictivas de energía y nutrientes.

Ambos **fagocitosis** y **autofagia** son procesos altamente conservados orientados al reciclaje de componentes extracelulares o propios, respectivamente, para mantener la homeostasis tisular. Estos dos procesos comparten muchas **similitudes** a **nivel intracelular**, al ser ambos parte del **sistema endosomal**, que converge en el lisosoma. Estas similitudes nos llevaron a formular la pregunta principal de esta tesis doctoral: ¿cuál es la relación funcional entre autofagia y fagocitosis? Para responder a esta pregunta, hemos estudiado el papel de la fagocitosis y la autofagia microgliales en un modelo in vitro de isquemia cerebral, además, hemos propuesto una nueva aproximación para analizar la autofagia usando el clásico ensayo de western blot, y hemos analizado la fagocitosis microglial en un modelo de epilepsia genética.

Si bien la autofagia de momento no esta bien caracterizada en la microglía, nuestro laboratorio ha descrito ampliamente el papel de la **fagocitosis microglial**, tanto en cerebro sano como enfermo, en respuesta a diferentes retos fagocíticos (Abiega et al., 2016; Diaz-Aparicio et al., 2020). Previamente, usando un modelo farmacológico de **epilepsia,** inducido mediante la administración de ácido kaínico (KA) intrahipocampalmente, demostramos que la **fagocitosis** microglial esta **bloqueada**, dando lugar a la acumulación de células apoptóticas, daño tisular e inflamación. Recientemente, hemos observado que este bloqueo de la fagocitosis también esta presente en un modelo de **isquemia cerebral**, generado mediante la oclusión transitoria de la arteria cerebral media (tMCAo). Durante la isquemia tiene lugar la interrupción del aporte de oxígeno y nutrientes, dos condiciones ampliamente relacionadas con la inducción de autofagia. Por lo tanto, el **Objetivo 1** ha sido describir los mecanismos subyacentes al bloqueo de la fagocitosis inducido tras la isquemia y determinar la relación funcional entre fagocitosis y autofagia en condiciones de privación de oxígeno y nutrientes. Para ello, hemos usado dos modelos in vitro: cultivos organotípicos de hipocampo y microglía primaria sometidos a la privación de oxígeno y nutrientes (OND). El tratamiento con OND demostró que la fagocitosis microglial estaba bloqueada después de 3 y 6 horas de privación pero era rápidamente recuperada después de una hora de reperfusión. Para entender por qué estaba bloqueada la fagocitosis en cultivos organotípicos, utilizamos microscopía de doble fotón y observamos que la motilidad de los procesos microgliales estaba reducida después de 3 horas de OND, evitando el reconocimiento de los cuerpos apoptóticos. Cuando extendimos nuestra investigación a cultivos de microglía primaria, donde podemos discriminar el englobamiento y la degradación de las células apoptóticas, determinamos que la OND bloqueó la degradación pero no en

englobamiento de los cuerpos apoptóticos. Además, observamos una basificación del compartimento lisosomal a causa de la OND, así como una reducción en su número y tamaño. Dichas alteraciones en el compartimento lisosmal nos llevaron a analizar los posibles cambios en la cascada autofágica. Después de 1 y 3 horas de OND no fuimos capaces de detectar cambios mediante el análisis por western blot de LC3-II (la forma unida a la membrana de LC3 usada como el método estándar para analizar la autofagia), probablemente debido a la limitada sensibilidad de la técnica; sin embargo, si que observamos un incremento en el número de vesículas autofágicas y el área que ocupaban mediante microscopía electrónica de transmisión (TEM). Estos descubrimientos desentrañaron in bloqueo tanto en el englobamiento como en la degradación de células apoptóticas, probablemente debido a las alteraciones en el compartimento lisosomal y a la inducción de una respuesta autofágica.

Considerando que una inducción de autofagia tuvo lugar después de OND, analizamos el papel de la autofagia basal en la microglía. Analizamos tres modelos in vivo de deficiencia de autofagia: ATG4B, TMEM119-Beclin1 y AMBRA$^{+/-}$, y determinamos que la autofagia era necesaria para mantener la función fagocítica de la microglía y su supervivencia. Asimismo, inhibimos la autofagia basal en microglía primaria para analizar los efectos de su inhibición exclusivamente en microglía. Para ello, usamos el inhibidor selectivo de la enzima ULK1, MRT68921, y demostramos una reducción en la supervivencia microglial, consistente con los descubrimientos in vivo, además de una inhibición de la fase de englobamiento durante la fagocitosis, con una pequeña tendencia a presentar un bloqueo también en la degradación. La autofagia es, por lo tanto, un proceso esencial para mantener tanto la fisiología como la función microglial.

Datos previos del laboratorio empleando el modelo de isquemia tMCAo, demostraron que la administración de la inductora de autofagia rapamicina, recobró parcialmente la fagocitosis microglial después de la isquemia. Nuestra próxima aproximación fue testar el efecto de la rapamicina en la autofagia y en la fagocitosis microgliales. El tratamiento de microglía primaria con rapamicina durante 6 y 24 horas no tuvo efectos detectables sobre la autofagia en condiciones basales, analizada por western blot, y tras la OND, solo observamos una pequeña tendencia a recuperar las ligeras alteraciones en el flujo autofágico. Probablemente la falta de efecto de la rapamicina sobre la autofagia analizada por western blot, se deba a la limitada sensibilidad de la técnica mencionada anteriormente. Sobre la fagocitosis, la rapamicina no revirtió los efectos detrimentales generados por la OND en cultivos organotípicos de hipocampo y no fue capaz de recuperar la fagocitosis. Por lo tanto, a pesar de ser un compuesto beneficioso para recuperar la fagocitosis in vivo, la rapamicina no revirtió el bloqueo de la fagocitosis

observado in vitro y no indujo cambio sobre la autofagia, al menos tras su análisis mediante western blot.

El **Objetivo 2** fue individualizar los diferentes pasos de la autofagia empleando el análisis clásico de western blot de LC3. Tradicionalmente, el flujo autofágico solo consideraba el paso de degradación como medida global de autofagia, mientras que el paso de formación quedaba sin analizar. La mayor parte de las proteínas controladoras y reguladoras de la autofagia actúan sobre pasos iniciales de la cascada, por lo que el paso de formación necesitaba ser analizado. Para superar esta limitación, propusimos una serie de ecuaciones sencillas para calcular tanto la formación como la degradación considerando la autofagia como un proceso con una entrada, formación de nuevos autofagosomas, y una salida, degradación de autofagosomas y un reservorio de autofagosomas considerado una caja negra. La distinción entre formación y degradación y la adición del término ratio neto de cambio (net turnover ratio, formación/degradación) nos permitió discriminar los efectos de drogas específicas, que podrían actuar de forma diferente sobre formación y degradación.

Finalmente, en el **Objetivo 3** estudiamos la fagocitosis microglial en un modelo genético de epilepsia, la **epilepsia mioclónica progresiva tipo I (EPM1)**. Se trata de una enfermedad genética de inicio temprano en la que el gen que codifica para la cistatina B (cstb) está mutado y da lugar a una proteína no funcional. La cistatina B (CSTB) actúa como inhibidor de las proteasas lisosomales denominadas catepsinas, por lo que en ausencia de actividad de CSTB hay un exceso de proteólisis, lo que genera muerte celular y daño tisular. Resultados previos del laboratorio demostraron que la fagocitosis microglial estaba bloqueada en este modelo de epilepsia tanto en ratones sintomáticos, a día posnatal 30. Nuestra hipótesis principal fue que la ausencia de CSTB en la microglía alteraba de manera autónoma la fagocitosis. Para responder a esta pregunta, primero determinamos la expresión de *Cstb* en microglía y otros tipos celulares, así como de sus catepsinas asociadas. A continuación, mediante un modelo de silenciamiento específico para cstb en microglía BV2 pudimos determinar que la ausencia de CSTB no afectaba a su capacidad fagocítica, no se trataba de un efecto autónomo celular. Estos resultados nos llevaron a plantearnos que la fagocitosis deficitaria en los ratones KO para CSTB podría deberse a factores ambientales, en particular a una hiperactivación del circuito previa a la aparición de crisis epilépticas visibles in vivo. Primero, analizamos la fagocitosis microglial en ratones presintomáticos de 14 días (P14), y observamos que la fagocitosis microglial ya era deficiente, pero únicamente en la capa granular del giro dentado del hipocampo, donde aparecen las neuronas maduras, pero no en la zona subgranular, donde residen los neuroprogenitores. Esta

deficiencia específica en la fagocitosis nos llevó a determinar la relación entre la activación neuronal (células cFos+), células apoptóticas y microglía usando microscopía confocal. A nivel global los ratones P14 *Cstb* KO no presentaban mayor activación que los ratones control pero observé que la proximidad entra las neuronas cFos+ y las células apoptóticas era inusualmente alta. En colaboración con el Dr. Paolo Bonifazi (Biocruces) desarrollamos un modelo matemático que nos permitió determinar si la elevada proximidad entre las neuronas activadas cFos+ y las células apoptóticas era causal o aleatoria. El análisis indicó que la relación global entre las neuronas cFos+ y las células apoptóticas era aleatoria, sin embargo, nuestro modelo nos permitió determinar que a nivel local, la proximidad entre las neuronas cFos+ y las células apoptóticas seguía siendo inusualmente alta. Concluimos por lo tanto que la deficiencia en la fagocitosis microglial no se debía a una activación global del circuito ni a la ausencia de *Cstb* por sí misma, sino a un fenómeno local más complejo.

2.2 SUMMARY

Microglia are the brain macrophages, in constant **surveillance** of the brain parenchyma to guarantee the maintenance of the tissue homeostasis. Among their many functions, microglia actively modulate neurogenesis, participate in myelination and vasculogenesis as well as control the blood brain barrier (BBB) permeability. Furthermore, microglia are widely known for their role as inflammatory mediators and the removal of extracellular content through **phagocytosis**.

Microglia are also known as the brain **professional macrophages**, devoted to the elimination extracellular material, like axonal debris, aggregated proteins, and dead cells. Our laboratory is interested in the removal of **apoptotic cells**, both in physiology and pathology. The clearance of apoptotic cells is an essential process to avoid the spillover of the cytotoxic content that results from the cell death and **limit** the **inflammation** due to the leakage of the toxic molecules. To properly phagocytose the dead corpses, microglia are provided with a wide variety of **receptors** that recognize specific molecules released form the dead cells to recruit the phagocytes and the ligands expressed on their surface. Once microglia have recognized the apoptotic cell, they will **engulf** it, forming the **phagosome**, and finally **degrade** it after its fusion with the **lysosome**. Microglial phagocytosis is then a crucial process to maintain tissue health.

In addition to phagocytosis, another main cellular process oriented to the preservation of tissue homeostasis by the recycling of own components is **autophagy**. Several types of autophagy have

been described, including microautophagy, chaperon mediated autophagy, and macroautophagy, but our main interest relies on macroautophagy (autophagy from now on). Through autophagy, the cell can recycle several **macromolecules**, such as proteins, and also damaged or long-lived or **organelles**, such as damaged mitochondria. The initiation of autophagy requires the formation of a **double membrane** that will dock and engulf own components, forming the **autophagosome**, which will mature and finally fuse with the **lysosome** for the degradation of the engulfed material. Autophagy is active at basal levels but can also be triggered under certain stimuli, like nutrient starvation, in order to preserve the cell homeostasis under energy and nutrient restrictive conditions.

Both **phagocytosis** and **autophagy** are highly conserved processes oriented to the recycling of extracellular or own components, respectively, to maintain the tissue homeostasis. These two processes, share many **similarities** at the **intracellular level**, as they are both part of the **endosomal pathway** that converges in the lysosome. These similarities drove us to formulate the main question of this PhD thesis: what is the functional relationship between phagocytosis and autophagy? To address this question, we have studied the role of phagocytosis and autophagy in an in vitro model of cerebral ischemia, proposed a new approach for the analysis of the conventional western blot assay to measure autophagy and assessed microglial phagocytosis in a model of genetic epilepsy.

Whereas autophagy is not yet a well characterized process in microglia, our laboratory has broadly described **microglial phagocytosis**, both in the healthy and in the diseased brain in response to several phagocytic challenges (Abiega et al., 2016; Diaz-Aparicio et al., 2020). We previously demonstrated that in a model of pharmacologically induced **epilepsy**, by intrahippocampal injection of kainic acid (KA), microglia presented a **phagocytosis blockage**, leading to the accumulation of apoptotic cells, tissue damage and inflammation. Recently, we have observed that this phagocytosis impairment is also present in a model of **cerebral ischemia** generated by the transient occlusion of the medial cerebral artery (tMCAO). During the ischemia, there is an interruption of the oxygen and nutrient supply, two conditions largely related to the induction of autophagy. Hence, **Aim 1** has been to unravel the mechanisms underlying tMCAO-induced phagocytosis impairment and determine the functional relationship of phagocytosis and autophagy under oxygen and nutrient deprivation conditions. For this purpose, we used two in vitro models: organotypic hippocampal slices and primary microglia treated with oxygen and nutrient deprivation (OND). The treatment with OND demonstrated that microglial phagocytosis was blocked in organotypic hippocampal slices after 3 and 6 hours

of deprivation but was rapidly recovered after 1 hour of reperfusion. To understand why phagocytosis was blocked in hippocampal slices, we performed two photon microscopy and observed that microglial process motility was reduced after OND, preventing the recognition of the apoptotic bodies. When we extended our research to primary microglial cultures, where we can discriminate between engulfment and degradation, we determined that OND blocked the degradation of apoptotic cells but not the engulfment. In addition, we observed that the lysosomal compartment was basified by OND and reduced in number and size. The alterations in the lysosomal compartment prompted us to address possible changes in the autophagy cascade. After 1 and 3 hours of OND, we were not able to detect any changes by western blot of LC3-II (the membrane bound form of LC3 used as the gold standard method to study autophagy), likely due to the limited sensibility of the technique, but we did observe an increase in the number of autophagy-like vesicles and the area they occupied by transmission electron microscopy (TEM). These findings unraveled a blockade in both engulfment and degradation of apoptotic cells, likely related to the observed alterations in the lysosomal compartment and the induction of an autophagic response.

Considering that autophagy was induced after OND, we next addressed the role of basal autophagy in microglia. We analyzed three in vivo models of autophagy deficiency: ATG4B, TMEM119-Beclin1 and AMBRA$^{+/-}$, and determined that autophagy was necessary to maintain the phagocytic function and ensure microglial survival. In addition, we inhibited autophagy in primary microglia to address the effects of its inhibition exclusively on microglia. For this purpose, we used the ULK1 selective inhibitor, MRT68921, and showed that it reduced microglial survival, consistent with the in vivo findings, and also impaired the engulfment step of phagocytosis, with also a small trend to reduce degradation. Autophagy is then an essential process to maintain microglial physiology and function.

Previous data from the laboratory using the tMCAo model, demonstrated that the administration of the autophagy inducer rapamycin, partially recovered microglial phagocytosis after stroke. Our next approach was to test the effect of rapamycin on microglial autophagy and phagocytosis. The treatment with rapamycin for 6 and 24 hours on primary microglia had no detectable effect on autophagy assessed by western blot in basal conditions and, after OND, it only showed a small trend to recover the slightly altered autophagy flux. Likely, the lack of effect of rapamycin addressed by LC3 western blot was related to its low sensitivity, as previously mentioned. On phagocytosis, rapamycin did not recover the deficient degradation induced by OND and had detrimental effects on microglial survival in microglia treated with OND in the

degradation step. Furthermore, rapamycin did not revert the detrimental effects generated by OND in organotypic hippocampal slices and was unable to recover phagocytosis. Thus, despite being an effective compound to partially recover microglial phagocytosis in vivo, rapamycin did not revert the phagocytosis impairment observed in vitro and it did no trigger any changes in autophagy, at least by western blot.

Aim 2 was to dissect the different steps of autophagy using the classical LC3 western blot assay. Traditionally, the autophagy flux only considered the degradation step as a global measurement of autophagy, whereas the formation of autophagosome has been overseen. Most of the autophagy controlling and regulating genes act on the initial steps of autophagosome formation, hence, the formation needed to be addressed. To overcome this limitation, we proposed a simple set of equations to calculate both formation and degradation considering autophagy as a process with an input, or formation of new autophagosomes, an output, or degradation of autophagosomes, and an autophagosome pool taken as a black box. The dissection of formation and degradation, and the addition of the term net turnover ration (formation/degradation) allowed us to discriminate the effect of specific drugs, that could differentially act on formation and degradation. We tested the applicability of the model on simulated scenarios and on experimental data obtained from autophagy inhibition and induction experiments, proving to be a useful tool to extend the analysis of the classical LC3 western blot assay.

Finally, in A**im 3** we studied microglial phagocytosis in a model of genetic epilepsy, progressive myoclonic epilepsy type I (EPM1). EPM1 is a genetic illness of early onset in which the gene encoding the cystatin b protein (CSTB) is mutated giving rise to a lack of function protein. CSTB is a protease inhibitor that limits the activity of lysosomal and cytoplasmic proteases, called cathepsins; consequently, its lack of activity leads to increased proteolysis, cell death and tissue damage. Previous results from the laboratory determined that microglial phagocytosis was blocked in a mouse model of CSTB absence, *Cstb KO*, in symptomatic P30 mice. Our main hypothesis was that the absence of CSTB in microglia was altering phagocytosis in a cell-autonomous way. To answer this question, we first determined the expression of *Cstb* in microglia and other cell types and its associated cathepsins. We next silenced the *Cstb* expression in BV2 microglia, using a siRNA, and performed a phagocytosis assay but neither engulfment nor degradation were affected by the lack of CSTB. Thus, the deficient phagocytosis was not due to a cell-autonomous effect. This result shed light onto the possible influence of the environment on microglial phagocytosis, in particular to a hyperactivation of the circuit prior to the seizure onset. To address this question, we first analyzed microglial phagocytosis in pre-

symptomatic P14 mice and observed that microglial phagocytosis was already deficient, but only in the granule cell layer of the dentate gyrus where mature neurons are found, but not in the subgranular zone where neuroprogenitors reside. This specific phagocytosis deficiency prompted us to determine the relationship between neuronal activation (cFos+ cells), apoptotic cells and microglia using confocal microscopy. Globally, P14 *Cstb KO* mice did not present an increased neuronal activation but the distance between cFos+ neurons and apoptotic cells was unusually high. In collaboration with Dr. Paolo Bonifazi, we developed a mathematical model that allowed us to determine if the high proximity between the cFos+ and apoptotic cells was causal or random. The analysis indicated that the global relationship was random; however, our model, allowed us to determine that, locally, the proximity between cFos+ and the apoptotic cells was unusually high. We concluded that microglial phagocytosis was not due to a global hyperactivation of the circuit neither to the *Cstb* absence per se but to a more complex local phenomenon.

Introduction

3. Introduction

3.1 MICROGLIA: AN OVERVIEW

3.1.1 Introduction to microglia

The early 20th century was governed by the neuron doctrine, formulated by Santiago Ramón y Cajal, who was awarded the Nobel Prize in 1906 together with Camilo Golgi for their research on the organization of the central nervous system (CNS) (López-Muñoz et al., 2006). The two researchers defended opposite theories: whereas Cajal was defender of a neuron-based structure, Golgi believed in a reticular organization that made the brain a continuum (Cimino, 1999; Jones, 1999). In addition to describing different types of neurons and how they were connected, Cajal described the presence of astrocytes, already reported by Virchow and Lenhossek in the 19th century, and discovered a non-neuronal component that he baptized as "the third element" (Sierra et al., 2016). He characterised the third element using the sublimated gold chloride method and was able to identify apolar cells that were neither neurons nor astrocytes (Tremblay et al., 2015). It was Pio del Río Hortega who, in 1919 gave name and identity to the third element as two different cell types: microglia and oligodendrocytes (del Rio-Hortega, 1919). He used a sophisticated method to stain the brain based on ammoniacal silver carbonate (Del Río-Hortega Bereciartu, 2020), and described the distribution and morphological phenotype of microglia (Sierra et al., 2016).

Microglia are the resident macrophages of the CNS, in constant surveillance of the brain parenchyma and the first cellular barrier of the brain innate immune system (Sierra et al., 2014). Microglia can be found ubiquitously throughout the CNS but vary in density and morphology (Gomez-Nicola & Perry, 2015; Stowell et al., 2018), and they can as well present differential phenotypes (Tan et al., 2020; Wolf et al., 2017), according to their protein expression (de Haas et al., 2008), transcriptional profile (De Biase et al., 2017) or motility (Smolders et al., 2019), among others. This heterogeneity is related to the spatio-temporal maturation of microglia and the encounter of physiological cues (Wurm et al., 2021) or immunological insults, such as inflammation or apoptotic cells (Hammond et al., 2019; Tay et al., 2017).

In the next sections we will discuss the developmental origin of microglia, which grants them with unique properties in the brain parenchyma, and their physiological functions, including an

extensive comment on the two processes that are the focus of this PhD thesis: phagocytosis and autophagy. Both processes are in the spotlight of this PhD, as they both share many similarities at the intracellular level and are part of the endosomal pathway. The high resemblance between the two processes allowed as to formulate the initial question: what is the functional relationship between phagocytosis and autophagy in microglia?

We will also detail the role of microglia in two models of disease. First, we will focus on a model of stroke, in which previous in vivo data from our laboratory demonstrated the impairment of microglia phagocytosis and the lack of oxygen and nutrients triggered autophagy induction. Then, we will study the mechanisms of phagocytosis impairment in progressive myoclonus epilepsy type I (EPM1), in mice lacking the lysosomal protein Cstb (cystatin B). Thus, the beginning of the story starts during the embryonic development when microglia are originated.

3.1.2 Microglial ontogeny: embryonic origin and brain colonization.

The original belief stated that microglia had an ectodermal origin as the rest of the CNS (Fujita & Kitamura, 1975); however, it is now known that they have a mesodermal origin. They arise from the extraembryonic mesoderm, unlike erythrocytes or muscle cells, which are originated in the embryonic mesoderm (Ross & Boroviak, 2020) (**Figure 1**).

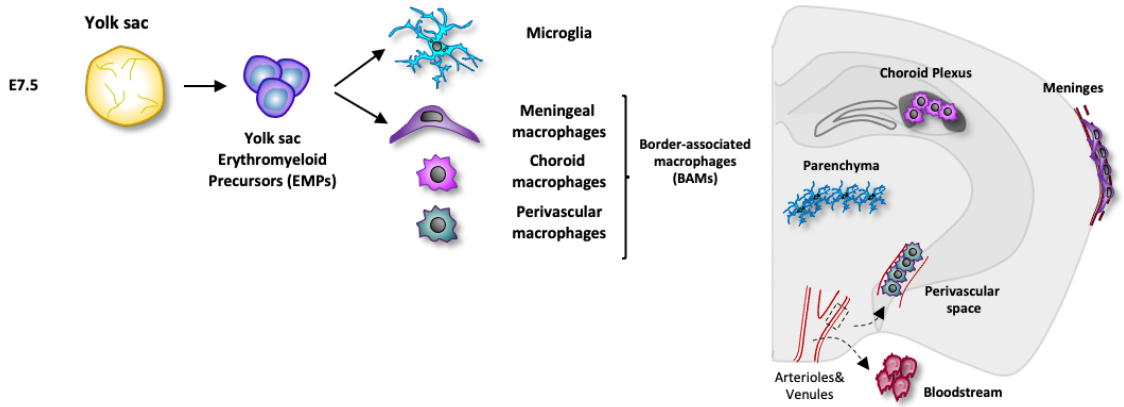

Figure 1. Origin of microglia and border associated macrophages. *Erythromyeloid precursors (EMPs) located in the yolk sac around E 7.5 generate microglia, as well as other border-associated macrophages (BAMs) located in the meninges, choroid plexus and in the perivascular space. This image was adapted from Sol Beccari´s PhD Thesis (2021).*

Microglia derive from a pool of Myb-independent macrophages generated during primitive haematopoiesis in the blood islands in the yolk sac (YS) during embryogenesis (Ginhoux & Guilliams, 2016; Gomez Perdiguero et al., 2015; Schulz et al., 2012). They give rise to several cell

types including immature microglia and border associated macrophages (BAMs), that colonise the brain from embryonic day E7.5-10 in mice (Ginhoux et al., 2010; Ginhoux & Guilliams, 2016; Goldmann et al., 2016; Prinz et al., 2019) and from gestational week 4 to 24 in the human brain (Menassa & Gomez-Nicola, 2018) (**Figure 1**). This colonisation occurs in parallel to the formation and remodelling of blood vessels in the brain parenchyma (Checchin et al., 2006; Kubota et al., 2009), which allows the dissemination of the radial glia that act as neuroprogenitors (Cunningham et al., 2013). The microglial progenitors enter the CNS through the leptomeninges and lateral ventricles, and later populate the brain at different speeds and proliferation rates, according to the development of each brain structure (Menassa & Gomez-Nicola, 2018; Monier et al., 2007; Verney et al., 2010). The complete colonisation of the brain takes place perinatally (Dalmau et al., 2003; Schwarz et al., 2012), along with the acquisition of the mature microglia phenotype (Verkhratsky et al., 2021).

In the adult brain, once the microglial population is established, it self-renews at very low rate with no contribution of bone-marrow derived circulating monocytes in physiological conditions (Ginhoux et al., 2010; Hashimoto et al., 2013; Hoeffel & Ginhoux, 2018; Schulz et al., 2012; Yona et al., 2013). Recent studies based on the depletion of microglia have been useful to demonstrate the source for microglial renewal, based on the proliferation of local progenitors (Elmore et al., 2015; Elmore et al., 2014). The role of microglia as the brain parenchyma macrophages leads to the development of highly specialised functions, like tissue surveillance, inflammatory response, and phagocytosis, which we will discuss in the next sections.

3.1.3 Microglia brain-specific functions in physiology and pathology

The capacity of microglia to constantly survey and react to the occurring changes in the brain parenchyma (Hickman et al., 2013) allows them to exert a wide variety of functions (Nayak et al., 2014). The signals sensed by microglia comprehend from invading microorganisms to dead cells (de Miranda et al., 2017; Hickman et al., 2018; Wolf et al., 2017), as well as chemical changes in the environmental pH or extracellular matrix composition (Ginhoux et al., 2013; Hickman et al., 2013; Nimmerjahn et al., 2005). The microglial response to these signals is translated into a broad-spectrum of microglial functions (Kettenmann et al., 2011; Verkhratsky et al., 2021), including the modulation of neurogenesis, vasculogenesis, myelination, and the innate immune response (**Figure 2**). In this section, we will describe these brain-specific roles of microglia in physiological conditions and discuss how they are altered in pathological conditions.

During neurogenesis in the developing brain, microglia colonize the brain in parallel to the emergence of the radial glial cells (Tong & Vidyadaran, 2016). Radial glia are a set of specialised cells that serve as a physical guide for the new-born neurons, as well as are the primary pool of progenitors that give rise to neurons, astrocytes, and oligodendrocytes during the brain development (Rakic, 1972). Microglia limit the proliferation and regulate the size of the neurogenic pool in the subventricular zone (SVZ) of the rat and macaque brain, presumably by phagocytosing neuronal precursors (Cunningham et al., 2013; Fourgeaud et al., 2016); yet the direct visualisation of live neuronal precursor phagocytosis has not been assessed in vivo, as it has only been demonstrated in cultured slices (Cunningham et al., 2013). In addition, during adulthood microglia are in charge of removing the new-born neuroblasts that die by apoptosis both in the dentate gyrus (DG) of the hippocampus (Sierra et al., 2010) as well as in the subventricular zone (SVZ) (Fourgeaud et al., 2016), clearing the neuronal debris and limiting the production of new-born neurons in the DG as well as in vitro (Diaz-Aparicio et al., 2020). In pathological conditions, microglia can negatively affect the neurogenic niche, as the release of pro-inflammatory cytokines can reduce the formation of new neurons in the DG of the adult mouse brain (Ekdahl et al., 2003; Monje et al., 2003) (**Figure 2**).

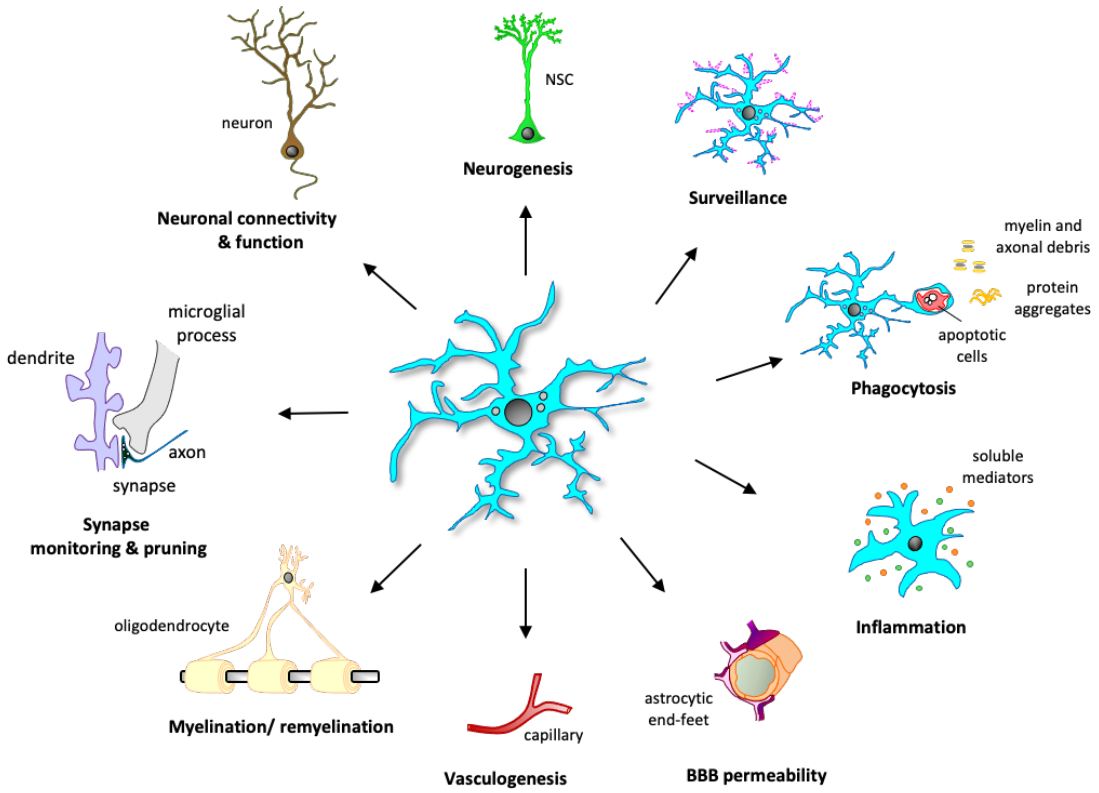

Figure 2. Microglial brain specific functions. *Microglia, in constant surveillance of the brain parenchyma, perform a wide variety of functions in pathology and physiology. For instance, microglia perform immune functions by the release of inflammatory cytokines and phagocytosis of cellular debris, like apoptotic cells,*

and axonal and myeline debris. In addition, microglia interact with other brain cell types regulating their function: neuronal activity and connectivity, neural stem cells (NSC) and neurogenesis, oligodendrocytes and myelination, endothelial cells and vasculogenesis, as well as astrocytes and the blood-brain barrier (BBB). This image was adapted from (Sierra et al., 2019).

In parallel to neurogenesis, brain vasculogenesis takes place to guarantee blood and nutrient supply for the correct development of the brain (Checchin et al., 2006; Kubota et al., 2009). Several studies suggest that microglia participate in the formation of new blood vessels, since the lack of specific trophic factors released by microglia result in the failure of vessel formation and embryo lethality (Fantin et al., 2010). Microglia has also been proposed to participate in the vascularization of brain tumours by the release of pro-angiogenic factors such as VEGF and CXCL2, at least in vitro (Brandenburg et al., 2016); as well as in the control of the neurovascular coupling (Császár et al., 2022). In neurodegenerative diseases, like Alzheimer's disease (AD) and multiple sclerosis (MS), microglia are attracted towards the bloods vessels, either by VEGF or fibrinogen release respectively, and its association might cause damage and compromise the vascular function in the regions of interaction (Zhao et al., 2018) (**Figure 2**).

During postnatal development, microglia have also been postulated as essential regulators of synapse formation (Coull et al., 2005; Parkhurst et al., 2013), maturation (Hoshiko et al., 2012; Paolicelli et al., 2011; Schafer et al., 2012), and refinement through synaptic pruning (Paloneva et al., 2002; Roumier et al., 2004; Stevens et al., 2007). During the CNS development there is an excessive synapse formation but only functional and active synapses are consolidated in an activity-dependent manner, whereas redundant synapses are erased (Hua & Smith, 2004). During adulthood, microglial-mediated synapse elimination has been proposed to occur through partial phagocytosis or trogocytosis (Weinhard et al., 2018), but it is still a controversial matter (Lim & Ruthazer, 2021). In addition, excessive or deficient synapse pruning can also aggravate neurological disorders such as AD or schizophrenia (Vilalta & Brown, 2018) (**Figure 2**).

Microglia have also been related to myelination through the release of growth factors that aid the survival and proliferation of oligodendrocytes (Pang et al., 2013). During remyelination, microglia phagocytose the degenerated myelin (Domingues et al., 2016), promoting the recruitment and differentiation of oligodendrocyte precursors (Domingues et al., 2016; Voet et al., 2019). However, the release of pro-inflammatory cytokines can also limit remyelination in pathologies such as MS (Guerrero & Sicotte, 2020) (**Figure 2**).

In addition to this brain-specific functions, the classical innate immune functions related to microglia are inflammation and phagocytosis, which we will review in the next sections.

3.2 INNATE IMMUNE RESPONSE OF THE BRAIN

Microglia in the parenchyma, together with the BAMs, located in the meninges, perivascular space, and choroid plexus, are the residing brain macrophages and act as one of the key players of the CNS innate immune system. The innate immune system is the organism´s earliest line of defence (McComb et al., 2019; Yatim & Lakkis, 2015) once the barriers formed by the skin and mucous membranes are broken and pathogens reach the inside of the organism (McComb et al., 2019; Yatim & Lakkis, 2015). The innate immune system is composed of tissue macrophages, natural killer cells (NKs), dendritic cells and white blood cells in the periphery, and microglia and BAMs in the brain (Parkin & Cohen, 2001; Vivier et al., 2008). Inflammation and phagocytosis are the main answers of the innate immune system against potentially harmful stimuli. First, we will discuss the molecular effectors of inflammation and in the next section, we will gain depth into the phagocytosis process (**Section 2.3**).

3.2.1 Inflammation

Inflammation response of the innate immune system triggered by harmful stimuli, such as pathogens, toxics substances, irradiation, or damaged cells (Isailovic et al., 2015), and it is characterised by redness, swelling, heat, pain and loss of tissue function (Lucas et al., 2006). The initiation of an inflammatory response is devoted to restoring the tissue function and clearing the threat (Chen et al., 2018); hence, it can be initiated by several cell types like astrocytes, oligodendrocytes, endothelial cells, meningeal macrophages or even neurons (Takeuchi & Akira, 2010). However, microglia are the major orchestrator of the inflammatory response and release inflammatory mediators such as cytokines, chemokines, complement proteins and other inflammatory mediators to promote and resolve inflammation (Cámara-Lemarroy et al., 2010; Jeong et al., 2013). In the next sections, we will define and classify the inflammatory mediators released by microglia during the inflammatory response: cytokines, complement proteins, prostaglandins and leukotrienes, and trophic factors (Nayak et al., 2014).

3.2.1.1 Cytokines

Cytokines are small released molecules, such as peptides, proteins or glycoproteins produced to trigger, influence and resolve the immune response (Takeuchi & Akira, 2010). Cytokines can act either on the cells that produce and secret them, in an autocrine way, and also on the

neighbouring cells in a paracrine way (Borish & Steinke, 2003). Once they are released, they bind to cell-surface receptors and trigger intracellular responses such as proliferation, differentiation, cell death as well as the release of other cytokines to promote or resolve the inflammatory response (Devi, 2000; Foster, 2001; Zhang et al., 2009). The cytokine family is characterised by its redundancy and the ability of several cytokines to present overlapping or even identical functions (Borish & Steinke, 2003). Cytokines can be gathered into different subgroups according to several criteria such as their protein structure, functional outcome, and inflammatory effect. Here, we will classify them according to their inflammatory outcome: pro- and anti-inflammation.

Pro-inflammatory cytokines. These cytokines are usually produced by macrophages and monocytes and are involved in the initiation and up-regulation of the inflammatory response (Dinarello, 2000; Zhang & An, 2007). The classically studied cytokines are interleukin-1β (IL-1β), Interleukin-6 (IL-6), tumour necrosis- α (TNF- α) and interferon- γ) (F. Su et al., 2016; Vezzani & Viviani, 2015), whose main function is to maintain a normal organic function. However, their uncontrolled release can lead to detrimental consequences, including tissue injury and organic failure (Kim et al., 2021). In the brain, several studies have demonstrated that increased cytokine levels are a common hallmark in many neurological diseases including AD, Parkinson´s disease (PD), MS, epilepsy, and stroke aggravating the progression of these diseases (Rocha et al., 2012; Zheng et al., 2016). Among the detrimental effects caused by the uncontrolled cytokine release are apoptosis of neurons and glial cells, increased blood brain barrier (BBB) permeabilization accompanied by increased migration and infiltration of immune cells towards the brain parenchyma, which increases the damage. These cytokines trigger the production and release of other inflammatory mediators like reactive oxygen species (ROS) and nitric oxide (NO), that can be neurotoxic if their action is not limited (Sastre et al., 2006; Smith et al., 2012).

Anti-inflammatory cytokines. These cytokines are released to maintain the correct balance between a pro-inflammatory status and its resolution. It is important to state that, apart from IL-1ra (receptor agonist) (Dayer et al., 2017), all the anti-inflammatory cytokines present pro-inflammatory properties depending on the timing when they are released, the environment, the receptor sensitivity and amount and of course, on the tissue itself (Opal & DePalo, 2000). The well-known anti-inflammatory cytokines include interleukin 4 (IL-4), interleukin 10 (IL-10), and transforming growth factor β (TGF-β) (F. Su et al., 2016). In addition to these cytokines, there are specific cytokine inhibitors and soluble cytokine receptors that help to attenuate the pro-inflammatory cytokine function (Opal & DePalo, 2000). The main role of the anti-inflammatory

cytokines is to promote the tissue repair and limit the synthesis of pro-inflammatory mediators (Loftis et al., 2010) to avoid the establishment of a chronic inflammatory state (Vezzani et al., 2013).

Cytokines can also be classified according to their functional outcome. Interleukins, interferons, tumour necrosis factors, colony stimulating factors and transforming growth factor β (TGF- β) trigger the release of inflammatory factors. Another class of cytokines, the chemokines, regulate the motility of several cell types, such as leukocytes, towards the site of the lesion where they will eventually produce inflammatory cytokines (Hughes & Nibbs, 2018). This migratory process, called chemotaxis, is involved not only in inflammation but in many physiological processes including the patterning of neuronal cells in the developing brain (Jin et al., 2008). Monocytes require the presence of the chemokine receptor CCR2 and its binding chemokine CCL2 to abandon the bone marrow and enter the circulatory system, similar to the CX3CR1 receptor and its ligand CX3CL1 essential for the neuron-microglia communication axis (Wolf et al., 2013). Some chemokines and their receptors have been proposed to be upregulated in pathological situations such as AD, MS, brain trauma or stroke (Mennicken et al., 1999; Savarin-Vuaillat & Ransohoff, 2007; Ubogu et al., 2006).

3.2.1.2 The complement system

The complement system is an essential part of the innate immunity to face infections or altered host cells and is as well a driver of inflammation (Ricklin et al., 2010). It is composed by more than 30 proteins, receptors and modulators soluble in plasma or present in cells, that are constantly activated at a basal level to guarantee a fast response against foreign substances or invaders (Morgan & Harris, 2015). The complement proteins are maintained in a zymogen in the circulation but are rapidly cleaved to active enzymes as early as the pathogen is identified (Ling & Murali, 2019). Their main role is to opsonize or “tag” the invading pathogen, amplify the inflammatory response to attract phagocytic cells and/or directly induce its lytic death (Sarma & Ward, 2011). The activation of the complement system depends on the nature of the foreign element: the classical pathway, activated by an antibody or by direct binding of C1q to the pathogen surface, MB-lectin pathway, by direct binding of lectin molecules to the pathogen surface and the alternative pathway, directly triggered by the pathogen´s surface (Sarma & Ward, 2011). All these three activation strategies are oriented to the activation of a protease, called C3 convertase, that activates zymogens sequentially to activate the complement cascade, inflammation and pathogen clearance (Bonifati & Kishore, 2007). However, the complement

malfunction, over or under activation, leads to and exaggerated or insufficient cytokine release, altered pathogen clearance and the generation of ROS species that can damage the tissue and even cause cell death (Bonifati & Kishore, 2007; Sinkovits et al., 2021).

3.2.1.3 Prostaglandins and leukotrienes

In addition to the protein inflammatory mediators above mentioned, cytokines and the complement system, lipidic molecules are also part of the innate inflammatory response. Prostaglandins (PGs) and leukotrienes (LTs) are inflammatory mediators derived from arachidonic acid (Funk, 2001; Kuehl & Egan, 1980). Prostaglandin E2 (PGE_2), the major PG produced in the body by almost every nucleated cell, plays a key role in physiology: it regulates the blood pressure, fertility processes and, of course, inflammation. On the other hand, LK are produced by leukocytes in the periphery (Funk, 2001; Peters-Golden & Henderson, 2007) but their source in the CNS remains unclear (Michael et al., 2020). The alteration of the pathways regulated by these molecules lead to detrimental consequences, e.g. deficient PGE2 synthesis or degradation is associated with a wide range of pathological conditions including MS, AD, PS, Huntington's disease (HD), and/or Amyotrophic Lateral Sclerosis (ALS) (Famitafreshi & Karimian, 2020; Legler et al., 2010)and LTs contribute to the neuropathology of many neurodegenerative diseases such as stroke (Fang et al., 2006; Hijioka et al., 2020; Ji et al., 2013; Zhao et al., 2011) or brain trauma (Hu et al., 2005; Zhang et al., 2004).

3.3 PHAGOCYTOSIS

Phagocytosis, from Ancient Greek *phagein* "to eat" and *kytos* "cell", can be literally translated as "cell eater". It is a cellular process that involves the recognition, ingestion and digestion of particles larger than 0.5 µm (Mukherjee et al., 1997), like apoptotic cells or microorganisms. Phagocytosis can be observed in unicellular organisms as their basic nutritional process. In multicellular organisms, many cell types execute phagocytosis to maintain tissue homeostasis (Mukherjee et al., 1997; Uribe-Querol & Rosales, 2020). However, only specialised cells, the professional phagocytes, perform phagocytosis efficiently. Phagocytosis efficiency is related to the ability of the phagocytes to respond to certain stimuli, such as inflammatory mediators or bacterial products, by producing phagocytosis related molecules, such as tumour necrosis factor- α (TNF- α) or insulin-like growth factor 1 (IGF1) (Uribe-Querol & Rosales, 2020). It is then an essential mechanism of the innate immune system, in combination with inflammation, to eliminate and clear the invading pathogens or substances and recover the tissue health. In the

next section, we will review the different cargos that can be taken up by microglia and the different steps they must accomplish during the phagocytosis process.

In this section, we will dissect the phagocytosis process from different angles: concerning the susceptible phagocytic cargo, we will describe the different steps of phagocytosis and the signals associated to each step and finally describe the current models to study phagocytosis and its functional outcome.

3.3.1 Phagocytic cargo

Microbes. If organisms such as bacteria, viruses, fungi or parasites enter the CNS microglia rapidly recognise these invaders as foreigners and trigger its immune response (Dando et al., 2014). However, the chances of CNS invasion by pathogens are extremely low due to the presence of the BBB, which acts a physical barrier against infections (Pardridge, 2005). Nevertheless, some pathogens break through the BBB causing infections, e.g., meningitis, or directly enter the CNS after a traumatic brain injury. In the peripheral nervous system (PNS), however, the infection is counteracted not by microglia, but by extravasated circulating monocytes (Liu et al., 2000) in combination with the resident macrophages of the PNS, which comprise 5% of the total endoneurial cell population (Mueller et al., 2003; Mueller et al., 2001).

Several studies have demonstrated the effective clearance of bacteria and fungi by microglia. In culture, microglia efficiently phagocytose and clear *Escherichia coli* bacteria in vitro after the stimulation with the endotoxin lipopolysaccharide (LPS) (Cockram et al., 2019; Diesselberg et al., 2018) as well as *Staphylococcus aureus* (Baldwin & Kielian, 2004; Kochan et al., 2012). LPS is a lipid molecule conjugated to a either an oligo- or polysaccharide, present in the membrane of Gram negative bacteria, and is widely used as an inflammatory model to mimic human sepsis (Deitch, 1998). Fungi are also targeted and cleared by microglia, in vitro and in vivo. For example, the BV2 microglia cell line phagocytoses and clear *Lomentospora prolificans* (Pellon et al., 2018). In vivo, microglia effectively surround *Candida Albicans* cists, directly phagocytosing the yeast (Blasi et al., 1991) and releasing cytokines to recruit neutrophiles to the lesion site (Lionakis et al., 2011). Hence, microglia effectively battle invading microbes in the CNS.

Aggregated proteins (Aβ aggregates). The Aβ peptide is generated by the proteolytic cleavage of the amyloid precursor protein (APP) by the by β- and γ-secretases (Hamley, 2012). The release, oligomerization, and deposition of Aβ is the major pathological hallmark in AD, which is suggested to trigger a detrimental cascade of events that ultimately leads to cognitive

impairment and loss of memory (Selkoe & Hardy, 2016). On the other hand, several studies have suggested that the progression of the disease is related to a deficient clearance of the Aβ deposits and not to the overproduction and release of the peptide (Mawuenyega et al., 2010). Several studies have stated that microglia are able to remove Aβ from Aβ deposits by phagocytosis; however, it is not yet clear if they degrade or extrude the phagocytosed Aβ.

The role of microglia in AD is still in debate. They are found surrounding the plaques both in AD patients as well as in murine models of the disease (Daria et al., 2017). Several in vitro studies have demonstrated the Aβ uptake by microglia (Hellwig et al., 2015; Majumdar et al., 2008; Mandrekar et al., 2009; Xu et al., 2020). However, a complete clearance of the internalized Aβ still remains to be confirmed (Grathwohl et al., 2009; Y. Huang et al., 2021; Krabbe et al., 2013; Spangenberg & Green, 2017). Furthermore, the role of microglial phagocytosis of Aβ in vivo has been proposed to be either neutral, as microglia depletion had no effect on the size of the Aβ plaques (Grathwohl et al., 2009); or beneficial, as microglia depletion resulted in plaque growth (R. Zhao et al., 2017). Thus, the role of microglia in AD remains a controversial matter still to be answered.

Synapses and spines. As mentioned in **Section 1.1.3**, the role of microglia in synapse remodelling has been a subject of study in the last years. In addition to microglial role during development, they can also phagocytose synaptic elements, like pre- and post-synaptic proteins, in the adult mice (Paolicelli et al., 2011; Schafer et al., 2012; Weinhard et al., 2018). The role of microglial phagocytosis of synapses and spines has also been studied in pathology. Going back to AD, microglia promote synapse loss due to an increased synapse targeting with the complement protein C1q (Hong et al., 2016). In Huntington disease (HD) and schizophrenia, excessive synapse loss has also been proposed (McGonigal et al., 2016; Williams et al., 2016). On the contrary, in ischemia, microglia contact longer with presynaptic terminals presumably trying to restore the synaptic function (Wake et al., 2009). Hence, the role of microglia in synapse remodelling still remains open to debate.

Axonal and myelin debris. After acute CNS injury, the axonal debris generated by the neuronal damage comprises a barrier for axonal regeneration and, hence, it should be cleared to promote axonal outgrowth. Microglial phagocytosis has been proposed as the mechanism to remove the debris through phagocytosis, yet few studies have demonstrated myelin debris phagocytosis by microglia (Cignarella et al., 2020; Lampron et al., 2015). However, recent data have demonstrated then role of microglia after spinal cord injury, where they are essential to initiate

regeneration (Zhou et al., 2020). In vitro experiments, using sectioned neurites from cortical rat explants (Tanaka et al., 2009) and axonal degeneration co-cultures (Hosmane et al., 2012), demonstrated the microglial clearance of axonal debris allowing axonal regeneration.

Among these phagocytosis substrates our main interest relies on the phagocytosis of apoptotic cells. We will next detail the concept of apoptotic cells as a susceptible phagocytic cargo and explain how microglia engulf and degrade dead cells following different steps.

Apoptotic cells. Apoptosis, or programmed cell death, is a controlled and regulated biological process, essential for multicellular organisms to maintain their homeostasis and regulate the balance between cell proliferation and cell death (Xu et al., 2019). It takes place ubiquitously in the adult organism and plays a major role during embryonic development (Voss & Strasser, 2020). Programmed cell death can also take place under pathological conditions, for example in neurodegenerative diseases (Madden & Cotter, 2008). In the brain, regardless of the physiological or pathological cause for apoptosis, microglia must execute the removal of the dead corpses to guarantee tissue homeostasis.

The initiation of apoptosis, either by internal or external signals, defines the type of programmed cell death. The intrinsic or mitochondrial pathway is initiated by internal signals dependent on factors produced by the mitochondria, whilst the extrinsic or death receptor pathway is mediated by death ligands that bind to surface receptor in the target cell (Igney & Krammer, 2002). Some of the internal signals that trigger apoptosis comprise damage in the DNA, lack of pro-survival signals like hormones, cytokines and growth factors; whereas external factors include the activation of immune cells, such as NK or macrophages, that produce the death ligands after infections or cells damage (D'Arcy, 2019; Zaman et al., 2014).

Both pathways require caspases as effector molecules, different at the initiation step but present common downstream executioner molecules: caspases 3, 6 and 7 (Elmore, 2007). The activation of these caspases generates the cleavage and degradation of essential proteins for normal cell function, such as cytoskeletal and nuclear proteins. Subsequently, the cell experiments nuclear fragmentation (karyorrhexis), chromatin condensation (pyknosis), cytoplasm reduction, cell shrinkage and the formation of blebs and apoptotic bodies as a result of the cytoskeletal break down (Santavanond et al., 2021). One of the most important morphological features of apoptosis is the maintenance of the plasma membrane integrity until the final stages. It avoids the spill over of the intracellular content and limits the generation of

an exacerbated inflammatory response and tissue damage, as in other types of uncontrolled cell death such as necrosis (D'Arcy, 2019). The limitation of the damage in the surrounding tissue through apoptosis must then be in tight communication with the phagocyte devoted to the elimination of the dead bodies, to guarantee the completion of a successful cell death and removal of the corpse.

In the next section, we detail the communication between the apoptotic cell and microglia.

3.3.2 Phagocytosis stages: find me, eat me, digest me

The physical process of phagocytosis can be split into three different steps: “find-me”, “eat-me” and “digest-me” (**Figure 3**). First, apoptotic cells must release “find-me” signals to alert and attract microglia towards them (Peter et al., 2010; Sierra et al., 2013). Once in close proximity, microglia engage the apoptotic cell by directly interacting with specific “eat-me” ligands in the apoptotic cell that allow microglia to recognise the cell as dead and enable phagocytosis (Gardai et al., 2006; Li, 2012; Sierra et al., 2013). After the recognition and docking of the apoptotic cell, microglia physically engulf the corpse by the formation of a phagocytic pouch and the reorganisation of the plasmatic membrane (Arandjelovic & Ravichandran, 2015). After the apoptotic cell is internalised, the phagosome is delivered to the lysosomes for the degradation and recycling of useful components during the “digest-me” step (Kinchen et al., 2008; Kinchen & Ravichandran, 2008; Levin et al., 2016; Park et al., 2011) (**Figure 3**). Phagocytosis is a highly conserved process regulated by a plethora of redundant receptors and molecules that guarantee its success. Next, we will revise the different each phagocytosis step individually based on their regulatory receptors and ligands.

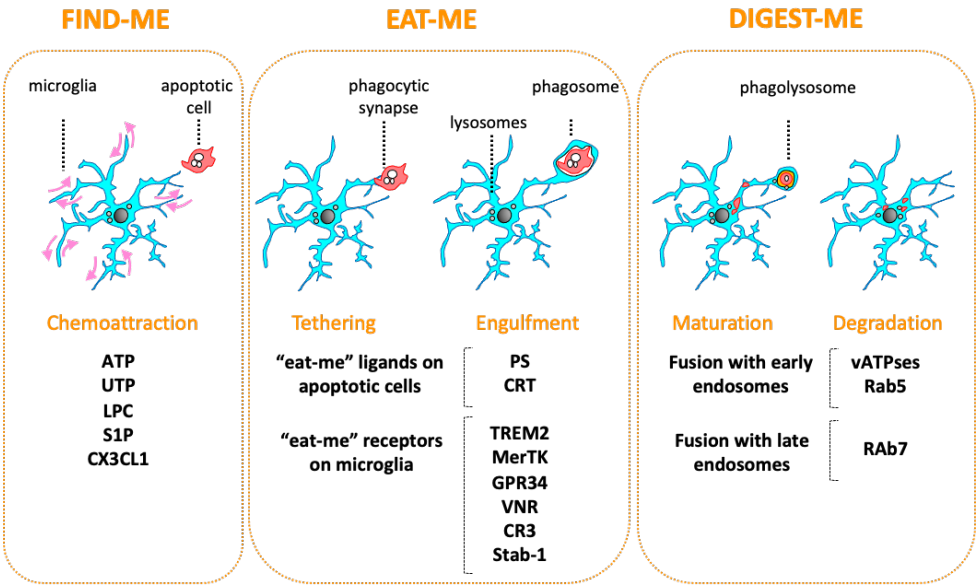

Figure 3. Sequential steps of microglial phagocytosis of apoptotic cells. *Phagocytosis of apoptotic cells comprises three different steps: "find-me", "eat-me" and "digest-me". In the "find-me" step, apoptotic cells release soluble and diffusible molecules, such as ATP or CX3CL1, to attract phagocytes. The "eat-me" step, the receptors expressed in the microglial surface, like TREM-2, meet the ligands in the apoptotic cell, such as PS, forming a phagocytic synapse that will tether apoptotic cell, leading to their engulfment in the phagosome. Finally, in the "digest-me" step, the phagosome matures by fusing with endosomes and the vesicular content is finally degraded after the fusion of the phagosome with the lysosome, forming the phagolysosome.*

3.3.2.1 "Find-me" step

The main goal of the "find-me" signals is to attract the phagocytes, microglia in our case, towards the location of the dead cell (**Figure 3**). The constant surveillance of the parenchyma performed by microglia allows them to respond to the secreted signals within a range of seconds (Avignone et al., 2015). The main "find-me" signals released by apoptotic cells are soluble nucleotides (adenosine triphosphate, ATP, and uridine triphosphate, UTP), lysophosphatidylcholine (LPC), sphingosine-1-phosphate (S1P) and Fractalkine (CX3CL1) (Arandjelovic & Ravichandran, 2015; Elliott et al., 2009; Gude et al., 2008; Lauber et al., 2003; Li, 2012; Park & Kim, 2017; Sierra et al., 2013; Truman et al., 2008).

Nucleotides (ATP and UTP). Nucleotides, mainly ATP and UTP, are released from apoptotic cells in a caspase-3-dependent manner (Elliott et al., 2009) through pannexin-1 channels (Chekeni et al., 2010; Koizumi et al., 2013). These nucleotides, and their hydrolysed metabolites ADP and UDP, bind to purinergic receptors, like P2Y12 and P2Y6 respectively, that are widely expressed in microglia and attract the phagocytes towards the dead cell (Haynes et al., 2006; Xu et al., 2016).

Lysophosphatidylcholine (LPC). LPC is released from the apoptotic cell after the cleavage of phosphatidylcholine (PC) by the calcium-independent phospholipase A2 (iPLA2 or PLA2G6) enzyme (Lauber et al., 2003; Peter et al., 2008). LPC binds to the G-coupled receptor G2A stimulating the chemotactic migration of microglia.

Sphingosine-1-phosphate (S1P). S1P is released in a caspase-3-dependent manner, after its generation from sphingosine by sphingosine kinase. It binds to S1P receptor on phagocytes (Gude et al., 2008) and their expression in microglia was only recently demonstrated (O'Sullivan et al., 2018); yet their role in microglial chemotaxis remains poorly explored.

Fractalkine (CX3CL1). CX3CL1 is a membrane-bound protein released by proteolytic cleavage from apoptotic cells (Sokolowski et al., 2014; Truman et al., 2008). The resultant soluble fragment binds to the CX3CR1 receptor in microglia and macrophages promoting the migration of the phagocytes (Eyo et al., 2016; Jung et al., 2000; Mizutani et al., 2012).

Once the dead cell has been approached, microglia physically meet the apoptotic body and initiates the second step of phagocytosis or "eat-me" phase, in which microglia recognize, tether and dock the apoptotic cell (Sierra et al., 2013).

3.3.2.2 "Eat-me" step

Microglia must properly recognize the apoptotic cells in order to engulf the correct target (Sierra et al., 2013) (**Figure 3**). Both apoptotic cells and microglia express a wide set of ligands and receptors to ensure the correct recognition of the cell to be eaten. To guarantee a correct recognition of the phagocytic target, healthy cell also express "don´t eat-me" ligands on their surface that interact with receptors in the phagocyte enabling their recognition as "own and non-edible" cells (Kourtzelis et al., 2020; Park & Kim, 2017; Westman et al., 2020). CD47 is expressed in the surface of eukaryotic cells and interact with the SIRPα receptor in the phagocyte to negatively modulate myosin assembly during the formation of the phagocytic synapse (Gardai et al., 2005; Tsai & Discher, 2008). Another example is CD31, expressed both in the healthy cell and in the phagocyte, whose homotypic interaction prevents the recognition of the healthy cells as foreign or damaged (Brown et al., 2002). In addition, CD46 in the surface of the healthy cells binds to C3b and C4 complement molecules, enabling their proteolytic degradation and avoid their opsonization and engulfment (Elward et al., 2005). All these molecules are expressed by tumour cells to "trick" the immune system and avoid their elimination (Banerjee et al., 2021).

- "Eat-me" ligands on apoptotic cells

"Eat-me" signals are displayed in the membrane of apoptotic cells but should not be displayed in the membrane of healthy ones. Several molecules have been proposed to act as "eat-me" signals; however, the most studied ones are the membrane anchored phosphatidylserine (PS) and calreticulin (CRT).

PS is phospholipid located in the inner leaflet of the plasma membrane of healthy cells, but it is exposed to the extracellular environment upon stressful stimuli (Fadok et al., 1992; Ravichandran & Lorenz, 2007). If a cell is healthy, there is an asymmetry between the inner and the outer leaflet of the plasma membrane, maintained by the action of ATP-dependent and independent flippases that transport certain lipidic components between leaflets. During apoptosis, PS is irreversibly exposed on the outer leaflet by the action of the Xk-related protein 8 (Xkr8), a phosphatidylserine scramblase (Suzuki et al., 2016), as well as by the inactivation of the ATP11C ATPase by caspase-3-mediated cleavage (Segawa et al., 2014).

CRT is an endoplasmic reticulum (ER)-associated protein involved in the quality control of new proteins and has chaperone activity. Upon ER stress or apoptosis signalling, CRT can be exposed on the surface of apoptotic cells, either alone or bound to PS by its C-terminal acidic region (Wijeyesakere et al., 2016). It will bind to the low-density lipoprotein receptor (LRP or CD91) present in the phagocyte surface (Gardai et al., 2005), promoting the engulfment of apoptotic cells.

- "Eat-me" receptors on phagocytes

Microglia display a plethora of "eat-me" receptors on their membrane that can bind to several ligands in the surface of the apoptotic cell. Among the best characterized receptors are triggering receptor expressed on myeloid cells-2 (TREM2), Mer tyrosine kinase (MerTK), G protein-coupled receptor 34 (GPR34), vitronectin receptor (VNR or αvβ3), complement receptor 3 (CR3), and stabilin- 1 (Stab-1).

Triggering receptor expressed on myeloid cells-2 (TREM2). TREM2 is a transmembrane receptor of the immunoglobulin superfamily expressed by dendritic cell (DCs), macrophages and microglia (Neumann & Takahashi, 2007). This receptor associates with adapter protein named DNAX-activation protein of 12 kD (DAP12) (Paloneva et al., 2002) and the malfunction of either TREM2 or DAP12 leads to a deficient uptake of apoptotic cells by microglia (Hsieh et al., 2009; Thrash et al., 2009). In vitro, apolipoprotein E was suggested to directly bind TREM2 in addition to connecting the receptor with PS (Atagi et al., 2015).Furthermore, TREM2 has been widely involved in the recognition of extracellular Aβ deposits in AD (Joshi et al., 2021; Parhizkar et al., 2019).

Mer tyrosine kinase (MerTK). MerTK is a member of the Tyro3, Axl and MerTK (TAM) receptor family (Lemke, 2013), expressed in DCs, macrophages and microglia (Behrens et al., 2003).

MerTK interacts with the apoptotic cell through soluble-bridging proteins bound to PS, like the arrest-specific protein 6 (GAS6) and protein S (ProS) (Lemke, 2013; Nagata et al., 1996; Wu et al., 2005; Zizzo et al., 2012) and galectin-3 (Gal-3) (Caberoy et al., 2012).

G protein-coupled receptor 34 (GPR34). GPR34 is part of the PY2 family, mainly expressed in macrophages and microglia (Bédard et al., 2007; Butovsky et al., 2014; Hickman et al., 2013) and to a lesser extent in other populations like DCs and NK (Schöneberg et al., 2018). Its dominant ligand is lysophosphatidylserine (LysoPS), a deacylated form of phosphatidylserine produced by phospholipases (PLA) (Makide et al., 2014). The role of LysoPS has been well characterized both in vivo and in vitro, where it has been demonstrated that it induces T-cell proliferation, fibroblast migration, neurite growth and apoptotic uptake by macrophages (Makide et al., 2014). GPR34 deficient microglia demonstrated less phagocytic capacity in vitro, removing less apoptotic beads and myelin (Preissler et al., 2015), hence, demonstrating the important role of GPR34 in the phagocytosis of apoptotic cells.

Vitronectin receptor (VNR or αvβ3). VNR is a member of the integrin superfamily of adhesion molecules expressed by macrophages (Lauber et al., 2004). It binds to the opsonin milk fat globule EGF factor (MFG-8) to mediate the phagocytosis of apoptotic cells, both in vivo and in vitro (Hanayama et al., 2002). The VNR activation triggers the remodelling of microglial cytoskeleton (Arcuri 2017; Yanuck 2019) and has also been proposed to present a synergistic crosstalk with MertK (Wu et al., 2005).

Complement receptor 3 (CR3). CR3, part of the family of beta-2 (CD18) integrins (Vorup-Jensen & Jensen, 2018), binds to molecules of the complement cascade such as C1q or C3b (Linnartz et al., 2012) and is well known to enable cellular adhesions and promote pathogen and apoptotic cell phagocytosis in vitro (Trouw et al., 2008). In addition, CR3 was also shown to trigger an anti-inflammatory response in microglia (Ehirchiou et al., 2007; Fraser et al., 2010; Hou et al., 2020).

Stabilin- 1 (Stab-1). Stab-1 is a transmembrane receptor expressed in macrophages and non-continuous sinusoidal endothelial cells of the liver, spleen, adrenal cortex, and lymph nodes (Naeini et al., 2020). Among its many functions, it mediated the engulfment of apoptotic cells through PS recognition (Park et al., 2009; Park & Kim, 2017).

To this point, microglia have been able to reach, recognize and engulf the apoptotic cells. During this process, microglia remodel their cytoskeleton to internalize and deliver the phagosome to

the lysosomes for its degradation (Zhou & Yu, 2008). In the next section, we will highlight some aspects of the phagosome digestion.

3.3.2.3 "Digest-me" step

Once the phagosome is internalised, it must mature and be transported to the lysosomes for its degradation (Desjardins et al., 1994; Kinchen & Ravichandran, 2008; Lee et al., 2020) (**Figure 3**). The maturation process implies the acidification and gain of hydrolytic function by fusion and fission events with endocytic organelles (early and late endosomes, autophagic and lysosomes) that transfer enzymes and proton pumps to the maturing phagosome by "kiss-and-run-events" (Desjardins, 1995). In the first step, the non-degradative early phagosome fuses with early endosomes and acquire vacuole ATPases (vATPases) and membrane associated proteins such as Rab5, acquiring a pH close to 6.5 (Bucci et al., 1992; Duclos et al., 2000). After several fusion-fission events, the phagosome acquires a mature phenotype, characterised by Rab7 expression and a luminal pH of 5.5 (Harrison et al., 2003) and can be considered a late phagosome. At this point, the phagosome is transported to the (-) end of the microtubules to fuse with the lysosomes, finally forming the fully degradative phagolysosome (Harrison et al., 2003). The lysosomal compartment will be described in detail in the **Section 1.6**. The signalling cascade triggered by the internalisation, maturation and degradation of the phagosome has been proposed to further regulate the phagocytosis process, by enhancing the uptake of additional targets and by remodelling the lysosomal compartment enhancing the generation of extra degradative potential (Hipolito et al., 2018).

In summary, phagocytosis is then a highly regulated and redundant process compartmentalised pin three major steps: "find-me", "eat-me" and "digest-me", susceptible of alterations that can affect microglial phagocytosis. Until now, we have described the potential phagocytic cargo and the different steps that the phagocytosis can be divided into. In the following section we will describe how microglial phagocytosis of apoptotic is assessed both in in vivo and in vitro.

3.3.3 Assessing microglial phagocytosis

Microglial phagocytosis has been historically overlooked and taken as a process occurring in the brain related to inflammation rather than as a relevant process itself (Griffiths et al., 2009). The analysis of microglial phagocytosis has been traditionally assessed using indirect methods, such as microglial morphology or the expression of "activation markers" (**Figure 4**).

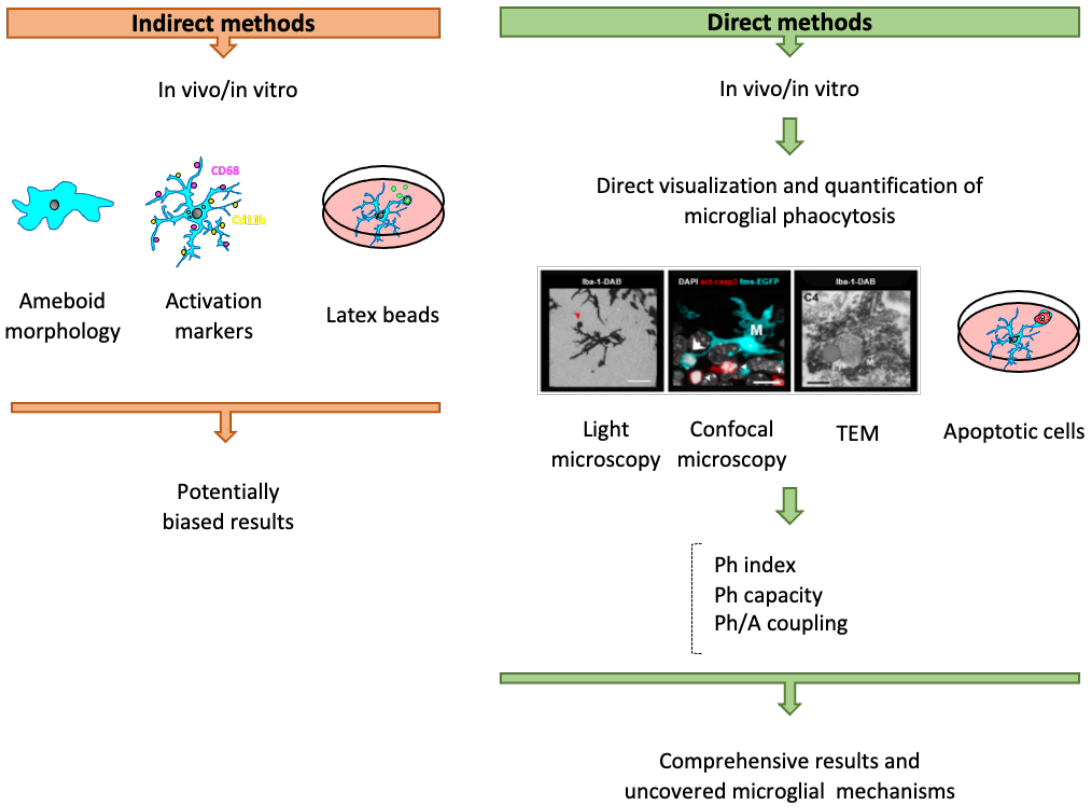

Figure 4. Methods to assess microglial phagocytosis. *Microglial phagocytosis has traditionally been assessed using indirect methods like ameboid morphology, or the expression of activation markers, such as the lysosomal CD68. The addition of latex beads is also frequently used as a system despite not reproducing the physiological environment. To overcome these limitations, direct methods like the in vivo observation of phagocytosis are spreading. The use of light microscopy, confocal microscopy or TEM, as well as a more physiological phagocytosis assay in vitro using apoptotic cells, allow the direct visualization of phagocytosis and its quantification. To understand the dynamics of phagocytosis, we developed a novel set of parameters based on the direct observation of confocal microscopy images: Ph index (i.e., proportion of apoptotic cells completely engulfed by microglia), Ph capacity (i.e., proportion of microglia with one or more phagocytic pouches, each containing one apoptotic cell), and Ph/A coupling (i.e., net phagocytosis (number of microglia multiplied by their phagocytic capacity) divided by the number of apoptotic cells. This image was adapted from (Diaz-Aparicio et al., 2016).*

Microglial ameboid morphology was long considered as the hallmark for phagocytosis, yet morphology is not always translated into function. Microglial phagocytosis is not only performed by ameboid microglia, contrary to the general belief (Kettenmann, 2007). Our laboratory demonstrated that microglia efficiently phagocytosed apoptotic cells either ramified in physiological conditions or more hypertrophic under a LPS challenge (Sierra et al., 2013). Thus, microglial morphology is not directly related to their phagocytic function.

"Activation markers" have also been considered as a hallmark for phagocytosis. Proteins such as macrosialin/ED1 (lysosomal protein CD68) and Cd11b (integrin α M) are considered to be indicators of phagocytosis (da Silva & Gordon, 1999; Schafer et al., 2012), whereas CD68 is, in fact, a lysosome associated membrane protein (LAMP)-like protein bound to the lysosome, and Cd11b is constitutively expressed in the plasma membrane of NK, macrophages and neutrophils. Both are overexpressed in the plasma membrane during inflammation, unrelated to phagocytosis (Chistiakov et al., 2017; da Silva & Gordon, 1999; Ekdahl et al., 2003; Sierra et al., 2010) (**Figure 4**).

In addition to the use of morphology and inflammatory markers as indicators of phagocytosis, phagocytosis has traditionally been studied in artificial in vitro systems, which are very useful to isolate individual processes or signalling cascades but do not fully recapitulate the steps of phagocytosis in vivo. In the next section, we will discuss the main in vitro systems to assess microglial phagocytosis and the functional outcome of phagocytosis.

3.3.3.1 Modelling phagocytosis in vitro

Microglial phagocytosis has been traditionally studied using in vitro models of cultured microglia derived from the postnatal brain (Sierra et al., 2013) (**Figure 5**). In 1986, Guilian and Baker (Giulian & Baker, 1986) established the culture of adherent microglia and since then phagocytosis assays have been performed by adding potentially phagocytic substrates to microglia. The main assets of the in vitro systems are their high controllability and the advantage of having individualized cells to assess direct effect of a certain treatment on microglia. Each in vitro model, like BV2 cell, primary microglia or iPSCs, renders different advantages and disadvantages that will change depending on the type of assay, for example, depending on the phagocytic substrate, beads or apoptotic cells, added to the culture (**Figure 5**).

One of the main advantages of primary cultures is genetic homogeneity and the specific pathogen free (SPF) mice, were pre- and post-mortem conditions can be controlled (Timmerman et al., 2018). However, the main concern about primary microglia derived from the postnatal brain is their lack of exposure to the environmental signals required for their maturation and, despite removing apoptotic cells, they do not present a mature transcriptional signature (Butovsky et al., 2014). In addition, in the brain parenchyma, microglia are kept in a homeostatic state by several signal coming from the surrounding cells, such as fractalkine, whose deletion has proven to reduce microglia phagocytosis and enhance inflammation (Wolf et al., 2013). The absence of the parenchymal signals in the in vitro cultures evidence the major difference with

the in vivo models, as the complexity of the environmental signalling cannot be recapitulated using artificial models, at least up to date (**Figure 5**).

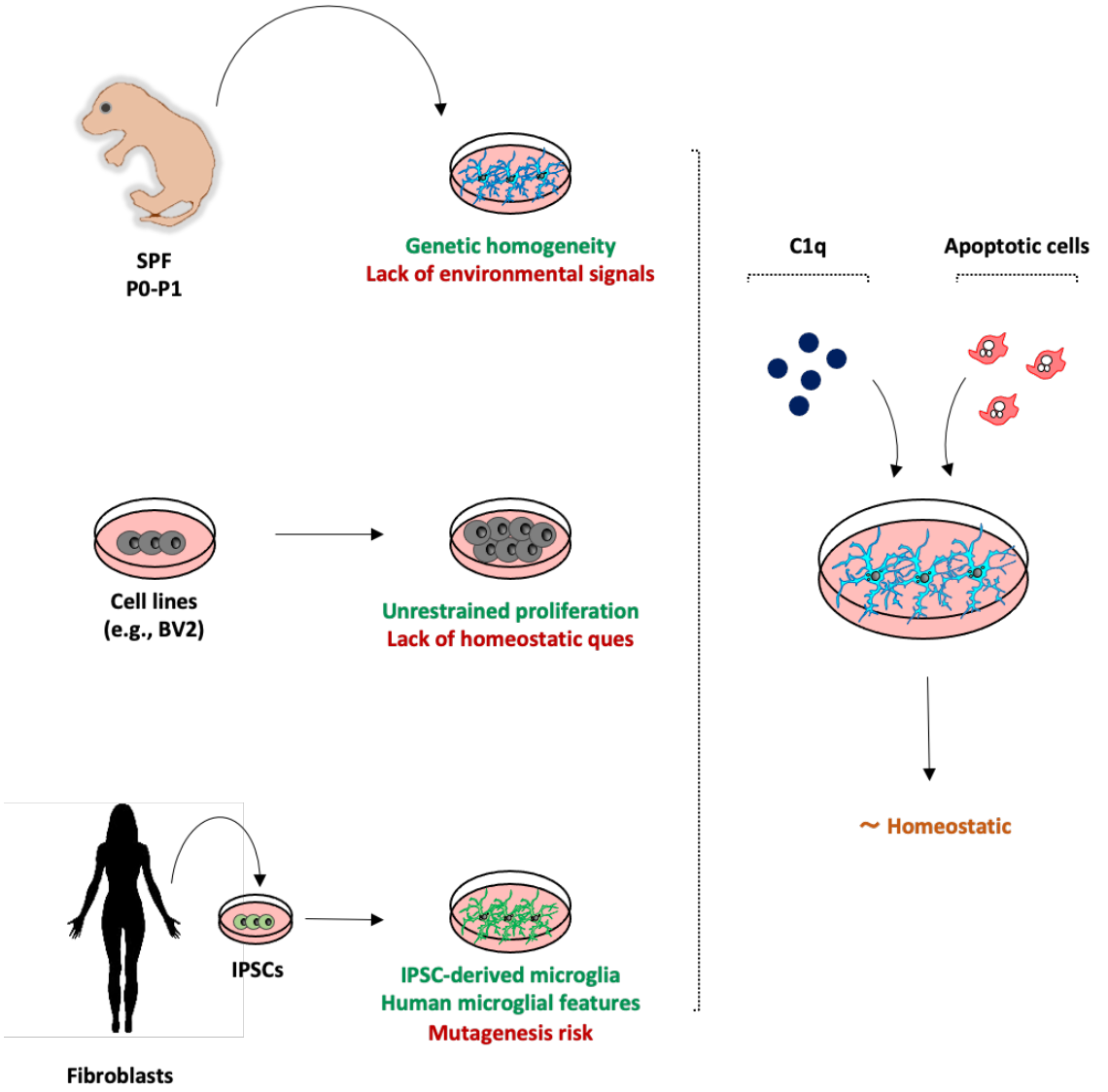

Figure 5. In vitro modeling of microglial phagocytosis. *Microglial phagocytosis has traditionally been assessed using in vitro systems, whose main assets are their high controllability and the individualization of cells. Among these models, microglial cell lines, like BV2 cells, and primary microglia are the most commonly used, both with advantages and disadvantages. Recently, IPSCs are emerging as a powerful alternative to overcome the limitations of traditional in vitro system but present their own limitations as well. To mimic the homeostatic conditions of the brain, molecules such as C1q have been demonstrated to be essential for microglial phagocytosis and are currently used in phagocytosis assays as well as apoptotic cells in substitution for the non-physiological latex beads.*

In addition to primary cultures, microglial cell lines like BV2 cells (Blasi et al., 1990) have been and are widely used in the field, due to their easy maintenance and availability because of their unrestricted proliferative capacity (Timmerman et al., 2018). For instance, BV2 cells present

similar enzymatic activity to primary microglia as the NADPH oxidase enzyme, related to the microglia-triggered neuronal damage (Yang et al., 2007). However, it has also been evidenced that BV2 cells are not able to recapitulate the full microglial phenotype. BV2 are less motile in response to chemokines, also less responsive to LPS and the characteristic TGF-β pathway is down regulated in this cell lines (Das et al., 2016; He et al., 2018). At the transcriptional level, the BV2 profile was significantly different from the profile of adult microglia isolated from the mouse brain (Butovsky et al., 2014), confirming the differences between these two models. The current step to overcome the limitations of murine primary cultures and cell lines are microglial cells derived from induced pluripotent stem cells (iPSC). Derived from human fibroblasts, they have been shown to recapitulate human microglial features (Healy et al., 2018) to a much higher extent than rodent microglia, but present mutagenesis and oncogene activation risks (Dawson et al., 2018; Friedman et al., 2018). Thus, they are the most accurate model to mimic human microglia (Hasselmann & Blurton-Jones, 2020) (**Figure 5**).

Another critical point when designing in vitro models is the choice of target. Commonly, phagocytosis assays have been performed using latex beads coated with serum to promote the interaction of the phagocyte with the beads. It has been recently proposed that the C1q molecule, present in the culture serum, is involved in the phagocytosis of apoptotic cells; hence, the use of non-inactivated serum to coat the latex beads could improve microglial phagocytosis (Diaz-Aparicio & Sierra, 2019b; Fraser et al., 2010). Nevertheless, these particles do not release chemokines to attract microglia and do not activate the initial “find-me” step of phagocytosis. Furthermore, the internalization of non-metabolizable latex beads does not allow degradation. The fluorescence pH sensor pHrodo is used as a measurement of the acidification of intracellular vesicles when they fuse with lysosomes. However, it has been wrongly used as a measurement of degradation (Lindner et al., 2020), as the acidification of intracellular vesicles does not imply the full degradation of the enclosed content but only the lower of the vesicular pH. In order to mimic the physiological conditions of the in vivo environment, we chose to perform the phagocytosis assays in the presence of C1q (non-inactivated serum) using apoptotic neurons that express the “find-me” signals and can be digested once phagocytosed by microglia (Diaz-Aparicio & Sierra, 2019b) to build a more physiological system. Nonetheless, the most direct method to assess phagocytosis is to visualise it in vivo.

3.3.3.2 In vivo phagocytosis: dentate gyrus of the hippocampus

Analysis of phagocytosis must be then based on the direct observation of the phagocytic pouch and the cargo inside microglia (**Figure 4**). To make these observations, several imaging techniques can be used. For example, electron microscopy (EM) has been used to directly visualize the phagocytosis of synaptic elements (Tremblay et al., 2010) but is a time-consuming technique limited to the imaging of small areas. The combination of light microscopy and immunostaining can be useful to image the phagocytic pouch but, as they are performed separately and only give common information when merged, the content of the phagocytic pouch cannot be guaranteed (Perez-Pouchoulen et al., 2015). Our technique of choice is immunofluorescence and confocal microscopy , as we can directly visualise the microglial phagocytic 3D pouch surrounding the apoptotic cell and further determine other possible contents, such as myelin or axonal debris, without overestimating the phagocytosis of apoptotic cells (Sierra et al., 2013). However, the imaging analysis on fixed tissue gives information at a given timepoint; live imaging techniques, such as 2-photon microscopy, render live visualisation of the phagocytosis process (Abiega et al., 2016; Sieger et al., 2012). In the next sections we will discuss the main approaches to study microglial phagocytosis both in vivo and in vitro.

To study microglia phagocytosis in vivo, we focused on the dentate gyrus of the hippocampus (**Figure 6**), where neurogenesis occurs throughout the lifespan (Altman, 2011; Gonçalves et al., 2016). We selected this brain region because the ongoing apoptosis of the neuroprogenitors form the neurogenic cascade (Sierra et al., 2010) allows us to establish a baseline of microglial phagocytosis in physiological conditions. In this section, we will discuss why the dentate gyrus of the hippocampus (DG) is an optimal region to assess phagocytosis in the healthy brain.

Neurogenesis, or the formation of new neurons, is a complex process that extends through adulthood in two brain regions of the mammalian brain, the subventricular zone (SVZ) and the DG (Obernier & Alvarez-Buylla, 2019). The production and emergence of new neurons is a multistep process that requires the proliferation of the neural stem cells, their differentiation, migration, and integration in the circuitry, gradually acquiring functional and physiological properties (Kempermann et al., 2004). However, along this process the majority of the new-born neurons die by apoptosis and are rapidly and efficiently phagocytosed by microglia (Sierra et al., 2010). Here, we will not discuss the neurogenic cascade in detail, but only refer to the ongoing apoptosis that takes place at the initial steps of the process, to study microglial phagocytosis in physiological conditions in the DG (**Figure 6**).

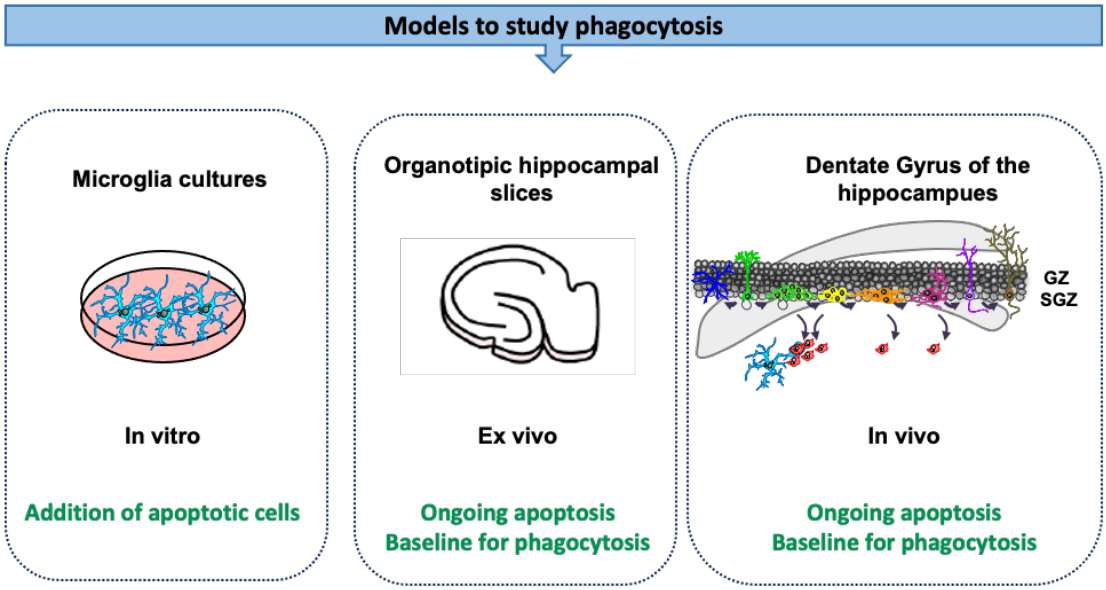

Figure 6. Models to study phagocytosis. *The study of microglial phagocytosis can be performed on isolated cells or more complex systems depending on the model of study. In vitro systems render the possibility to study microglial phagocytosis in isolated cells with a controlled amount of apoptotic cells, whilst organotypic hippocampal slices and the DG offer the possibility to study microglia in physiological conditions. Basal apoptosis that occurs both in organotypic cultures and in the DG allow establishing a baseline for phagocytosis and its comparison with pathological situations.*

In 2010, our group studied microglial efficiency in the DG, and determined that 90% of the apoptotic cells were phagocytosed and cleared by microglia, whereas the remaining 10% were not phagocytosed as they were early apoptotic and were not recognized yet by microglia (Sierra et al., 2010). The percentage of phagocytosed apoptotic cells engulfed by microglia is defined as the phagocytic index (Ph index) and we use it as a measurement of microglial efficiency. Phagocytosis occurs very rapidly, taking around 1.5 hours to engulf and fully clear an apoptotic cell (Sierra et al., 2010), in agreement with the phagocytosis efficiency of macrophages (Henson & Hume, 2006). The short clearance time implies that, at a given time point, we can only observe a small proportion of the actual cells that have undergone apoptosis and have been phagocytosed by microglia (Barres et al., 1992; Sierra et al., 2010).

Under an apoptotic challenge induced by inflammation or excitotoxicity, microglia can follow three different strategies to cope with the increase in apoptotic cells, revealing their phagocytic potential: 1, they can recruit more phagocytic cells; 2, they can increase their phagocytic capacity by phagocytosing more apoptotic cells per microglial cell; 3, they can increase the number of microglia (Abiega et al., 2016). These strategies allow microglia to efficiently remove the apoptotic cells maintaining phagocytosis tightly coupled to apoptosis (Abiega et al., 2016).

Thus, the in vivo study of phagocytosis not only allowed us to establish a baseline for phagocytosis but also to study microglial phagocytosis in the healthy brain that we can compare with pathological scenarios. In this PhD Thesis we have used the neurogenic cascade as a model to study microglia phagocytosis using different models of disease: autophagy deficient mice and a genetic model of epilepsy. These models will be revised in **Sections 1.8.2** and **1.8.4**. respectively.

As a compromise solution between in vivo models and primary cultures, organotypic cultures can mimic some aspects of the in vivo environment improving the primary culture model (**Figure 6**). Apoptosis occurs naturally, the connectivity is largely preserved, and all neural cell types are present (Gähwiler et al., 1997); therefore, they serve as a useful model to mimic several diseases such as epilepsy (Abiega et al., 2016) or stroke (Garbayo et al., 2011; Gerace et al., 2021). However, the replacement of the cerebrospinal fluid with culture medium once again modifies the original environment rendering a different response of microglia to the same stimulus, as we have already described (Abiega et al., 2016). Thus, organotypic cultures do not fully recapitulate the in vivo environment but help to overcome in vitro limitations of primary cultures and cell lines such a as the presence of other cell types and their interconnection.
Up to this point, we have addressed the different cargo and steps of phagocytosis as well as how we can quantify phagocytosis following direct and physiological approaches. But what is the outcome of phagocytosis? What are the functional consequences of the phagocytosis of apoptotic cells?

3.3.3.3 Functional outcome of phagocytosis

The rapid and efficient removal of apoptotic cells from the parenchyma is essential to maintain tissue homeostasis both in physiological and pathological conditions. The absent or delayed clearance of apoptotic cells leads to the loss the apoptotic cell membrane integrity and their development towards secondary necrotic cells (Nagata et al., 2010; Poon et al., 2014; Roth et al., 2021). The loss of the membrane integrity allows the spill over of the cytotoxic content that results from the cells death generating a generalized inflammatory response, tissue damage or even autoimmune diseases (Nagata et al., 2010; Poon et al., 2014). Thus, the inefficient phagocytosis of apoptotic cells eventually generates a harmful situation for the tissue (**Figure 7**).

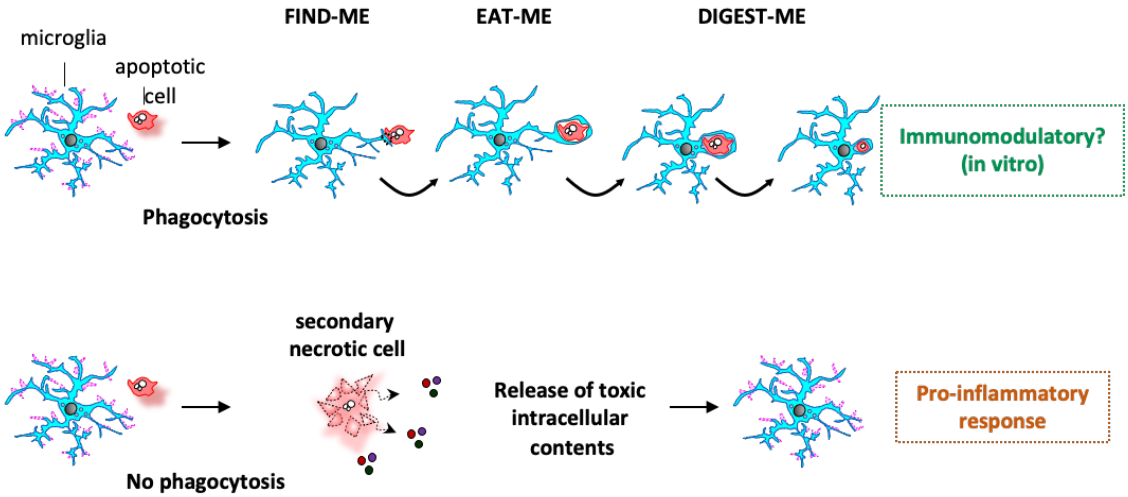

Figure 7. Functional consequences of apoptotic cell removal. *Microglial phagocytosis is not a silent process, but it is immunologically active. The removal of apoptotic cells has been proven to be immunomodulatory, at least in vitro; and it prevents the spill over of the cytotoxic content that results from the cell death, limiting the possible subsequent inflammation.*

However, phagocytosis is not just a process to get rid of the corpses but it is immunologically active (Gordon & Plüddemann, 2018). Several evidence demonstrated that the phagocytosis of apoptotic cells generated an anti-inflammatory response, at least in vitro (Stern et al., 1996; Voll et al., 1997), characterized by the release of TGF-β (Lucas et al., 2006). In addition, myelin debris removal generated an anti-inflammatory response in vitro (Liu et al., 2006). On the contrary, the removal of microbes and necrotic cells by macrophages through toll-like receptors (TLR) generates a pro-inflammatory response (Aderem, 2003; Erdman et al., 2009). Hence, phagocytosis can be considered as an immunomodulatory process depending on the engulfed substrate.

In cultured microglia, phagocytosis dampens the response to inflammatory stimuli such as LPS by reducing TNF-α and increasing TGF-β release (De Simone et al., 2003; Magnus et al., 2001); However, phagocytosis does not seem to provide a global anti-inflammatory effect, since in our hands , we only observed a reduction in LPS-induced TNF- α expression but no changes in other pro- and anti-inflammatory cytokines, such as IL6, IL1 or TGF-β expression in the (De Simone et al., 2003; Diaz-Aparicio et al., 2020). Overall, it has been demonstrated that the removal of apoptotic cells renders an anti-inflammatory outcome in vitro as well as the production of pro-inflammatory cytokines after pathogen removal. In primary microglia, the final outcome remains controversial as phagocytosis can modulate inflammation in a pro-inflammatory environment but does not suppress the production of pro-inflammatory cytokines. Thus, the influence of

microglial phagocytosis on the inflammatory response remains to be clarified and in vivo analysis should be performed to corroborate the in vitro data.

Until now, we have discussed the role of phagocytosis as not a mere process to get rid of the corpses but as an immunologically active process participating in inflammation and antigen presentation among others. In addition to phagocytosis, autophagy has been proposed to play an essential role in the maintenance of cellular homeostasis and thus, tissue homeostasis. In the next sections, we will revise the autophagy process and its similarities with phagocytosis, as they are both part of the endo-lysosomal pathway that converges in the lysosome.

3.4 AUTOPHAGY

Autophagy, from Ancient Greek *auto* "oneself" and *phagein* "to eat", can be literally translated as "self-eating". This self-eating process is present in all mammalian cells and tissues, including the CNS, and its main goal is the elimination of intracellular components, from long-lived proteins to damaged organelles, no longer useful for the cell; hence, it is essential to maintain cell fitness (Levine & Kroemer, 2019; Plaza-Zabala et al., 2017). Autophagy is a constitutive mechanism that serves as checkpoint for quality control in basal conditions, but it can also be induced under stressful situations, such as nutrient starvation or functional damage, to restore cellular homeostasis (Kaur & Debnath, 2015). The autophagy induction after a stressful stimulus provides the cell with nutrients and energy during metabolic shortage as well as it relives the burden of toxic components during functional damage (Mizushima, 2011).

Autophagy, as phagocytosis, is part of the endosomal pathway and converges in the lysosome for the degradation of the docked and engulfed cytoplasmic cargo (Mahapatra et al., 2021). The completion of autophagy in the lysosome is essential both to actively maintain basal autophagy and restore the cellular homeostasis after a stressful stimulus; thus, autophagy is not just a process to recycle deficient material but controls several processes in the cell (Boya et al., 2013). In the brain, it has been proposed to control neuronal survival and, indeed, neurons rely on basal autophagy to clear damaged organelles and cytotoxic substances as they cannot dilute their effect through cellular division (Hara et al., 2006; Komatsu et al., 2006). Recently, the role of autophagy has been extended to other cell types and, specifically, in microglia autophagy has been suggested to control metabolic fitness (Ulland et al., 2017), inflammation, phagocytosis of amyloid beta in rodent models of Alzheimer's disease (Heckmann et al., 2019), degradation of extracellular beta-amyloid fibrils (Cho et al., 2014) and synuclein (Choi et al., 2020), myelin phagocytosis in acute experimental encephalomyelitis (Berglund et al., 2020), as well as synaptic

pruning and social behaviour in mice (Kim et al., 2017). Thus, autophagy likely plays a major role in the control of the immune response in microglia, as does phagocytosis.

However, assessing autophagy is a complex task and several complementary methods are required to avoid misleading results (Klionsky et al., 2021). In the following sections, we will discuss the main types of autophagy according to the mechanisms used to deliver the cargo to the lysosomes. We will also detail the different steps of the autophagy cascade focusing on how to assess autophagy in microglia. Finally, we will establish the shared bases aspects between autophagy and phagocytosis that drove us to ask the main question of this PhD Thesis: what is the functional relationship between phagocytosis and autophagy?

3.4.1 Types of autophagy

The general term autophagy gathers three different types of autophagy: microautophagy, chaperone-mediated autophagy (CMA) and macroautophagy (commonly termed autophagy). These processes are classified according to the substrate selectivity and the mechanism used to deliver that cargo to the lysosome (**Figure 8**).

Microautophagy was at first considered a lysosomal process to enwrap cytoplasmic content for its degradation (De Duve & Wattiaux, 1966). Originally only lysosomes were thought to be involved in this type of microautophagy but recently, endosomes have been described to participate too (Oku & Sakai, 2018). Hence, microautophagy can be classified into three different types depending on the vesicular compartment that executes the membrane remodelling: type 1 or lysosomal protrusion; type 2 or lysosomal invagination; and type 3 endosomal invagination. Then, microautophagy captures soluble cytoplasmic content through lysosome- and endosome-dependent mechanisms (Li et al., 2012; Mijaljica et al., 2011; Oku & Sakai, 2018) (**Figure 8**).

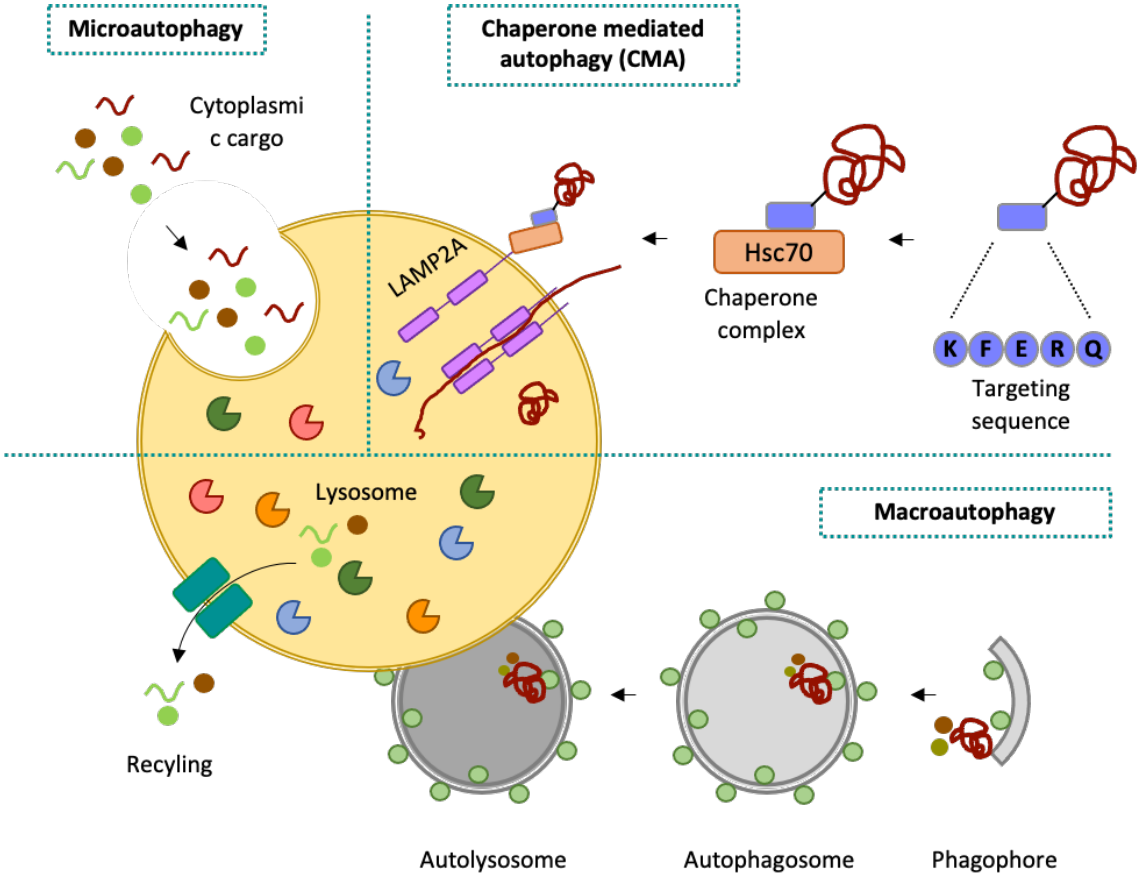

Figure 8. Types of autophagy in mammalian cells. *Autophagy is a conserved process essential to maintain the cell and tissue homeostasis. Macroautophagy (autophagy) is the most studied type of autophagy and requires the formation of and autophagosome that encloses the potentially degradative cargo that will be recycled in the lysosome. During microautophagy, full portions of the cytoplasm are internalized and degraded by the lysosome. Last, during the chaperone mediated autophagy, the HSP70 protein recognizes the targeting sequence in the autophagy substrates, that will be internalized through LAMP2 located in the lysosomal membrane.*

The chaperone mediated autophagy (CMA) is the most selective type of autophagy regarding their substrates, which are exclusively proteins. The proteins are tagged with the pentapeptide KFERQ-like motif (Lys-Phe-Glu-Arg-Gln amino acids) (Dice, 1982) recognized by the heat shock cognate 71 kDa protein (HSP70) cytosolic protein (Agarraberes et al., 1997) that delivers the protein cargo to the lysosome for its degradation. Proteins are then translocated one by one to the lysosomal lumen through the lysosomal membrane receptor lysosomal associated membrane protein 2A (LAMP2A), dimerized after the protein docking (Kaushik & Cuervo, 2018); and later degraded by intracellular proteases such as cathepsins (Drobny et al., 2022). Hence, CMA is a selective lysosomal degradative pathway for the degradation of tagged proteins. Both microautophagy and CMA mediate the cargo sequestration mainly in a lysosomal-dependent

manner; however, macroautophagy docks and encloses the selected cargo independently of the lysosome (**Figure 8**).

Macroautophagy, autophagy from here on, is the best characterized autophagy pathway to date (Parzych & Klionsky, 2014). Autophagy requires the formation of *de novo* structures, or autophagosomes, to enclose the cargo (Yamamoto & Noda, 2020) and deliver it to the lysosomes for their degradation (**Figure 8**). In the following sections, we will disclose the different steps of the autophagy cascade and the key molecules for each step.

3.4.2 The autophagy cascade

As we mentioned above, autophagy is constitutively active in basal conditions and can also be triggered in response to stressful stimuli, such as nutrient deprivation (Kaur & Debnath, 2015). The cell presents several extracellular and intracellular nutrient and damage sensors, whose signalling usually converges in the mechanistic target of rapamycin complex 1 (MTORC1), sensing amino acids and growth factors (Sarkar, 2013); and AMP-activated protein kinase (AMPK), sensing low glucose levels and ATP (Sanchez-Garrido & Shenoy, 2021) (**Figure 9**). The initiation of autophagy requires the formation of a pre-autophagosomal structure, named phagophore, which will subsequently elongate and dock the cytosolic cargo until their complete closure forming the autophagosome (Yu et al., 2018). The autophagosome will then mature by interacting with the endosomal compartment during its transport towards the nucleus (Hilverling et al., 2022), where lysosomes are located (Pu et al., 2016), and will eventually fuse with the lysosomes for the degradation of the intravesicular content. In this section, we will describe the autophagy cascade and the molecules implicated in each step of the process.

3.4.2.1 Autophagy stages

Initiation. The initiation of autophagy takes place after the verification of the nutrient and damage status of the cell. MTORC1, the central suppressor of autophagy, is constitutively active blocking the upregulation autophagy (Dossou & Basu, 2019) (**Figure 9**). During canonical autophagy, or MTORC1 dependent (Sarkar, 2013), the inhibition of MTORC1 by AMPK, allows the activation of the unc-51 like autophagy activating kinase 1 (ULK1), essential kinase to activate the pre-initiation complex composed by ULK1, autophagy related protein (Atg) Atg101 Atg13 and focal adhesion kinase family interacting protein of 200 kD (FIP200). Upon activation, ULK1 phosphorylates Atg13, which is stabilized by FIP200 and Atg101 (Zachari & Ganley, 2017),

and the whole ULK1 complex docks to the source membrane forming the pre-autophagosomal structure (PAS); yet the membrane source remains under debate (Wei et al., 2018).

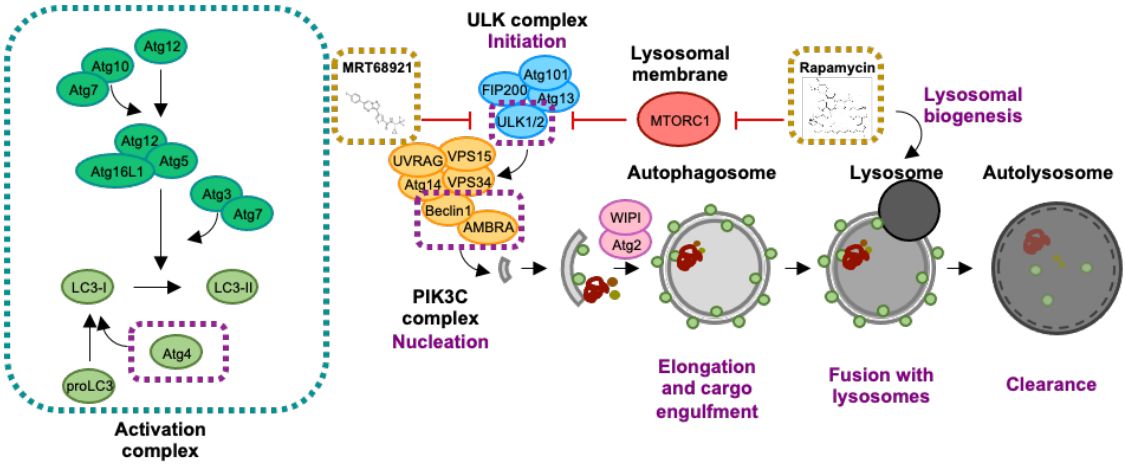

Figure 9. The autophagy cascade. *The autophagy cascade is a tightly regulated process at different steps of the pathway. The ULK complex regulates the initiation of autophagy whilst the PI3KC complex regulates the nucleation step required for the formation of the phagophore. In addition, the pre-processing and lipidation of LC3 is controlled by a set of Atg proteins that conform the activation complex.*

Nucleation. Next, the PI3K complex, formed by beclin-1 (BECN), vacuolar protein sorting 34 and 15 (VPS34, VPS15), Ambra1, and Atg14 and bind to the ULK1 complex at the PAS site and catalyses the formation of phosphatidyl-inositol-3-phosphate (PI3P) necessary for the structuration of the pre-autophagosomal membrane or phagophore (**Figure 9**). The PI3K complex is in addition regulated by the action of the antiapoptotic Bcl-2 family that sequesters BECN inhibiting autophagy and releases it upon stressful stimuli (Decuypere et al., 2012). In parallel to the PI3K complex activity, Atg9 positive vesicles bind to the Atg2-WIPI complex and interact with the PAS structure through FIP200 (Li et al., 2020) completing the nucleation step.

Elongation. Once the nucleation has occurred, the elongation step is highly regulated by the subsequent action of several Atg proteins (Noda & Inagaki, 2015; Suzuki et al., 2017); it is a critical step for the elongation of the membrane and for the substrate selectivity and recognition (Pang et al., 2019) (**Figure 9**). The elongation phase requires two different conjugation systems of Atg proteins: the Atg12 conjugation system and the Atg8/LC3 (microtubule-associated light chain protein 3) conjugation system, which rely on the Atg7 activity for their functionality (Li et al., 2020). They act as a ubiquitin-like conjugation system based on the subsequent action of three enzymes: activating, conjugating, and ligating (Dengjel & Dumit, 2012). In the Atg12 system, Atg12 is activated by the action of Atg7, conjugated to Atg5 by the action of Atg10 and

finally ligated to Atg16L1 (Li et al., 2020; Pang et al., 2019). The Atg8/LC3 system, from now on LC3 system, starts with the pre-processing of pre-proLC3 by Atg4. Later, Atg7 activates LC3 and with the action of Atg3, LC3 is conjugated to a molecule of phosphatidylethanolamine (PE). The active Atg12 system participates in the ligation of the lipidated LC3 to the membrane. The soluble or non-lipidated form of LC3 is known as LC3-I, whereas the membrane bound or lipidated form is termed LC3-II and are both used as the classical measurement of autophagy (we will discuss the main techniques to assess autophagy in **Section 1.4.3**). Finally, Atg4 can also deconjugate the PE molecule from LC3 and leave it bound to the autophagosome membrane (Yang et al., 2021). The closure of the autophagosome membrane is performed by the action of the Atg2-WIPI system, located at the terminal ends of the elongating autophagosome (**Figure 9**).

Degradation. Once formed, the autophagosomes are actively transported through the microtubules, while they mature by interacting with endosomes, and finally fuse with the lysosomes for their degradation (Eskelinen, 2005; Hyttinen et al., 2013). This process has been reviewed in several excellent articles (Lőrincz & Juhász, 2020; Nakamura & Yoshimori, 2017; Yim & Mizushima, 2020) In brief, autophagosomes are transported towards the cell nucleus, by dynein-dynactin motor complexes, where thy will meet the lysosomes. These transport proteins interact with motor adaptor proteins, among which PLEKHM1 is essential for the fusion of autophagosomes. Along this transport, autophagosome experience “kiss-and-run” events with early and late endosomes and acquire a specific molecular identity that will determine their fate. They incorporate small Rab-GTPases to their membranes, essential for their trafficking and fusion. Rab7 plays a key role as bridging molecules by interacting with LC3 and phosphoinositides (e.g., PI3P) in the membrane of the autophagosome and lysosome. These three molecules, Rab7, LC3 and phosphoinositides interact with tethering and adaptor proteins, such as HOPS, anchoring the autophagosome and the lysosome for further fusion. Real fusion cannot take place without the formation of the SNARE complexes: for example, STX17 interacts with VAMP7/VAMP8 and SNAP29, among other to promote the fusion of the autophagosome and lysosome, generating the autolysosome in which the enclosed cargo will be degraded.

3.4.2.2 Cargo recruitment

The selectivity of the autophagy response depends on the cellular context and on the initial stimulus. Hence, autophagy can be either non-selective or selective (Jin et al., 2013). If the initial stimulus is nutrient starvation, the cell will initiate a non-selective autophagy program and

directly engulf cytoplasmic portions to guarantee substrate and energy supply and ensure proper cell function and metabolic balance (Reggiori et al., 2012). On the other hand, selective autophagy is oriented to the degradation of specific cargo, such as misfolded proteins or long-lived organelles; thus, the recognition of the substrates is very specific. This selectivity is achieved by a set of autophagy receptors that specifically recognize and serve as a bridge between the selected cargo and the autophagosome (Khaminets et al., 2016). Aggregated proteins are docked by the NBR1 receptor; zymogenes or unprocessed proteins and lipid droplets are recognized by the sequestosome-1 (SQTSM1) or p62; organelles, including peroxisomes, lysosomes, endoplasmic reticulum (ER) and mitochondria, are recognised by NBR1/p62, p62, ATL3/C53 and AMBRA1/Bcl2C13/NIX, respectively, among others (Gubas & Dikic, 2022; Johansen & Lamark, 2020). These receptors present an Atg8-interacting motif (AIM)-like LC3 interaction motif that allows the interaction with the membrane-docked LC3 to the autophagosome membrane, therefore, the receptors recognize both the substrate and LC3 (Gatica et al., 2018). In addition to this function, it is important to mention that these receptors can also bind to proteins from the initiation and complex. For example, FIP200 that can subsequently activate ULK1 and the downstream machinery to select the cargo and promote phagophore growth (Gubas & Dikic, 2022).

The complexity of the multistep autophagy cascade and its protein regulation at different levels, make this pathway a difficult subject to assess. In the next section, we will describe the main techniques classically used to assess autophagy and their limitations.

3.4.3 Monitoring autophagy

Assessing autophagy is a complex task and current guidelines recommend the use of complementary techniques to avoid the acquisition of inconclusive data (Barth et al., 2010; Klionsky et al., 2021). The gold standard method to assess autophagy is the analysis of the autophagy flux using LC3 western blot (Kabeya et al., 2000; Karim et al., 2007; Klionsky et al., 2021; Tanida et al., 2008). In addition to the western blot, several techniques such as live imaging or transmission electron microscopy (TEM) have proven very useful to complete and clarify the, sometimes, misleading results from the western blot.

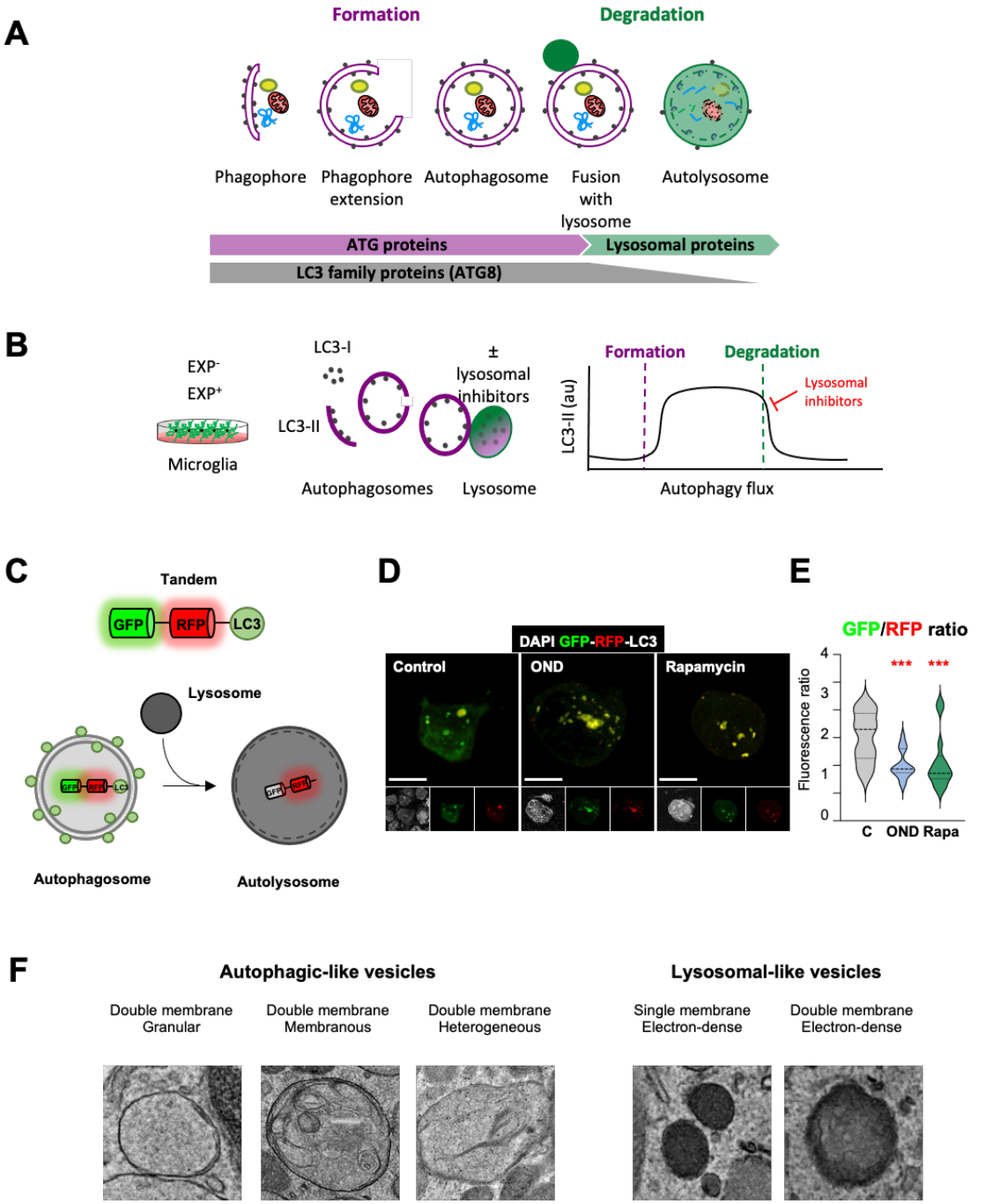

Figure 10. Estimation of the autophagy flux variations using LC3 turnover assay, tandem GFP-RFP-LC3 and TEM. ***[A]*** *Early stages of autophagy, which lead to the novo formation of autophagosomes, are mainly regulated by Atg proteins. The LC3 family of proteins (ATG8) participate in the formation of autophagosomes and progressively disappear after lysosomal fusion and cargo degradation in autolysosomes. Late stages of autophagy depend on the functionality of lysosomal proteins and enzymes.* ***[B]*** *Total protein homogenates obtained from microglia under control (EXP-) and experimental conditions (EXP+) are analyzed by western blot to evaluate LC3 levels in the presence and absence of lysosomal inhibitors. When autophagy is activated, LC3-I (soluble form) is lipidated to the phophatidylethanolamine of the nascent phagophore forming LC3-II (membrane-bound form). LC3-II accumulates along the*

extension of the autophagic vacuoles as it closes and it is used as an estimate of the number of autophagosomes. Upon fusion with lysosomes, LC3-II levels decrease due to the degradation of the inner autophagosomal membrane simultaneously with the luminal cargo. In the presence of lysosomal inhibitors, no degradation occurs, and LC3-II levels are maintained. The subtraction of LC3-II quantities in the presence and absence of lysosomal inhibitors provides an estimate of the autophagosomes that have been degraded during the experimental period of time. ***[C]*** *The GFP-RFP-LC3 tandem binds to the autophagosome membrane, with emission from both GFP and RFP. After the fusion with the lysosome, the GFP fluorescence is quenched, and the ration between GFP and RFP is used as a measurement of ongoing autophagy.* ***[D]*** *Representative images of BV2 cells transfected with the plasmid encoding the GFP-RFP-LC3 tandem; GFP (green), RFP (red), DAPI (white), in control, OND and rapamycin treated cells.* ***[E]*** *GFP/RFP mean fluorescence intensity ratio, indicative of autophagy flux.* ***[F]*** *Representative TEM images from autophagy-like structures (left panels) and lysosomal-like vesicles (right panels). Data was analyzed by one-way ANOVA followed by Bonferroni post hoc test. Scale bars=10µm, z=1.9µm (control), 3.3µm (OND), and 3.9µm (Rapamycin)* ***[A]****; 2µm (control), 5µm (OND), 500nm (high magnification). Data from Mikel García-Zaballa Master Thesis (2021).*

3.4.3.1 LC3 western blot

As mentioned above, autophagy is complex process composed by several steps: formation, maturation, fusion with the lysosome and degradation of the vesicular content. Classically, this process has been measured indirectly by determining the amount of LC3 bound to the autophagosome membrane (Kabeya et al., 2000; Karim et al., 2007) (**Figure 10A**). During autophagy, the soluble form of LC3 or LC3-I is recruited to the phagophore membrane, where it is transformed into the membrane-bound LC3-II, which will later mature and be delivered to the lysosomal compartment for its degradation (Kabeya et al., 2000; Karim et al., 2007). Taking the LC3 protein as a reference, the amount of ongoing autophagy, or autophagy flux, is calculated as the differential amount of LC3-II in the presence and absence of lysosomal inhibitors such as bafilomycin A1 or chloroquine, among others (An et al., 2017; Yamamoto et al., 1998; Yang et al., 2013) (**Figure 10B**). Lysosomal inhibitors are used to block LC3-II degradation in the lysosomal compartment to monitor its accumulation over a specific period of time, both in control and after a certain treatment. Therefore, the autophagy flux is only a measurement of the amount of autophagosomes that would have been degraded along that period of time and does not reflect the autophagosomes formation (Rubinsztein et al., 2009).

The formation and degradation of autophagosomes are tightly but independently regulated: the initial steps are mostly regulated by Atg proteins (Mercer et al., 2018; Plaza-Zabala et al., 2017), whereas the degradation steps are mainly regulated by fusion and degradation proteins located

in the lysosome (Lőrincz & Juhász, 2020). Hence, to overcome the limitation of only assessing the degradation step using the LC3 western blot, we proposed a two-step model to assess the formation step in addition to degradation. This model will be presented in the **Results section 5.5**.

LC3 western blot is then an indirect measurement of the amount of the autophagosomes that would have been degraded at a given time point and not a dynamic assessment of the process. To overcome this limitation, a direct visualization of the autophagosomes could give extra information about the autophagy flux.

3.4.3.2 Tandem GFP-RFP-LC3

The tandem GFP-RFP-LC3 is a fluorescent assay to monitor the autophagy flux by directly visualizing the developing vesicular structures during autophagy (Kimura et al., 2007; Klionsky et al., 2021; Lopez et al., 2018) (**Figure 10C**). The tandem GFP-RFP-LC3 can be used both in vitro (Kimura et al., 2007) and in vivo (Lopez et al., 2018) to assess formation, fusion and degradation events. After transfecting the plasmid, the tandem reporter is expressed and located in the nascent membrane of the phagophore. The GFP signal is pH sensitive and thus will be quenched when entering acidic compartments such as late endosomes or lysosomes. In contrast, the RFP protein is more resistant to acid pH and will maintain its fluorescence. According to the fluorescence intensity and colocalization of each fluorophore, the different stages of the autophagy cascade can be identified: colocalization of RFP and GFP indicate the presence of the tandem in the phagophore or closed autophagosome with a more basic pH that does not quench the GFP fluoresce; the RFP alone indicates that the autophagosome has already fused with the lysosome, generating the autolysosome and quenching the GFP fluorescence; and the sole expression of GFP can be due to its faster expression in the phagophore than RFP. Using this plasmid, we have recently shown how the basal levels of autophagy in microglia increased after the treatment with OND to comparable levels of autophagy obtained after the addition of rapamycin (**Figure 10D**, **E**). The GFP/RFP ratio inversely correlates with the amount of fusing and acidifying autophagosomes with lysosomes, suggestive of ongoing autophagy (Mikel García-Zaballa Master Thesis 2021) (**Figure 10E**).

This method serves as a useful tool to directly visualize and quantify the autophagy structures (e.g., phagophores, autophagosomes and autolysosomes) at a given timepoint. However, this method cannot be used to directly visualise the degradation of the cargo, as it only allows to

visualize fusion events between the different vesicular types and the disappearance of the fluorescence marker due to acidification, but not the full degradation of the cargo and its recycling. The interpretation of the tandem GFP-RFP-LC3 results have both strengths and limitations. As mentioned above, it is a very useful tool to directly visualize the autophagy process, but it could also lead to misleading conclusions. One example is the deficient GFP quenching after the fusion of the autophagosome and the lysosome, which would indicate a blockade of the autophagy flux and not the induction or ongoing autophagy, as it could be concluded from the maintained GFP expression. In spite of the accuracy of the tandem visualization, electron microscopy remains the original and most reliable method to directly assess autophagy (Klionsky et al., 2021).

3.4.3.3 Transmission electron microscopy (TEM)

Autophagy was first described as lysosomal degradation events of cytoplasmic content using TEM in 1950 (Eskelinen et al., 2011) and, to date, it is considered the most reliable method to directly visualize autophagy. Using TEM, the different autophagic vesicles can be visualised in the cellular environment, considering the subcellular localisation in the nanometer scale and the quantification of the autophagy vesicles. The accuracy of this technique depends on the correct identification of the different species (Lucocq & Hacker, 2013). Starting from the beginning of the cascade, the phagophore and autophagosome can be identified by the double membrane surrounding the docked cargo, separated by a translucent cleft that can sometimes be lost depending on the fixation procedure (Jung et al., 2019) (**Figure 10F**). The latter stages, autolysosomes and lysosomes, are characterised by their electrondensity and are usually considered as a single degradative compartment (Hurbain et al., 2017) (**Figure 10F**). To distinguish the degradative compartment, the use of complementary staining, like immune-electron microscopy of degradative enzymes (hydrolases and proteases e.g., cathepsins) have been proposed to be very useful (Yang et al., 2009; Yokota et al., 1989).

The quantification of autophagy by TEM can be very reliable but certain aspects should be taken into consideration. Quantifying the number of autophagy vesicles in a specific section, of either a cell or tissue fraction, might render misleading results as the cell areas are not homogenous as well as the vesicles. Thus, it is more accurate to refer the number of vacuoles to the area and later correlate it to the cell volume (Kovács et al., 1989). TEM, remains the most reliable method to visualise autophagy despite being time-consuming and in requirement of expertise in the visualization and analysis.

3.4.4 Autophagy modulators used in this PhD thesis

To assess autophagy and its relationship with phagocytosis, we have used several models: first, we analysed microglial phagocytosis in vivo in three different knock-out (KO) models: ATG4B KO, TMEM119-Beclin KO and AMBRA $^{-/+}$; and second, we pharmacologically modulated autophagy using the MRT68921 inhibitor and the autophagy inductor rapamycin.

3.4.4.1 In vivo autophagy KO models

ATG4B KO mice. Atg4b or autophagin-1, is one of the four homologs of the Atg4 human cysteine proteases (Mariño et al., 2003). Its main role is to pre-process the LC3 pro-form, enabling its conjugation to the phagophore (**Figure 9**), thus, its absence leads to incomplete LC3 conjugation to the membrane a deficient autophagosome formation (Fujita et al., 2008). Mice lacking Atg4b, present a partial impairment of the autophagy process, enough to trigger the accumulation of spheroid-like bodies in several brain nuclei, such as the vestibular nuclei (Read et al., 2011). ATG4B KO mice develop normally; however, they develop balance problems with aging, likely associated with alterations in the vestibular system (Marino et al., 2010). In this PhD thesis, we studied microglial phagocytosis in ATG4B KO mice taking into account that it is not a microglia specific KO model, and that the autophagy inhibition is only partial, as it is compensated by its Atg4 homologs. Dr. Guillermo Mariño, from the Universidad de Oviedo, kindly provided us with tissue from ATG4B KO mice and their wild type (wt) littermates.

TMEM119-Beclin KO mice. Beclin-1 is a core protein from the PI3K complex (**Figure 9**), essential for the initiation of autophagy (Levine & Kroemer, 2019). The TMEM119-Beclin KO mice is a microglia specific KO, as the Beclin-1 deletion is under the expression of the microglial TMEM119 promoter (Bennett et al., 2016; Satoh et al., 2016). The phenotype of this specific transgenic mouse model is currently under study, but it has been described that the full deletion of Beclin-1 is embryonically lethal, confirming the essential role of this protein for the autophagy process (Yue et al., 2003). These mice were kindly provided by Dr. Dorothy Schafer, from the University of Massachusetts Medical School.

AMBRA $^{-/+}$ mice. AMBRA1 is the regulating protein of the Beclin-1 complex (**Figure 9**). It is a key protein in the regulation of autophagy and has been determined to be essential in the embryonaric and CNS development (Fimia et al., 2007). Full AMBRA KO are not born, hence, the heterozygous model is used to study the role of autophagy and its implications. AMBRA $^{-/+}$ do

not present evident phenotypical alterations but they have been described to develop an autistic-like behavior, exclusively in female mice (Dere et al., 2014). Dr. Patricia Boya, from the Centro de Investigaciones Biomedicas (CIB), kindly provided brain tissue from AMBRA $^{-/+}$ mice.

3.4.4.2 Pharmacological modulation of autophagy

MRT68921 inhibitor. MRT68921, from now on MRT, is a selective ULK1 inhibitor (**Figure 9**) that has proven to successfully inhibit the autophagy pathway at the pre-initiation step, in vitro (Petherick et al., 2015). The inhibition of the cascade at the initiation level can lead to the accumulation of truncated autophagosomes expressing LC3-II (Zachari & Ganley, 2017; Zachari et al., 2020). This situation can be confused with ongoing autophagy, using indirect methods such as western blot, as the amount of LC3-II is associated with functional autophagy. However, it can also be due to the blocked of autophagy related to the deficient formation of the autophagosomes and their fusion with lysosomes. The main advantage of this compound relies on the specific inhibition of the autophagy pathway without altering phagocytosis.

Rapamycin. Rapamycin (sirolimus) was discovered in the Easter Island, after the isolation of the microorganisms that grew in its soil ("A long and winding sTORy," 2017). Initially, rapamycin, was used as a potent antifungal but it was later described to have antiproliferative effects and was widely used as an antitumoral agent (Li et al., 2014), as well as an immunosuppressant in certain transplantations (Baroja-Mazo et al., 2016; Wang et al., 2009). Mechanistically, rapamycin blocks the MTORC1 activity enhancing the autophagy pathway and enhances lysosomal biogenesis by promoting the translocation of the transcription factor EB (TFEB) to the nucleus (Martina et al., 2012) (**Figure 9**). We selected rapamycin as it has been described to have beneficial effects in stoke by preventing neuronal death (Hadley et al., 2019; Li & Huang, 2020b; Wu et al., 2018) and since our main goal is to study the functional relationship between autophagy and phagocytosis, rapamycin was the best candidate to promote autophagy in the context of stroke.

Until now, we have described the different types of autophagy, highlighted the main steps of the autophagy cascade, their regulation, and the main methods to assess it. In the previous section, we had discussed the phagocytosis process, the phagocytic cargo and the signals involved in the process, and the different techniques to assess phagocytosis; but what is the relationship between autophagy and phagocytosis in microglia?

3.5 AUTOPHAGY IN MICROGLIA: inflammation and phagocytosis

Whilst autophagy in the CNS has mostly been studied in neurons, increasing evidence demonstrates that it also has key roles in peripheral macrophages, such as fine regulation of inflammation (Netea-Maier et al., 2016), or the regulation of phagocytosis promoting engulfment and cargo degradation (Green et al., 2016). In microglia, the role of autophagy has also been proposed as a key pathway to regulate inflammation through modulation of the inflammasome (P. Su et al., 2016; Zhao et al., 2021) and phagocytosis, through LC3-associated phagocytosis (LAP) and/or modulating the efficiency of phagocytosis (Fazeli & Wehman, 2017; Lima et al., 2011; Martinez et al., 2011). In the next section we will discuss the role of autophagy in different microglial functions: inflammation, LAP, and phagocytosis.

3.5.1 Inflammation

Inflammasomes are cytosolic multimeric complexes that are assembled in response to the activation of pathogen-associated (PAMPs) or danger-associated (DAMPs) molecular patterns (Malik & Kanneganti, 2017). They usually comprise a sensor that serves to categorize the inflammasome type, e.g., NRLP3 or NRLP1 (Malik & Kanneganti, 2017), an adaptor known as Apoptosis-associated Speck-like protein containing CARD (ASC), which bridges the inflammasome sensor to caspase-. Upon activation, the proforma or zymogen of caspase-1 (pro-caspase-1), is activated, leading to the maturation of pro- inflammatory cytokines such as interleukin-1β (IL-1β) and interleukin-18 (IL-18) (Broz & Dixit, 2016; Guo et al., 2015; Malik & Kanneganti, 2017), as well as gasdermine D , that leads to cell death through pyroptosis (Burdette et al., 2021).

In microglia, autophagy has specifically been related to the NRLP3 inflammasome. In AD patient´s brains, there is a conserved activation of the NRLP3 inflammasome and IL-1β release by microglia (Heneka et al., 2013). Moreover, the silencing of LC3 and Atg-7 in primary murine microglia treated with Aβ increased the expression of several components of the NRLP3 inflammasome and exacerbated the inflammatory response (Cho et al., 2014), proving the regulatory role of autophagy the microglial inflammatory response in AD. In addition, in mice with heterozygous deletion of Beclin1 ($Becn^{+/-}$), isolated microglia treated with LPS/ATP increased the NRLP3 expression compared to wt mice (Houtman et al., 2019). Similarly, the silencing of Atg-5 in BV2 cells and its suppression in vivo, also rendered an increased expression of NRLP3 in a PD mouse model (Qin et al., 2021). Therefore, autophagy seems to limit the microglial inflammatory response in pathological situations.

Suggestive evidence demonstrated that there is a crosstalk between autophagy and phagocytosis during the innate immune response in the peripheral macrophages and in microglia (Berglund et al., 2020; Bonilla et al., 2013; Lee et al., 2019; Runwal et al., 2019). However, the exact crosstalk between autophagy and phagocytosis still remains unclear.

In the next sections, we will discuss the relationship between autophagy and phagocytosis in the LC3-associated phagocytosis (LAP) process, in the modulation of the phagocytic efficiency and in the inflammatory outcome.

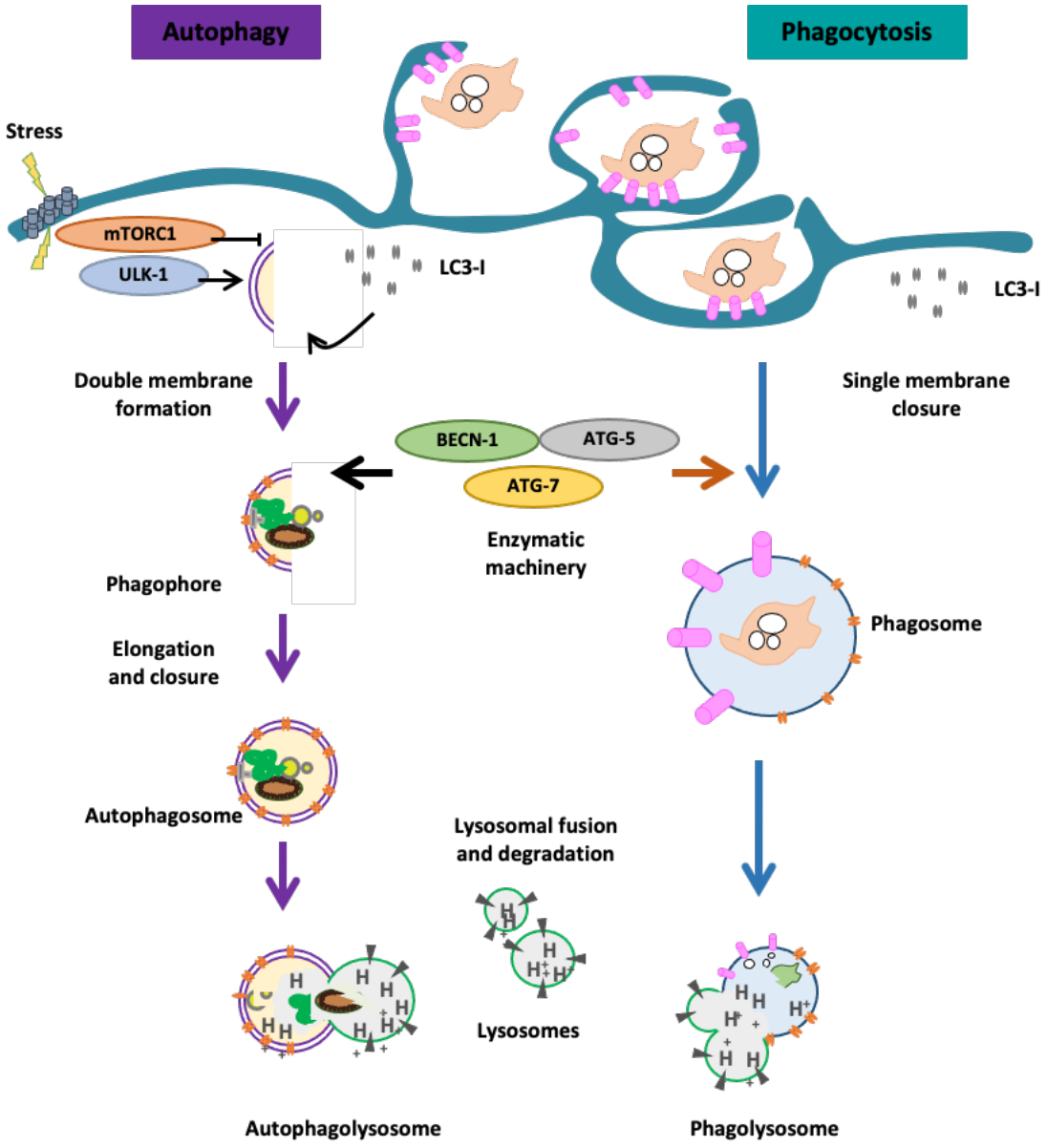

Figure 11 Autophagy and phagocytosis lysosomal clearance pathways and share many similarities at the intracellular level. *Autophagy and phagocytosis are lysosomal clearance pathways that share mechanistic and functional similarities. In response to cellular stress, autophagy (purple flow) is activated*

by signals that inhibit mechanistic target of rapamycin complex 1 (MTORC1) and activate unc-51 like autophagy activating kinase 1 (ULK-1), whereas phagocytosis (blue flow) is activated by extracellular ligands that bind to phagocytosis receptors in the surface of the microglial plasma membrane. Then, cargo engulfment structures start to form: the phagophore is de novo formed using different cellular sources, such as the endoplasmic reticulum (ER) (autophagy) and the phagocytic cup is formed from invaginations of the plasma membrane (phagocytosis). These structures elongate and close up, forming the double-membrane-bound autophagosome (autophagy) and the single-membrane-containing phagosome (phagocytosis), which contain intracellular and extracellular degradative substrates, respectively. The formation of the autophagosome depends on the sequential and coordinated action of autophagy-related (ATGs) proteins, including microtubule-associated light chain 3 (LC3). In contrast, the formation of the phagosome may depend on the recruitment of autophagy machinery (ATGs and LC3) during LC3-associated phagocytosis (LAP) (orange arrow) or may be completed independently of ATGs in other types of phagocytosis. Finally, the autophagosome (autophagy) and the phagosome (phagocytosis), progressively mature and fuse with lysosomes, forming the autophagolysosome and the phagolysosome, respectively. Figure modified from Plaza-Zabala et al., 2017.

3.5.2 LC3-associated phagocytosis (LAP)

LAP is the most representative example of interaction between autophagy and phagocytosis, as a form of phagocytosis assisted by the autophagy machinery (**Figure 11**). During LAP, part of the autophagy machinery is translocated to the phagosome to promote the internalisation and degradation of the phagocytic cargo (Fazeli & Wehman, 2017). In macrophages, LAP regulates antigen presentation (Münz, 2016; Romao et al., 2013) and their inflammatory profile (Martinez et al., 2011; Martinez et al., 2016; Mehta et al., 2014), events that have also been proposed to occur in microglia (Berglund et al., 2020). Upon Toll-like receptor (TLR) or T cell immunoglobulin mucin protein 4 (TIM4)-stimulated phagocytosis of bacteria (Sanjuan et al., 2007) or apoptotic cells (Martinez et al., 2011) by macrophages, LC3 binds to the phagosome membrane in a Becn1/Rubicon, Atg-5 and Atg-7 (Martinez et al., 2011; Sanjuan et al., 2007) dependent manner but independent of ULK-1 (Martinez et al., 2011). Thus, LC3 conjugates to the single membrane phagosome without inducing an autophagy response (Sanjuan et al., 2007). Deficient LAP has been related to the development of systemic lupus erythematosus (SLE), where the deficient clearance of dead cells leads to a peripheral autoimmune disease (Martinez et al., 2016).

The recruitment of autophagy machinery to the phagosome promotes an effective degradation and clearance of the phagocytosed cargo; however, the necessary recruitment of LC3 to complete phagocytosis is not clear. For instance, Atg-5 and Atg-7 KO mice do not exhibit a delay in the maturation of opsonized particle- or zymosan-containing phagosomes to phagolysosomes

(Cemma et al., 2016), suggesting that LC3 might not be required for every type of phagocytosis. On the contrary, the inhibition of autophagy using 3-methlyadenine (3-MA) had detrimental effects both on the survival and phagocytic function of macrophages in vitro (Zhou et al., 2016), suggesting not only an essential role of autophagy regulating phagocytosis but also ensuring cell survival. However, 3-MA has been proposed to directly inhibit LAP (Martinez et al., 2016), thus, future research on the interaction between autophagy and phagocytosis needs to be performed. In this PhD project, we tested the effects the selective autophagy inhibitor MRT68921 on autophagy and its repercussions on microglial survival and phagocytosis.

In brief, the convergence of autophagy and phagocytosis has been proved in macrophages, where both pathways intersect to promote the phagocytic cargo degradation and its dysregulation renders detrimental effects both for macrophage survival and function. Scarce evidence is available determining the role of LAP in microglia (Choi et al., 2020; Heckmann et al., 2019; Xu et al., 2021). Recent evidence hits towards an essential role of LAP clearing β-Amyloid, as BV2 cells lacking Atg5 or Rubicon displayed a reduced recruitment of LC3 to the endosomal vesicle containing Aβ and reduced degradation (Heckmann et al., 2019). In addition, Atg7 and Atg4 KO primary microglia failed to degrade internalized α-synuclein as well as p62 KO microglia did not engulf neither degrade α-synuclein (Choi et al., 2020) and additionally Atg7 KO microglia are not capable of degrading lipid droplets and fail to maintaining lipid homeostasis (Xu et al., 2021). Thus, LAP in microglia is emerging as key process to promote the degradation and internalization of specific substrates, yet this process should be further studied in the forthcoming years.

3.5.3 Autophagy modulation of phagocytosis efficiency

In addition to the translocation of the autophagy machinery to promote phagocytosis during LAP, the functional outcome of autophagy could also regulate phagocytosis (**Figure 11**). The activation of autophagy has been suggested to both reduce (Lima et al., 2011) and promote phagocytosis in macrophages (Martinet et al., 2009). The first study showed that both nutrient starvation or rapamycin reduced the uptake of yeast by cultured macrophages, presumably by inducing autophagy, although this was not directly tested (Lima et al., 2011). In the second study the data showed opposite results, as autophagy induction by nutrient starvation increased the uptake of bacteria by macrophages (Martinet et al., 2009). However, this study analysed phagocytosis in macrophages deficient in Atg7, which also participates in LAP (Martinet et al., 2009) and therefore, the role of autophagy on microglial phagocytosis deserves further

exploration. The available evidence shows opposite results concerning the modulation of phagocytosis through the autophagy pathway; hence, more evidence needs to be gathered to clarify the role of autophagy on phagocytosis. In addition, since autophagy is involved in the recycling of cellular components, it could also regulate the presence of phagocytosis receptors (Levine & Kroemer, 2019). For example, Atg-7 deficient macrophages presented enhanced scavenger receptor expression and also, increased phagocytic uptake of bacteria; yet this study did not discard the participation of LAP during the uptake, and the results remain inconclusive (Bonilla et al., 2013). None of these studies were performed in microglia, and thus the impact of autophagy induction in microglial phagocytosis remains to be tested. In this PhD project, we tested the effect of the well-known autophagy inductor, rapamycin, on the microglial function both in basal and pathological conditions, as well as the modulation of phagocytosis through autophagy.

3.6 THE LYSOSOME: WHERE AUTOPHAGY AND PHAGOCYTOSIS MEET

3.6.1 Introduction to the lysosome

Lysosomes are intracellular organelles devoted to the digestion and recycling of enclosed material. As mentioned above, lysosomes were considered as “suicide bags” with no other function than digestion but, currently, their role has been found to be much more complex as they are key regulating organelles of cellular function (Yang & Wang, 2021). Lysosomes are signalling hubs essential for energy and amino acid sensing, calcium signalling transduction, and autophagy regulation (Ballabio & Bonifacino, 2020; Perera & Zoncu, 2016). Among others, they are present in all animal cells, except for mature erythrocytes, and range from 50 to 1000 lysosomes per cell. They are mainly located in the perinuclear area (Jongsma et al., 2016) but can be relocated to other cytoplasmic regions under the cell´s demand (Cabukusta & Neefjes, 2018); and also be delocalized in pathological conditions such as HD (Caviston et al., 2011; Erie et al., 2015). They render 5% of the total cytoplasmic volume and are heterogenous in size and morphology, as well as variable in their electron density and intravesicular content. Lysosomes can break a wide variety of macromolecules: proteins, nucleic acids, fatty acids and carbohydrates, due to the presence of almost 50 acid hydrolases which are active at acid pH (~5). The different types of lysosomal hydrolases and the acidification mechanism of the lysosomal lumen will be discussed in the next section as part of its biogenesis process and identity acquisition (Ballabio & Bonifacino, 2020).

3.6.2 Lysosomal biogenesis

Lysosomal biogenesis requires the coordination of the endosomal and the secretory pathway in the trans Golgi network (Yang & Wang, 2021) (**Figure 12**). Lysosomes emerge from mature endosomes that acquire the characteristic lysosomal hydrolases in "kiss and run" events and complete fusion with pre-existing lysosomes. The hybrid species or endolysosomes will transform into the classical electrodense lysosomes after the re-formation of their structure (Luzio et al., 2014). The re-formation process consists of the removal of endosomal proteins, such as the SNARE proteins in charge of the vesicular fusion, and their recycling to early endosomes. Vesicular ATPases are also incorporated into the membrane of the emerging lysosome to maintain the acidic environment inside the vesicle and generate the core-dense structures (Hirota et al., 2004) (**Figure 12**). This process takes place in tubular structures that emerge from the endolysosome and will give rise to the classical electrondense lysosome. Pure lysosomes are likely to be involved in the secretory pathway, involved in the extrusion of recycled molecules to the extracellular space, and are storage vesicles of functional hydrolases that will be delivered to the degradation site after their fusion with mature endosomes, where the majority of the degradation presumably takes place (Ballabio & Bonifacino, 2020; Luzio et al., 2014). In addition to endosomes, lysosomes can also emerge from the autophagy pathway, after the fusion of autophagosomes and lysosomes, following the same process as endolysosomes. A tubular structure will emerge from the autolysosome forming proto-lysosomal structures, regulated by the activity of MTORC1 that will eventually generate new lysosomes (**Figure 12**).

The acquisition of the lysosomal identity relies on the incorporation of lysosomal proteins to both the lumen and lysosomal membrane. Lysosomal proteins are targeted by a mannose-6-phosphate (M6P) sugar that serve as a location-specific sequence to deliver the protein to the lysosome. M6P is recognized by mannose-phosphate receptors (MRP) in early endosomes that will release the protein along with the acidification of the endosome conforming the lysosome. The MRP will be recycled to early endosomes after the excision of the lysosome (Luzio et al., 2014). There is also an indirect rout to deliver proteins to the lysosome that involves the plasma membrane. M6P proteins are delivered to the plasma membrane and are re-internalized in clathrin-coated vesicles that will fuse with maturing endosomes, releasing the proteins, and recycling the clathrin structures to the plasma membrane.

The main characteristic of lysosomes is their acidic nature and the degradation of macromolecules. In the next section we will revise the main lysosomal proteins and the mechanisms by which the lysosome maintains acid its luminal pH.

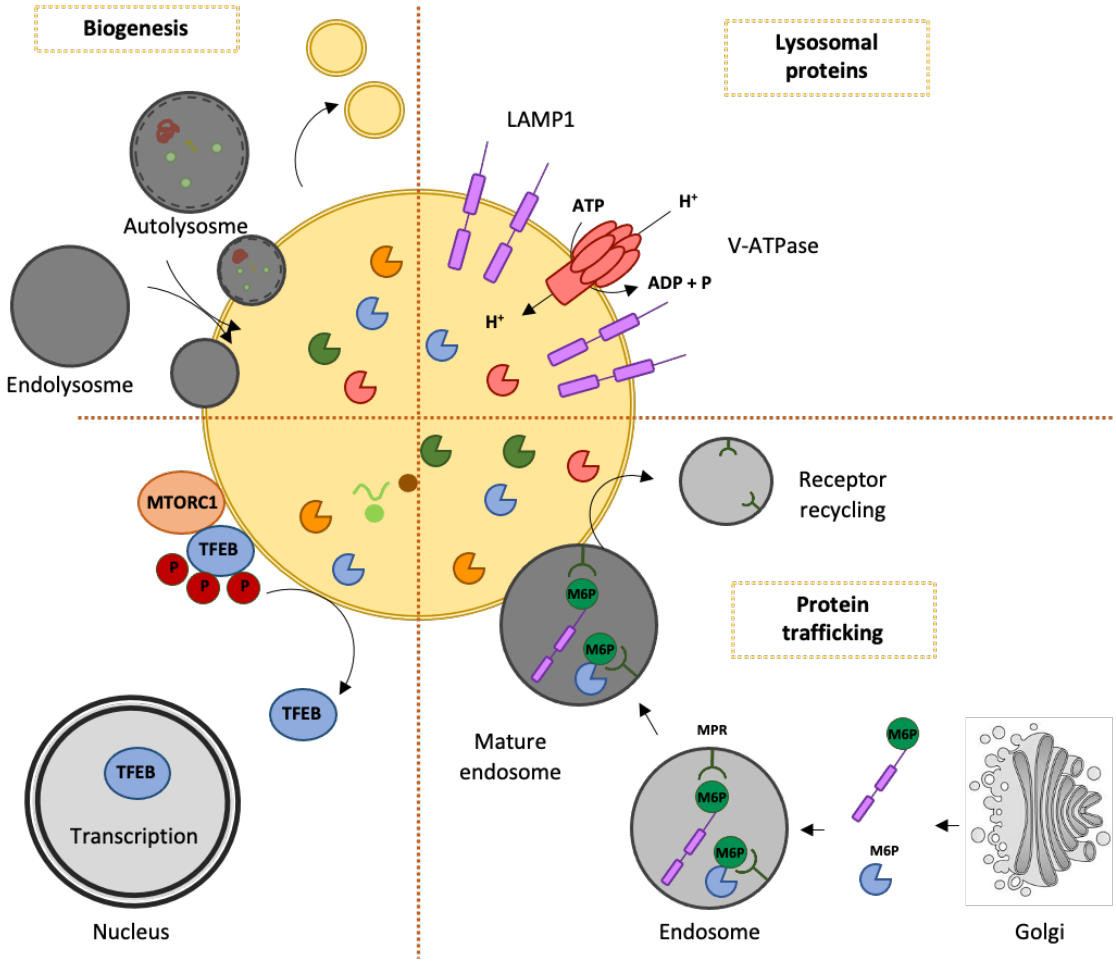

Figure 12. Lysosomal biogenesis. *Schematic design of the lysosomal biogenesis process from endolysosomes and autolysosomes and their re-formation after the fusion with pre-existing lysosomes. LAMP2 is the most abundant membrane associated protein in lysosomes, actively participating in CMA, as well as the v-ATPase, essential for the maintenance of the intraluminal acidic pH. The de novo synthesized lysosomal proteins in the Golgi network, are tagged with mannose-6-phosphate (M6P), which are recognized by mannose-6-phosphate receptors (MPR) in endosomes, in which they will be delivered to the lysosome. The lysosomal biogenesis and protein expression are regulated by the translocation of the transcription factor EB (TFEB), highly phosphorylated and docked in the lysosomal membrane, in close proximity to MTORC1.*

3.6.3 Lysosomal proteins and proton pumps

Lysosomes present more than 100 proteins in their membrane to ensure its integrity and maintain the acidic environment. Lysosomal proteins are classified into lysosome-associated

membrane proteins (LAMPs) (**Figure 12**), lysosomal membrane glycoproteins (LGPs) and lysosomal integral membrane proteins (LIMPS) (Eskelinen et al., 2003). LAMPs and LIMPs comprise up to 50% of the total lysosomal membrane proteins, among which, LAMP1 and LAMP2 are the most abundant. LAMP2 has been proposed to be a selective receptor for cytosolic proteins expressing the KFERQ motif, essential for the recognition of the cargo in the chaperone-mediated autophagy process (revised in **Section 1.4.1**). In addition, their highly glycosylated intraluminal tails, form a protective glycocalyx that serves as a barrier to avoid the leakage of the lysosomal protons and acid hydrolases that have detrimental consequences if released to the cytosol (Holland et al., 2020). On the other hand, LIMPs participate fusion events with the plasma membrane to secrete the lysosomal content (LIMP1) and promote lysosomal biogenesis by interacting with the fusion/fission machinery (Eskelinen et al., 2003). LGPs, present overlapping functions with LAMPs, mainly in the maintenance of the glycocalyx structure and integrity.

Within the secure lysosomal membrane, the acid hydrolases degrade macromolecules for their recycling and energy obtention. Some examples of the degradative enzymes are glycosidases, proteases, lipases, nucleases, phosphatases, and sulfatases, that exert their action at acidic pH. The V-type H^+ ATPase, present as well in the plasma membrane, maintains this already acidic environment in lysosomal lumen (Mindell, 2012) (**Figure 12**). It uses the energy released from the ATP hydrolysis to pump protons into the lumen against their electrochemical gradient, accompanied by the movement of counterions, like Ca^{2+}, K^+ and Cl^-, to avoid the inhibition of the proton pump. The structure and mechanism of the V-type H^+ ATPase has been excellently reviewed elsewhere (Mindell, 2012). The V-type H^+ ATPase activity is controlled by glycolysis, promoting the subunit assembly and function. It can also be regulated by cytoplasmic acidification, to remove the excess of protons from the basic cytosol (Ballabio & Bonifacino, 2020; Holland et al., 2020). The degradative activity of the acid hydrolases is not only regulated by the intraluminal pH but also by enzymes such as cystatin B, CSTB (Nakanishi, 2020). CSTB regulates and limits the activity of cysteine proteases (CTSs) avoiding an excessive proteolysis within the lysosome (Joensuu et al., 2007; Lalioti et al., 1997; Lehtinen et al., 2009). The role of CSTB will be discussed din depth in **Section 5.8.3** in a disease context. Hence, the lysosome is not just a degradative organelle but participates in many regulatory functions. Next, we will discuss the main mechanisms of lysosomal regulation and the feedback loop to autophagy.

3.6.4 Lysosomal regulation and feedback loop to autophagy

Lysosomes are not static organelles but respond to several environmental insults, like starvation, cell growth or the accumulation of storage products. This lysosomal adaptation is mediated by a gene network termed "the coordinated lysosomal expression and regulation", or CLEAR, controlled by its master regulator TFEB (Sardiello & Ballabio, 2009). TFEB positively regulates the expression of lysosomal genes, promotes the lysosomal degradative capacity and numbers (Settembre et al., 2011). Under basal conditions, TFEB is highly phosphorylated and bound to the cytoplasmic face of the lysosomal membrane, whilst its dephosphorylated form is located in the nucleus. Upon stimulation, like starvation, or in certain diseases, TFEB translocates to the nucleus where it promotes the synthesis of acid hydrolases and other lysosomal proteins to enhance the lysosomal function (Luzio et al., 2014; Settembre et al., 2013) (**Figure 13**).

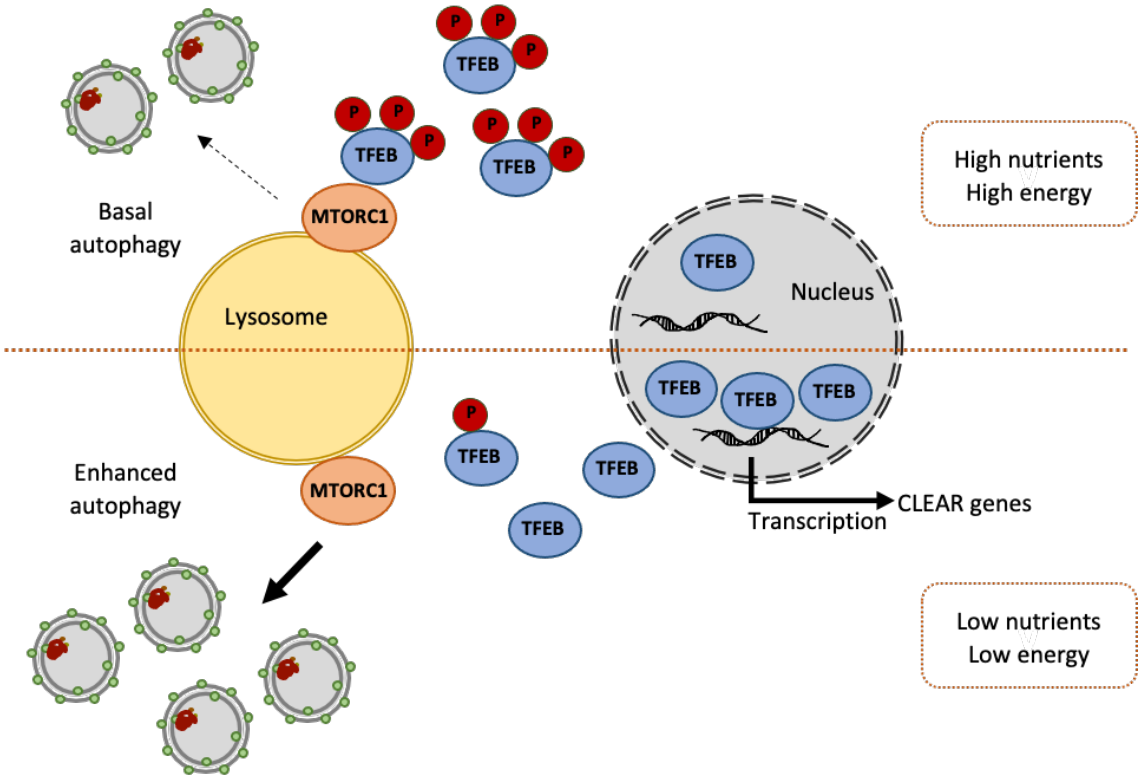

Figure 13. Feedback loop to autophagy. *In basal conditions, the lysosomal regulator TFEB is phosphorylated by MTORC1 and sequestered both in the lysosomal membrane and in the cytoplasm, with minimum translocation of the non-phosphorylated TFEB to the nucleus. MTORC1 is active promoting only basal levels of autophagy. Under nutrient and energy restriction, TFEB is de-phosphorylated because of the MTORC1 inhibition, and translocated to the nucleus, where it will drive the expression of lysosomal genes to enhance the lysosomal activity. The reduced MTORC1 activity will promote autophagy in response to nutrient starvation.*

In the lysosomal membrane, TFEB interacts with MTORC1 that phosphorylates TFEB, enhancing its cytoplasmic location. However, in energy shortage situations, MTORC1 becomes inactive and hence, TFEB is no longer phosphorylated and translocate to the nucleus, to transcriptionally regulate the lysosomal function (Settembre et al., 2011) (**Figure 13**). In addition, the level of amino acids within the lysosome determines the docking of MTORC1 to its membrane. The lysosome serves as a nutrient sensor that regulates the activity of MTORC1 and consequently the initiation of autophagy. In nutrient rich conditions, MTORC1 is active, limiting the autophagy pathway and sequestering TFEB in the cytosol. However, under nutrient and more precisely, amino acid starvation, MTORC1 inhibition triggers the initiation of autophagy and promotes lysosomal function through TFEB (Luzio et al., 2014; Settembre et al., 2011; Settembre et al., 2013) (**Figure 13**). Overall, the autophagy and lysosomal functions are regulated in a coordinated manner, to ensure energy and macromolecular supply under stressful conditions for the cell.

The lysosome is not merely a disposal organelle but is a dynamic compartment in constant remodelling and signalling towards the cell. It regulates autophagy and its own biogenesis and function depending in the environmental input. It is the convergence point of the autophagy and phagocytosis, where the docked substrates are degraded.

Until now, we have discussed the main characteristics of phagocytosis and autophagy and approached their relevance from a physiological angle. In the next section we will frame these two processes in a disease model of stroke.

3.7 MICROGLIAL PHAGOCYTOSIS AND AUTOPHAGY IN DISEASE: STROKE

3.7.1 Introduction to stroke

Stroke, or cerebrovascular accident, is one of the leading causes of death and disability worldwide. It affects over 13.7 million people every year and claims 56.7 million lives according to recent trends ("Global, regional, and national burden of stroke, 1990-2016: a systematic analysis for the Global Burden of Disease Study 2016," 2019; Lindsay et al., 2019). It is characterised by the interruption of the blood supply to a certain brain region, either by a broken or clogged blood vessel, resulting in oxygen and nutrient starvation, brain damage and loss of function (Moskowitz et al., 2010; Mozaffarian et al., 2016); and has different outcomes depending on the affected region, including deficits in motor memory, language, attention, and motor performance (Ferro et al., 2016). Clinically, stroke patients not only suffer from physical

disease but also develop mood disorders, like depression, and emotional deficits that make the recovery a very complex journey (Chen et al., 2013; Cumming et al., 2013). This disease is then a major health issue that needs to be urgently appeased.

The generic term stroke comprises two major types, according to the origin of the blood limitation: haemorrhagic and ischemic stroke.

Haemorrhagic stroke. Haemorrhagic strokes happen when a blood vessel ruptures and bleed into the brain parenchyma, generating a physical pressure in the flooded tissue and oxygen and nutrient deprivation along with the build-up of inflammation and excitotoxicity (Dirnagl et al., 1999; Knight-Greenfield et al., 2019; Krafft et al., 2012). They comprise between 5 and 21% of acute strokes, related to hypertension and/or vascular malformations (arteriovenous malformation, AVM) and is also associated with cerebral amyloid angiopathies in elder patients (Knight-Greenfield et al., 2019). Hemorrhagic stroke may be further subdivided into intracerebral hemorrhage (ICH) and subarachnoid hemorrhage (SAH), with bleeding into the brain parenchyma and subarachnoid space, between the brain and the leptomeninges, respectively (Unnithan & Mehta, 2022). It has a very poor prognosis, and it often requires osmotherapy and/or surgery to reduce the hematoma and repair the damaged vessel (Chen et al., 2014; Michelozzi & Cognard, 2019). The available treatments are only palliative oriented to reduce the swelling, like corticosteroids or diuretics, and also painkillers and anti-hypertensive drugs (Arai et al., 2011; Krafft et al., 2012; Morotti & Goldstein, 2016).

Ischemic stroke. Ischemic strokes occur as a result of the narrowing or obstruction of a blood vessel due to several causes, among which clots are the most common. They comprise up to 85% of all strokes (Mozaffarian et al., 2016) and gather two different types of ischemic strokes: global and focal ischemia (Lee et al., 1999). Global ischemia occurs when the cerebral blood flow is reduced in the majority or all the brain; on the contrary to focal ischemia where the reduction or cut of the blood flow is restricted to a specific area (Traystman, 2003). In humans, the most common occluded artery during focal ischemia, is the middle cerebral artery (MCA), that irrigates temporal, parietal and frontal lobes (Navarro-Orozco & Sánchez-Manso, 2022). Currently, the only treatment available for the ischemic stroke is to tackle de clot using recombinant tissue plasminogen activator (rt-PA) to promote thrombolysis and restore the normal cerebral blood flow (Rabinstein, 2020). However, thrombolysis has associated a hemorrhage risk (6%) after reperfusion, responsible for 50% of the deaths under these conditions (Powers et al., 2019; Rabinstein, 2020). Hence, treatments are oriented to the restoration of the blood flow and to minimize the effect of reperfusion.

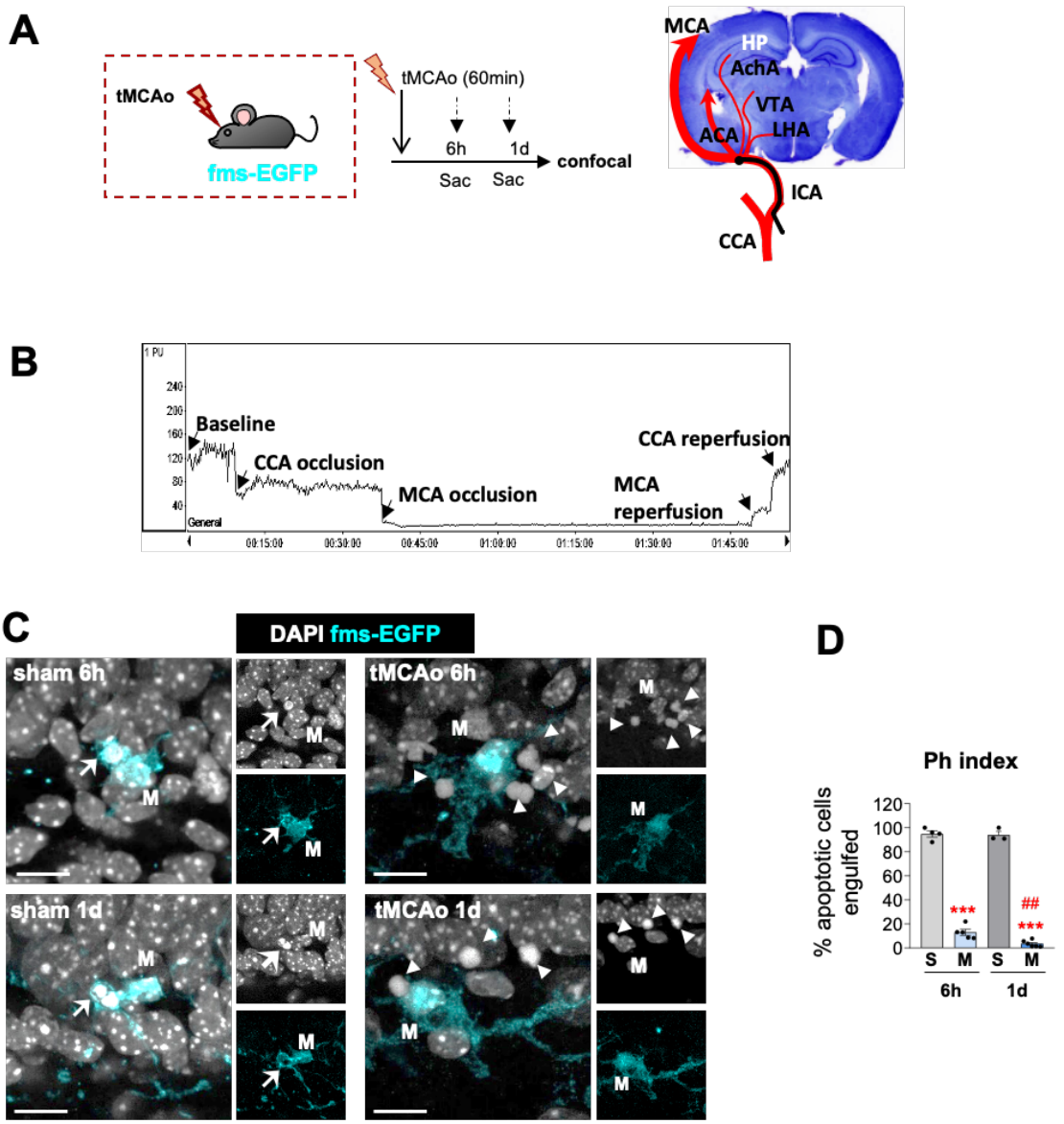

Figure 14. Microglial phagocytosis is impaired in a mouse model of tMCAo. ***[A]*** *Experimental design of tMCAo in 2-month-old fms-EGFP mice and coronal slice with cresyl violet showing the areas irrigated by the MCA.* ***[B]*** *Laser Doppler signal graph showing cerebral blood flow (CBF) in the territory supplied by MCA during baseline, CCA and MCA occlusion, and reperfusion. Successful MCA occlusion, determined by CBF >70% drop from the baseline, recovers after reperfusion.* ***[C]*** *Representative confocal z-stacks of the DG of fms-EGFP mice at 6h and 1d after tMCAo. Cell nuclei were visualized with DAPI (in white) and microglia by EGFP (in cyan). Apoptotic cells are marked with arrowheads.* ***[D]*** *Ph index in the septal hippocampus (% of apoptotic cells engulfed by microglia). Bars show mean ± SEM* ***[E-H]****. n=3 mice (sham at 6h), n=4 mice (sham at 1d), n=5 mice (tMCAo at 6h) and n=6 mice (tMCAo at 1d). The effect of sham/tMCAo at 6h and 1d on Ph index was analyzed using 2-way ANOVA. Significant interactions were found between the two factors (tMCAo treatment x time); therefore, data was split into two 1-way ANOVAs to analyze statistical differences due to the time after sham/ tMCAo at each time. Holm-Sidak was used as a post hoc test. (* and #) represent significance compared to sham and/or tMCAo at 6h,*

respectively. Two symbols represent p<0.01; three p<0.001. Scale bars14µm, z=16µm. Figure from Sol Beccari´s PhD Thesis

To study the mechanisms and consequences of the ischemic stroke, several animal models have been used to accurately mimic the disease, most of which occlude the MCAo using different techniques (Lopez & Vemuganti, 2018; Trotman-Lucas & Gibson, 2021). MCA can be occluded after craniotomy (Tamura et al., 1981), by photothrombosis (Kleinschnitz et al., 2008), by embolism (Niessen et al., 2003), by endothelin-1 administration Hughes et al., 2003), or by intraluminal filament insertion (Koizumi et al., 1986; Longa et al., 1989). Our laboratory chose the filament insertion model and reperfusion to assess the effects of ischemia on microglial phagocytosis in the DG of the hippocampus. Briefly, the intraluminal filament insertion model consists of the insertion of a filament to occlude the MCA and its collateral branches either permanently or transitorily by removing the filament (**Figure 14A**). To confirm the occlusion, we used Laser Doppler flowmetry to monitor the occlusion and reperfusion after the filament removal (**Figure 14B**) and ensure the reproducibility of the model. The intraluminal filament technique to induce focal MCAo is one of the methods that most closely simulate human ischemic stroke (Ansari et al., 2011; Morris et al., 2016).

Therefore, the transitory occlusion of the MCA (tMCAo) served as a very powerful tool to induce a reproducible damage, reaching the hippocampus in our model, and study the role of microglia in stroke.

3.7.2 Microglia in stroke

Microglia is not free from the ischemic damage. After ischemia, microglia experiment a dramatic morphological change (Ito et al., 2001; Morrison & Filosa, 2013; Otxoa-de-Amezaga et al., 2019; Thored et al., 2009) and initiates an inflammatory response, first contributing to neurotoxicity by triggering a pro-inflammatory response, cytokine release and ROS production (Hu et al., 2012; Iadecola & Anrather, 2011; Lambertsen et al., 2009; Lan et al., 2017; Zhang et al., 2017; S. C. Zhao et al., 2017); and later helping to restore the tissue health and homeostasis by the release of trophic factors (Iadecola & Anrather, 2011; Kim et al., 2014; Lai & Todd, 2006). In addition, microglia shift their receptor profile by increasing the expression of purinergic receptors (Franke et al., 2004; Melani et al., 2006), fractalkine receptors (Fumagalli et al., 2019; Tarozzo et al., 2002), Toll-like receptors (TLRs) (Anttila et al., 2017), and TREM2 (Heldmann et al., 2011; Sugimoto et al., 2014), likely to respond to the pathological environment. In the necrotic core, where the blood flow is interrupted and necrotic death occurs, microglia undergo cell death,

whereas in the penumbra or the area surrounding the core and likely to be either recovered or damaged, microglia proliferate (Denes et al., 2007; Lalancette-Hébert et al., 2007; Li et al., 2013; Moraga et al., 2015; Otxoa-de-Amezaga et al., 2019; Thored et al., 2009). Many studies have addressed the role of microglia in stroke in terms of M1/M2 phenotypes (Guo et al., 2022; Ma et al., 2017), originally related to pro- and anti-inflammatory profiles but already outdated, as microglia do not polarize to either of these states (Ransohoff, 2016). This phenotyping is currently surpassed by more sophisticated RNA-sequencing (RNA-seq) methods (Androvic et al., 2020; Kang Guo et al., 2021; Rajan et al., 2019; Zheng et al., 2021). These studies, however, make no or little comment on microglial phagocytosis only referring to the inflammatory profile after stroke. Thus, despite the morphological and molecular studies above mentioned, the functional implications of stroke on microglia still remain to be assessed. In the next section, we will discuss the state of the art on microglial phagocytosis in stroke and compare it with our own results in the DG of the hippocampus of male mice.

3.7.2.1 Microglial phagocytosis in stroke

Several groups have attempted to address microglial phagocytosis after stroke, but the methods used did not directly assess the engulfment of apoptotic cells by microglia. Initial reports suggested an increase of phagocytosis between 1- and 2-days post tMCAo in the striatum, determined as a co-localization between NeuN and microglia (Schilling et al., 2003). However, as NeuN is degraded during phagocytosis (Sierra et al., 2010), this method results in a sub-estimation of the amount of phagocytosis. In addition, the authors did not provide a baseline measurement of phagocytosis and therefore they could not conclude whether phagocytosis efficiency was preserved after tMCAo.

In addition to the in vivo experiments, years later, in vitro assays using FACS-sorted microglia from tMCAo mice, demonstrated that microglia were able to phagocytose latex beads one day after tMCAo and peaked after 3 days (Ritzel et al., 2015). However, as we have discussed before latex beads are not an accurate model to study phagocytosis as they do not express “find-me” signals and cannot complete the degradation step. More recently, it was reported that microglia were able to interact and phagocytose the infiltrating neutrophils in photothrombotic stroke (Neumann et al., 2018) and MCAo (Otxoa-de-Amezaga et al., 2019); as well as in vitro, where primary microglia and human cultured microglia phagocytosed added neutrophiles (Otxoa-de-Amezaga et al., 2019). These data confirm the phagocytic potential of microglia after stroke, at least outside of the necrotic core where microglia do not survive (Otxoa-de-Amezaga et al., 2019).

However, none of these studies directly assessed microglial phagocytosis of dead corpses. In Dr. Sol Beccari´s PhD Thesis, she studied the effects of tMCAo on microglia, directly quantifying microglial phagocytosis (**Figure 14C**, **D**). She demonstrated that microglial phagocytosis was impaired as early as 6 hours after the ischemic insult and maintained up to 1 day (**Figure 14D**). This finding prompted us to study the mechanisms underlying the phagocytosis impairment and to propose a recovery strategy of the lost phagocytic function. In this PhD project we will test microglial phagocytosis in two in vitro systems: organotypic slices and primary microglia treated with oxygen and nutrient deprivation (OND) to mimic the lack of blood supply in the ischemic stroke. Furthermore, we will address the still poorly described the role of autophagy in microglia after OND and relate the autophagy pathway to phagocytosis under the deprived conditions.

3.7.2.2 Microglial autophagy in stroke

The role of autophagy in stroke remains a controversial matter, as opposite studies have demonstrated both protective (Buckley et al., 2014; Jeong et al., 2016) and cytotoxic (Buckley et al., 2014; Wen et al., 2008) effects. Similarly, modulation of microglial autophagy in stroke has also resulted in contradictory resultsas we will discuss next. Furthermore, in most cases, a direct assessment of microglial autophagy was not performed. finally, most studies have focused on the interaction between autophagy and inflammation, whereas its role on phagocytosis has been overlooked.

In vivo studies have demonstrated that the inhibition of autophagy is related to decreased inflammation after stroke, presumably through its action on microglia (Yang et al., 2015; Zhou et al., 2011). For example, mice subjected to permanent MCA occlusion (pMCAo) expressed high levels of inflammatory genes/proteins, (IL-1β, IL-6 and TNF- α) that were reduced after the treatment with the autophagy inhibitor 3-MA, which acts at the initiation of the autophagy cascade by inhibiting the PI3K complex (Yang et al., 2015). On the contrary, the administration of the autophagy inducer rapamycin increased the production of pro-inflammatory cytokines; however, the effect of rapamycin on autophagy was not assessed and, specifically, its relationship with microglial autophagy was overlooked (Yang et al., 2015). In contrast, isolated microglia from pMCAo rats, treated with a glycogen synthase kinase-3β (GSK-3β) inhibitor presented reduced inflammation and increased autophagy. The reduction of inflammatory cytokines after the administration of the GSK-3β inhibitor was abolished when the autophagy gene Beclin1 was silenced in microglia, confirming the relationship between autophagy and

inflammation (Zhou et al., 2011). Other studies demonstrated this relationship using different autophagy deficient models, for example, the Atg5 silencing induced an increase in inflammation after OGD/R and the pharmacological induction of autophagy through the activation of the transient receptor potential vanilloid 1 (TRPV1) protected microglia against the detrimental effects of hypoxia and nutrient deprivation (Lin et al., 2022). In addition, the suppression of autophagy has been related to microglial survival, as the silencing of Atg5 in primary microglia lead to increased apoptosis after oxygen and glucose deprivation and reperfusion (OGD/R) (T. Huang et al., 2021). Thus, the current evidence on the role of autophagy in stroke is contradictory, suggesting that it could trigger both a pro- and anti-inflammatory response, but no other functional assays were performed. Further in vivo studies should be performed to confirm the role of microglial autophagy in stroke.

Considering that autophagy could be a target pathway to modulate the microglial response against stroke, in this PhD project, we chose the well know autophagy inductor, rapamycin. In the next section, we will revise the main effects of rapamycin in models of stroke.

3.7.2.3 Rapamycin as a therapeutic approach for tMCAo

Rapamycin is a recognized inhibitor of the MTOR pathway (Sarkar, 2013) (**Figure 9**) that triggers the induction of autophagy but can also have off target effects in time and dose dependent manner (Klionsky et al., 2021). Our choice of rapamycin as a therapeutical approach to modulate phagocytosis is based on its reported benefits in several disease models (Galluzzi et al., 2016). In particular, rapamycin has been described to reduce the infarct volume and ameliorate the neurological score after stroke in two different models, pMCAo (Wu et al., 2018) and tMCAo (Li & Huang, 2020b). It has also been shown to reduced neuronal death (Wu et al., 2018) and increased mice survival after its administration (Buckley et al., 2014; Xie et al., 2014).

While autophagy has been largely studied in neurons after stroke, its role on microglia remains largely unknown. Autophagy and its pharmacological modulation are currently associated with inflammation and not with the phagocytic function. The effect of rapamycin is not an exception, it has been related to a decreased inflammatory response after stroke (Tang et al., 2021; Xie et al., 2014) but it has neither been properly assessed in microglia nor related to the phagocytosis function.

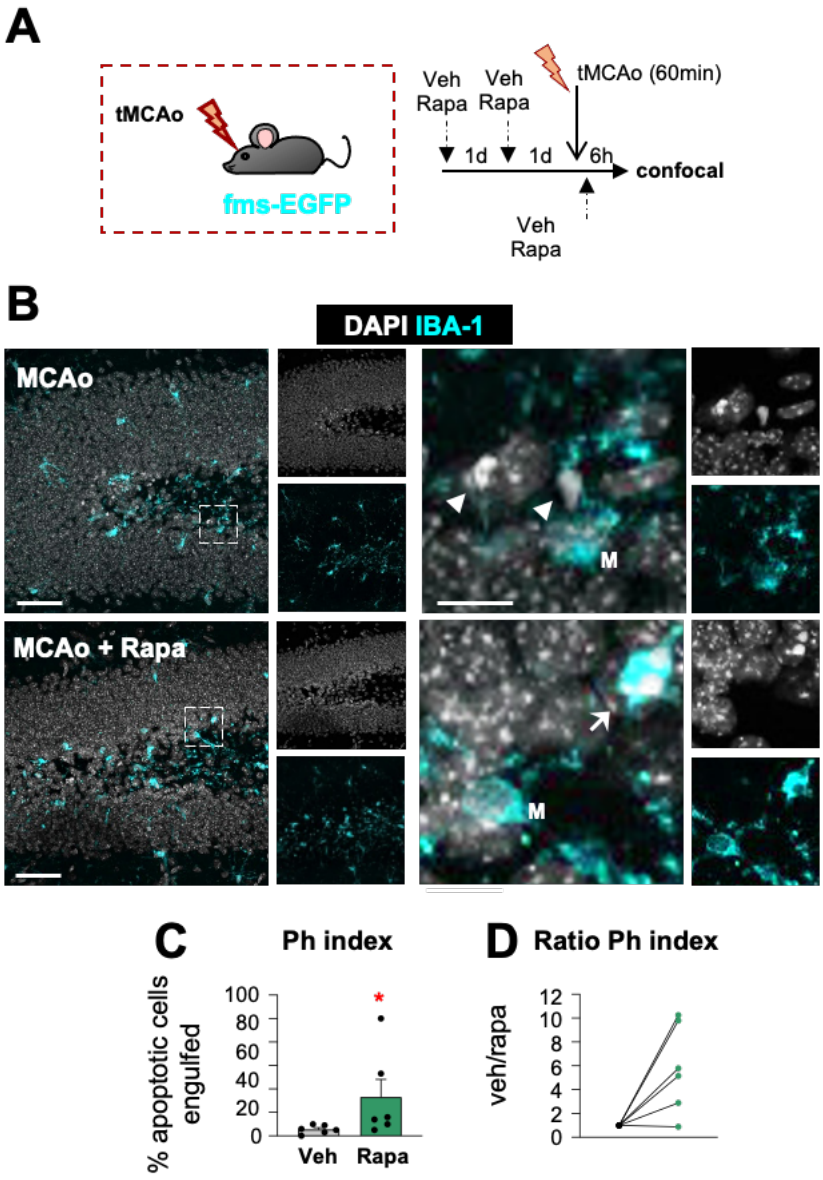

Figure 15. Rapamycin reverts the tMCAo-induced phagocytic dysfunction in vivo but not in vitro.

[A] *Experimental design showing the daily administration of rapamycin (10mg/kg, ip) two days prior to the tMCAo in 2-month-old fms-EGFP mice. Mice received a third rapamycin injection right after reperfusion and were sacrificed 6h later.* ***[B]*** *Representative confocal z-stacks of the DG of fms-EGFP mice 6h after tMCAo, treated with vehicle or rapamycin (10mg/kg, ip). Cell nuclei were visualized with DAPI (in white) and microglia (fms-EGFP⁺, in cyan). Arrowheads point to non-phagocytosed apoptotic cells and arrows to phagocytosed apoptotic cells. M labels a microglial soma.* ***[C]*** *Ph index in the septal hippocampus (% of apoptotic cells engulfed by microglia).* ***[D]*** *Normalized ratio of Ph index change in each rapamycin-treated mice over its same day vehicle-treated mice. Bars show mean ± SEM. n=6 mice per group. Data was analyzed using a Student´s t-test. Asterisks represent significance between untreated and rapamycin-treated mice.: (*) represents p<0.05 Scale bars=50µm, z=19.6µm; inserts bar=10µm z=9.8µm. Figure from Sol Beccari´s PhD Thesis*

Considering the beneficial effects of rapamycin in stroke and its modulation of autophagy, we assessed its effects on the tMCAo model to try to recover the microglial function lost after stroke (**Figure 15A**). The pre-treatment with rapamycin for 2 days prior to the surgery had a partially protective effect on the microglial function (**Figure 1B**-**D**). It did not fully recover phagocytosis but significantly restored the microglial function compared to the non-treated tMCAo mice (**Figure 15C**, **D**). The recovery of phagocytosis was once again, suggestive of the interaction between autophagy and phagocytosis, thus, in this PhD project we will try to address the functional effects of rapamycin using in vitro models of OND.

The ischemic stroke is not the only pathology associated with deficient phagocytosis. We recently described that microglial phagocytosis was impaired in a model of mesial temporal lobe epilepsy (MTLE) both in mice and human (Abiega et al., 2016). In the next section, we will discuss microglial phagocytosis in a model of genetic epilepsy where the lysosomal protein Cystatin B lacks its function.

3.8 MICROGLIAL PHAGOCYTOSIS IN DISEASE: GENETIC EPILEPSY

3.8.1 Introduction to epilepsy.

The term epilepsy is used to describe a wide spectrum of neurological disorders characterised by seizures, which are defined as abnormal synchronised neuronal activities that are translated into external symptoms like uncontrolled shaking or loss of conscience (Fisher et al., 2014; Savage, 2014). Epilepsy is the third most common cause of chronic disorders, affecting more than 50 million people worldwide (Thurman et al., 2011). Importantly, the life quality of epilepsy patients is conditioned by the development of psychological comorbidities, such as mood disorders, including depression and anxiety (Quintas et al., 2012); as well as cognitive impairment, among which attention, memory and language deficits are most common (Holmes, 2015). In addition, people that suffer from epilepsy have been reported to exhibit 2-3 times increased mortality rate compared to the general population (Forsgren et al., 2005; Gaitatzis & Sander, 2004). Hence, epilepsy is a public health concern that should not be unattended.

Epilepsy has many possible known and unknown causes, from genetic factors, developmental abnormalities, brain trauma, infections, stroke and/or brain tumours (Ahl et al., 2016; Temkin, 2009); however, almost 50% of the epilepsies are idiopathic. Pharmacological treatments are available to control but not cure epilepsies and almost 30% of the patients are pharmacoresistant or refractory to the available treatments (Fattorusso et al., 2021). Moreover,

the treatments are associated with negative side effects; thus, there is a strong need to develop efficient therapies not to tame but to heal and limit the detrimental consequences of the disease (Eyo et al., 2016).

According to the region where seizures are initiated, epilepsies can be classified as focal or generalized (Fisher et al., 2017). Focal or partial seizures are initiated in a particular brain region and are associated with the lack of function that often correlate with the area of initiation (Ahl et al., 2016). Generalised epilepsies involve uncontrolled neural activity throughout the whole brain, loss of consciousness and violent convulsion (Ahl et al., 2016). The most frequent form of human epilepsy is Mesial Temporal Lobe Epilepsy (MTLE) (Tatum, 2012), on which we will make a brief comment on to set the bases for the analysis of the genetic model of epilepsy.

3.8.2 MTLE

MTLE encompasses a group of disorders associated with the dysregulation of the hippocampal function caused by neuronal hyperexcitability (Schwartzkroin, 1986); and are the most common form of drug-resistant epilepsy (Duveau et al., 2016). Hippocampal resection is the only available treatment to control seizures in pharmaco-resistant patients (Mathon et al., 2015). The pathophysiology of MTLE comprises unprovoked seizures, hippocampal sclerosis, including neuronal loss, granule cell dispersion, gliosis and inflammation (Bae et al., 2010; de Lanerolle et al., 2003; Sharma et al., 2007; Sierra et al., 2015).

To understand the mechanisms underlying MTLE, several animal models are used to mimic the electroencephalographic, behavioural, and neuropathological features (Kandratavicius et al., 2014; Lévesque et al., 2016). The most commonly used are pilocarpine (Vezzani, 2009) and kainic acid (KA) administration (Ben-Ari & Cossart, 2000; Fritsch et al., 2014). Both models resemble the appearance of seizure and affect similar brain structures, such as the amygdala and the hippocampus. They can be administered systemically or directly in the structure of interest (amygdala or hippocampus). Among these models, the intrahippocampal administration of KA has proven to be the most reliable model to reproduce human MTLE, as it mimics the effect of hippocampal focal seizures and their extended damage over related healthy tissue (Lévesque & Avoli, 2013). KA acts as an agonist of the KA glutamate receptor and partially activates AMPA receptors (Ben-Ari & Cossart, 2000). Its administration shows low mortality and is characterized by the initial status epilepticus, followed by a latent period that precedes the appearance of recurrent seizures, consistent with the human pathology (Lévesque & Avoli, 2013). Our

laboratory chose the KA model to study microglia phagocytosis in the DG hippocampus KA treated mice (Abiega et al., 2016).

3.8.3 Progressive myoclonus epilepsy type

Progressive Myoclonus Epilepsy 1 (EPM1) or Unverricht-Lundborg disease, is the most prevalent genetic neurodegenerative disease among the progressive myoclonus epilepsies (PMEs) group, comprised by a heterogenous family of inherited and poorly understood disorders that are generally pharmacoresistant (Lehesjoki & Kälviäinen, 1993) (Tegelberg et al., 2012). It is characterised by stimulus-sensitive myoclonus and tonic-clonic epileptic seizures of early onset, between 8 and 16 years of age (Äikiä et al., 2021). As EPM1 progresses, patients develop severe neurological manifestations, like ataxia, dysarthria, incoordination, and intention tremor. Advanced stages of the disease are characterised by mild cognitive impairment as well as intellectual dysfunction (Chew et al., 2008; Magaudda et al., 2006).

The autosomal recessive disease is caused by biallelic loss-of-function, related to a dodecamer repeat expansion, in the cystatin B gene (*CTSB*), which encodes the cystatin B protein (CSTB) (Joensuu et al., 2008; Lalioti et al., 1997; Pennacchio et al., 1996). CSTB, or Stefin B, is a cytoplasmic protease that limits the activity of nuclear and lysosomal cysteine proteases known as cathepsins (Koskenkorva et al., 2012; Riccio et al., 2001) to limit the protease activity outside the lysosomal context (cystatins and cathepsins have been revised in **Section 2.6**). Its dysregulation has been associated with several neurodegenerative diseases (Nakanishi, 2003; Nixon & Cataldo, 2006; Stoka et al., 2016); however, the precise mechanism that leads to the development of EPM1 remain unclear. The lack of activity of CSTB has also been related to an impaired response to oxidative stress (Lehtinen et al., 2009). To study the physiopathology of EPM1, the murine *Cstb* KO model is widely used (Maher et al., 2014; Manninen et al., 2014; Pennacchio et al., 1998; Tegelberg et al., 2012).

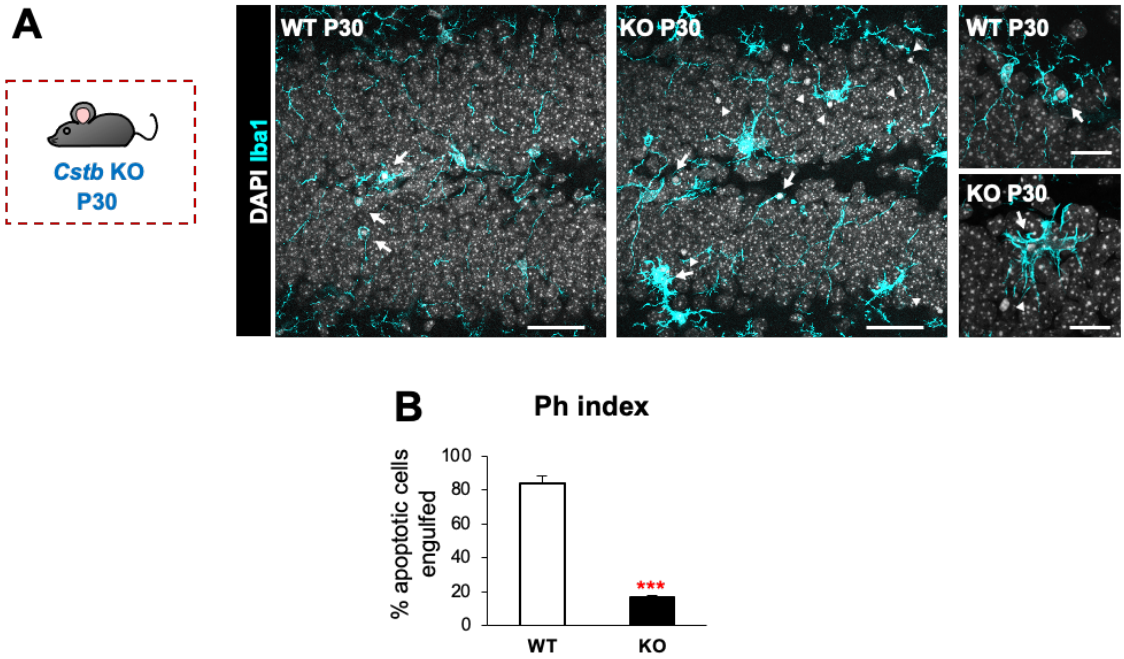

Figure 16. Microglial phagocytosis is impaired in the DG of P30 Cstb KO mice. ***[A]*** *Representative confocal images of the DG in WT and Cstb KO P30 mice (A). Healthy or apoptotic (pyknotic/karyorrhectic) nuclear morphology was visualized with DAPI (white) and microglia were stained for Iba1 (cyan). High magnification examples of phagocytic microglia following the typical "ball and chain" (upper panel) form with the tip of their processes and phagocytosing with their soma (lower panel).* ***[B]*** *Phagocytic index (in % of apoptotic cells being engulfed by microglia) in the septal hippocampus. Bars represent the mean ± SEM. *** indicates p < 0.001. Scale bars= 40µm (**A**, low magnification), 20 µm (**A**, high magnification); z=7µm (**A**, low magnification), 3.5µm (**A**, high magnification). Figure from Oihane Abiega´s PhD Thesis*

The *Cstb* KO model recapitulates many clinical features of the EPM1 pathology (Koskenkorva et al., 2012; Mascalchi et al., 2002) (**Figure 16**). *Cstb* KO mice develop seizures after one month and progressive ataxia by six months of age (Maher et al., 2014; Manninen et al., 2013; Pennacchio et al., 1998; Shannon et al., 2002) consistent with findings in humans. Mice suffer from progressive atrophy, cortical thinning, and neuronal and white matter loss, particularly in the cerebellum and in the thalamocortical system (Koskenkorva et al., 2012; Manninen et al., 2014; Pennacchio et al., 1998; Shannon et al., 2002; Tegelberg et al., 2012). It is important to mention that one of the earliest neuropathological features in the *Cstb* KO mice is the altered microglial inflammatory profile and morphology (Korber et al., 2016; Okuneva et al., 2015; Tegelberg et al., 2012), as early as two weeks of age, as well as genetic alterations associated with immunological genes, studied at later timepoints (Joensuu et al., 2014), followed by alterations in astrocytes and progressive neuronal loss from one month onwards. In addition to the histological alterations in the cerebellum, there is an alteration in the genetic profile of the

GABAergic signalling at one week of age. These alterations in the pre- and post-synapses, lead to decreased inhibition and reduced biding of the GABA ligands (Joensuu et al., 2014), rendering the *Cstb* KO model as a very useful tool to study the EMP1 pathology.

3.8.4 Microglia in epilepsy

Microglia respond both morphologically and molecularly to seizures in human and in animal models. The most notable morphological changes in rodent models of epilepsy include changes in their body size, process length and number, branching complexity and motility (Abiega et al., 2016; Eyo et al., 2014). Microglia have been found to present an ameboid morphology with few processes, particularly in the areas affected by MTLE, like CA3, CA1 and the DG (Morin-Brureau et al., 2018). Microglia also alter the expression of purinergic receptors, fractalkine receptors and cytokines in epilepsy models (Avignone et al., 2015; Banerjee et al., 2015; Eriksson et al., 2000; Vezzani, 2009). Importantly, the "find-me" signals and their receptors have been described to be upregulated in the cerebrospinal fluid of MTLE patients and in rat models of pilocarpine (Ali et al., 2015) but not in the KA model (Hughes et al., 2002). The purinergic receptors P2X7, P2Y6 and P2Y12 increased both at the transcriptional (Avignone et al., 2008) and immunohistochemical level (Rappold et al., 2006) after KA administration, confirming the molecular changes in microglia. Using a mouse model of KA, we confirmed that after 1 day, the expression of the purinergic receptors P2X4, P2X7, P2Y6 and P2Y12 was increased (Abiega et al., 2016). However, only few studies have assessed microglial phagocytosis in epilepsy.

Initial studies (Koizumi et al., 2013) demonstrated that microglial phagocytosis latex beads applied in the cortex of KA mice increased compared to healthy mice. However, the direct administration of the beads on the cortex and the lack of "find-me" signals as well as the completion of phagocytosis through degradation, make this model a useful preliminary but not conclusive study. The expression of CD68 and the immunoglobulin Fc receptor CD16/32a have also been taken as indirect measurements of phagocytosis (Morin-Brureau et al., 2018), but CD68 expression does not correlate with phagocytosis, as we have discussed earlier. In contrast, our laboratory directly assessed microglial phagocytosis in the DG of KA mice (Abiega et al., 2016) and showed that microglial phagocytosis was impaired after KA administration from 6 to 24 hours. The impairment was related to two different phenomena: 1, the reduced expression of "find-me" receptors in microglia, like TREM2, CR3, GPR34 and MerTK and 2, the massive release of ATP during the seizures that reduced microglial motility. The combination of the two events lead to a decrease recognition of the apoptotic cells present as a result of the KA administration, and also to the "blinding" of microglia by the release of ATP that disrupted the

microgradientes that allow the finding of the apoptotic cells in basal conditions (Abiega et al., 2016).

To confirm if this phagocytosis impairment also occurred in other type of epilepsy, in this PhD Thesis we studied microglial phagocytosis in EPM1. Previous data from Dr. Ohiane Abiega obtained during her PhD demonstrated that microglial phagocytosis, in symptomatic P30 *Cstb* KO mice, was deficient at the seizure onset (**Figure 16A**, **B**) (Sierra-Torre et al., 2020). In addition, microglial phagocytosis was not compensated by astrocytes that did not remove the apoptotic cells not engulfed by microglia (data not shown). Hence, she confirmed that microglia are deficient in *Cstb* KO mice at P30.

Here, we have used the *Cstb* KO model to extend our studies on microglial phagocytosis in the context of a genetic epilepsy, and confirm our findings obtained from the MTLE model. In addition, this model comprises a model of lysosomal disease, as CSTB, one of the main regulators of the cathepsin activity, is dysfunctional in this disease.

Hypothesis and objectives

4. Hypothesis and objectives

Autophagy and **phagocytosis** are two highly conserved process devoted to the maintenance of the tissue homeostasis through the recycling of cytoplasmic content in the case of autophagy and extracellular material, like apoptotic cells, in the case of phagocytosis. Both processes share many similarities at the intracellular level and are part of the **endosomal pathway** that converges in the **lysosome**, which suggest a functional relationship between autophagy and phagocytosis (Plaza-Zabala et al., 2017).

The role of microglial autophagy has not been yet properly characterized; however, our laboratory has broadly described microglial phagocytosis both in the healthy and in the diseased brain, in response to different phagocytic challenges (Abiega et al., 2016; Diaz-Aparicio et al., 2020). We have previously demonstrated that in a pharmacological model of **epilepsy** generated by the injection of KA intrahippocampally, microglia present a **blockage in phagocytosis**, leading to the accumulation of apoptotic cells, tissue damage and inflammation (Abiega et al., 2016). Recently, we have extended our studies on microglial phagocytosis and determined that the microglial phagocytic blockage in the KA model, also occurred in a model of cerebral ischemia (**tMACo**). During ischemia, the oxygen (**hypoxia**) and nutrient supply (**starvation**) is suppressed, two conditions widely described as inductors of **autophagy**. Hence, based on the phagocytic blockage and the autophagy inducing conditions that take place during stroke, we hypothesised that autophagy and phagocytosis are not independent processes but are tightly related in microglia. Thus, the main objective of this PhD is the study of the **functional relationship between autophagy and phagocytosis** both in basal conditions and using an in vitro model of ischemia.

In addition, we have extended our research on microglial phagocytosis in a model of **genetic epilepsy**, characterised by the lack of a lysosomal gene, ***Cstb***, where we previously demonstrated that microglial **phagocytosis** was **blocked** in *Cstb* KO mice. Our goal was to determine the functional cause for the microglial phagocytosis impairment, thus, we hypothesised that the lack of Cstb in microglia altered microglial phagocytosis in a cell-autonomous way or the phagocytosis deficiency could be related to increased neuronal activity as it occurred in the KA model.

In this PhD Thesis, we have analysed the role of microglial phagocytosis and autophagy in basal and oxygen and nutrient deprivation (OND) conditions using primary microglial and organotypic hippocampal slices as models of study. Furthermore, we have assessed the functional implications of the absence of the lysosomal gene *Cstb*, in cultured BV2 microglia and in in vivo *Cstb* KO mice. The results are divided in three sections:

In the first section, we analysed microglial phagocytosis in primary microglia and organotypic hippocampal slices treated with OND; monitored the lysosomal health and assessed the autophagy compartment by western blot and TEM in primary microglia. Next, we characterized the functional outcome of microglial autophagy in basal conditions and tried to modulate autophagy to recover the phagocytosis deficits that occur after stroke.

In the second section, we have proposed a two-step model to analyse autophagy using the classical LC3 assay by western blot. We have described simple equations to assess the formation and degradation of autophagosomes and tested the in simulated and experimental scenarios.

In the last section, we have studied the microglial phagocytosis in EMP1 using an in vitro model of *Cstb* silencing in BV2 microglia and determined the role of neuronal activity in pre-symptomatic P14 *Cstb* KO mice. In addition, in collaboration with Dr. Paolo Bonifazi, we have developed mathematical model that allows us to establish the relationship between active neurons and microglial phagocytosis.

Aim 1. To analyse microglial phagocytosis and autophagy in an ischemia in vitro model and determine the role of basal autophagy on microglia.

Aim 1.1 Effect of OND on microglial phagocytosis. We subjected organotypic hippocampal slices and primary microglia to OND and assessed its effects on microglial phagocytosis from fms-EGFP mice. Quantitative analysis of apoptosis and phagocytosis were performed by immunofluorescence in sections imaged by confocal microscopy. Two-photon microscopy was performed in organotypic hippocampal slices from CX3CR1$^{GFP/+}$ mice. The lysosomal compartment was analyzed in primary microglia by confocal microscopy.

Aim 1.2 Effect of OND on microglial autophagy. Autophagy was assessed in primary microglia and BV2 cells, treated with OND through a time course by western blot of LC3. The autophagy and lysosomal compartments were directly visualised by TEM in OND treated primary microglia.

Aim 1.3 Basal autophagy in microglia. To determine the role of basal autophagy in microglia, we used the autophagy inhibitor MRT69821, selective for the ULK1 kinase essential for the initiation of autophagy. We performed a time and dose-response assay to find the optimal dose to inhibit autophagy in microglia by western blot and imaging. Once the concentration was established, we performed a phagocytosis assay under autophagy in inhibition conditions and assessed the microglial function. Quantitative analysis of apoptosis and phagocytosis were performed by immunofluorescence using confocal microscopy.

Aim 1.4 Autophagy modulation with rapamycin. To modulate autophagy using rapamycin, we performed a time and dose-response assay and analysed it by western blot. We tested the effect of rapamycin on autophagy and assessed its effect on microglial phagocytosis under OND conditions. In addition, we analysed microglial phagocytosis in organotypic hippocampal slices treated with OND in the presence of rapamycin. Quantitative analysis of apoptosis and phagocytosis were performed by immunofluorescence using confocal microscopy.

Aim 2. To dissect formation and degradation of autophagosomes using the classical LC3 western blot

Aim 2.1 Equations to describe the steps of autophagy. We proposed a simple set of equations to differentiate the formation, degradation, and net turnover ratio of autophagosomes.

Aim 2.2 Theoretical scenarios to test the proposed equations. We have simulated the different biological scenarios to test the power of the equations and determine how the different steps of the process can be affected independently by a certain stimulus.

Aim 2.3 Experimental confirmation of the proposed equations. To test the equations, we have used BV2 cells treated with rapamycin and primary microglia treated with MRT68921 and OND. The experimental data was obtained by LC3 western blot.

Aim 3. To determine the effect of *Cstb* absence on microglial phagocytosis. Aim 3.1. Cstb in vivo expression and silencing in BV2 cells. We determined the basal expression of Cstb and its associated cathepsins in FACS-sorted microglia from fms-EGFP mice. To assess the isolated effect of the Cstb deficiency on microglia, we silenced its expression in BV2 microglia using siRNA and quantified by RT-qPCR and immunofluorescence by confocal microscopy. The effects on phagocytosis were assessed after the Cstb silencing. Quantitative analysis of apoptosis and phagocytosis were performed by immunofluorescence using confocal microscopy.

Aim 3.2. ***Phagocytosis in P14 Cstb KO mice*****.** We analysed microglial phagocytosis in the DG of P14 mice differentiating between the GL and the SGZ. Quantitative analysis of apoptosis and phagocytosis were performed by immunofluorescence in sections imaged by confocal microscopy.

Aim 3.3. ***Neuronal activity and apoptosis.*** We analysed the neuronal activity in P14 *Cstb* KO mice and its relationship with the apoptotic cells present in the same region. In collaboration with Dr. Paolo Bonifazi, we modelled the distribution of activated neurons and apoptotic cells to determine their relationship with microglial phagocytosis.

Experimental procedures

5. Experimental procedures

5.1 ANIMALS

fms-EGFP (MacGreen, B6. Cg-Tg(Csf1r-EGFP)1Hume/J; Jackson Laboratory stock #018549) mice were used to perform in vitro experiments (primary microglia cultures and hippocampal organotypic slices) and FACS-sorting experiments. In these mice, microglia constitutively express the green fluorescent protein (GFP) under the expression of the c-fms gene (Sasmono et al., 2003),(Sierra et al., 2007). Two-photon microscopy experiments were performed in CX3CR1$^{GFP/+}$ where microglia express the GFP protein (Jung et al., 2000). The effects of autophagy inhibition were analyzed in several transgenic mouse models: ATG4B KO (C57BI6/129 Sv; Guillermo Mariño, Universidad de Oviedo); Beclin1 KO (Tmem119-CreER) (CD57BL/6, all 3 from D. Schafer, University of Massachussetts, USA); AMBRA1+/- (CD1; Patricia Boya, Centro de Investigaciones Biológicas (CIB), Madrid); FIP200 cKO (CX3CR1-CreER) Jun-Lin Guan, University of Cincinnatti, College of Medicine); *Cstb* KO mice (129S2/SvHsd5-*Cstb* ^{tm1Rm}; Lehesjoki´s lab at Folkhälsan Research Center and University of Helsinki) (**Table 1**).

Experimental Models		
Model	Center	Recombination paradigm
AMBRA1+/- brain samples	Bred at Centro de Investigaciones Biológicas (CIB)	Constitutive
ATG4B KO brain samples	Bred at Universidad de Oviedo	Constitutive
CX3CR1$^{GFP/+}$ mice	Bred at Achucarro Basque Center for Neuroscience	Constitutive
fms-EGFP (MacGreen) mice	The Jackson Laboratories	Constitutive
Microglia specific BECN1 KO (TMEM119-CreER) brain samples	Bred at University of Massachussetts	75 mg/Kg tamoxifen i.p: P21-23 → sacrifice P28
Wildtype mice C57BL/6	Bred at Achucarro Basque Center for Neuroscience	N/A

***Table 1**. List of experimental models used in this PhD thesis.*

5.2 ORGANOTYPIC HIPPOCAMPAL CULTURES

Hippocampal organotypic slices were prepared as previously described (Beccari et al., 2018a). Postnatal day 7 (P7) fms-EGFP mice pups were sacrificed by decapitation and the brains were extracted. Both hippocampi were dissected using a binocular magnifier and were sectioned into 350 μm slices using a tissue chopper (McIlwain). Individual slices were then transferred to 0.4 μm polystyrene culture inserts (Millipore) each of them placed in 6-well plates, each well containing 1 mL of organotypic culture medium. The medium consisted of 50% Neurobasal medium (Gibco) supplemented with 0.5% B27 (Gibco), 25% horse serum (Gibco), 1% Glutamax (Gibco), 1% penicillin/streptomycin (Fisher), and 1% glucose solution in HBSS (Gibco). The medium was changed the day after the culture and every 2 days until the day of the experiment. The hippocampal slices were kept in culture for 7 days prior to the experiment. Slices were fixed after the experiment in cold 4% paraformaldehyde solution for 40 minutes and after thorough rinsing with 1X PBS were stored at 4ºC until immunofluorescence processing.

5.3 CELL CULTURES

5.3.1 Red fluorescent SH-SY5Y cell line (vampire SH-SY5Y)

The vampire SH-SY5Y cell line is a human neuroblastoma cell line developed as a stable transfection of the SH-SY5Y cell line with the red fluorophore tFP602 (InnoProt, P20303) expressed as a free cytoplasmic protein. It derives from neuroepithelioma cell line SK-N-SH, generated from the bone marrow of 4-year-old female with metastatic neuroblastoma (American Type Culture Collection). Cells were grown as adherent culture in non-coated T-75 flasks in the presence of 10-15 mL of high glucose Dulbecco's Modified Eagle's Medium (DMEM, Gibco) supplemented with 10% fetal bovine serum (FBS, GE Healthcare Hyclone) and 1% antibiotic-antimycotic (Gibco) and 0.25mg/ml Geneticin (G418, Gibco) to select the transfected cells. When confluence was reached, cells were trypsinized (Trypsin-EDTA 0,5% no phenol red, Gibco) and replated at a 1:3 density. SH-SY5Y cells were used to perform phagocytosis assay for which they were trypsinized and replated at the same density 24 hour prior to the phagocytosis assay to avoid the addition of cell clusters to the microglia culture. For western blot experiments, cells were plated at a density of 750.000 cells in 6 well plates 24 hours prior to the experiment.

5.3.2 BV2 cell line

BV2 cells (Interlab Cell Line Collection San Martino-Instituto Scientifico Tumori-Instituto Nazionale per la Ricerca sul Cancro), a cell line derived from raf/myc-immortalized rat neonatal

microglia were used to perform western blot experiments and the *in vitro* knock-down model of *Cstb*. BV2 cells were grown as an adherent culture in non-coated 90mm^2 Petri dishes in the presence of 10 mL of culture medium. The culture medium consisted in high glucose DMEM, (Gibco) supplemented with 10% FBS (GE Healthcare Hyclone) and 1% antibiotic-antimycotic (Gibco). When confluence was reached, cells were trypsinized (Trypsin-EDTA 0,5% no phenol red, Gibco) and replated at 1:5. BV2 cells were plated at a density of 150.000 cells per well in 6 well plates for western blot experiments and 30.000 cells per well for transfection and phagocytosis assays 24 hours prior to the experiment.

5.3.3 Primary microglia cultures

Primary microglia cultures were performed as previously described (Abiega et al., 2016) (Beccari et al., 2018a). Postnatal day 0-1 (P0-P1) fms-EGFP pups were sacrificed by decapitation and brains were extracted. Meninges were dissected off in Hank´s balanced salt solution (HBSS, Gibco) under a binocular magnifier. The cerebellum and the olfactory bulbs were discarded, and the remaining brain was manually chopped and enzymatically digested (enzymatic solution, in mM: 116 NaCl, 5.4 KCl, 26 NaHCO3, 1 NaH2PO4, 1.5 CaCl2, 1 MgSO4, 0.5 EDTA, 25 glucose, 1 L-cysteine) in the presence of papain (20U/mL, Sigma), and desoxyribonuclase I (DNAse I, 150U/μL, Gibco) for 15 minutes at 37°C after which the remaining fragments were mechanically homogenized by gentle pipetting. The resulting cell suspension was then filtered through a 40μm polypropylene cell strainer (Fisher) to individualize the cell suspension. Cells were transferred to a 50 mL Falcon tube containing 5 mL of 20% FBS (Gibco) in HBSS to inactivate the papain after the enzymatic digestion. Next, the cell suspension was centrifuged at 200 g for 5 minutes and the resulting pellet was resuspended in 1 mL of DMEM (Gibco) supplemented with 10% FBS and 1% antibiotic-antimycotic (Gibco). Cells were seeded in poly-L-Lysine (15μL/mL, Sigma) coated T-75 flasks with a density of two brains per flask. The medium was changed the day after the culture and every 3-4 days, enriched with the granulocyte-monocyte colony stimulating factor (5ng/mL GM-CSF, Sigma) to promote microglia proliferation at 37°C, 5% CO_2. When confluence was reached, after approximately 11-14 days, microglia cells were harvested by shaking at 120-140 rpm, at 37°C for 4 hours. The isolated cells were counted and plated at the desired density: 100,000 cells per well in 24-well plates for immunofluorescence experiments, 500,000 cells per well in glass bottom imaging dishes (Ibidi, 81158) for live imaging and 2,000,000 cells per well in 6-well plated for western blot; all of them coated with poly-L-Lysine to guarantee optimal cell adhesion. Before performing experiments, microglia were allowed to settle for at least 24 hours.

5.4 OXYGEN AND NUTRIENT DEPRIVATION ASSAY (OND)

Organotypic slices, primary microglia and BV2 cells slices were treated with oxygen and nutrient deprivation to mimic hypoxia in vitro. Organotypic slices were rinsed twice with 1X PBS to remove medium remains, incubated in nutrient deprived buffered salt solution (130 mM NaCl, 5,4 mM KCl, 1.8 mM $CaCl_2$, 26 mM $NaHCO_3$, 0.8 mM $MgCl_2$, 1.18 mM NaH_2PO_4, pH 7.4 in milliQ water) (Cuartero et al., 2014) and transferred to a hypoxia chamber (Biospherix, US) for 3 or 6 hours inside a standard thermal incubator with an oxygen concentration between 0-3% and no CO_2. For reperfusion experiments slices were placed back in fresh complete medium containing propidium iodide (PI) (5 µg/ml, Sigma) for an additional hour in a regular cell culture incubator (20% O_2, 5% CO_2). Primary microglia and BV2 cells were rinsed twice with 1X PBS and incubated in the buffered salt solution inside the hypoxia for 30 minutes, 1 or 3 hours with no reperfusion.

5.5 DRUG TREATMENT

Bafilomycin A1 (Selleckchem): specific and reversible lysosomal inhibitor that acts on the vacuolar H^+-ATPase (V-ATPase) avoiding the acidification of the lysosome and thus, its degradative capacity (Gagliardi et al., 1999). It was used for western blot experiments to allow the accumulation of autophagosomes through a time course to determine the autophagy flux in primary microglia and BV2 cells at 100 nM for 3 hours. It was dissolved in DMSO to a concentration of 500 µM.

MRT68921 (Sigma): autophagy inhibitor specific for ULK1 that prevents the correct formation of the initiation complex (Petherick et al., 2015). In organotypic slices, MRT68921 was added at 30 and 100 µM (Sigma) for 3 hours under control conditions and during the OND challenge to assess its effects on phagocytosis. Primary microglia were treated with MRT68921 for 3 and 6 hours at 1, 10, and 30 µM under control conditions to assess both the basal effects of its inhibition and the repercussions in autophagy. It was dissolved in water to 1 mM concentration.

Rapamycin (Selleckchem): autophagy inducer that acts through direct inhibition of mTORC1, potentiating autophagy (Sehgal, 2003) . It was used in organotypic slices at a concentration of 200 nM for 3 or 21 hours before the OND challenge and in control conditions to assess its effects on phagocytosis. For primary microglia and BV2 cells, rapamycin was used at a final concentration of 100 nM for 24 hours and 6 hours to assess its effects on phagocytosis and its

repercussions on autophagy. It was dissolved in DMSO (3.65 mM) and diluted in water to 10 µM reducing the final DMSO concentration and hence, avoiding its possible detrimental effects.

5.6 siRNA TRANSFECTION

siRNA targeting *Cstb* (*Cstb* siRNA) and scrambled siRNA (shuffled *Cstb* sequence) (Thermo Fisher) were used to transfect BV2 cells. Both *Cstb* and scrambled siRNA were labeled for immunofluorescence assays using the Silencer Labeling Kit with FAM dye (Invitrogen, AM1634) following the manufacturer´s instructions. BV2 cells were seeded in 24 or 6 well plates 24 hours prior to the transfection assay in high glucose DMEM supplemented with 10% FBS (GE Healthcare Hyclone) and 1% antibiotic-antimycotic (Gibco) to ensure ~80% confluence the day of the experiment. 30,000 and 150,000 cells per well were seeded in 24-well and 6-well plates, respectively. The transfection assay was performed following the manufacturer´s instructions. Lipofectamine 2000 (2µg/mL, Invitrogen) and 5nM siRNAs were separately pre-incubated with Opti-MEM (Gibco) for 20 minutes at room temperature and then added to the plated BV2 cells in low glucose DMEM supplemented with 5% FBS and no antibiotics to ensure full transfection efficiency for 15 hours. Cells were washed with regular growth medium, high glucose DMEM supplemented with 10% FBS and 1% antibiotic-antimycotic. siRNA knock-down was assessed 6, 24 and 48 hours after transfection both by FAM-immunofluorescence (24-well plates) and RT-qPCR (6-well plates).

5.7 IN VITRO PHAGOCYTOSIS ASSAY

The in vitro phagocytosis assay was adapted from (Beccari et al., 2018a) for both BV2 cells and primary microglia to distinguish engulfment and degradation of apoptotic cells. Primary microglia cells were allowed to rest for 24 hours before phagocytosis assay while BV2 cells were transfected, and the phagocytosis assay was performed after 24 hours of expression. Phagocytosis was performed in high glucose DMEM, supplemented 1% antibiotic-antimycotic (Gibco) and 10% FBS (GE Healthcare Hyclone) to ensure the presence of the complement molecules, such as C1q, that have been related to phagocytosis in vivo (Diaz-Aparicio & Sierra, 2019b) and determine the immunomodulatory outcome of phagocytosis (Fraser et al., 2010). Primary microglia and BV2 cells were fed with apoptotic vampire SH-SY5Y, previously treated with staurosporine (3µM, 4h, Sigma) to induce apoptosis. Only the floating fraction of apoptotic cells were added in a 1:1 ratio after their visualization and quantification with trypan blue in a Neubauer chamber. Apoptotic cells were identified by trypan blue staining: primary apoptotic cells are not permeable to trypan blue due to their membrane integrity whereas necrotic and

secondary apoptotic cells are stained with trypan blue due to their membrane disruption. Primary microglia and BV2 cells were left to interact with the added apoptotic cells for 1 hour to assess their engulfment. In some experiments, apoptotic cells were added at 1:9 proportion and were left to interact with microglia for 30 minutes. After that time, the non-phagocytosed apoptotic cells were removed by thoroughly washing with 1X PBS twice after which primary microglia and BV2 cells were left to degrade the engulfed cell for 3 more hours to assess degradation.

In some experiments microglia were pre-treated and/or treated during the phagocytosis assay. For OND experiments cells were pre-treated for 3 hours and OND was applied during the engulfment (1 hour) and degradation (3 hours) of the phagocytosed cargo. For MRT experiments, cells were pre-treated for 5 hours and MRT was added during the engulfment (1 hour) and degradation (6 hours) of the phagocytosed cargo. For rapamycin experiments, the engulfment groups were pre-treated for 20 hours followed by 1 hour of rapamycin or vehicle during engulfment. The degradation groups were pre-treated for 20 hours flowed by 1 hour of engulfment and 3 hours of degradation in the presence or absence of rapamycin.

5.8 LYSOSOMAL pH MEASUREMENT ASSAY: LIVE IMAGING

The lysosomal pH was measured using a fluorescence ratiometric assay. Primary WT microglia were incubated with a dextran molecule conjugated to two fluorophores fluorescein (FITC, pH sensitive) and tetramethylrohadamine (TRITC, pH stable) (70,000 MW, anionic, Fisher). The fluorescence of both fluorophores was measured by confocal microscopy and the ration between FITC/TRITC was calculated (Majumdar et al., 2007). The fluorescence emitted by FITC, which is pH sensitive, was proportionally quenched to the lysosomal pH values and, thus, the ratio between the two fluorophores allowed us to indirectly quantify the lysosomal pH in control conditions and after OND. Microglia were incubated with 2mg/mL of dextran for 15 hours for its internalization. Then, dextran excess was removed by thorough washing with PBS and control cells were incubated in complete high glucose DMEM medium, supplemented 1% antibiotic-antimycotic (Gibco) and 10% FBS (GE Healthcare Hyclone) for 3.5 hours allowing the dextran to be delivered to the lysosomes (chase pulse). For the OND group the chase was partially done under OND conditions (control 0.5 hours plus OND 3 hours). Next, control cells were washed with imaging medium (150 mM NaCl, 20 mM HEPES, pH 7.4, 1 mM CaCl2, 5 mM KCl, and 1 mM MgCl2, 0.2% glucose) and the OND group was imaged in OND buffer to avoid the addition of nutrients and glucose and hence the loss of the treatment effect. Single plane images were taken using a Leica TCS STED CW SP8 laser scanning microscope using the 63X oil-immersion objective

and 2X zoom. Images were analyzed using the Fiji/ImageJ free software and fluorescence intensity was measured for each individual cell. Brightness, contrast, and background were adjusted equally for the entire image using the "brightness and contrast" and "levels" controls from the "image/adjustment" set of options without any further modification. In each experiment, calibration curves were generated from dextran-loaded cells to a range of pH (50mM Tris Maleate adjusted to pH 3.5, 4.0, 4.5 and 5.5), fixed in 4% paraformaldehyde for 10 minutes at RT and equilibrated for 20 minutes in the corresponding pH buffer. Data are shown normalized to the control of each experiment to reduce interexperimental variability.

5.9 LYSOSOMAL ENZYMATIC ACTIVITY ASSAY

Lysosomal activity was measured using the commercial Lysosomal Intracellular Activity Assay Kit according to the manufacturer´s instructions (Abcam, ab234622). Cells were incubated with a self-quenched substrate, washed with 1mL of ice-cold 1X assay buffer and immediately imaged. Single plane images were taken using a Leica TCS STED CW SP8 laser scanning microscope using the 63X oil-immersion objective and 1.5X zoom. Images were analyzed with the Fiji/ImageJ free software and mean fluorescence intensity was measured for each individual lysosome. Brightness, contrast, and background were adjusted equally for the entire image using the "brightness and contrast" and "levels" controls from the "image/adjustment" set of options without any further modification. The de-quenching of the substrate and the fluorescence emission proportionally correlated with the amount of the degradative lysosomal activity (Humphries & Payne, 2012). Intensity, lysosomal number, and occupied area values were normalized to the cell area. Data are shown normalized to the control of each experiment to reduce inter-experimental variability.

5.10 WESTERN BLOT

Primary microglia and BV2 cells were lysed in RIPA buffer (Sigma) containing protease and phosphatase inhibitor cocktail (Fisher). The cell lysate was collected and centrifuged (10.000xg, 10 min). The solubilized protein was quantified by BCA Assay Kit (Fisher) in triplicates at 590nm using a microplate reader (Synergy HT, BioTek). 15 to 20 µg of ß-mercaptoethanol denatured protein were loaded in Tris-glycine polyacrylamide gels (14%) and run for 90 minutes at 120V. The resolved proteins were then transferred to a nitrocellulose membrane at 220mA for 2 hours and the transfer efficiency was verified by Pounceau staining (Sigma). The membranes were then blocked for 1hour in 5% milk prepared in Tris Buffered Saline with 0.1% Tween-20 (TBS-T) buffer. Membranes were afterwards incubated with rabbit primary antibody to LC3 (1:3.000,

NB100-2220, Novus Biologicals), and mouse primary antibody to β-actin (1:5.000, Sigma), in TBS-T containing 4% Bovine Serum Albumin (BSA) overnight (4°C, shaker). Next day, membranes were rinsed and incubated with Horseradish Peroxidase (HRP) conjugated anti-rabbit (1:5,000) and anti-mouse (1:5,000) secondary antibodies (Cell Signaling) for BV2 experiments or the fluorescent secondary antibodies StarBright Blue 700 anti-mouse (1:5,000, BioRad) and StarBright Blue 700 anti-rabbit (1:5,000, BioRad) for primary microglia, vampire SH-SY5Y and astrocytes experiments in TBS-T containing 5% milk powder. After rinsing membranes, protein was analyzed in a ChemiDoc imaging system (BioRad). Band intensity was quantified using the Gel Analyzer method of Fiji software.

5.11 IMMUNOFLUORESCENCE

5.11.1 Brain tissue sections and organotypic slices

Six series of 50µm-thick sections of brain were cut using a Leica VT 1200S vibrating blade microtome (Leica Microsystems GmbH, Wetzlar, Germany). Immunostaining was performed following standard procedures (Abiega et al., 2016; Beccari et al., 2018a). Free-floating sagittal sections were incubated in blocking and permeabilizing solution (0.3% Triton X-100, 0.5% BSA in 1X PBS) for 2 hours at RT and de incubated overnight at 4°C with the primary antibodies diluted in the permeabilizing solution (**Table 2**). Organotypic hippocampal slices were processed using 0.2% Triton X-100, 3% BSA in 1X PBS as permeabilizing solution. After thorough washing with 1X PBS, the brains sections and organotypic slices were incubated with fluorochrome-conjugated secondary antibodies and DAPI (5 mg/ml) diluted in the corresponding permeabilizing solution for 2 hours at RT. Brain sections and organotypic slices were mounted on glass slides with DAKOCytomation Fluorescent Mounting Medium (Agilent) after washing with 1X PBS (**Table 2**).

5.11.2 Primary microglial cultures and BV2 cells

Primary microglia cultures were fixed in 4% PFA for 10 minutes al RT after which they were transferred to 1X PBS and stored at 4°C until immunofluorescence was performed. Fluorescent immunostaining was carried out following standard procedures (Abiega et al., 2016; Beccari et al., 2018a). Primary microglia attached and fixed to 12 mm coverslips, were blocked and permeabilized in washing solution (0.2% Triton X-100, 0.5% BSA in 1X PBS) for 30 minutes at RT. Next, cells were incubated with primary antibodies in the washing solution overnight at 4°C. After, cells were rinsed twice with 1X PBS incubated in the secondary antibodies containing DAPI (5 mg/ml) in the washing solution for 1 hour at RT. Last, cells were rinsed in 1X PBS and mounted on glass slides with DAKOCytomation Fluorescent Mounting Medium (Agilent).

Antibodies				
Primary	Host	Dilution	Source	Catalogue #
activated caspase 3	Rabbit	1:1000	Cell Signaling	#9664
CD11b	Rat	1:200	BioRad	MCA711
cFos	Rabbit	1:750	Santa Cruz, Biotechnologies	sc-52/ sc-166940
GFP	Chicken	1:1000	Aves Lab	#GFP-1020
Iba1	Rabbit	1:1000	Abcam	#019-19741
NeuN	Mouse	1:750	Millipore	#MAB377
P2Y12	Rabbit	1:1000	Anasec	#AS-55043A
Secondary	Host	Dilution	Source	Catalogue #
AlexaFluor 488 goat anti-chicken		1:1000, 1:500	Life Technologies	#A11039
AlexaFluor 488 goat anti-rabbit		1:500	Jackson Immunology Research	111-545-144
AlexaFluor 488 goat anti-rat		1:1000	Jackson Immunology Research	112-545-167
AlexaFluor 647 goat anti-mouse		1:500	Jackson Immunology Research	#115605003
AlexaFluor 647 goat anti-rabbit		1:1000, 1:500	Jackson Immunology Research	#111605003
AlexaFluor RRX goat anti-rabbit		1:1000, 1:500	Jackson Immunology Research	#111295144
AlexaFluor RRX goat anti-rat		1:1000	Jackson Immunology Research	112-295-167
AlexFluor 647 donkey anti-mouse		1:500	Fisher (Spain)	#A31571
AlexFluor RRX donkey anti-goat		1:500	Jackson Immunology Research)	705-295-147
AlexFluor RRX donkey anti-rabbit		1:500	Jackson Immunology Research	711-295-152

DAPI		1:1000	Sigma-Aldrich	#D9542.10mg
Western blot antibodies	Host	Dilution	Source	Catalogue #
Horseradish Peroxidase (HRP) anti-mouse secondary antibodies		1:5000	Cell Signaling	#7076
Horseradish Peroxidase (HRP) conjugated anti-rabbit		1:5000	Cell Signaling	#7074
LC3 (rabbit)		1:3000	Novus Biologicals	NB100-2220
ß-actin (mouse)		1:5000	Sigma	A5441
StarBright Blue 700 Goat anti-mouse IgG		1:5000	BioRad	12004159
StarBright Blue 700 Goat anti-rabbit IgG		1:5000	BioRad	12004162

***Table 2**. List of antibodies used in this PhD thesis.*

5.12 PHAGOCYTOSIS ANALYSIS

Apoptotic cells were defined based on their nuclear morphology visualized by the nuclear marker DAPI, which stains DNA. In apoptotic cells the chromatin structure was lost and appeared condensed and/or fragmented (pyknosis/ karyorrhexis), whereas live cells euchromatin (loosely packed and lightly stained) and heterochromatin (densely packed and darkly stained) are well defined and structured. Phagocytosis was defined as the formation of a fully enclosed and three-dimensional pouch around each apoptotic cell, either emerging from a microglial process or by phagocytosis through direct apposition of the microglial soma (Abiega et al., 2016; Sierra et al., 2010).

All fluorescence immunostaining images were collected using a Leica SP8 laser-scanning microscope using a 40x oil-immersion objective and a z-step of 0.7µm. All images were imported into the Fiji distribution of ImageJ in Tiff format. Brightness, contrast, and background were adjusted equally for the entire image using the “brightness and contrast” and “levels” controls from the “image/adjustment” set of options without any further modification. For primary cultures 3-5 random z-stacks were analyzed from 3 independent coverslips. For mouse tissue

sections, 2-5 20µm-thick z-stacks located at random positions containing the DG were collected per hippocampal section, and a minimum of 6 sagittal sections per series were analyzed.

5.12.1 Phagocytosis analysis in tissue sections and organotypic slices

In tissue sections and organotypic slices, the number of apoptotic cells, phagocytosed cells, and microglia were estimated using unbiased stereology in the volume of the DG contained in the z-stack (determined by multiplying the thickness of the stack by the area of the DG at the center of the stack using ImageJ, Fiji). To obtain the total numbers in tissue sections, this density value was then multiplied by the volume of the septal hippocampus (spanning from -1 to -2.5 mm in the AP axes, from bregma; 6 slices in each of the 6 series) which was calculated using Fiji from Zeiss Axiovert epifluorescent microscope images collected at 20X. To calculate the phagocytosis parameters, the following formulas are used (Beccari et al., 2018a):

Phagocytic Index: proportion of apoptotic cells engulfed by microglia. Phagocytosed apoptotic cells (apo^{Ph}); total apoptotic cells (apo^{tot}).

$$Ph\ index = \frac{apo^{Ph}}{apo^{tot}} \times 100$$

Phagocytic capacity: proportion of microglia with one or more phagocytic pouches, each containing one apoptotic cell (Sierra et al., 2010) Microglia (mg); microglia with one or more phagocytic pouches (Phn).

$$Ph\ capacity = \frac{mgPh1 + 2mgPh2 + 3mgPh3\ \ldots nmgPhn}{mg}$$

Phagocytosis/Apoptosis coupling: net phagocytosis (number of microglia multiplied by their phagocytic capacity) divided by the number of apoptotic cells (Abiega et al., 2016).

$$Ph/A\ coupling = \frac{Ph\ capacity \times microglia}{apotot}$$

5.12.2 Phagocytosis analysis in cells

In primary cultures and BV2 cells phagocytosis experiments, the number of total microglial cell was calculated, and microglial processes were scanned for DAPI or RFP (from apoptotic SH-SY5Y)

inclusions. The number of microglia with DAPI or RFP inclusions was divided by the total number of microglia to calculate the percentage of phagocytic microglia. In the engulfment-degradation experiments, the engulfment percentage was calculated as mentioned, normalized to the control group. The degradation in each experimental condition was calculated by subtracting the percentage of phagocytic microglia at 3 hours from the percentage of phagocytic microglia in the control group at 1 hour.

5.13 TRANSMISION ELECTRON MICROSCOPY (TEM)

Five-million primary microglial cells were cultured in 60 mm diameter plates (Nunclon, ThermoFisher) and exposed to OND for 3 hours. Subsequently, primary microglia were rinsed in PBS and pre-fixed as an adherent cell monolayer using 0.5% glutaraldehyde solution in Sörensen buffer 0.1M pH=7.4 (SB) (10 mins, RT). After scraping the pre-fixed cells, primary microglia were centrifuged (800g, 5 mins, RT) to form a pellet and fixed in 2% glutaraldehyde solution in SB (overnight, 4ºC). Primary microglia were then rinsed with 4% sucrose in SB and post-fixed with 1% osmium tetroxide in SB (1h, 4ºC, darkness). After rinsing, primary microglia were dehydrated in a growing concentration series of acetone. After dehydration, primary microglia samples were embedded in epoxi resin EPON Polarbed 812 (Electron Microscopy Sciences). Semi-thin sections (1 µm thick) were stained with toluidine blue to identify the regions of interest. Ultra-thin sections were cut using a LEICA EM UC7 ultramicrotome and contrasted with uranyl-acetate and lead citrate. The ultrastructural analysis was done with a Transmission Electron Microscope Jeol JEM 1400 Plus at 100 kVs equipped with a sCMOS digital camera.

5.13.1 TEM analysis

Image analysis (4-6 images per cell) was performed in 36-38 cells per experimental condition using Fiji. Autophagic-like vesicles (containing at least a portion of double membrane with granular, membranous, and heterogeneous cargo) and lysosomal-like vesicles (electron-dense vesicles with single or double membrane) were identified manually, and their perimeter was selected to generate regions of interest (ROIs) in each image. The area of the cellular cytoplasm (μm^2) was also identified and selected manually to generate a ROI in each image. Subsequently, the number (vesicles) and area (vesicles and cytoplasm, μm^2) of ROIs were measured. Finally, the quantitative data coming from ROIs of the images belonging to the same cell were grouped and the number of autophagic-and lysosomal-like vesicles per μm^2 was calculated dividing the number of vesicles present in the cell by its cytoplasm area (μm^2). The percentage of cytoplasm area occupied by autophagic- and lysosomal-like vesicles per each cell was calculated by

summing up the areas of individual vesicles and relating it to the cellular cytoplasmic area, which was considered 100%.

5.14 FACS SORTING

Microglia were isolated from 1 month old mouse hippocampi (Abiega et al., 2016; Sierra et al., 2007). In brief, the brains from fms-EGFP mice were enzymatically disaggregated (enzymatic solution, in mM: 116 NaCl, 5.4 KCl, 26 NaHCO3, 1 NaH2PO4, 1.5 CaCl2, 1 MgSO4, 0.5 EDTA, 25 glucose, 1 L-cysteine; with papain (20 U/ml) and DNase I (150 ul; Invitrogen) for at 37°C for 15 min. The enzymatic digestion was accompanied by mechanical disaggregation through careful pipetting. After homogenization, the cell suspension was filtered through a 40µm nylon strainer to a 50 ml Falcon tube quenched by 5 ml of 20% FBS in HBSS. To enrich the microglial population, myelin was removed by using Percoll gradients; cells were centrifuged at 200g for 5 min and resuspended in a 20% solution of isotonic Percoll (SIP; 20% in PBS), obtained from a previous SIP stock (9 parts Percoll, 1-part 10X PBS). Each sample was layered with HBSS poured very slowly by fire-pulled pipettes. Afterwards, gradients were centrifuged for 20 min at 200g´s with minimum acceleration and no brake so the interphase was not disrupted. Then, the interphase was removed, cells were washed in HBSS by centrifuging at 200g´s for 5 min and the pellet was resuspended in 500 µl of sorting buffer (25 mM HEPES, 5 mM EDTA, 1% BSA, in HBSS). Microglia cell sorting was performed by FACS Jazz (BD Biosciences, in which the population of green-fluorescent cells was selected, collected in lysis buffer (Qiagen) containing 0.7% beta-mercaptoethanol and stored at -80°C until processing.

5.15 RNA ISOLATION AND RETROTRANSCRIPTION

RNA from FACS-sorted microglia was isolated by RNeasy Plus micro kit (Qiagen) according to the manufacturer's instructions and retrotranscribed using the iScript Advanced cDNA Synthesis Kit (BioRad). RNA from transfected BV2 cells was isolated by RNeasy Plus mini kit (Qiagen) according to the manufacturer´s instructions and retrotranscribed using the Superscript III Reverse Transcriptase (Invitrogen) in a Veriti Thermal Cycler (Applied Biosystems).

5.16 REAL-TIME qPCR

Real-time qPCR was performed following MIQE guidelines (Minimal Information for Publication of Quantitative Real Time Experiments) (Bustin, 2010). Three replicas of 1.5µl of a 1:3 dilution of cDNA were amplified using SsoFast EvaGreen Supermix (Bio-Rad) for FACS-sorted microglia and Power SYBR Green (Bio-Rad) for BV2 transfected cells in a CFX96 Touch Real-Time PCR

Detection System (Bio-Rad). The amplification protocol for both enzymes was 3 min 95°C, and 40 cycles of 10 s at 95°C, 30 s at 60°C.

5.16.1 Primers

Cstb, cathepsins B L and *S* commercial primers were purchased from Sigma-Aldrich (**Table 3**). Their specificity was assessed using melting curves and electrophoresis in 2% agarose gels. For each set of primers, the amplification efficiency was calculated using the software LinRegPCR (Ramakers et al., 2003)or standard curve of 1:2 consecutive dilutions, and was used to calculate the relative amount using the ΔΔCt following formula:

$$\Delta\Delta Ct = \frac{(1 + eff.target\ gene)^{(Ct\ sample - Ct\ control)}}{(1 + eff.reference\ gene)^{(Ct\ sample - Ct\ control)}}$$

Up to three independent reference genes were compared: L27A, which encodes a ribosomal protein of the 60S subunit (Sierra et al., 2007); OAZ-1, which encodes ornithine decarboxylase antizyme, a rate-limiting enzyme in the biosynthesis of polyamines and recently validated as a reference gene in rat and human (Kwon et al., 2009); and HPRT, which encodes hypoxanthine guanine phosphoribosyl transferase (van de Moosdijk & van Amerongen, 2016). The expression of L27A, OAZ-1, and HPRT remained constant independently of time and treatments, validating their use as reference genes. The reference gene that rendered lower intragroup variability was used for statistical analysis.

Primers				
	Gene	**Gene Bank**	**Amplicon size (bp)**	**Sequence 5´-3**
Reference Genes	**HPRT**	NM_013556.2	150	Fwd ACAGGCCAGACTTTGTTGGA
				Rv ACTTGCGCTCATCTTAGGCT
	OAZ	NM_008753	51	Fwd TGGCCTTCCGTGTTCCTAC
				Rv CCCCGGACCCAGGTTACTAC
	L27A	BC086939	101	Fwd TGTTGGAGGTGCCTGTGTTCT
				Rv CATGCAGACAAGGAAGGATGC
Interest Genes	**Cystatin B (mouse)** (FACSsorted microglia)	NM_007793.3	111	Fwd GTGCTACCCCGACTACTGCT
				Rv ATTCAAGCTGGGACTTCACCTGG
	Cystatin B (rat)	NM_012838.2	145	Fwd GAGATCGCCGACAAGGTGAA

	(BV2 transfection assays)			Rv GCACACATTTTTCTTCGCCG
	Cathepsin B	NM_007798.3	120	Fwd TGCGTTCGGTGAGGACATAG
				Rv CCAAATGCCCAACAAGAGCC
	Cathepsin L	NM_009984.4	104	Fwd TCGGTGACATGACCAATGAG
				Rv GGATCTTAAGCATCAGCGG
	Cathepsin S	NM_001267695.2	105	Fwd CCGAAGACTGTCACTTTCAGG
				Rv CACAAGAACCCTGGTATTTCAC

***Table 3**. List of primers used in this PhD thesis.*

5.17 APOPTOTIC CELL TO cFOS$^+$ NEURONS DISTANCE DETERMINATION

For each image, the 3D coordinates of cFos$^+$ and apoptotic cells of the granule layer (GL) were visually identified and saved using the Point tool of the Fiji distribution of ImageJ. Then, we used these coordinates to estimate the cartesian distances of each apoptotic cell to its closest cFos$^+$ neuron (nearest neighbor, NN) and to the nearest border of the image stack (X, Y and Z borders). This direct analysis, however, was hindered by the fact that most apoptotic cells were closer to a border of the z-stack (the upper or bottom Z border in most cases) than they were to a cFos$^+$ neuron (**Figure 48**). Therefore, the inclusion criteria for analyzing apoptotic-cFos+ distances were: $d_{cFosNN}<d_{border}$ (i.e., the calculated distance to cFos NN must be shorter than the distance to the closest border), and apoptotic-cFos+ distances that were further away than the distance to the closest border, which was the case for the vast majority of apoptotic cells, were discarded. We analyzed a total of 25 and 253 apoptotic cells collected from 2 series of sections from the GL of wild-type (WT) and KO mice, respectively. Out of these, only 5 phagocytosed and 15 non phagocytosed cells from n=9 KO mice, and one cell of each type in n= 9 WT mice passed the inclusion criteria. To ensure that our z-stacks did not have an intrinsic bias in either of the cell types, we confirmed that both phagocytosed and non- phagocytosed apoptotic cells were located in z-stacks of similar thickness (23.4 ± 0.6 vs 24.3 ± 0.4 □m, respectively), and therefore had similar chance of detection.

5.18 MODELLING APOPTOTIC CELL TO cFOS$^+$ NEURONS DISTANCES

To generate the model, we first generated virtual 3D (v3D) cell location grids based on real granule neurons. On these grids, we placed apoptotic cells and cFos$^+$ neurons in 10,000 simulations and calculated cumulative probability distribution function of the distance between apoptotic and NN cFos$^+$ cells

1. Generation of v3D cell location grids from real WT and KO z-stack images. To model the distances between apoptotic and cFos+ cells we generated v3D grid locations of all granule neurons ($NeuN^+$) and apoptotic cells from 16 representative confocal z-stack images from WT and KO mice (8 z-stacks each). For each set of z-stack images, the 3D coordinates of $NeuN^+$ granule neurons and apoptotic cells of the GCL were visually identified and saved using the Point tool of Fiji. These coordinates were pooled to generate a v3D grid for each z-stack, on which $cFos^+$ and apoptotic cells were later positioned in four different random models (see below). The computations for the models were performed in Matlab (MathWorks, Natick, MA).

2. *Number of cFos-positive and apoptotic cells located in each virtual 3D grid*. The number of apoptotic cells located in each v3D grid was derived randomly from a Gaussian probability distribution with mean and standard deviation (SD) obtained from the experimental apoptotic cell density (**Table 4**), multiplied by the total number of cells in the grid and finally approximated to the closest integer positive number. In the case of models 1-3, WT- and KO-derived v3D grids were filled according to the corresponding WT and KO densities, respectively. In model 4 we used inverted densities and filled the WT v3D grid from the KO density, and vice versa for the KO v3D grid. The number of $cFos^+$ cells located on the v3D grids either corresponded to the real count in the correspondent original z-stack (models 1, 2 and 4) or was assigned randomly from a Gaussian probability distribution (model 3) based on the cFos cell density (**Table 4**) and the total number of cells in the grid, similarly to what above described for the apoptotic cell number.

3. Simulations. For each v3D grid and each of the four models, 10,000 randomizations were performed, and the Euclidean distance between each apoptotic cell and its nearest $cFos^+$ cell was computed in each randomization. Specifically, we performed 100 cell number (*rn*) randomizations, each followed by 100 cell location *(rl)* randomizations. In each *rm*, the number of $cFos^+$ and apoptotic cells in the grid was defined by different criteria according to the four different models detailed above. For each model and for each condition (WT or KO), the cumulative probability distribution of the NN distances between cFos and apoptotic cells was next calculated with 1 m step and with 99% confidential intervals, by pooling data from the 10,000 simulations and the eight corresponding (WT or KO) v3D grids.

Experimental value	Group	Mean	SD	n
Apoptotic/NeuN$^+$	**WT**	0.0005	0.0003	4
	KO	0.0052	0.0007	4
cFos/NeuN$^+$	**WT**	0.0240	0.0075	4
	KO	0.0265	0.0073	4

Table 4. *Summary of experimental values used for mathematical modelling.*

5.19 STATISTICAL ANALYSIS

SigmaPlot (San Jose, CA, USA) and GraphPad Prism (San Diego, CA, USA) were used to perform the statistical analysis. Data was tested for normality and homocedasticity. When the data did not comply with these assumptions, a logarithmic transformation (Log_{10}, Log_{10}+1, of Ln) or a square root was performed, and the data was analyzed using parametric tests. Two-sample experiments were analyzed by Students´ t-test and more than two sample experiments with one-way or two-way ANOVA. In case that homoscedasticity or normality were not achieved with a logarithmic transformation, data were analyzed using a Kruskal-Wallis ranks test, followed by Dunn method as a *posthoc test. Two sample non-parametric data was analyzed using Mann Whittney U test.* Only $p < 0.05$ is reported to be significant.

Resources	
Equipment	Source
FACS Jazz (2B/4YG)	BD Biosciences
Chemidoc MP imaging system	Bio-Rad
TCS STED CW SP8 laser scanning microscopy	Leica
VT 1200S vibrating blade microtome	Leica
Hypoxia chamber	Biospherix
Microplate reader	SynergyHT, BioTek

Pannoramic MIDI II, automated digital slide scanner	3DHistech
Software	**Source**
ImageJ (Fiji)	https://imagej.nih.gov/ij/
SigmaPlot	http://sigmaplot.co.uk/index.php
GraphPad Prism	https://www.graphpad.com
LinRegPCR	https://www.gear-genomics.com
CFX Manager™ Software	https://www.bio-rad.com

Table 5. *Summary of equipment used in this PhD thesis.*

Results

6. Results

Microglial phagocytosis and autophagy are mechanistically similar processes oriented to the recycling of extracellular own and components to ensure the maintenance of the tissue homeostasis. as we have described in the introduction, microglial phagocytosis of apoptotic cells is a fast and efficient process, actively immunomodulatory, essential to avoid the tissue damage as a consequence of the spill-over of the cytotoxic content that results from the cell death. We have demonstrated that phagocytosis is blocked in a pharmacological model of MTLE (Abiega et al., 2016) and that phagocytosis actively regulates hippocampal neurogenesis (Diaz-Aparicio et al., 2020). We have also observed an impaired phagocytosis in a model of stroke, tMCAo, where microglia are not able to remove the apoptotic corpses (**Figure 14**). The lack of oxygen and nutrients that occurs during stroke, could trigger the initiation of an autophagy response that might interfere with phagocytosis, as they are very similar and convergent processes in the lysosomal compartment.

To confirm this hypothesis, in the first section, we will study the cellular and molecular mechanisms underlying the phagocytosis impairment we had initially observed during stroke (**Figure 14: Aim 1**) and its relationship with the lack of oxygen and nutrients during stroke, including the induction of autophagy. In the second section, we will describe a conceptual model to discriminate between autophagosome formation and degradation using conventional western blot LC3 flux assays (**Aim 2**) and establish with precision where a certain stimulus is acting on the autophagy cascade. Finally, in the third section I will study the role of a lysosomal gene, *Cstb*, on microglial phagocytosis in a model of genetic epilepsy (**Aim 3**) and confirm the mechanisms by which microglial phagocytosis.

6.1 IN SILICO ANALYSIS OF MICROGLIAL PHAGOCYTOSIS-RELAYED GENES IS NOT ENOUGH TO UNRAVEL THE MECHANISMS SUBSEQUENT TO STROKE

To determine whether transcriptional changes underlie the MCAO-induced phagocytosis impairment, we first analysed recently published RNA sequencing (RNA-Seq) databases from mice or rat MCAo models (Androvic et al., 2020; Beuker et al., 2022; Kang Guo et al., 2021; Rajan et al., 2019; Zheng et al., 2022). To compare among databases, we set a threshold of significance for genes with a fold-change (FC) in expression above 0.5 or below -0.5, and an adjusted p-value<0.05. While none of these studies originally discussed alterations in phagocytosis-related

genes in their unbiased analysis, we used the functional annotation tool DAVID to determine whether the significantly regulated genes in each of those databases was related to the Gene Ontology (GO) term Phagocytosis (GO:0006909) (**Figure 17**). We found that the Phagocytosis GO term was only significantly regulated in a bulk RNA-Seq study of permanent MCAo in mice at 3d by Androvic and cols (Androvic et al., 2020)and in a microglial cluster in single cell (sc) RNA-Seq study of transient (90min) MCAo in mice at 1d (Zheng et al., 2022). In addition, the sub-term Positive regulation of phagocytosis (GO:0050766) was regulated in the Androvic study (Androvic et al., 2020) and in another bulk RNA-Seq study of transient MCAo (60min) at 1d by Guo and cols. (Guo et al., 2015). However, in these three studies, the percentage of phagocytosis-related genes over the total significant genes was very small (0.7-3.9%), which is likely the reason why the original papers did not report it as a relevant finding. In addition, the most recent scRNA-Seq study of FACS-sorted leukocytes by Beuker and cols. did not identify changes in phagocytosis in either of the microglial clusters (Beuker et al., 2022). They also discovered a new cluster of stroke-associated myeloid cells (SAMCs), in which they reported changes in lipid metabolism genes and increased lipid uptake in vitro, suggestive of myelin engulfment, but in which we found no significant regulation of the Phagocytosis GO term (**Figure 17**).

To delve more into the expression of individual genes related to phagocytosis, we cross-referenced the 380 genes listed in the Phagocytosis GO term with the five databases and found that the Androvic study reported significant changes in expression in only 24.2% of the Phagocytosis GO genes. This percentage dropped in the rest of the studies, down to 0.5% in some of the microglial clusters of the Beuker study (Supp. Figure 8B). Even more importantly, the majority of the genes with significant differential expression in either of the five studies had a very small FC (Supp. Figure 8C). We then used a Spearman rank order correlation matrix to understand whether the FC of individual genes followed the same expression pattern (up- or down-regulation) across databases. We only found a significant correlation (Spearman correlation coefficient 0.868, p=2E-07) between the Androvic and the Guo studies but not among the rest of the databases (largely due to the reduced number of significant genes; data not shown). In addition, most of the significantly regulated genes related to the Phagocytosis GO term in these two databases were upregulated: 88/92 genes in the Androvic study; and 24/28 genes, in the Guo study. Among these upregulated genes the positive regulators outnumbered the negative regulators of phagocytosis: 30 to 7 genes in the Androvic study and 10 to 1 gene in the Guo study. In light of the consistent dysfunction of phagocytosis we found in the in vivo model of stroke (**Figure 14**), these gene changes could be interpreted as a compensatory mechanism to recover phagocytosis efficiency. Altogether, this analysis suggests

that RNA-Seq studies are not necessarily the optimal strategy to identify functional changes in microglia, and that in MCAo models microglial phagocytosis is not regulated at the transcriptional level.

A

										Phagocytosis (GO:0006909)		Positive regulation of phagocytosis (GO:0050766)	
Database	**Model**	**Species, age & sex**	**Occlusion time**	**Analysis time**	**Region**	**Sample**	**Population**	**Analysis method**	**Comparison**	**% genes**	**adj p-value**	**% genes**	**adj p-value**
Androvic et al., 2020	MCAo	Mouse, 3mo, F	Permanent	3d	Ipsilateral parietal cortex	Whole tissue	All cell types	Bulk-RNAseq	tMCAO vs control	1.7	4.1*E-7	0.7	7.9*E-5
Guo et al., 2021	tMCAo	Mouse, 2.5mo, M	60min	24h	Ipsilateral penumbra cortex	Whole tissue	All cell types	Bulk-RNAseq	tMCAO vs control	2.5	n.s.	0.9	2.4*E-2
Rajan et al., 2019	tMCAo	Rat, adult	90 min	24h	Ipsilateral hemisphere	FACS-sorted microglia	Microglia	Bulk-RNAseq	tMCAO vs control	1.39	n.s.	0.54	n.s.
Zheng et al., 2021	tMCAo	Mouse, 2.5mo, M	60min	24h	Ipsilateral hemisphere	Whole tissue	Microglia Cluster	scRNAseq	tMCAO vs control	3.9	2.0*E-2	2.15	n.s.
Beuker et al., 2022	tMCAo	Mouse 3-4 mo, M	30-45 min	24-72h	Ipsilateral hemisphere	FACS-sorted leukocytes	Cluster 1	scRNAseq	tMCAO 24 vs 72h	5.4	n.s.	4,1	n.s.
							Cluster 2		tMCAO 24 vs 72h	3.2	n.s.	3.2	n.s.
							Cluster 3		tMCAO 24 vs 72h	3.7	n.s.	3.7	n.s.
							Cluster stress		tMCAO 24 vs 72h	5.8	n.s.	4.4	n.s.
							SAMC		tMCAO 24 vs 72h	4	n.s.	1.84	n.s.

B

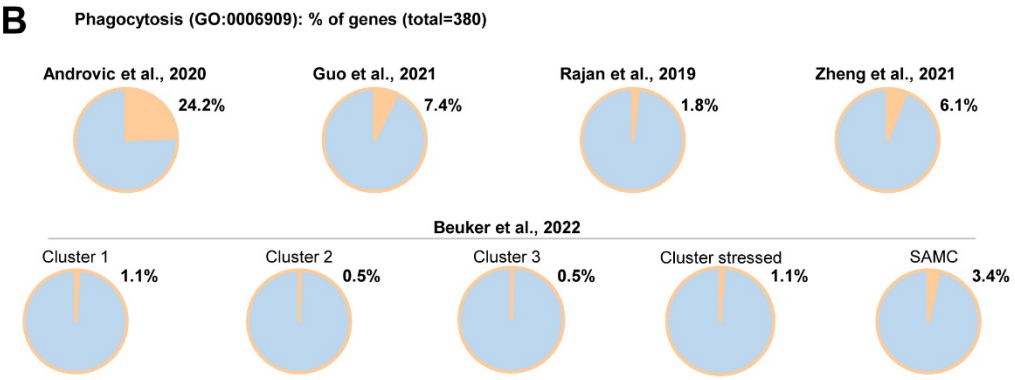

C

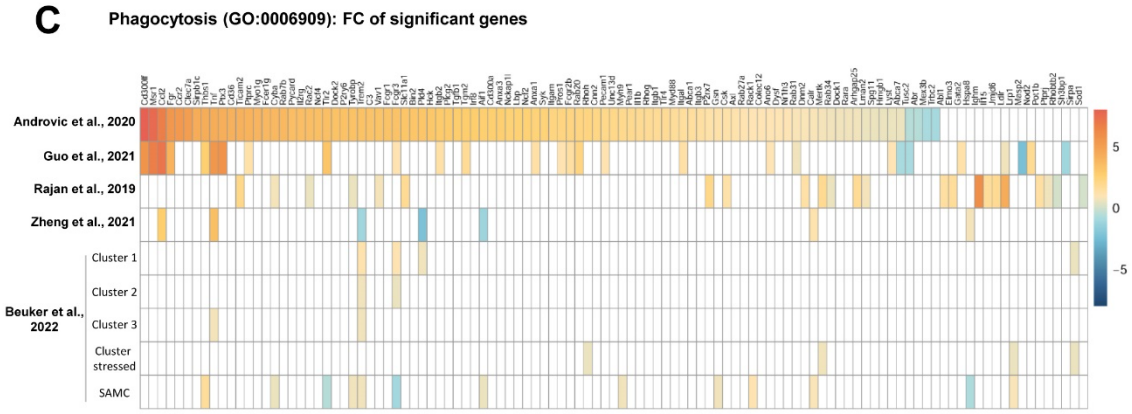

Figure 17. In silico analysis of RNA sequencing databases in stroke models. *[**A**] Table summarizing the variables of each of the bulk and single cell databases. The % of significantly changed genes (adjusted p-value<0.05 and -0.5>fold change >0.5) that belonged to the gene ontology terms (GO) Phagocytosis or Positive regulation of phagocytosis are shown, and whether they were found to significantly affect such GO terms using the DAVID functional annotation analysis tool (orange boxes) (p-value adjusted using Benjamini-Hochberg correction). [**B**] Pie charts summarizing the % of genes (orange) of the Phagocytosis*

GO term that were significantly regulated (adjusted p-value<0.05 and -0.5>fold change >0.5). C, Color-coded fold change of the significantly regulated genes of the Phagocytosis GO term found in at least one study (total=380 genes). SAMC are stroke-associated myeloid cells, a cluster of cells found in (Beuker et al., 2022).

6.2 OND REDUCED MICROGLIAL PHAGOCYTOSIS AND ALTERED ITS PHYSIOLOGY

In the in vivo model of stroke (tMCAo), we had initially demonstrated that microglial phagocytosis was impaired, preventing the removal of apoptotic cells (**Figure 14**). Herein, we hypothesize that this deficient phagocytosis could be related to the shortage of oxygen and nutrients associated to the reduced blood supply during stroke. To test this hypothesis, we used a model of oxygen and nutrient deprivation (OND) in hippocampal organotypic slices and primary microglial cultures.

6.2.1 Lack of oxygen and nutrients impaired microglial phagocytosis and reduced microglial motility in organotypic hippocampal slices

To assess the effects of OND on microglial phagocytosis, we first studied microglia in hippocampal organotypic slices. Cultures from P7 fms-EGFP mice were deprived of oxygen and nutrients (OND, salt solution and 1% oxygen) for 3 and 6 hours, followed by reperfusion for 1 more hour (**Figure 18A**, **B**). These cultures have ongoing cell death in basal conditions (Abiega et al., 2016), allowing us to measure basal phagocytosis and compare it to phagocytosis after OND. Apoptotic cells were identified by their nuclear morphology: condensed (pyknotic) and/or fragmented (karyorrhectic); and phagocytosis was defined as the formation of a fully enclosed three-dimensional pouch around the apoptotic cell (**Figure 18B**). First, we measured the number of apoptotic cells to assess the effect of OND on global cell death. Apoptosis increased after 3 and 6 hours of OND, regardless of reperfusion (**Figure. 18C**). This increased number in apoptotic cells was accompanied by a reduction in the phagocytic index (i.e., percentage of apoptotic cells engulfed by microglia) after 3 and 6 hours of OND (**Figure 18D**), confirming the phagocytosis impairment that took place in vivo after tMCAo (**Figure 14**). Importantly, this decrease in phagocytosis was reverted to control levels after 1 hour reperfusion (**Figure. 18D**), showing recovery of engulfment after the restoration of energetic conditions. Next, we measured the phagocytic capacity (Ph capacity, i.e., the number of phagocytic pouches with apoptotic cells per microglia cell) to determine if microglia were engulfing more apoptotic cells to overcome the increase of dead bodies after OND. The phagocytic capacity was also decreased after 3 and 6 hours of OND but was enhanced even beyond controls levels after reperfusion (**Figure 18E**). We found that after OND the number of microglia with no phagocytic pouches increased compared

to control conditions and microglial cells with one or more phagocytic pouches decreased after OND (**Figure 18F**). However, after reperfusion the number of non-phagocytic microglia decreased and microglia with more than one phagocytic pouch increased (**Figure 18G**), strengthening the hypothesis that microglial phagocytosis was restored after reperfusion.

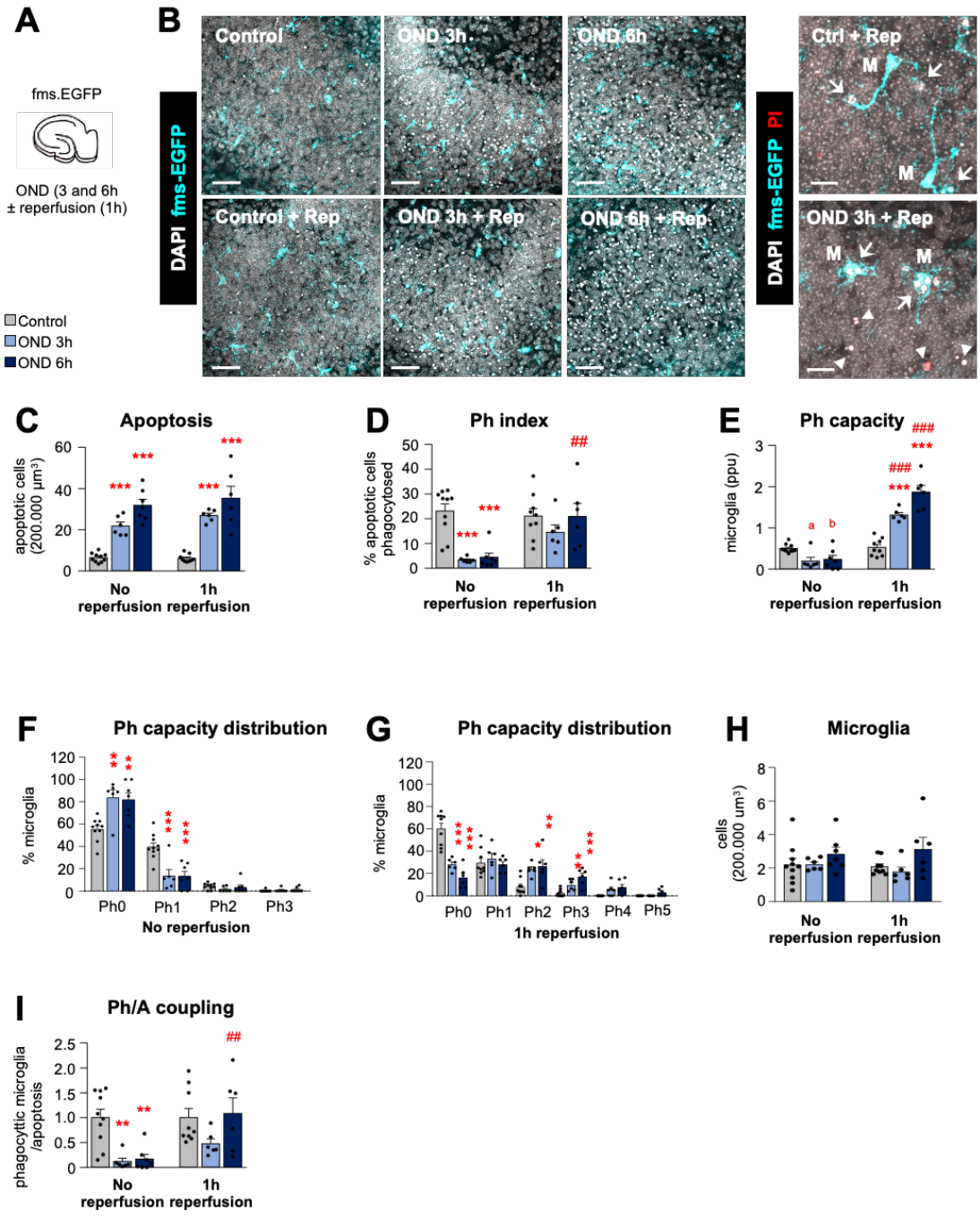

Figure 18. Engulfment of apoptotic cells in hippocampal organotypic slices was impaired after OND.

[A] *Experimental design showing the exposure of hippocampal organotypic slices (fms-EGFP) to OND (3 and 6 hours) in the presence and absence of 1h reperfusion.* ***[B]*** *Representative confocal images of the DG after OND. Normal or apoptotic (pyknotic/karyorrhectic) nuclear morphology was visualized with DAPI*

(white) and microglia by the transgenic expression of fms-EGFP (cyan). Under reperfusion conditions, membrane permeability (characteristic of necrotic cells) was observed with PI (red). High magnification images show primary apoptotic cells (pyknotic/karyorrhectic, PI^-) or secondary necrotic cells (pyknotic/karyorrhectic, PI^+) engulfed (arrows) or not-engulfed (arrowheads) by microglia (M) ($EGFP^+$). Secondary necrotic cells were very few and were pooled together with the rest of pyknotic/karyorrhectic cells and labeled as apoptotic thereafter. ***[C]*** *Number of apoptotic cells in 200.000µm^3 of the DG.* ***[D]*** *Ph index (% of apoptotic cells phagocytosed by microglia).* ***[E]*** *Weighted Ph capacity (number of phagocytic pouches containing an apoptotic cell per microglia, in parts per unit (ppu).* ***[F, G]*** *Ph capacity histogram after OND in non-reperfused* ***[F]*** *and reperfused* ***[G]*** *conditions.* ***[H]*** *Number of microglia in 200.000 µm^3 of the DG.* ***[I]*** *Ph/A coupling expressed as fold-change, ratio between net phagocytosis and total levels of apoptosis. Bars show mean ± SEM. n = 6-10 mice per group Data was analyzed by two-way ANOVA followed by Holm-Sidak post hoc tests* ***[C]****. When an interaction between factors was found, one-way ANOVA (factor: treatment) was performed followed by Holm-Sidak post hoc tests* ***[D-E, H-I]*** *or one-way ANOVA (factor: number of pouches) followed by Holm-Sidak post hoc tests* ***[F-G]****. To comply with homoscedasticity, some data was Log_{10} transformed* ***[C]*** *or Ln transformed* ***[I]*** *(* and #) represent significance between control and OND or between bafilomycin and no bafilomycin respectively: one-symbol represents p<0.05; two-symbols represent p<0.01; three-symbols represent p<0.001 (OND vs control). Scale bars=50µm, z=10.5µm* ***[B,*** *left panels****]****;15 µm, z=16.8µm* ***[B,*** *right panels****]****.*

We next assessed the impact of OND on microglial survival and found that microglial numbers were not altered by OND (**Figure 18I**). However, as OND induced net apoptosis, these results suggested that microglia might have a higher resilience to energetic depletion compared to other cell types (**Figure 18C**, **I**). Last, we assessed the coupling between phagocytosis and apoptosis, or the capacity of microglia to compensate the increase in apoptotic cells by increasing phagocytosis. Microglia have the capacity to proportionally adapt their phagocytic output to increased apoptotic cells, maintaining the coupling between apoptosis and phagocytosis. This Ph/A coupling is calculated as the product of the phagocytic capacity and microglia divided by total apoptosis, normalized to the control conditions (Beccari et al., 2018a). If microglia effectively match the increase in apoptosis by triggering their phagocytic potential, the coupling has a value of 1, whereas if microglia fail to overcome the increase in apoptosis, the coupling value is lower than 1. After OND, microglia were not able to face the increasing number of apoptotic cells, leading to an uncoupling between phagocytosis and apoptosis after 3 and 6 hours of OND that was reverted after 1 hour of reperfusion (**Figure 18H**). All together, these data show that microglial phagocytosis was severely impaired after OND, similar to the phagocytosis impairment found after tMCAo in vivo, but was rapidly recovered after 1 hour reperfusion due to the restoration of the oxygen and energy supply. However, this recovery was

not observed in vivo, where the impairment of phagocytosis continued up to 24h despite the reperfusion of the MCA (**Figure 14**). This discrepancy between in vitro and in vivo models is likely explained by the fact that in vivo, there is continued hypoxia due to pericyte death in rigor that prevents reperfusion of the damaged area (Hall et al., 2014). Moreover, the degradation of the extracellular matrix after stroke due to the release and action of metalloproteinases (MPP) leads to a disruption of the neurovascular function (Arai et al., 2011). Thus, in vivo there are more complex and additive mechanisms underlying the pathology of stroke that led to continued tissue hypoxia in spite of reperfusion. Nonetheless, our results in organotypic cultures confirm that energy depletion impairs microglial phagocytosis. To determine the cause of the impaired engulfment of apoptotic cells during OND, we next hypothesized that it could be related to a reduction in the motility of microglial processes during OND.

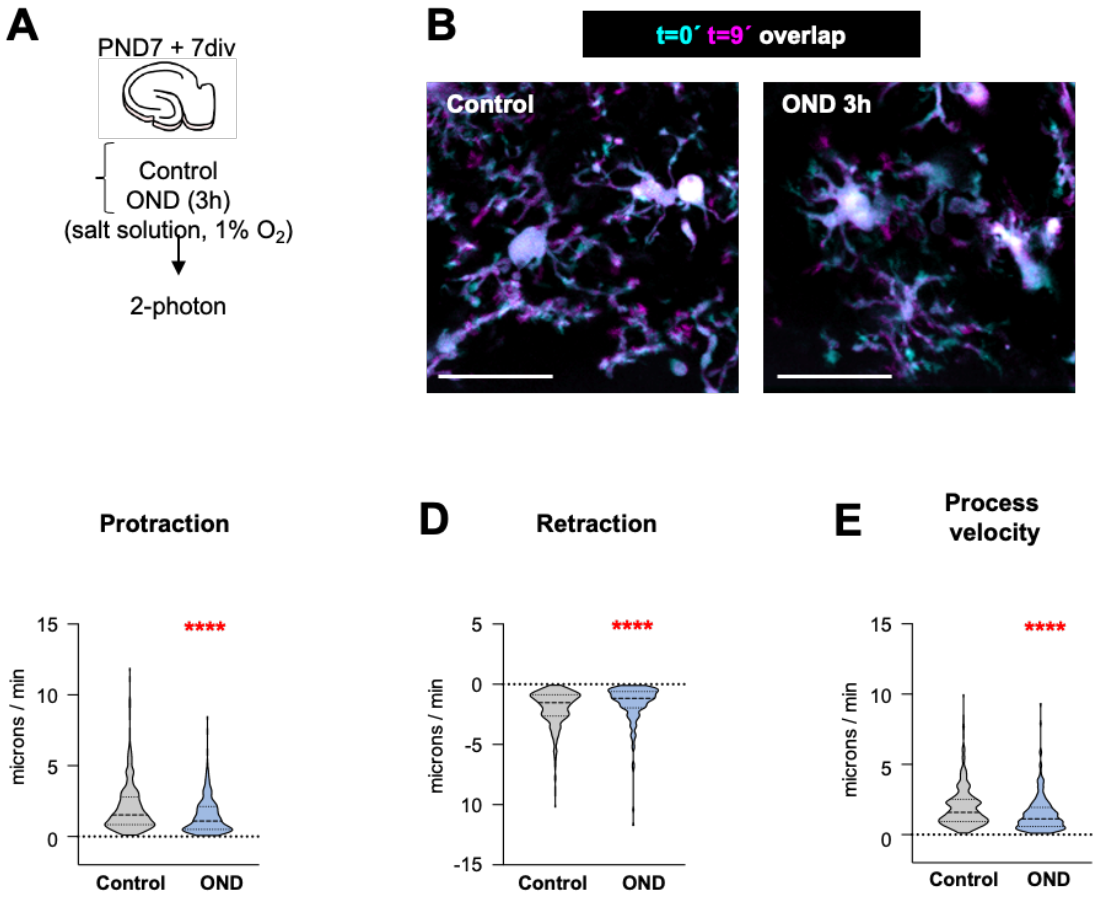

Figure 19. Microglial motility was reduced after OND. ***[A]*** *Experimental design showing the exposure of hippocampal organotypic slices (fms-EGFP) to OND (3 hours)* ***[B]*** *Representative projections of 2-photon images of microglial cells at t0 (cyan) and t9 (magenta) from hippocampal organotypic slices (CX3CR1$^{GFP/+}$) under control and OND conditions.* ***[C, D, E]*** *Microglial process motility: protraction* ***[C]****, retraction* ***[D]****, and process velocity* ***[E]****. Violin plots show the data distribution including extreme values; lower and upper hinges correspond to the first and third quartile respectively. n=355 processes from 98 cells from 12*

*animals (control), and n=222 processes from 57 cells from 9 animals (OND). Data was analyzed by Kruskal-Walli's rank test. **** indicates p<0.0001 Scale bars=20µm, z=22µm.*

Reduced process motility and surveillance due to the energy depletion under OND could prevent the finding and engulfment of apoptotic cells, leading to a reduction in phagocytosis. To confirm this hypothesis, we treated organotypic hippocampal slices with OND for 3 hours and assessed their process motility by two-photon microscopy (**Figure 19A**). This analysis was performed in CX3Cr1$^{GFP/+}$, where microglia constitutively express the green fluorescent protein (GFP) under the CX3Cr1 promoter and was not performed in fms-EGFP mice due to their lower endogenous fluorescence, which was not enough to perform the two-photon microscopy. Microglial process motility in the slices was assessed every 60 seconds for 10 minutes (**Figure 19B**). During imaging, organotypic slices were perfused with either DMEM in atmospheric conditions (control), or OND medium bubbled with nitrogen to remove the oxygen and maintain hypoxia. We found that both protraction (extension) and retraction (shortening) of microglial processes were reduced after OND compared to control (**Figure 19C, D**). Total process motility, including both protraction and retraction, was reduced after 3 hours of OND (**Figure 19E**). Thus, the lack of oxygen and nutrients reduced microglial motility and surveillance, likely preventing the engulfment of apoptotic cells in hippocampal organotypic slices, as microglia would not be able to extend their processes towards the apoptotic bodies.

6.2.2 Oxygen and nutrient deprivation impaired microglial degradation of apoptotic cells

To further identify the cellular mechanisms underlying the phagocytosis deficiency and dissect out the effect of oxygen and nutrient deprivation on engulfment and degradation of apoptotic cells by microglia, we used an in vitro model of phagocytosis in which primary microglia were fed with apoptotic cells (Beccari et al., 2018a; Diaz-Aparicio et al., 2020). We quantified the amount of phagocytosis at two time points to discriminate between engulfment and degradation (**Figure 20A**). Microglia were treated either with control media (DMEM) or OND for 3 hours and then co-cultured for 1h with SH-SY5Y apoptotic neurons, which expressed the red fluorescent protein tFP602 (RFP), in a 1:1 ratio, to assess engulfment. For the degradation experiments, the engulfment of apoptotic cells was performed under control conditions followed by degradation in control or OND: the non-phagocytosed neurons were removed from the culture and microglia were left to degrade the engulfed content for 3 more hours to assess degradation in DMEM or OND (**Figure 20A, B**). We quantified the percentage of microglia that formed a complete pouch around the apoptotic neurons and/or fragments of DAPI/vampire to

calculate the amount of cells engulfed (1h) and degraded (3h) in control and in OND conditions (**Figure 20C, D**). We used normalized data to discriminate more clearly the effect of OND on engulfment and degradation, by referring it to the phagocytosis percentage in control conditions (**Figure 20D-F**). We assessed engulfment by comparing the change in phagocytic microglia at 1 hour and found no significant changes between control and OND engulfment (**Figure 20E**). To assess degradation, we subtracted the percentage of phagocytic microglia after 3 hours to the engulfment percentage in the respective 1-hour control group. We observed a significant reduction in the amount of degradation under OND compared to control conditions (**Figure 20F**). Thus, OND induced a significant reduction in degradation but not in the engulfment of apoptotic cells in primary microglia.

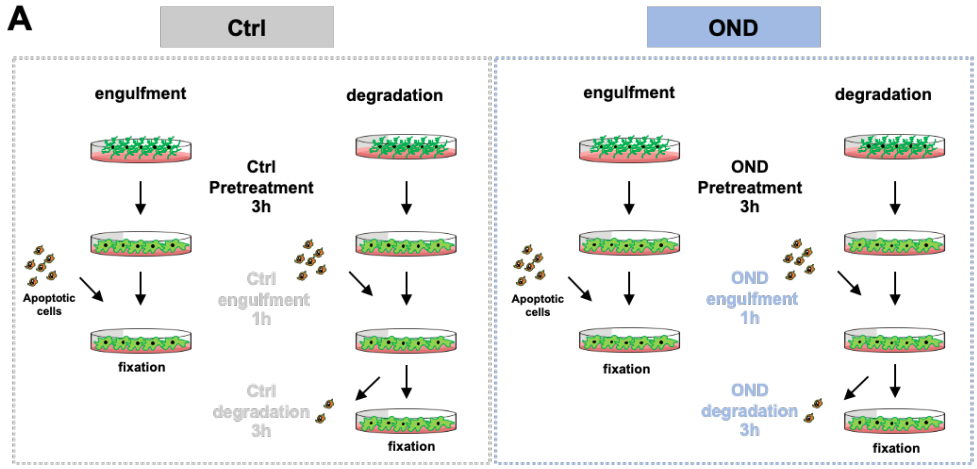

B

Group	Pretreatment (3h)	Engulfment (1h)	Degradation (3h)
Control ENG	Veh	Veh	-
Control DEG	Veh	Veh	Veh
OND ENG	OND	OND	-
OND DEG	Veh	Veh	OND

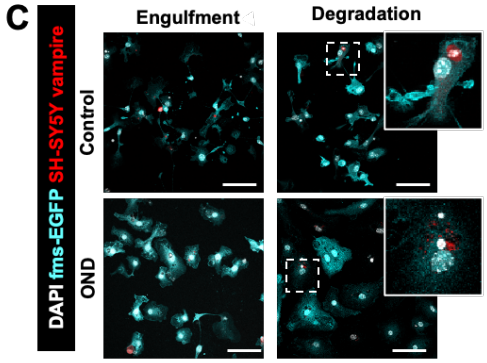

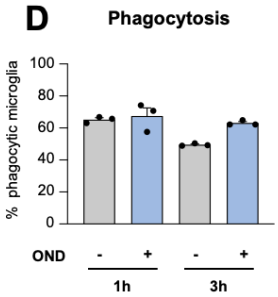

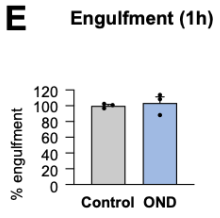

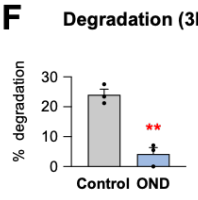

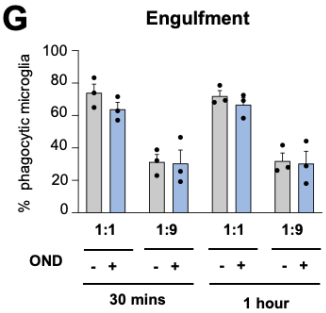

Figure 20. Degradation of apoptotic cells was impaired by OND in primary microglia. ***[A]*** *Experimental design of the phagocytosis assay to assess engulfment and degradation of apoptotic cells under control and OND conditions.* ***[B]*** *Table summarizing the treatments.* ***[C]*** *Representative images of primary microglia fed with apoptotic SH-SY5Y vampire cells during engulfment and degradation. Nuclei were visualized with DAPI (white), microglia by expression of EGFP (cyan), and SH-SY5Y neurons by expression of the red fluorescent protein Vampire.* ***[D]*** *Percentage of phagocytic microglia 1 and 3h after the addition of apoptotic cells (raw data).* ***[E, F]*** *Percentage of phagocytic microglia after engulfment (1h) and degradation (3h after engulfment). Only particles fully enclosed by microglia were identified as being phagocytosed.* ***[G]*** *Percentage of phagocytic microglia after the addition of different apoptotic SH-SY5Y vampire neuron to microglia ratios (1:1 and 1:9) after 30 min and 1h of engulfment under OND conditions. Bars show mean ± SEM. n=3 independent experiments. Data was analyzed Student´s t-test* ***[E-F]****. ** indicates p<0.01. Scale bars=5µm, z=8.5µm.*

The lack of effect of OND on engulfment was to some extent unexpected, given the reduction of phagocytosis we found in the tMCAo model in vivo and in organotypic slices (**Figure 14, 18**), and we speculated that it could be related to the super-optimal engulfment conditions in the in vitro model. Thus, we performed a second experiment in more stringent conditions, with a reduced number of apoptotic cells (1:9) at the standard (1h) and a shorter engulfment time (30 min). We found that decreasing the ratio of apoptotic cells to microglia (from 1:1 to 1:9) reduced the amount of phagocytic microglia in all groups, but OND still had no significant effect on engulfment either at 30min or 1h (**Figure 20G**). These results suggest that, regardless the ratio of apoptotic cells to microglia and the engulfment time, OND did not affect the engulfment step of phagocytosis in this in vitro model. However, it should be noticed that in vitro models do not fully recapitulate all the phagocytosis stages. In vivo, microglia have to find the apoptotic cells, following “find me” cues in the brain parenchyma, interpret “eat me” signals and, finally, engulf and degrade the apoptotic cell (Arandjelovic & Ravichandran, 2015; Sierra et al., 2013). In contrast, in vitro, all the signals and complexity of the brain are lost, as the apoptotic cells are directly placed next to microglia in a 2D system where spatial diffusion and fluid brain dynamics are absent. Nonetheless, this model allowed us to uncover the effect of OND in apoptotic cell degradation, which could not be observed in vivo because the deficient engulfment prevented us from observing downstream effects on degradation. To determine the cause of the degradative failure, we next assessed the health status of the main degradative organelle, the lysosome.

6.2.3 The lysosomal compartment was affected by the lack of oxygen and nutrients

Lysosomes are the main degradation organelles that digest the phagocytosed cargo. The observed alterations in apoptotic cell degradation under OND could result from a dysfunctional lysosomal compartment, for example due to decreased numbers or increased lysosomal pH, which must be acidic to activate lysosomal degradative enzymes (Hasilik, 1992; Saftig & Klumperman, 2009).

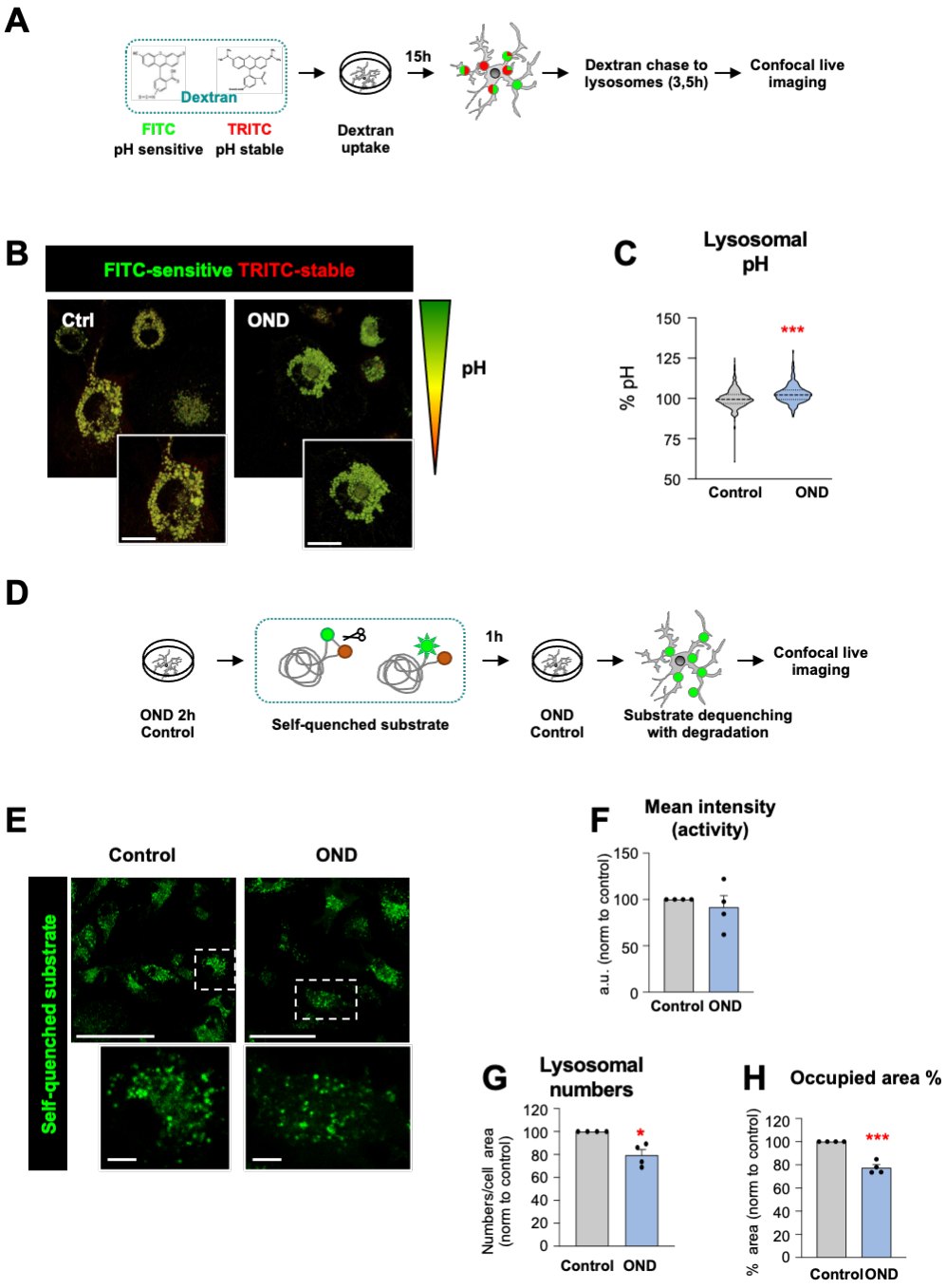

Figure 21. OND altered the lysosomal compartment in primary microglia. ***[A]*** *Experimental design showing a dextran molecule conjugated to FITC (pH sensitive) and TRITC (pH stable) whose ratio serves as an indirect measurement of the lysosomal pH.* ***[B]*** *Representative confocal images of microglia incubated with the dextran molecule, FITC (green) and TRITC (red).* ***[C]*** *Lysosomal pH expressed as % normalized to control values. Note the truncated Y axis.* ***[D]*** *Experimental design showing a self-quenched substrate (green).* ***[E]*** *Representative confocal images of microglia loaded with the self-quenched substrate.* ***[F]*** *Mean intensity (representative of lysosomal activity) represented in arbitrary units and referred to control values* ***[G]*** *Percentage of lysosomal numbers normalized to control values under control and OND conditions* ***[H]*** *Percentage of the area occupied by lysosomes, referred to control values. Violin plots show the data distribution including extreme values; lower and upper hinges correspond to the first and third quartile respectively* ***[C].*** *Bars show mean ± SEM* ***[F-H]****. n=4 independent experiments. Data was analyzed by Student´s t-test* ***[C, G-H].*** ** indicates p<0.05, *** p<0.001. Scale bars=7µm* ***[C]****, 50µm low magnification, 5µm high magnification* ***[E]****, z= single plane.*

To test if a lysosomal dysfunction could underlie the altered degradation observed after OND, we analysed lysosomal pH, enzymatic activity, and number of lysosomes. First, we measured the lysosomal pH of microglia in control and OND using a fluorescent ratiometric assay by live imaging (Majumdar et al., 2007) (**Figure 21A**). Primary microglia from wild type (wt) mice were incubated overnight with a fluorescein-rhodamine-dextran molecule, in which fluorescein (FITC: fluorescein) fluorescence declines with decreased pH whereas the rhodamine (TRITC: tetramethylrohadamine) fluorescence is stable. Thus, the ratio FITC/TRITC is pH-dependent and serves as a measurement of the lysosomal pH (Humphries et al., 2011) (**Figure 21B**). After the overnight incubation, the excess of dextran was removed from the medium to allow the endocytosed dextran to be delivered to the lysosomes. Next, microglia were subjected to control or OND conditions for 3 hours and the lysosomal pH was assessed by confocal live imaging (**Figure 21A, B**).

To assess the lysosomal pH we measured fluorescence intensity, calculated as the integrated density, in both FITC and TRITC channels for the pool of lysosomes in each cell using the ImageJ software (Schneider et al., 2012) (**Figure 21C**). The pH was calculated by interpolating the FITC/TRITC intensity ratios in a calibration curve of fixed pH values (see Methods). The obtained pH values were normalized to control levels due to the high variability of the technique. When we compared the control values to the OND treated group, we found that microglia had a small increase in the lysosomal pH after 3 hours of OND (**Figure 21C**). To address whether this small but significant and consistent increase in the lysosomal pH could be enough to alter the

enzymatic function of the lysosome and hence the degradation of the phagocytosed cargo we next assessed the lysosomal activity under OND.

Lysosomal enzymes, such as cathepsins (McGrath, 1999), require a very specific pH regulation not only to exert their hydrolytic function but also to be processed from zymogen to their active form (Chapman et al., 1997; Claveau & Riendeau, 2001).To test the functional effects of the OND-related lysosomal basification, we performed an activity assay based on the dequenching of a self-quenched substrate whose fluorescence emission is proportional to the lysosomal activity (**Figure 20D**) (Humphries & Payne, 2012). For this purpose, we incubated wt primary microglia for 3 hours under OND in the presence of the quenched substrate for the last hour and immediately image afterwards to avoid the loss of the OND effects (**Figure 21D**). We measured the mean intensity of each individual lysosome and referred it to total lysosomal numbers normalized by the cell area. We found no significant differences in the lysosomal activity between control and OND treated microglia (**Figure 21F**), but we did find a decrease in the lysosomal numbers (**Figure 21G**) and in the cytoplasmic area they occupied (**Figure 21H**). Thus, OND triggered a small basification of the lysosomal pH that did not affect the overall lysosomal activity but did induce a depletion of the number of lysosomes in microglia. This reduction in the number of lysosomes after OND could render fewer lysosomes to degrade the phagocytosed apoptotic cells, explaining the reduced degradation observed after OND.

We then considered possible mechanisms to explain the lysosomal depletion during OND. Among the possible causes, we focused on autophagy, a major lysosomal degradative pathway that shares cellular and molecular machinery with phagocytosis (Plaza-Zabala et al., 2017), and is induced by stressful stimuli, including nutrient starvation (Kaur & Debnath, 2015) or hypoxia (Fang et al., 2015). We hypothesized that the induction of autophagy in response to OND may consume lysosomes, leaving fewer available degradative organelles to degrade the apoptotic cells. The following sections are divided in two major blocks: first, we described how autophagy is modulated by OND in microglia using western blot analysis and electron microscopy; and second, we determined the relevance of basal autophagy for microglial function and survival through genetic and pharmacological manipulations of the process.

6.3 OND REMODELLED THE AUTOPHAGY COMPARTMENT

The induction of autophagy has been well characterized under nutrient starvation or energetic stress conditions in several cell types (Mercer et al., 2018; Plaza-Zabala et al., 2017). However, the combined effect of lack of oxygen and nutrients has been poorly explored. Our microscopy

data using the fluorescent tandem GFP-RFP-LC3 plasmid demonstrated that similar to rapamycin, OND enhanced the autophagy flux in microglia (**Figure 10D, E**). Indeed, the up regulation of the autophagic response after OND could be responsible for the observed lysosomal depletion, as lysosomes would be expended for autophagosome cargo degradation. This lysosomal expenditure would leave few lysosomes for the digestion of the phagocytosed apoptotic cells, which might in turn lead to a blockage in degradation. Thus, to further confirm the effects of OND, we analysed microglial autophagy by western blot and transmission electron microscopy (TEM).

6.3.1 Autophagy flux does not change after OND

We first assessed autophagy flux using LC3 turnover assay by western blot, the classical method used to monitor autophagy in cultured cells (Klionsky et al., 2021). In this assay, the amount of LC3-II is evaluated in the presence and absence of lysosomal inhibitors, such as bafilomycin A1, chloroquine and others (Klionsky et al., 2021). LC3-II accumulation in the presence of lysosomal inhibitors serves as an indirect measure of the autophagosomes that would have been degraded during the experimental period, allowing the determination of the autophagy flux for a specific time interval (Mauthe et al., 2018; Mauvezin & Neufeld, 2015). Further details concerning the analysis of the autophagy flux can be found in the Results Section 1.8 (Assessing autophagy in microglia: formation, degradation and net turnover).

To determine the autophagy flux in microglia, we treated primary cultures with OND though a time course (1 and 3 hours) in the presence/absence of bafilomycin A1and assessed LC3 expression by western blot (**Figure 22A**, **F**). We selected these early time points because microglia started to die after 6 hours of OND (data not shown). At 1h, OND did not alter the expression of either LC3-I or LC3-II, normalized to the reference gene ß-actin (**Figure 22C, D**) nor the ratio between LC3-II/LC3-I (**Figure 22E**). We did not observe significant changes in the autophagy dynamics in primary microglia at this early time-point, maybe due to the short exposure of microglia to OND. Next, we increased the time of OND to 3h to ensure a more robust response. At 3h, OND did not induce changes in the LC3-II/actin expression (**Figure 22H**) but reduced LC3-I/actin values. (**Figure 22I**). However, the LC3-II/LC3-I ratio remained at control levels (**Figure 22J**). Despite not identifying any changes in LC3-II flux, the reduction in LC3-I levels suggested an induction of autophagy, as the soluble form could be expended through conjugation to the autophagosome membrane.

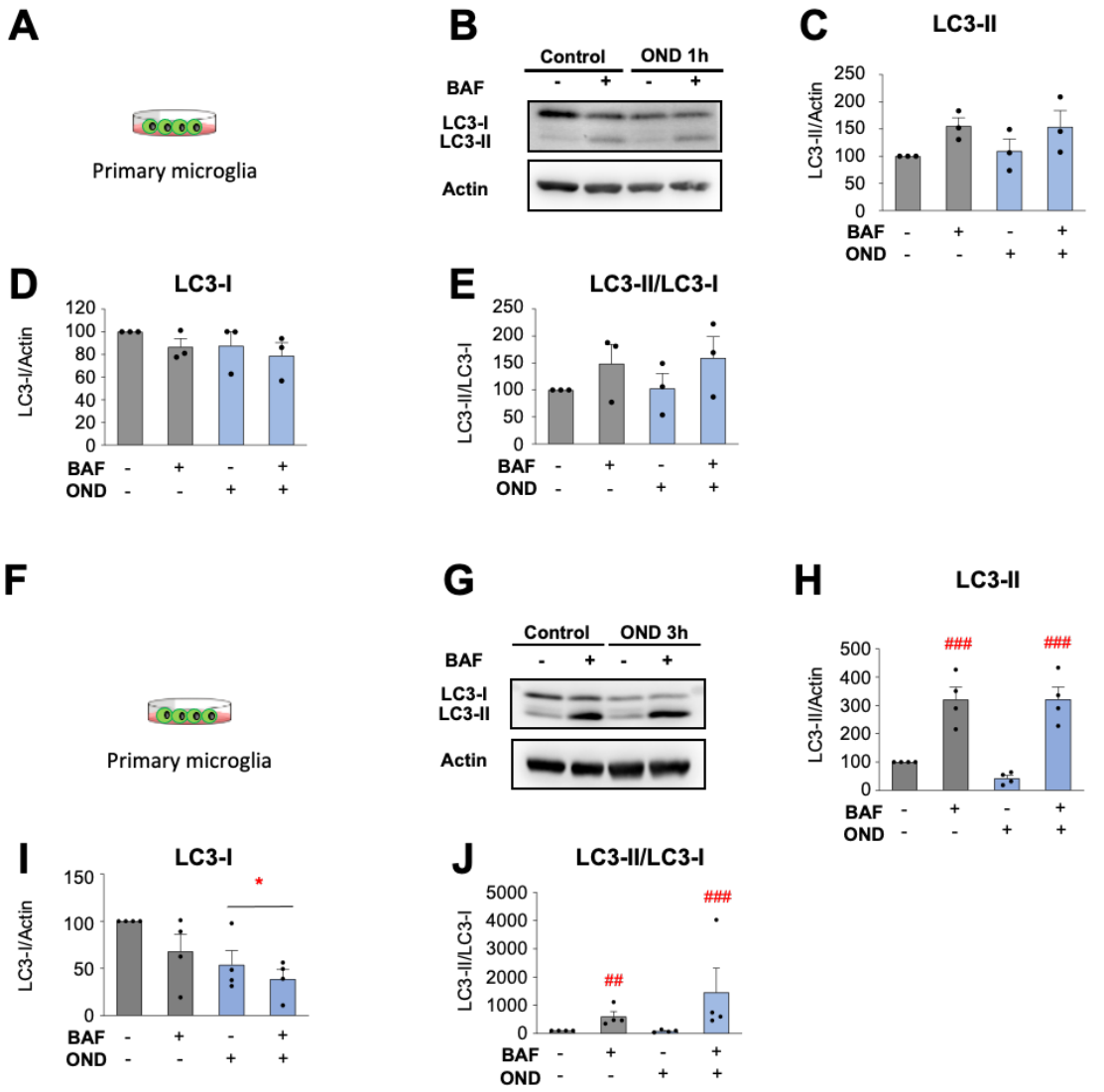

Figure 22. OND did not alter the autophagy flux assessed by western blot in primary microglia. ***[A, F]*** *Primary microglia were exposed to OND for 1 and 3 hours in the presence and absence of bafilomycin-A1 (BAF, 100 nM, 1 and 3 hours) to assess autophagy flux by LC3 turnover assay. Delipidated (~1 KDa) and lipidated (~17 KDa) LC3 levels were analyzed by western blot. Beta-actin (~42 KDa) was used as a loading control.* ***[B, G]*** *Representative blots showing LC3-I, LC3-II and actin bands,* ***[C, H]*** *LC3-II levels normalized to actin* ***[D, I]****, LC3-I levels normalized to actin,* ***[E, J]*** *LC3-II levels normalized to LC3-I levels. Bars show mean ± SEM. n=4 independent experiments. Data was analyzed by two-way ANOVA followed by Holm-Sidak post hoc test* ***[I].*** *To comply with homoscedasticity some data was square root* ***[H]*** *or* Log_{10} *transformed* ***[J].*** *(* and #) represent significance between bafilomycin and no bafilomycin. one symbol represents p<0.05, two symbols represent p<0.01 and three symbols represent p<0.001.*

To confirm these results, we assessed autophagy flux after 3 hours of OND in BV2 cells, a microglia cell line (**Figure 23A**, **B**). Consistent with the results in primary microglia, LC3-II/actin values (**Figure 23C**) were similar to control levels. Nevertheless, LC3-I/actin levels significantly

decreased after 3 hours of OND (**Figure 23D**), leading to increased LC3-II/LC3-I ratio (**Figure 23E**), thus confirming the LC3-I exhaustion described in primary microglia after OND.

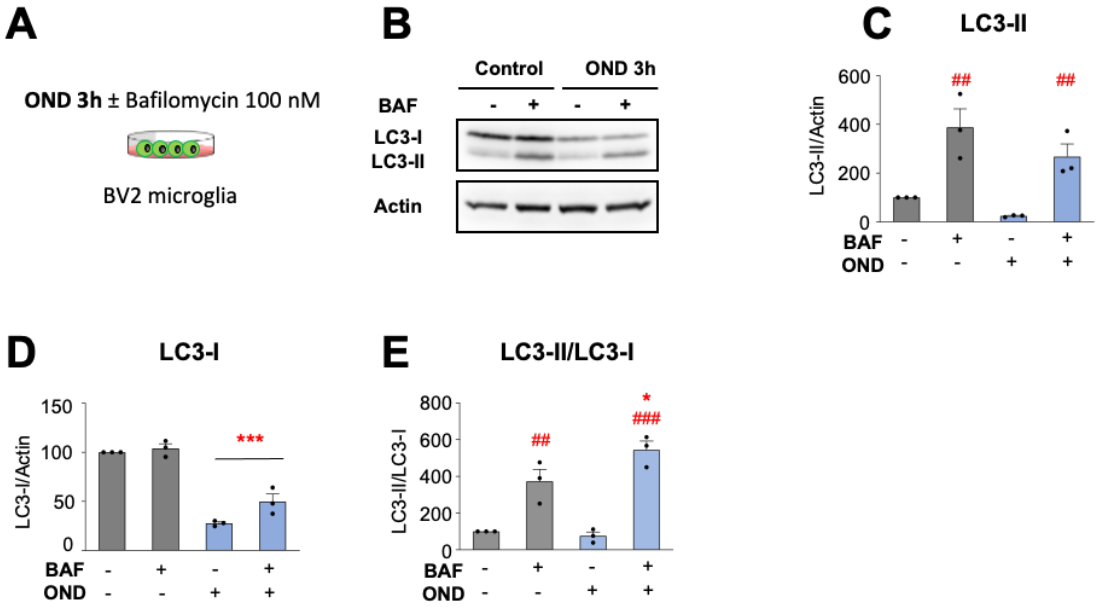

Figure 23. OND indued LC3-I exhaustion in BV2 cells. ***[A]*** *BV2 cells were exposed to OND for 3 hours in the presence and absence of bafilomycin-A1 (BAF, 100 nM, 3 hours) to assess autophagy flux by LC3 turnover assay. Delipidated (~1 KDa) and lipidated (~17 KDa) LC3 levels were analyzed by western blot. Beta-actin (~42 KDa) was used as a loading control.* ***[B]*** *Representative blots showing LC3-I, LC3-II and actin bands,* ***[C]*** *LC3-II levels normalized to actin* ***[D]****, LC3-I levels normalized to actin,* ***[E]*** *LC3-II levels normalized to LC3-I levels. Bars show mean ± SEM. n=4 independent experiments. Data was analyzed by two-way ANOVA followed by Holm-Sidak post hoc test. When an interaction between factors was found, one-way ANOVA was performed followed by Holm-Sidak post hoc tests* ***[E].*** *(* and #) represent significance between bafilomycin and no bafilomycin. one symbol represents p<0.05, two symbols represent p<0.01 and three symbols represent p<0.001.*

Altogether, these data indicated that the autophagy induction described by confocal microscopy using tandem GFP-RFP-LC3 plasmid was not detectable by the Western Blot LC3 turnover assay. However, we were able to describe a depletion of LC3-I by western blot after OND, which was possibly related to its conjugation to the autophagosome membrane and indicative of ongoing autophagy. To further confirm the effects of OND on autophagy, we performed transmission electron microscopy (TEM) to directly assess the microglial vesicular content.

6.3.2 Autophagy-like compartment expands after OND

Through TEM, we can discriminate and quantify of autophagic- and lysosomal-like vesicles within microglia after OND compared to the intracellular content in control conditions. We exposed primary microglia to OND for 3 hours and immediately fixed in glutaraldehyde for TEM processing (**Figure 24A**). The vesicular content in control and OND exposed microglia was significantly different (**Figure 24B**): both groups presented autophagic-like (double membrane-containing) and lysosomal-like (electron-dense) vesicles but in different proportions. We classified the vesicles in different types: 1, autophagosome-like vesicles, with at least a portion of double membrane surrounding the cargo, which could be granular, membranous, or heterogenous (**Figure 24C**); or 2, lysosome-like vesicles, which were electron-dense with either single or double membrane and mostly with no cargo (primary lysosomes) (**Figure 24D**). After OND, we found a significant increase in the number of autophagosome-like vesicles (**Figure 24E**), which were similar in size (**Figure 24F**) but occupied more area within the cell (**Figure 24G**), supporting the idea of autophagy induction after OND described with the tandem GFP-RFP-LC3 confocal images and the LC3-I consumption observed by western blot (**Figure 5I, 6D**). OND decreased the number of lysosomes, (**Figure 24H**), which were smaller in size (**Figure 24I**) and occupied less cytoplasm (**Figure 24J**). These results are in agreement with the reduction in the lysosomal numbers and occupied area that we previously described by confocal imaging methods (**Figure 4G, H**), strengthening our previous results. We speculated that the lysosomal consumption was related to their fusion with the increasing autophagosomes during OND, leading to their exhaustion and reduced availability for the degradation of the phagocytosed cargo.

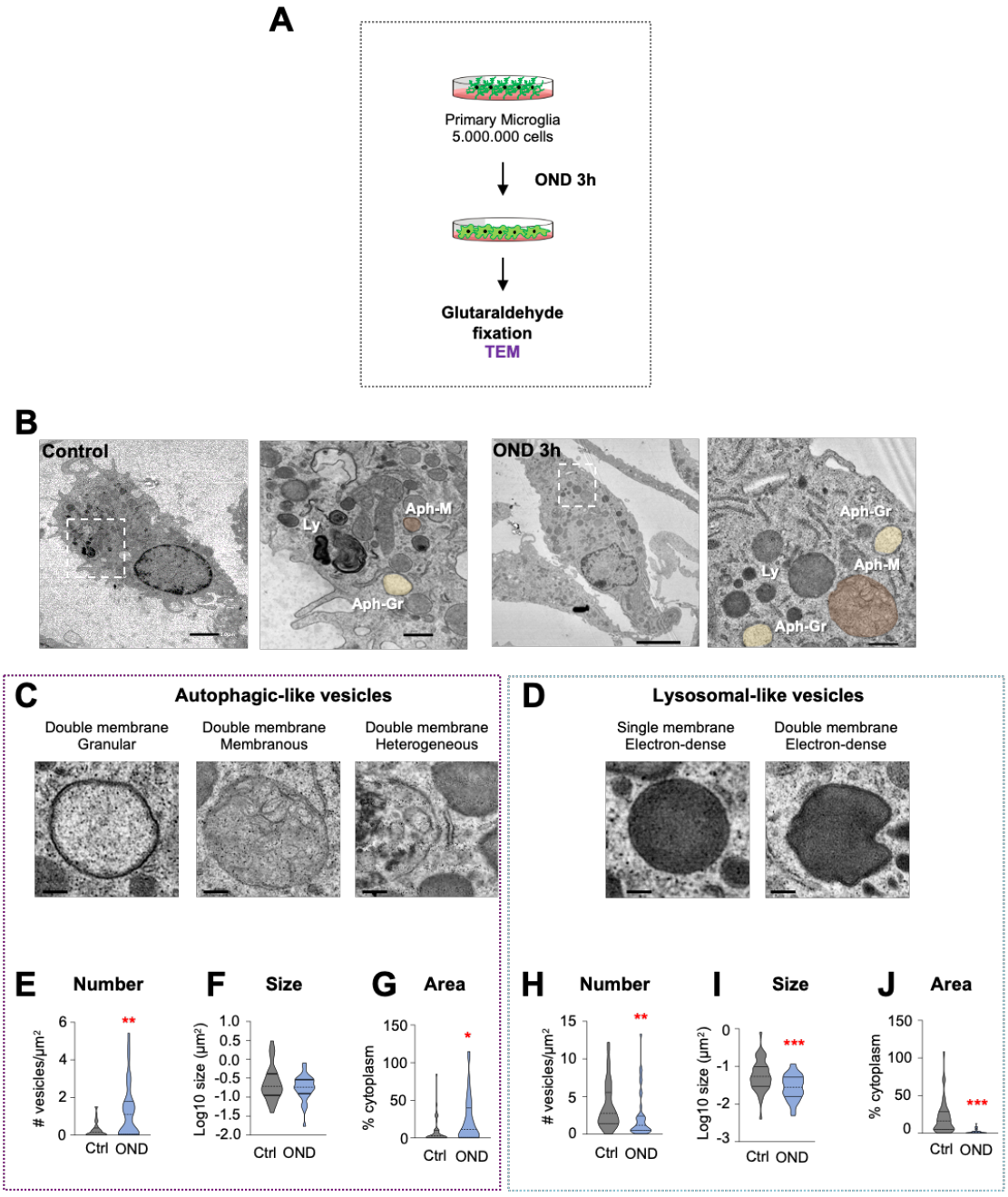

Figure 24. The autophagy compartment is remodeled after OND assessed by TEM. ***[A]*** *Primary microglia were exposed to OND for 3 hours and fixed for TEM.* ***[B]*** *Representative transmission electron microscopy images of primary microglia in control and OND conditions. Ly: lysosomes; Aph-Gr: autophagosomes with granular cargo (yellow); Aph-M: autophagosomes with membranous cargo (orange).* ***[C]*** *Details of autophagic-like vesicles identified as containing at least a portion of double membrane with different types of cargo (granular, membranous, heterogeneous).* ***[D]*** *Details of lysosomal-like vesicles identified as electron-dense vesicles with single or double membrane.* ***[E-G]*** *Quantification of autophagic-like vesicle number per µm²* ***[E]****, size in µm² (in logarithmic scale)* ***[F]****, and percentage of cytoplasm occupied* ***[G]****.* ***[H-J]*** *Quantification of lysosomal-like vesicle number per µm²* ***[H]****, size in µm² (in logarithmic scale)* ***[I]****, and percentage of cytoplasm occupied* ***[J]****. Violin plots show the data distribution, including extreme values;*

lower and upper hinges correspond to the first and third quartile, respectively. n=36-38 cells from 3 independent experiments. ***[E-G, H-J]****. Data was analyzed by non-parametric Mann-Whitney test* ***[E-G, H-J]****. * indicates p<0.05, ** p<0.01, *** p<0.001. Scale bars=2µm (control), 5µm (OND), 500nm (high magnification)* ***[B]****; 500nm* ***[C, D]****.*

In summary, we observed that OND led to reduced apoptotic cell engulfment, which could be explained by a reduced process motility; and reduced apoptotic cell degradation, likely related to an exhausted and basified lysosomal pool. The basification and exhaustion of the lysosomal pool could be related to their fusion with the increasing autophagosomes, although we acknowledge that there are alternative, unexplored mechanisms. For instance, OND could have a direct effect on lysosomal basification by blocking the v-ATPase proton pumps, which rely on ATP to pump protons into the lysosome and acidify their lumen (Futai et al., 2019; Mindell, 2012). The proposed mechanistic and functional relationship between phagocytosis efficiency and autophagy prompted us to determine the role of basal autophagy in microglial physiology and function, including the phagocytosis of apoptotic cells.

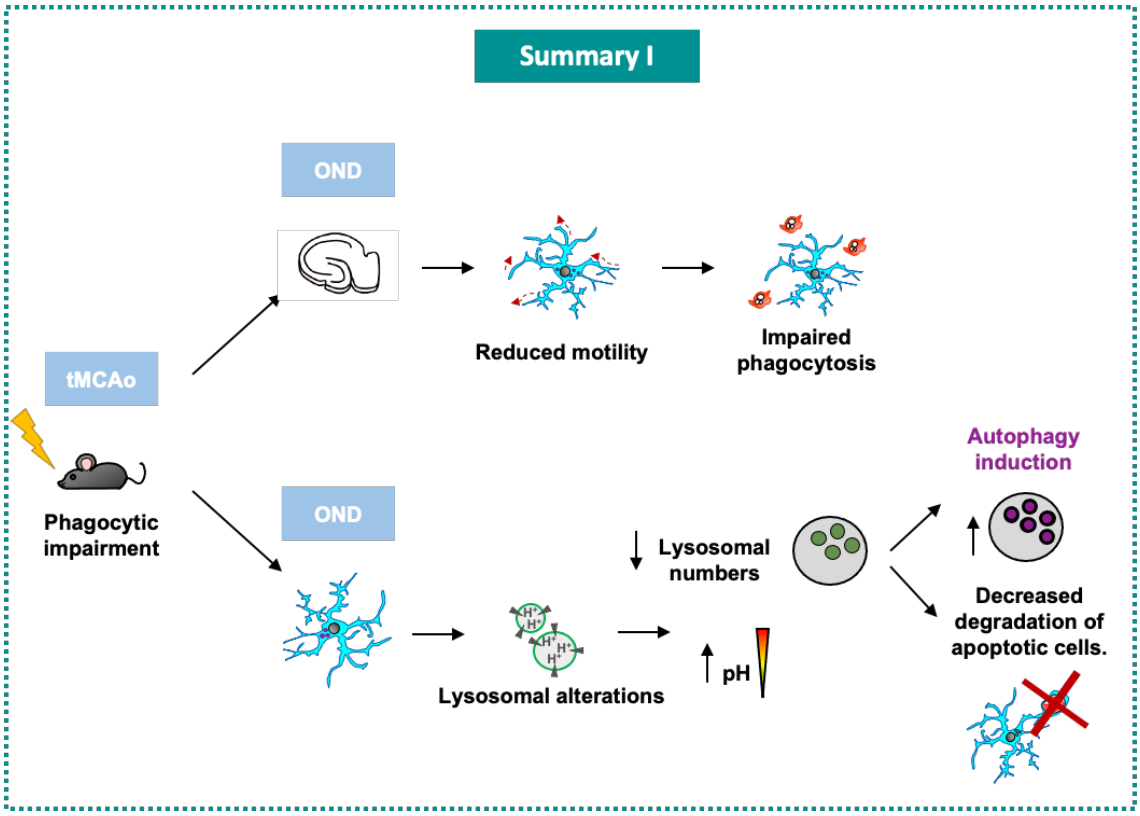

Figure 25. Summary I. *Main findings from the in vitro OND experiments.*

6.4 BASAL AUTOPHAGY PLAYED A CRUCIAL ROLE ON MICROGLIAL PHYSIOLOGY

Basal autophagy is an essential process to maintain cellular homeostasis in many cell types, as it is not only devoted to the recycling of defective proteins and organelles (Mizushima & Komatsu, 2011) but is also involved in cell survival and apoptosis (Fuchs & Steller, 2015). However, little is known about the role of autophagy on microglial physiology and how it might affect phagocytosis (Plaza-Zabala et al., 2017). To determine the role of basal autophagy on microglia we analysed several in vivo models of autophagy deficiency and characterized in vitro the effects of the pharmacological inhibition of autophagy.

6.4.1 Genetic deletion of autophagy genes had detrimental effects on microglial survival and phagocytosis.

Our first approach to determine the role of basal autophagy on microglia was to directly assess phagocytosis in 3 different in vivo models with deficient expression of autophagy-related genes: ATG4B knock-out (KO) mice, where the LC3 protease ATG4B is constitutively absent, leading to a downregulation of the autophagy pathway (Marino et al., 2010); TMEM119-creER-Beclin-1 KO mice, which lack the core protein of the PI3K complex exclusively in microglia; and the heterozygous AMBRA$^{+/-}$, which lack the regulatory protein of the Beclin-1 complex AMBRA1 (Fimia et al., 2007) (**Figure 9**). In the last two models, the absence of Beclin-1 and AMBRA lead to the total or partial absence of the novo formation of autophagosomes.

To determine the phagocytic efficiency in these mice, we quantified microglial phagocytosis in the dentate gyrus (DG) of the hippocampus, where there is ongoing neurogenesis in the subgranular zone (SGZ) in adult mice (Obernier & Alvarez-Buylla, 2019). Most of the new-born neurons undergo apoptosis and microglia are in charge of removing the dead bodies in physiological conditions (Sierra et al., 2010). This physiological phagocytosis allowed us to establish a baseline for microglial phagocytosis and hence compare it with phagocytosis in pathological situations (Abiega et al., 2016; Sierra et al., 2010).

First, we analysed phagocytosis in the hippocampus of ATG4B KO mice (**Figure 26A**, **B**). We found no differences in the number of apoptotic cells (**Figure 26C**), but we did observe a reduction in the phagocytic index (Ph index) (**Figure 26D**). Furthermore, microglia numbers were reduced in the absence of ATG4B (**Figure 26E**). These data suggest that microglia could depend on autophagy to optimally perform phagocytosis and maintain their survival.

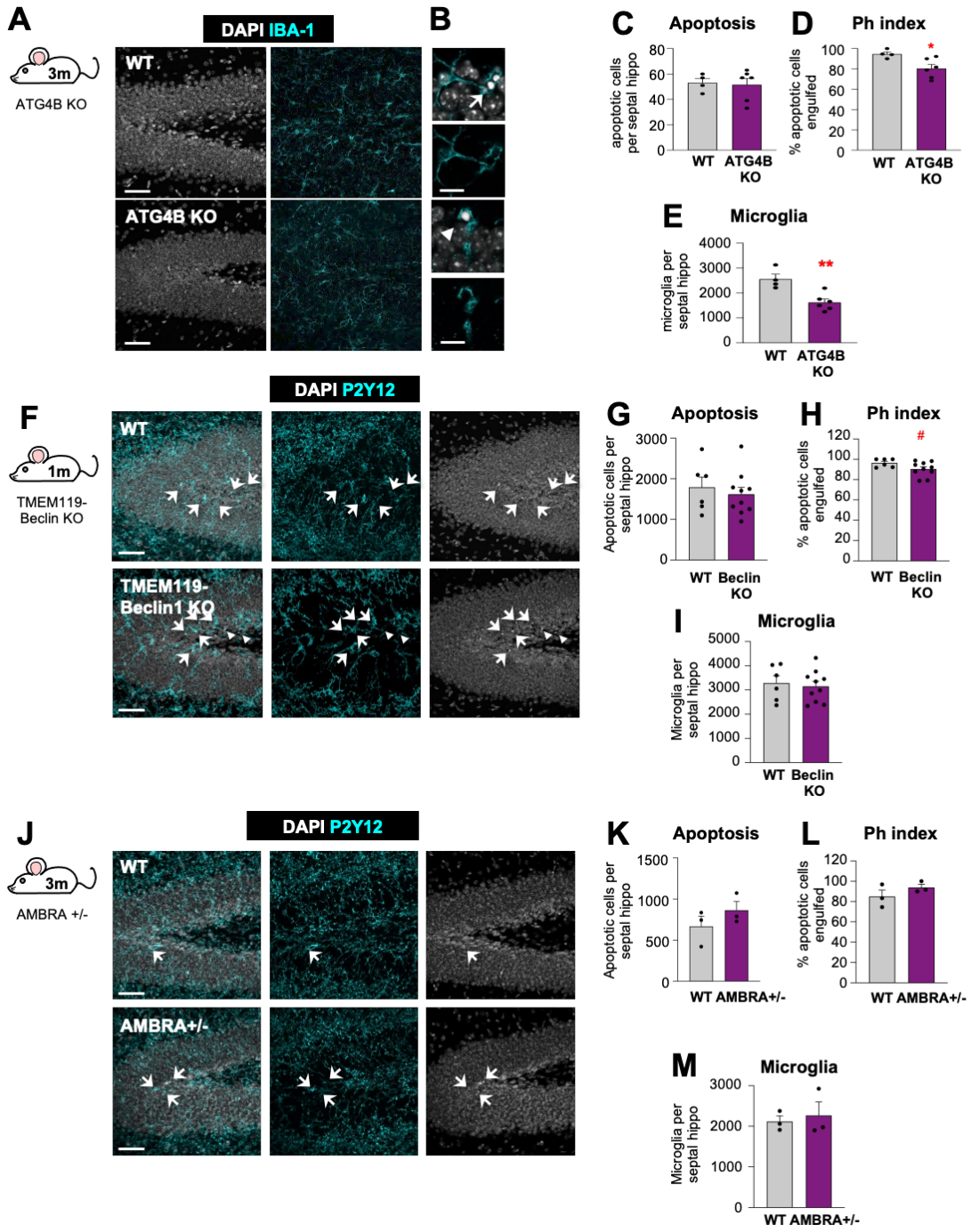

Figure 26. Microglial survival and phagocytosis were affected by the genetic deletion of autophagy genes in vivo. ***[A, F, J]*** *Representative confocal z-stacks of the DG of 3-month-old wild-type (WT) and ATG4B knock-out (ATG4B KO) mice; 1-month-old WT and TMEM-Beclin KO; and 3-month-old WT and AMBRA$^{+/-}$. Healthy or apoptotic nuclei (pyknotic/karyorrhectic) were visualized with DAPI (white) and microglia were stained for IBA-1 (cyan).* ***[B]*** *High magnification examples of phagocytosed (arrows) and non-phagocytosed (arrowheads) apoptotic cells in WT and ATG4B KO mice.* ***[C, G, K]*** *Number of apoptotic cells per septal hippocampus in WT, ATG4B KO mice, TMEM-Beclin KO and AMBRA$^{+/-}$.* ***[D, H, L]*** *Ph index in the septal hippocampus (% of apoptotic cells engulfed by microglia) of WT, ATG4B KO mice, TMEM-Beclin KO and AMBRA$^{+/-}$.* ***[E, I, M]*** *Number of microglial cells per septal hippocampus in WT, ATG4B KO mice,*

TMEM-Beclin KO and AMBRA$^{+/-}$. Bars show mean ± SEM. n=4-6 ***[A-E]****, n=6-10* ***[F-I]****, n=3* ***[J-M]*** *mice per group. Data was analyzed using Student´s t-test analysis. * indicates p<0.05, # represents p=0.080. Scale bars=50µm* ***[A, F, J],*** *z=36.4µm* ***[A],*** *50µm, z=8.5µm****[B]****; z=26.6µm* ***(WT)****, 21µm (TMEM119-Beclin1 KO)* ***[F],*** *16.1µm* ***[J].***

Next, we analysed TMEM119-creER-Beclin-1 microglia specific KO (**Figure 26F**). To induce recombination and the specific deletion of Beclin1, TMEM119-creER-Beclin-1 KO mice were treated with tamoxifen (75 mg/Kg) at P21 and P23 and sacrificed at P28. This acute and limited tamoxifen administration, likely, avoided the initiation of compensatory mechanisms to overcome the Beclin-1 deficiency. At P28 we did not find changes in apoptosis (**Figure 26G**) but had a trend to reduced phagocytosis (**Figure 26H**). In this model, microglia numbers were not altered and remained at control levels (**Figure 26I**). Thus, the specific deletion of Beclin-1 in microglia did not present such a strong phenotype as the deletion of ATG4B in all cell types.

Last, we analysed the functional implications of AMBRA1+/- deletion (**Figure 26J**) and found no changes in either apoptosis (**Figure 26K**), Ph index (**Figure 26L**) or microglia numbers (**Figure 26M**), suggesting that the heterozygous deletion of AMBRA1 might be compensated by other regulatory proteins and is not enough to trigger changes in phagocytosis and microglial survival.

Altogether, these data suggest that the deletion of different autophagy genes renders different results at the functional and survival level. The constitutive deletion of ATG4B in all cell types generated significant alterations in microglial physiology and function, whereas the microglia-specific deletion of Beclin-1 that was only altered for a short period of time (7 days) to avoid compensatory mechanisms, had milder effect on microglia. Last, the constitutive heterozygous deletion of AMBRA1 in all cell types, had no effect on microglia. To further study the functional implications of autophagy on microglia, we used primary cultures and organotypic hippocampal slices treated with a pharmacological inhibitor of autophagy.

6.4.2 Pharmacological inhibition of basal autophagy reduced microglial survival and phagocytosis

To study autophagy flux inhibition in vitro we used the selective ULK1/2 inhibitor MRT68921, MRT from now on (**Figure 9**), which blocks the serine/threonine kinase activity of ULK1/2, leading to the blockade of autophagy at its pre-initiation step (Petherick et al., 2015). In addition, MRT induces the accumulation of stalled autophagosomes, suggestive of the role of ULK1/2 also in the maturation step of autophagosomes (Zachari et al., 2020).

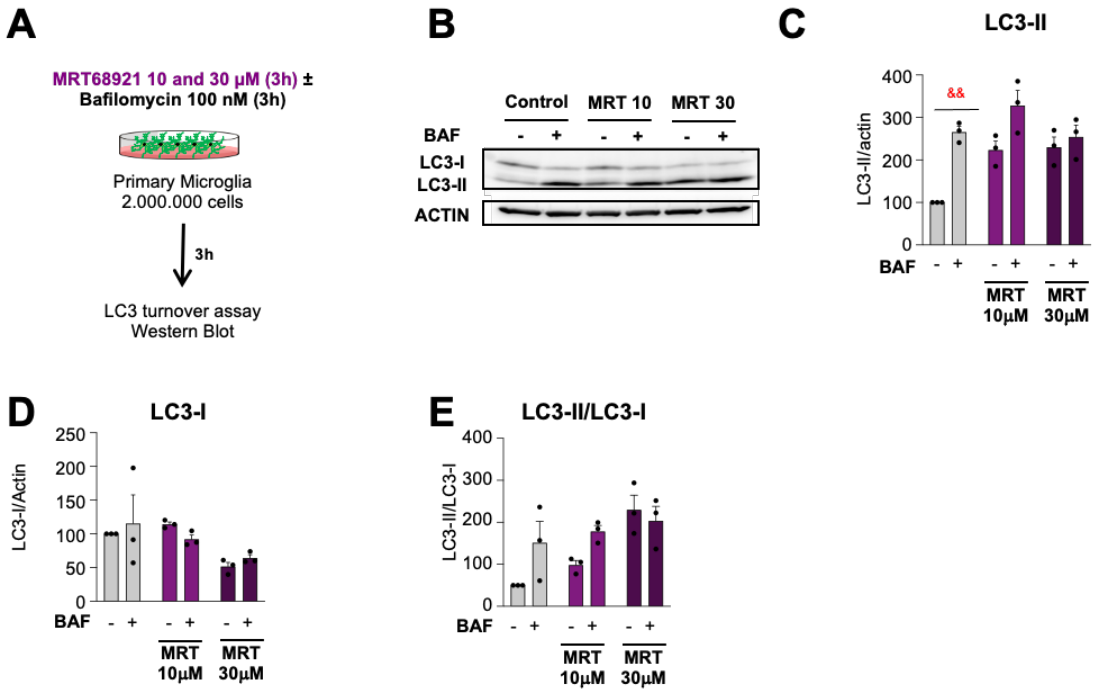

Figure 27. Microglial autophagy was effectively blocked by 30 µM MRT after 3 hours. ***[A]*** *Experimental design of the dose-response administration of Ulk1/2 inhibitor MRT68921 to primary microglia.* ***[B]*** *Representative blot showing relative levels of LC3-I and LC3-II after 10 and 30µM MRT68921 administration for 3h.* ***[C]*** *Quantification of the LC3-II levels (referred to actin) after 10 and 30µM MRT68921 in the presence and absence of the lysosomal inhibitor, bafilomycin A (BAF, 100 nM),* ***[D]*** *LC3-I levels normalized to actin,* ***[E]*** *LC3-II levels normalized to LC3-I levels. Bars show mean ± SEM n=3 independent experiments. Data was analyzed by two-way ANOVA followed by Holm-Sidak post hoc tests. (&) represents significance between bafilomycin-treated and non-treated groups: two symbols represent p<0.01.*

To avoid off-target effects, we screened for the minimal effective concentration to inhibit autophagy flux in primary microglia by LC3 western blot (**Figure 27A**). First, we tested 10 and 30 µM MRT for 3 hours in the presence and absence of bafilomycin A1 to assess the autophagy flux. We found no effects at 10µM but an evident blockade of autophagy at 30µM (**Figure 27C**). In control cells, bafilomycin A1 increased the levels of LC3-II/actin, indicative of autophagosome accumulation and ongoing autophagy flux, but this effect was lost in MRT treated cells in a concentration dependent manner, where we did not observe an increased LC3-II accumulation in the bafilomycin A1 treated group compared to the untreated group, suggesting that MRT had already impaired autophagosome degradation (**Figure 27C**). We did not see changes in the LC3-I/actin ratio, which remained constant in the presence of the inhibitor (**Figure 27D**). We could further confirm the autophagy blockade when we analysed the LC3-II-/LC3-I ratio, where LC3-II did not accumulate in the presence of MRT and bafilomycin A1 (**Figure 27E**). 30 µM MRT

effectively blocked the autophagy flux after 3 hours but because; high concentration of MRT could have detrimental side effects, such as cell death (Hwang et al., 2020; Petherick et al., 2015), we scanned for lower concentrations that effectively blocked autophagy.

We next reduced the autophagy inhibitor concentration and increased the treatment time, testing 1 and 10 µM MRT for 6 hours (**Figure 28A**, **B**). Bafilomycin A1 was added for the last 3 hours of the treatment period as it has detrimental effects on cell survival at longer time points (Rubinsztein et al., 2009) (Klionsky et al., 2021). The LC3-II/actin and LC3-II/LC3-I ratios indicated that MRT had no effect on autophagy at 1 µM, as LC3-II kept accumulating over time, but it did significantly block autophagy at 10 µM, as there was no accumulation of LC3-II in the MRT treated group in the presence of bafilomycin A1 compared to the untreated cells (**Figure 28C**). No changes were observed in the LC3-I/actin ratio in either concentration (**Figure 28D**). The LC3-II/LC3-I ratio indicated ongoing autophagy in control conditions and after 6 hours of 1 µM MRT but was not changed after 6 hours of 10 µM MRT, suggestive of an autophagy blockade (**Figure 28E**). Thus, only 10 µM MRT effectively blocked autophagy flux after 6 hours of treatment.

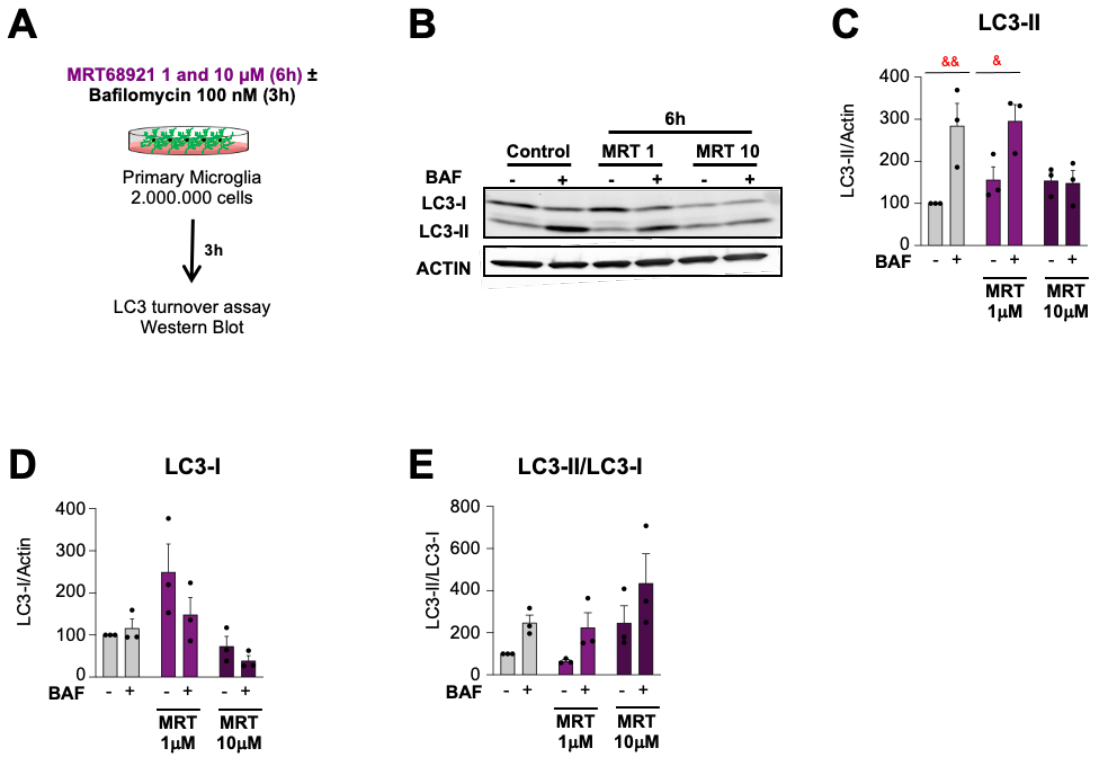

Figure 28. Microglial autophagy was effectively blocked by 10 µM MRT after 6 hours. ***[A]*** *Experimental design of the dose-response administration of Ulk1/2 inhibitor MRT68921 to primary microglia.* ***[B]*** *Representative blot showing relative levels of LC3-I and LC3-II after 1 and 10µM MRT68921 administration for 3h.* ***[C]*** *Quantification of the LC3-II levels (referred to actin) after 1 and 10µM MRT68921 in the presence and absence of the lysosomal inhibitor, bafilomycin A (BAF, 100 nM),* ***[D]*** *LC3-I levels normalized to actin,*

[E] *LC3-II levels normalized to LC3-I levels. Bars show mean ± SEM n=3 independent experiments. Data was analyzed by two-way ANOVA followed by Holm-Sidak post hoc tests. (&) represents significance between bafilomycin-treated and non-treated groups: one symbol represents p<0.05, two symbols p<0.01.*

Once we effectively blocked autophagy at 10 µM for 6h or 30 µM MRT for 3 hours, our next step was to determine the functional effects of this inhibition on microglial physiology (survival and phagocytosis) and describe the functional relationship between phagocytosis and autophagy.

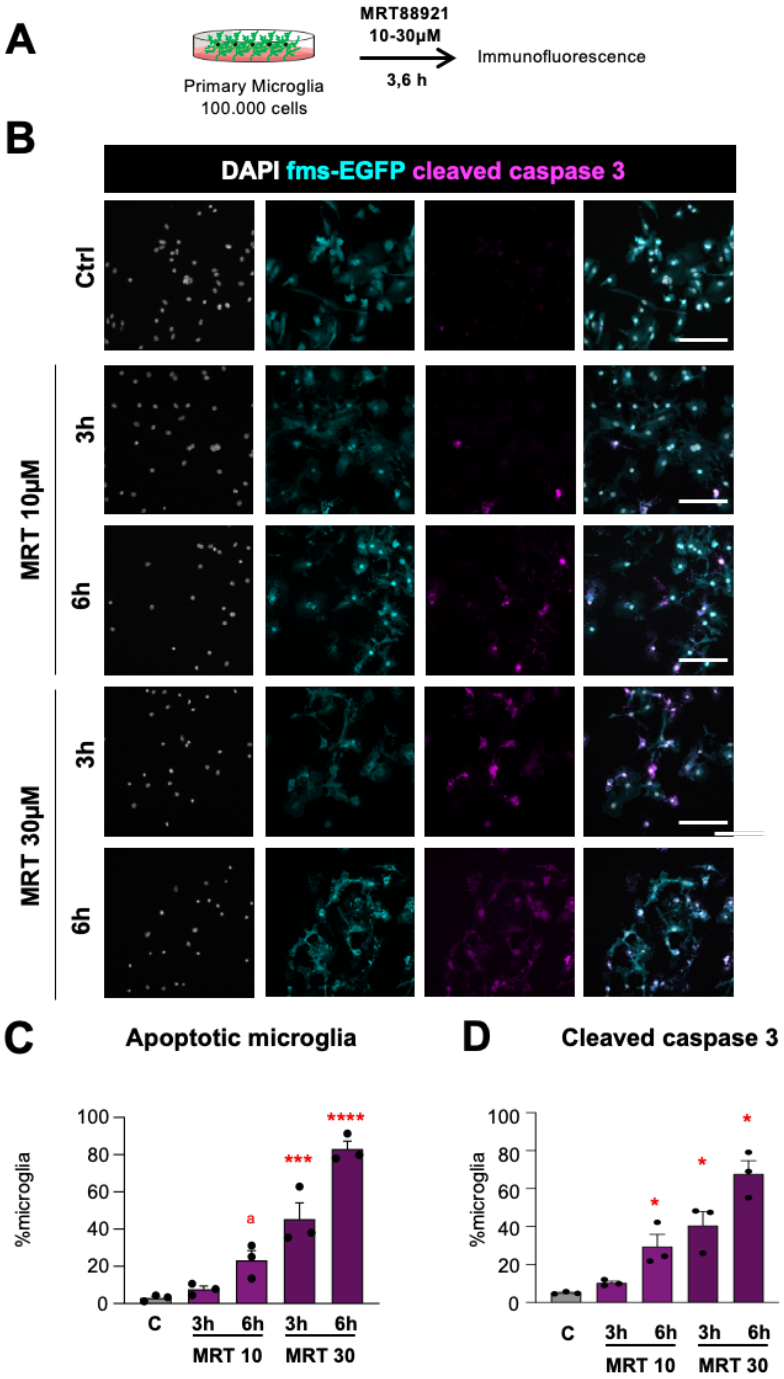

Figure 29. Autophagy inhibition reduced microglial survival in a time and dose dependent manner. ***[A]*** *Experimental design of the dose-response administration of Ulk1/2 inhibitor MRT68921 to primary*

microglia. ***[B]*** *Representative confocal images of primary fms-EGFP microglia treated with MRT68921 (1, 10 and 30µM, 3 and 6 hours). Nuclei were visualized with DAPI (white), microglia with their constitutive EGFP expression (cyan), and apoptotic cells with activated caspase 3 (act-casp3^{+}, magenta).* ***[C]*** *Percentage of apoptotic microglia assessed by their healthy or apoptotic nuclei (pyknotic/karyorrhectic).* ***[D]*** *Percentage of activated caspase 3 positive microglia. Bars show mean ± SEM. n=3 independent experiments. Data was analyzed by 1-way ANOVA followed by Tukey´s multiple comparisons. (a) represents p=0.051. * represents p<0-05, *** p<0.001, **** p<0.0001. Scale bar=50µm, z=8.5µm.*

We then assessed the effects of autophagy inhibition on microglial survival and phagocytosis in vitro to confirm the results found in ATG4B KO mice (**Figure 26**). By immunofluorescence, we analysed the effects of 10 and 30 µM MRT for 3 and 6 hours in microglial survival/death (**Figure 29A**). Primary microglia were stained for DAPI (white) to assess nuclear morphology and determine the nuclear health: apoptotic (pyknotic/karyorrhectic) or healthy (well defined heterochromatin and euchromatin); cleaved caspase 3+ (magenta) as an additional marker for apoptosis; and fms-EGFP (green) for microglia (**Figure 29B**). Autophagy inhibition induced microglial death in a dose and time dependent manner, determined both by DAPI and expression of cleaved caspase 3+ (**Figure 29C**, **D**): at the highest dose (30µM), MRT induced microglial apoptosis at both 3 and 6h. However, at the lowest dose (10µM), MRT only showed a trend to induce microglial apoptosis at 6h but had no significant effects at 3h (**Figure 29C**, **D**).

To assess the effect of autophagy inhibition on phagocytosis we selected the 10 µM MRT concentration for 6 hours, as it effectively blocked autophagy flux (**Figure 28**) without significantly inducing microglial death (**Figure 29**). We used the previously mentioned in vitro model in which primary microglia were fed with apoptotic cells and assessed phagocytosis at two different time points to discriminate engulfment and degradation (**Figure 30A**). To test the effects of the autophagy inhibition on engulfment, microglia were treated with 10 µM MRT or vehicle for 5 hours, and then fed with the apoptotic vampire SH-SY5Y for 1 more hour (total MRT treatment time, 6h). To assess degradation, the engulfment was performed under control conditions without MRT but, after washing out the non-phagocytosed cells, degradation was assessed after the addition of 10 µM MRT or vehicle for 6 hours to the medium (**Figure 30B**). The analysis of phagocytosis was performed as previously mentioned (**Section 1.3**): only fully enclosed apoptotic cells or DAPI/vampire particles were quantified as phagocytosis (**Figure 30C**, **D**). To assess engulfment, we compared the change in phagocytic microglia at 1 hour and after 6 hours of degradation. To quantify the amount of degradation, we subtracted the percentage of phagocytic microglia after 6 hours degradation to the engulfment percentage in the

respective 1-hour control group. 10 µM MRT significantly reduced the percentage of engulfing microglia (**Figure 30E**) and showed a small trend to reduce degradation (**Figure 30F**). These data suggest that the execution of phagocytosis requires autophagy for both engulfment and degradation of apoptotic cells, thus confirming a functional relationship between autophagy and phagocytosis in microglia.

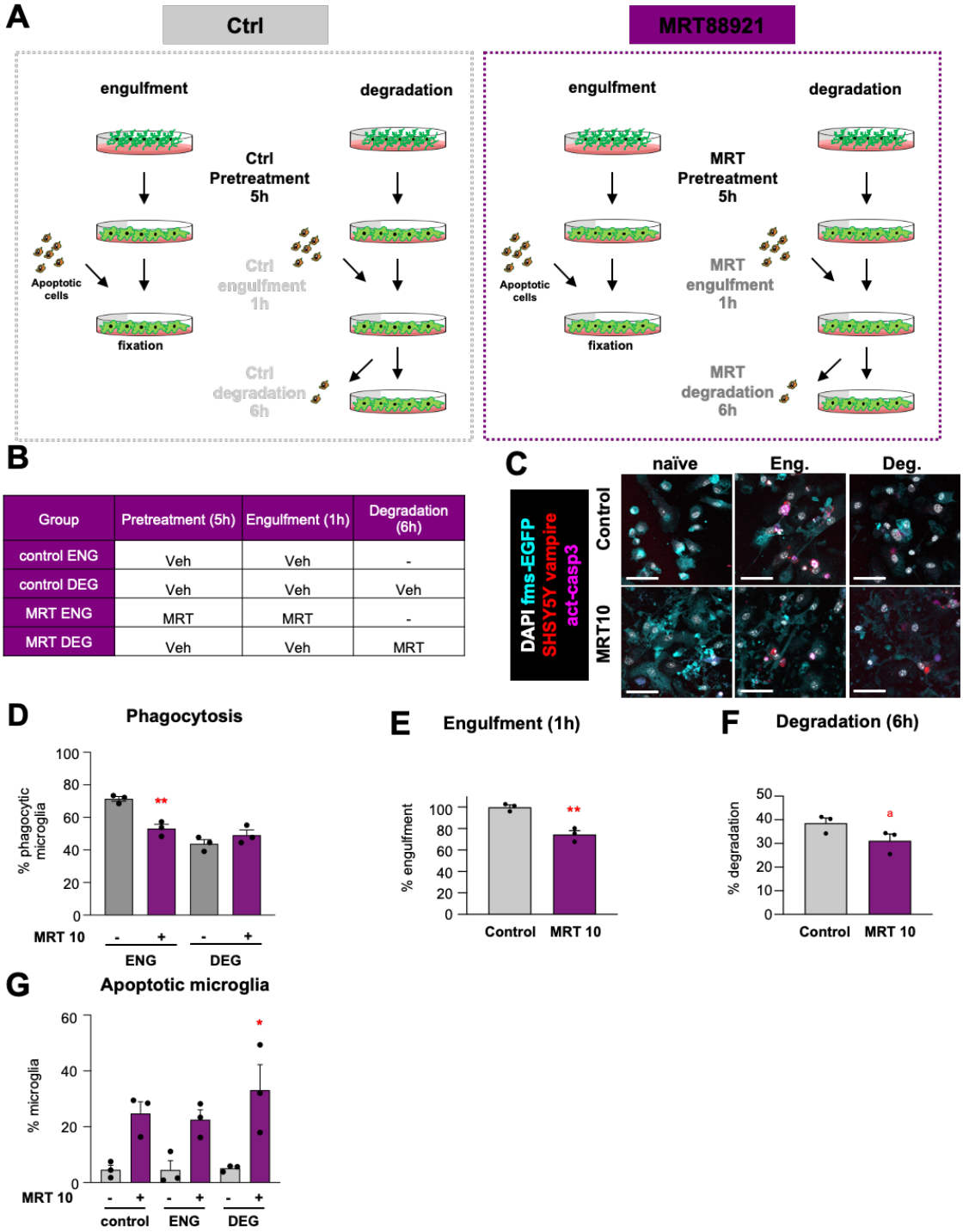

Figure 30. Engulfment of apoptotic cells was reduced after autophagy inhibition in primary microglia.

[A] *Experimental design of the phagocytosis assay to assess engulfment and degradation of apoptotic cells*

under control and autophagy inhibition conditions. ***[B]*** *Table summarizing the treatments.* ***[C]*** *Representative images of naïve and primary microglia fed with apoptotic SH-SY5Y vampire cells during engulfment and degradation. Nuclei were visualized with DAPI (white), microglia by expression of EGFP (cyan), and SH-SY5Y neurons by expression of the red fluorescent protein Vampire.* ***[D]*** *Percentage of phagocytic microglia 1 and 3h after the addition of apoptotic cells (raw data).* ***[E, F]*** *Percentage of phagocytic microglia after engulfment (1h) and degradation (3h after engulfment). Only particles fully enclosed by microglia were identified as being phagocytosed.* ***[G]*** *Percentage of apoptotic microglia in naïve and phagocytic microglia (engulfment and degradation) assessed by their healthy or apoptotic nuclei (pyknotic/karyorrhectic). Bars show mean ± SEM. n=3 independent experiments. Data was analyzed by 1-way ANOVA followed by Tukey´s multiple comparisons in case significant differences were identified* ***[D, G]*** *Student´s t-test analysis* ***[E-F].*** *(a) p=0.1080, * represents p<0.05, ** p<0.01. Scale bar=50µm, z=8.5µm.*

In addition, we analysed microglial survival in the presence of MRT during the phagocytic challenge. MRT induced an equivalent percentage of microglial apoptosis regardless of whether the cells were engaged in phagocytosis, as apoptosis was maintained to naïve MRT treated microglia levels (**Figure 30C**, **G**), suggesting that the inhibition of autophagy was the cause of microglial cell death per se, and that phagocytosis had no additional effects on microglial survival. These data confirm the effects of the autophagy deficiency in vivo observed in the ATG4B KO mice: the pharmacological inhibition of autophagy with MRT reduced microglial survival and impaired microglial phagocytosis in vitro. Thus, microglial autophagy was essential for microglial physiology, including survival and phagocytosis.

Next, we extended the analysis of the in vitro autophagy inhibition to organotypic hippocampal slices and assessed its effect both in control and under OND conditions.

6.4.3 Pharmacological inhibition of autophagy impaired microglial phagocytosis in organotypic slices

To ensure the bioavailability of the MRT and counteract for its diffusivity throughout the tissue slice, we used higher concentrations of MRT in organotypic slices compared to primary cultures (30 and 100 µM). We assessed the effects of both concentrations in control and after 3 hours of OND (**Figure 31A**). We stained for GFP to visualize microglia (green, **Figure 31B**, **C**) and for cleaved caspase 3 to assess apoptosis (magenta, **Figure 31C**), and used DAPI to visualize nuclear morphology (white, **Figure 31B**, **C**). MRT did not induce changes in global apoptosis in control conditions or after OND (**Figure 31D**). However, 100 µM MRT did induce a small increase in microglial apoptosis both in control and OND conditions (**Figure 31E**), which was reflected in

significantly reduced microglial numbers after OND and showed a trend to be reduced in control conditions (**Figure 31F**). This reduction in microglial numbers after the autophagy blockade in control and OND-treated cells, supports the idea that autophagy is an ongoing and essential process to ensure microglial survival in both control and OND-challenged microglia.

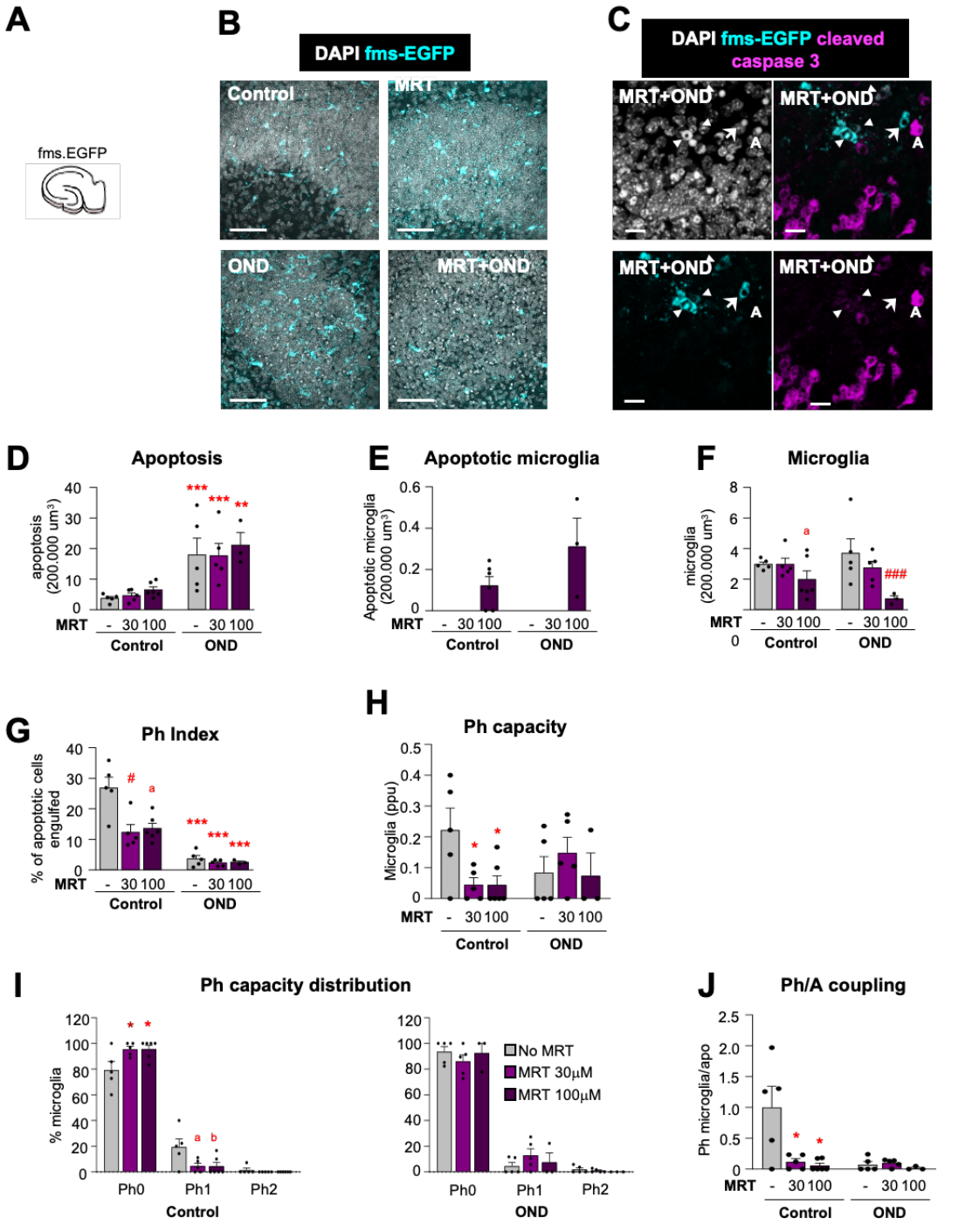

Figure 31. Microglial phagocytosis was impaired in organotypic hippocampal slices after the pharmacological inhibition of autophagy. ***[A]*** *Experimental design showing the exposure of hippocampal organotypic slices (fms-EGFP) to 100 and 300 µ M MRT for hours).* ***[B]*** *Representative confocal images of the DG after treatment with MRT68921 (100 µM) for 3 hours in the presence and absence of OND. Normal*

or apoptotic (pyknotic/karyorrhectic) nuclear morphology was visualized with DAPI (white) and microglia by the transgenic expression of fms-EGFP (cyan); ***[C]*** *apoptosis was confirmed by activated caspase-3 staining (magenta), Arrowheads, apoptotic microglia (fms-EGFP$^+$, act-casp3$^+$); arrow, phagocytic microglia (fms-EGFP$^+$, act-casp3$^-$); A, apoptotic cell (act-casp3$^+$ with pyknotic/karyorrhectic nuclear morphology).* ***[D]*** *Number of apoptotic cells in 200.000 µm^3 of the DG.* ***[E]*** *Number of apoptotic microglia. Apoptotic microglia were discriminated from apoptotic cells contained in microglial pouches thanks to their expression of EGFP within the nuclei and the lack of a process connecting it to a healthy microglial soma.* ***[F]*** *Number of microglia in 200.000 µm^3 of the DG.* ***[G]*** *Ph index (% of apoptotic cells phagocytosed by microglia).* ***[H]*** *Weighted Ph capacity (number of phagocytic pouches filled with apoptotic nuclei per microglia) in parts per unit (ppu).* ***[I]*** *Ph capacity histogram in control and OND conditions.* ***[J]*** *Ph/A coupling in fold-change (net phagocytosis with respect to total levels of apoptosis). Bars show mean ± SEM. n=3-6 mice per experimental condition. Some data was transformed to comply with homoscedasticity using Log$_{10}$* ***[H]*** *or square root* ***[J]****. Data was analyzed by two-way ANOVA followed by one-way ANOVA (factor: MRT treatment) when an interaction was revealed in data split in control and OND conditions and Holm-Sidak post hoc tests after logarithmic transformation* ***[D, J]*** *and one-way ANOVA (factor: number of pouches) followed by Holm-Sidak post hoc tests* ***[I].*** *(* and #) represent significance vs the control group or between MRT-treated and untreated groups: one symbol represents p<0.05, two symbols represent p<0.01 and three symbols represent p<0.001; (a) p=0.127* ***[F],*** *p=0.055* ***[G]*** *and (a) represents p=0.06 (MRT30 vs untreated), (b) represents p=0.07 (MRT100 vs untreated)* ***[I]****. Scale bars= 50 µm z=11.2µm* ***[B],*** *15µm, z=12.6 µm* ***[C]****.*

Once we determined the effects of MRT on microglial survival, we analysed phagocytosis (**Figure 31G**). MRT reduced microglial phagocytosis in control conditions (**Figure 31G**, **H**), similar to the effect observed in primary cultures (**Figure 30**). However, it had no effect in slices already treated with OND, suggesting that the inhibition of autophagy had similar detrimental effects on phagocytosis as OND, and, hence, basal autophagy is essential for phagocytosis efficiency. Similarly, MRT completely abolished the Ph/A coupling in control conditions and had no effect on the OND-induced uncoupling (**Figure 31J**). In conclusion, basal autophagy inhibition with MRT reduced microglial phagocytosis, suggesting that microglia require autophagy for its correct function. In contrast, autophagy inhibition after OND had no effect on the already impaired phagocytosis, suggesting a relationship between the two processes, that could be relying on the same cellular substrates.

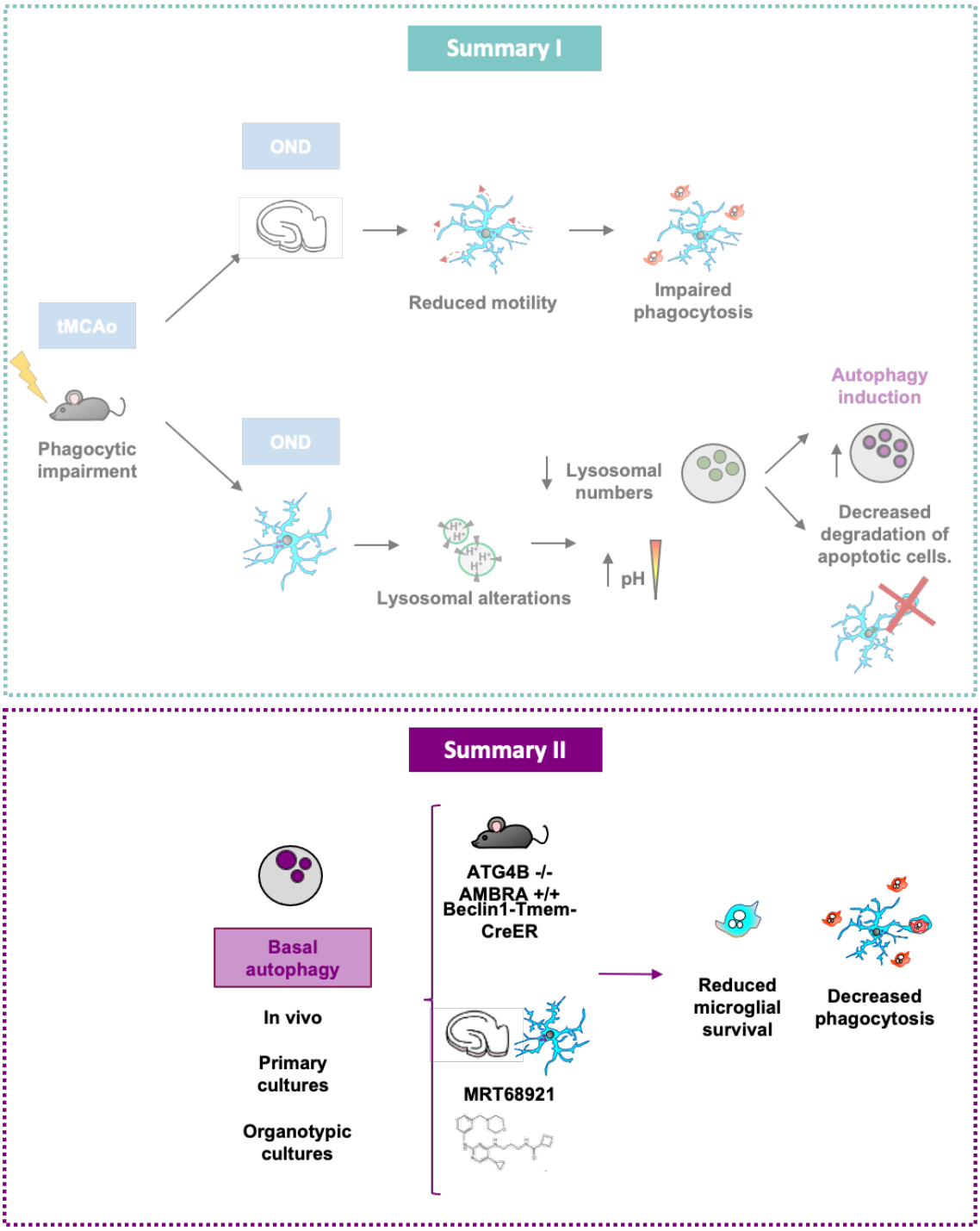

Figure 31. Summary II. Main findings from the autophagy inhibition experiments.

Up to this point, we have determined that the inhibition of basal autophagy both in vivo and in vitro reduced microglial survival and impaired microglial phagocytic capacity in basal conditions. We also found that blocking autophagy induction during OND increased microglial death but had no further detrimental effect on microglial phagocytosis, which was already blocked likely related to other cellular alterations, such as reduced process motility. We then concluded that autophagy is an essential process to maintain microglial survival and function. After OND, the

induction of autophagy could be a protective strategy oriented to the maintenance of microglial phagocytosis, as its inhibition tended to increase microglial death (**Figure 31E, F**). For this reason, we tested the opposite strategy and triggered autophagy with the well-known autophagy inducer rapamycin (Arriola Apelo & Lamming, 2016) and assessed microglial function in primary microglia and organotypic hippocampal slices during OND.

6.5 RAPAMYCIN DID NOT POTENTIATE MICROGLIAL AUTOPHAGY AND PHAGOCYTOSIS

We selected rapamycin to improve microglial function as it has been described to have beneficial effects on several brain disease models (Galluzzi et al., 2016) (Erlich et al., 2007) and specifically in stroke, where it prevents neuronal cell death (Beard et al., 2019; Hadley et al., 2019). In addition to its well-known function as inhibitor of the mTORC1 complex to promote autophagy, rapamycin also promotes lysosomal biogenesis (Civiletto et al., 2018) and could act directly on the altered lysosomal compartment after OND (**Figure 4, 7**) to recover phagocytosis.

Previous data from our lab, obtained by Dr. Sol Beccari (PhD, 2020), demonstrated that the pre-treatment with rapamycin partially reverted the phagocytosis impairment induced by tMCAo (**Figure 15**). To determine if this protection was related to a direct effect of rapamycin on microglia, we tested its effects on primary and organotypic cultures both on control and OND conditions.

6.5.1 The effects of rapamycin in basal and OND conditions were not detectable by LC3 western blot

Rapamycin has been reported to have different cellular outcomes depending on the concentration: for example, high doses in the micromolar range, can reduce cell survival and induce apoptosis (Mukhopadhyay et al., 2016); whereas low doses, in the nanomolar range, are known to induce autophagy. We selected the 100 nM concentration for 6 hours as we determined that it effectively induced autophagy in transfected BV2 microglia by confocal microscopy (**Figure 10D, E**). We treated primary microglia with 100 nM rapamycin for 6 hours and measured autophagy flux by western blot, (**Figure 33A**). At this concentration and time point, rapamycin was not able to induce the accumulation of LC3-II (**Figure 33B**, **C**) and it did not alter the LC3-I levels (**Figure. 33D**), nor the LC3-II/LC3-I ratio (**Figure 33E**).

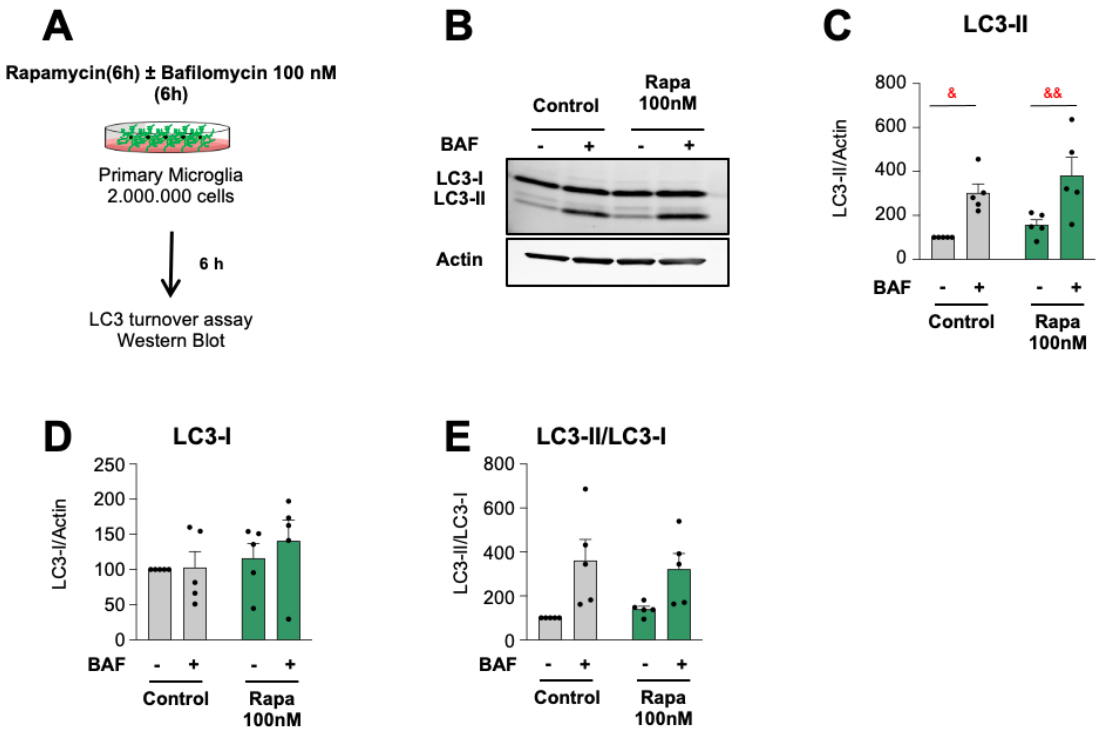

Figure 33. Rapamycin did not modulate basal autophagy in primary microglia assessed by western blot. ***[A]*** *Experimental design of the dose-response administration of rapamycin to primary microglia for 6 hours.* ***[B]*** *Representative blot showing relative levels of LC3-I and LC3-II after 100 nM rapamycin for 6h.* ***[C]*** *Quantification of the LC3-II levels (referred to actin) 100 nM rapamycin in the presence and absence of the lysosomal inhibitor, bafilomycin A (BAF, 100 nM),* ***[D]*** *LC3-I levels normalized to actin,* ***[E]*** *LC3-II levels normalized to LC3-I levels. Bars show mean ± SEM n=3 independent experiments. Data was analyzed by two-way ANOVA followed by Holm-Sidak post hoc tests. (&) represents significance between bafilomycin-treated and non-treated groups: one symbol represents p<0.05, two symbols p<0.01.*

Next, we extended the concentration and treatment time and tested 100mM for 24h and 500nM for 24h (**Figure 34A**). Rapamycin tended to increase LC3-II levels at 100 nM but no effects were observed after 500 nM (**Figure 34B**, **C**), and LC3-I/actin and LC3-II/LC3-I values were not changed after the addition of rapamycin (**Figure 34D, E**). We speculate that the different results obtained by confocal microscopy of tandem LC3 and LC3 western blot were due to a lower sensitivity of the western blot technique, since after OND, by western blot we did not detect changes in autophagy that were clearly visible by TEM (**Figure 24**). These data suggest that the modulation of autophagy in primary microglia is a complex task, undetectable by low sensitivity techniques, as it is likely tightly regulated process to ensure microglial function and survival.

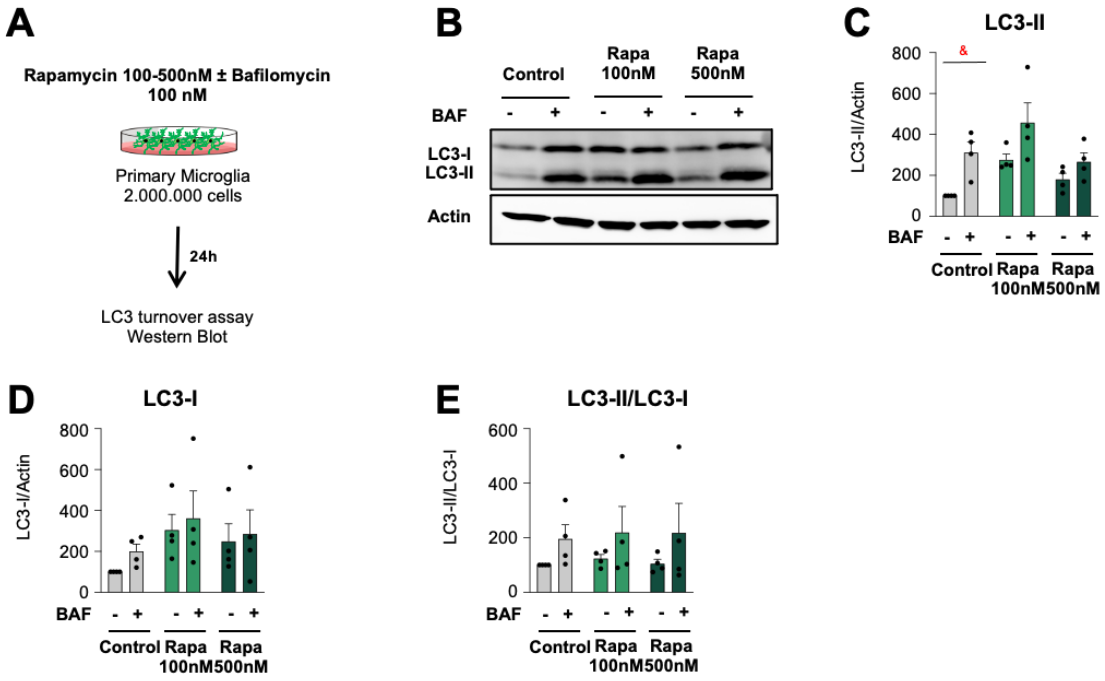

Figure 34. Basal autophagy was not significantly changed after 24 hours of rapamycin. ***[A]*** *Experimental design of the dose-response administration of rapamycin to primary microglia for 24 hours.* ***[B]*** *Representative blot showing relative levels of LC3-I and LC3-II after 100 and 500 nM rapamycin for 24h.* ***[C]*** *Quantification of the LC3-II levels (referred to actin) 100 and 500 nM rapamycin in the presence and absence of the lysosomal inhibitor, bafilomycin A (BAF, 100 nM),* ***[D]*** *LC3-I levels normalized to actin,* ***[E]*** *LC3-II levels normalized to LC3-I levels. Bars show mean ± SEM n4 independent experiments. Data was analyzed by two-way ANOVA followed by Holm-Sidak post hoc tests. (&) represents significance between bafilomycin-treated and non-treated groups: one symbol represents p<0.05.*

Our next approach was to test rapamycin under stressful conditions, such as OND, where we already described that microglia attempted to initiate autophagy in response to the lack of oxygen and nutrients and, for this purpose we selected the 100 nM concentration for 24 hours to test it effects in OND.

The potentiation of the already initiated autophagy response in microglia during OND could be beneficial to ensure microglial function. To answer this question, we first assessed the effects of rapamycin on autophagy after OND. Primary microglia were pre-treated with 100 nM rapamycin for 21 hours and then placed under OND conditions for 3 hours in the presence of rapamycin (**Figure 35A**). Surprisingly, we did not observe any effects on LC3-II/actin levels after rapamycin (**Figure 35B**, **C**), prompting us once again to consider the low western blot sensitivity for autophagy as no changes were observed in LC3-I/actin and LC3-II/LC3-I values either (**Figure 35C**,

D). Regardless of the western blot results, we further assessed the role of rapamycin directly on microglial function and test whether it ameliorated the deficient phagocytosis after OND.

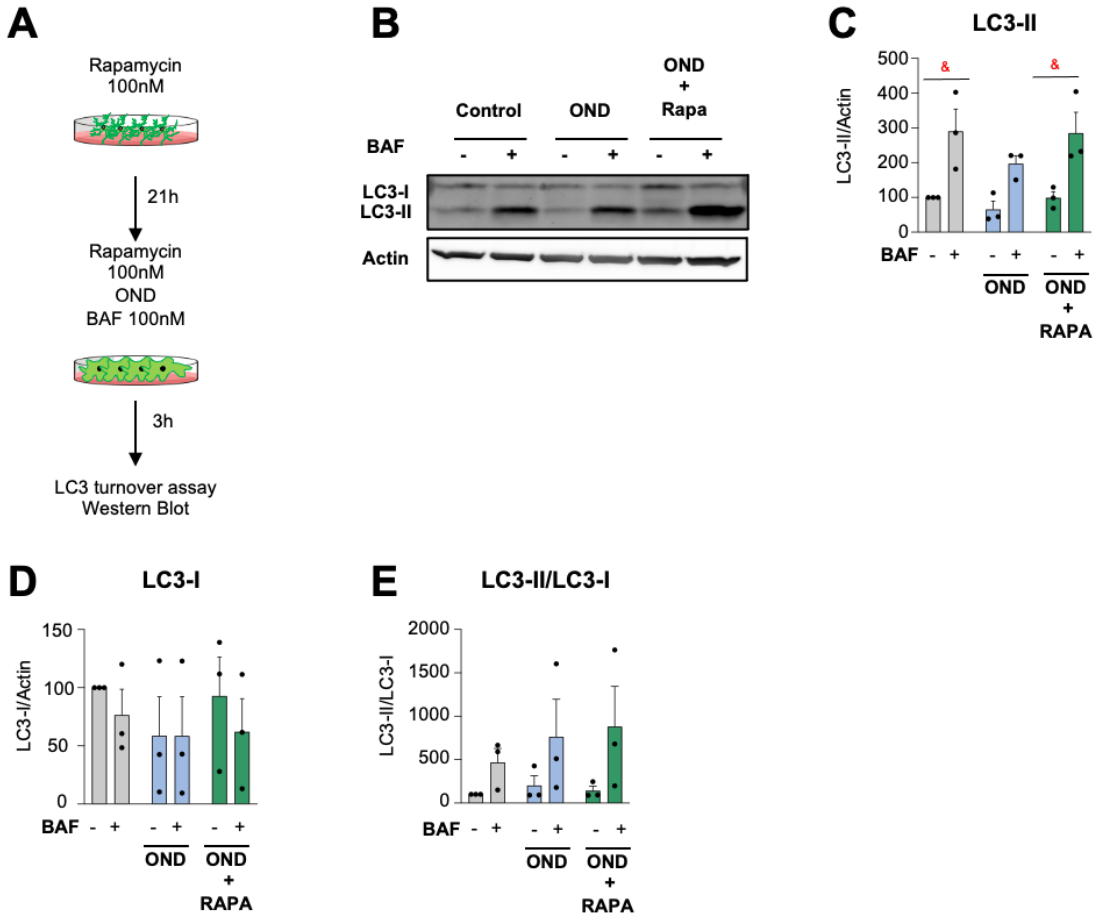

Figure 35. Rapamycin had no effect on microglial autophagy after OND. ***[A]*** *Experimental design of the dose-response administration of rapamycin to OND treated primary microglia for 24 hours.* ***[B]*** *Representative blot showing relative levels of LC3-I and LC3-II after 100 nM rapamycin for 24h.* ***[C]*** *Quantification of the LC3-II levels (referred to actin) 100 nM rapamycin in the presence and absence of the lysosomal inhibitor, bafilomycin A (BAF, 100 nM),* ***[D]*** *LC3-I levels normalized to actin,* ***[E]*** *LC3-II levels normalized to LC3-I levels. Bars show mean ± SEM n=3 independent experiments. Some data was transformed using a square root to comply with homoscedasticity. Data was analyzed by two-way ANOVA followed by Holm-Sidak post hoc tests. (&) represents significance between bafilomycin-treated and non-treated groups: one symbol represents p<0.05, two symbols p<0.01.*

6.5.2 Rapamycin did not recover the deficits in degradation after OND

To test this hypothesis, we performed the in vitro phagocytosis assay in the presence of rapamycin during OND (**Figure 36A**). Primary microglia were pre-treated with rapamycin, diluted in control medium, or vehicle (control medium) (**Figure 36B**). To assess the engulfment step,

microglia from either control or OND (3 hours) were treated with vehicle or rapamycin. Then they were fed with apoptotic cells for 1 hour to assess engulfment in control and OND conditions with and without rapamycin. After 1 hour, the non-phagocytosed apoptotic cells were washed out and microglia engaged in phagocytosis were left for 3 more hours to degrade the phagocytosed cargo (**Figure 36A**, **B**). Rapamycin had no effect on engulfment either in control or OND conditions (**Figure 36C**), suggesting that microglial phagocytosis was already functional in both control and OND. Rapamycin did not revert the deficient degradation induced by OND (**Figure 36D**), suggesting that, in vitro, rapamycin did not exert the protective effect described in vivo (**Figure 15**).

A

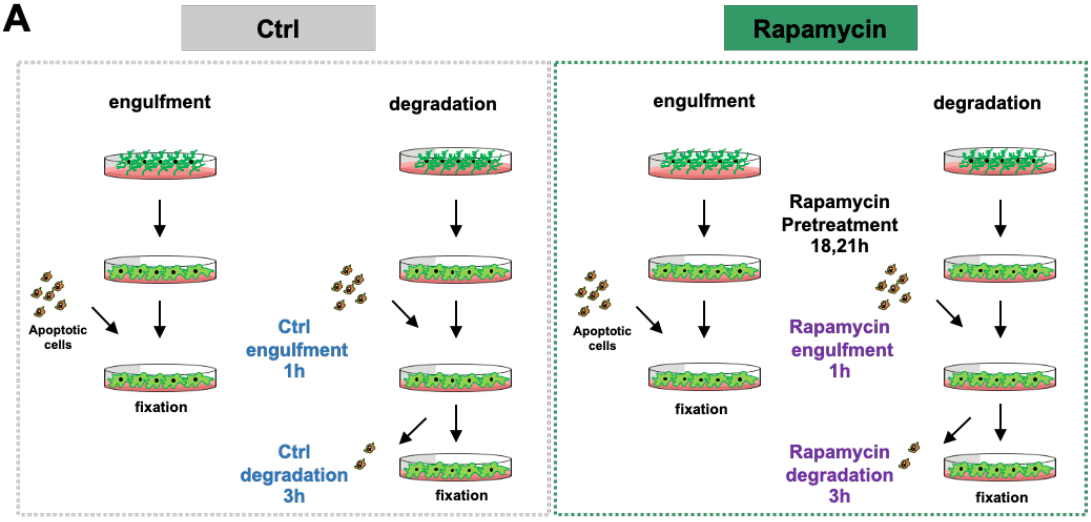

B

Group	Rapamycin (20h)	OND (3h)	Engulfment (1h)	Degradation (3h)
Control ENG	Veh	Veh	Veh	-
Control DEG	Veh	Veh	Veh	Veh
Rapa ENG	Rapa	-	Rapa	-
Rapa DEG	Rapa	-	Rapa	Rapa
OND ENG	Veh	OND	OND	-
OND DEG	Veh	Veh	Veh	OND
OND Rapa ENG	Rapa	OND + Rapa	OND + Rapa	-
OND Rapa DEG	Rapa	-	Rapa	OND + Rapa

C

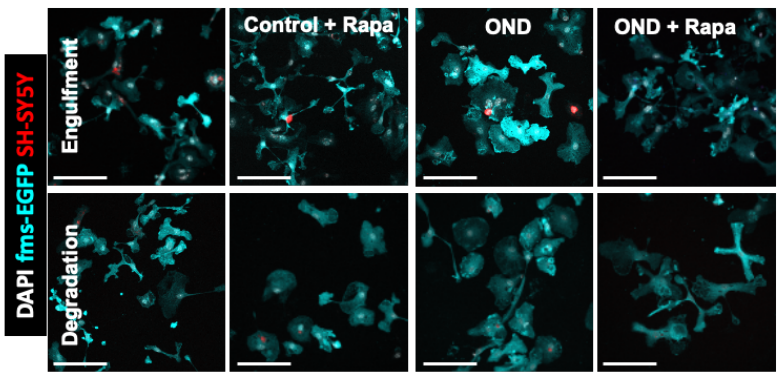

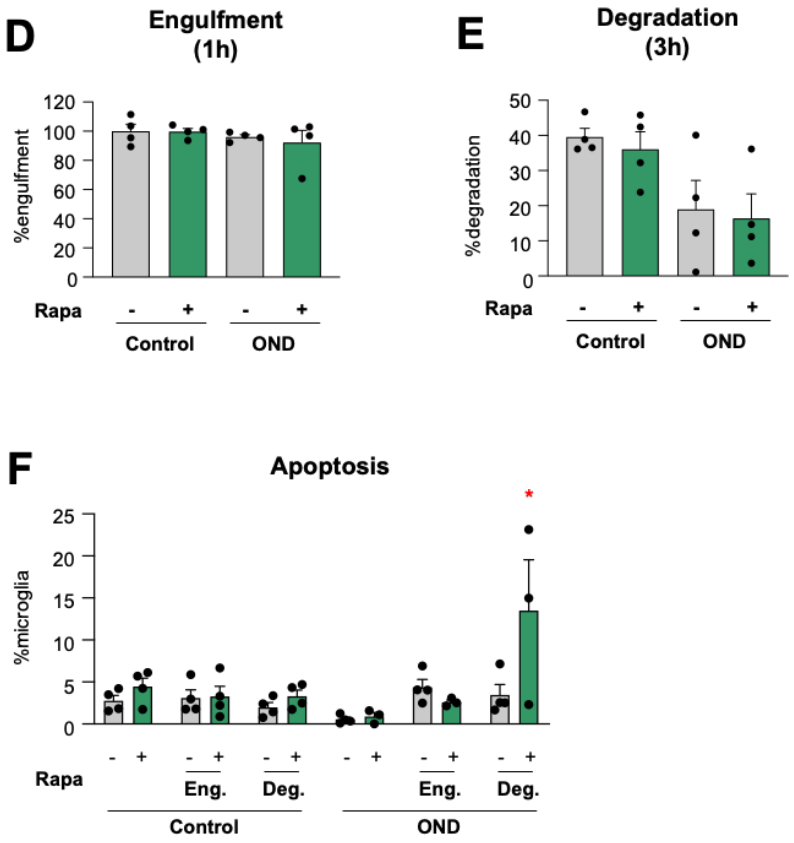

Figure 36. Rapamycin did not revert the deficits in degradation induced by OND. ***[A]*** *Experimental design of the phagocytosis assay to assess engulfment and degradation of apoptotic cells after the addition of rapamycin in control and OND treated primary microglia.* ***[B]*** *Table summarizing the treatments.* ***[C]*** Representative confocal images of microglia (fms-EGFP^{+}, cyan) engulfing (1h) and degrading (3h) *apoptotic SH-SY5Y vampire neurons (red) under control and OND conditions in the presence of rapamycin. Nuclear morphology was assessed with DAPI (white). Only particles fully enclosed by microglia were identified as phagocytosis.* ***[D, E]*** *Percentage of phagocytic microglia after engulfment (1h) and degradation (3h after engulfment). Only particles fully enclosed by microglia were identified as being phagocytosed.* ***[G]*** *Percentage of apoptotic microglia in naïve and phagocytic microglia (engulfment and degradation) assessed by their healthy or apoptotic nuclei (pyknotic/karyorrhectic). Bars show mean ± SEM. n=4 independent experiments. Data was analyzed or by one-way ANOVA followed by Tukey´s post hoc test when a significant interaction in two-way ANOVA was found* ***[G]. Scale bar****=50µm, z=8.5µm.*

We previously demonstrated that the inhibition of autophagy inhibition, was translated into an increase in microglial apoptosis, both in vivo (**Figure 10**) and in vitro (**Figure 30**, **31**). Hence, we next analysed microglial apoptosis in the context of autophagy induction in the presence of rapamycin in the different experimental conditions. Unexpectedly found that rapamycin specifically induced microglial death in OND-treated cells during apoptotic cell degradation (**Figure 36E**). In conclusion, rapamycin was not able to revert the degradative defects induced

by OND in primary microglia and induced cell death; however, to test the action of rapamycin in a more complex experimental set up and determine the possible tangential effects of other cell types, we assessed microglial phagocytosis in organotypic hippocampal slices treated with rapamycin under OND.

6.5.3 Rapamycin did not recover the deficits in phagocytosis after OND in organotypic slices.

To determine the effects of rapamycin in OND treated hippocampal slices, we pre-treated the cultures for 3 or 21 hours with either vehicle (control medium) or 200 nM rapamycin and later performed OND for 3 hours in control medium and in the presence of rapamycin (**Figure 37A**, **B**).

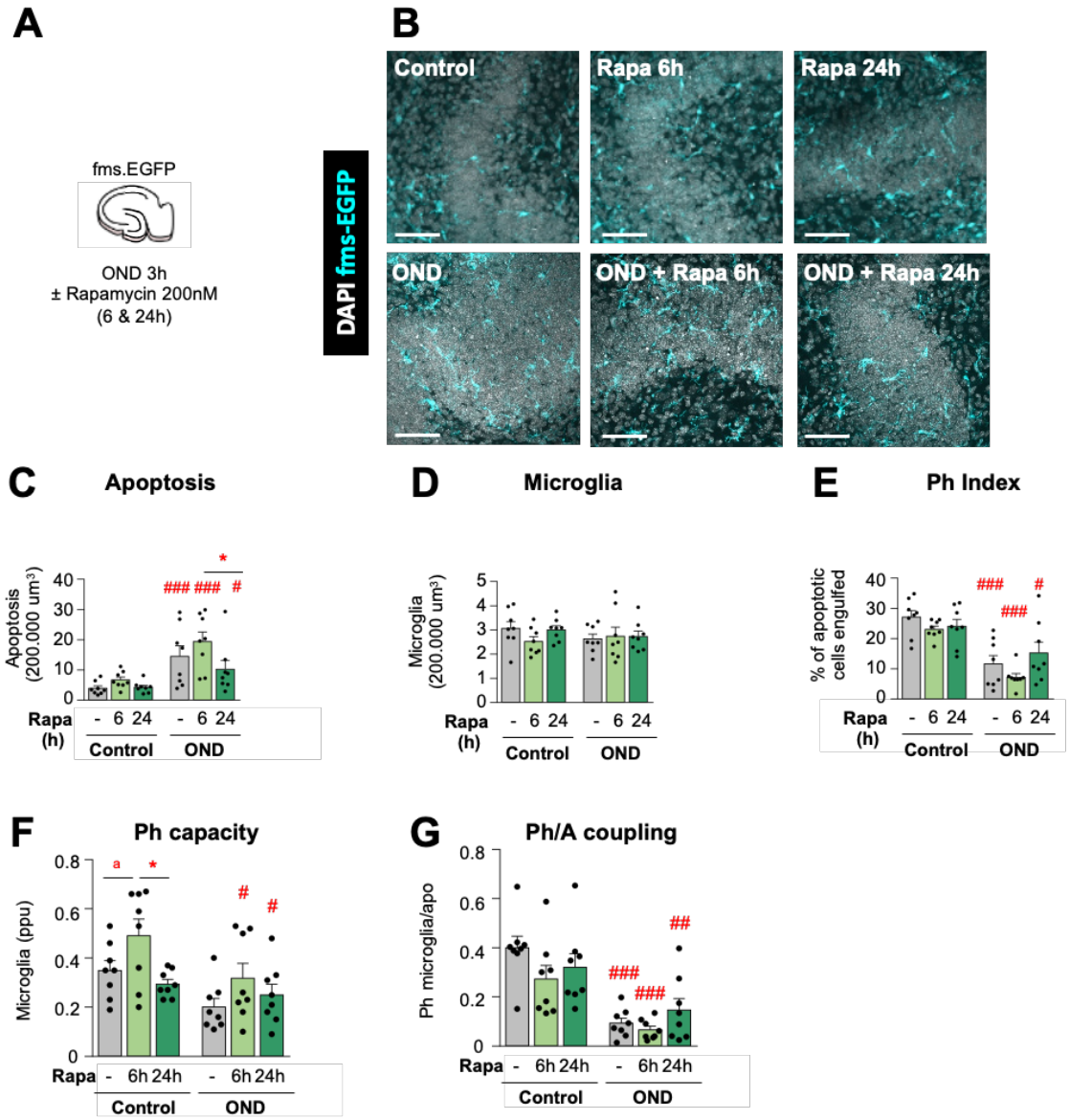

Figure 37. The phagocytosis deficits after OND were not recovered by rapamycin in organotypic hippocampal slices. ***[A]*** *Experimental design of hippocampal organotypic cultures. treated with vehicle or rapamycin (200nM; 6 and 24h) exposed to OND (3h).* ***[B]*** *Representative images of control and OND groups treated with rapamycin. Normal or apoptotic (pyknotic/karyorrhectic) nuclear morphology was visualized with DAPI (white) and microglia by the transgenic expression of fms-EGFP (cyan).* ***[C]*** *Number of apoptotic cells in 200.000 µm^3 of the DG.* ***[D]*** *Number of microglia in 200.000 µm^3 of the DG.* ***[E]*** *Ph index (% of apoptotic cells phagocytosed by microglia).* ***[F]*** *Weighted Ph capacity (number of phagocytic pouches filled with apoptotic nuclei per microglia) in parts per unit (ppu).* ***[G]*** *Ph/A coupling in fold-change (net phagocytosis with respect to total levels of apoptosis. Bars show mean ± SEM. n=8 mice per group. Data was analyzed by two-way ANOVA followed by Holm-Sidak post hoc tests when appropriate. Some data (**[C]**) was Log$_{10}$ transformed to comply with homoscedasticity. Asterisks represent significance between untreated and rapamycin-treated mice or cultures: (*) represents p<0.05. (#) represent significance between OND and control cultures: # represents p<0.05, and ### represents p<0.001. (a) represents p=0.079 (rapamycin 6h vs control). Scale bars=50µm, z=11.2µm* ***[B]****.*

In control conditions, rapamycin did not alter basal apoptosis, but it did reduce the OND-induced cell death in the 24-hour group (**Figure 37A**), suggesting a protective effect of rapamycin on global cell survival. The reduced apoptosis was not directly related to microglia, as microglial numbers remained constant despite the addition of rapamycin (**Figure 37D**). Furthermore, rapamycin did not recover the phagocytosis impairment in OND (**Figure 37E**) and had variable effects modulating the Ph capacity, slightly increasing microglial capacity after 6 hours in basal conditions and showing a small trend to recover it in OND (**Figure 37F**). However, the Ph/A coupling was not recovered by rapamycin (**Figure 37G**) indicating that microglia were not able to cope with the increase in apoptosis after OND despite the addition of rapamycin. The in vivo recovery after the rapamycin pre-treatment and the inconclusive in vitro data suggested that the possible effect of rapamycin in vivo could be related to its action on other cell types involving a more complex mechanism that we could not assess in vitro.

In summary, we have shown that OND has detrimental effects on microglial phagocytosis, reducing microglial motility, which was likely involved in preventing the engulfment of apoptotic cells; and reducing and basifying the lysosomal compartment, which was presumably related to the deficient degradation of the phagocytosed cargo. Autophagy was also initiated as a protective response after OND to guarantee microglial survival but seemed to compete with phagocytosis for the pool of lysosomes. In basal conditions, autophagy was essential to ensure microglial survival and function. Moreover, its inhibition dramatically reduced microglial survival and phagocytosis in OND. The autophagy response triggered by microglia during OND focused

our attention on the mTORC1 inhibitor, rapamycin, and promote autophagy to recover phagocytosis. In vivo, we were able to partially preserve microglial phagocytosis after the pre-treatment with rapamycin; however, we were not able to recover microglial phagocytosis in organotypic cultures nor overcome the deficits in degradation in primary microglia, where it induced microglial cell death. These results suggest that the potentially beneficial effects of rapamycin observed in vivo could be mediated by other cell types (**Figure 15**).

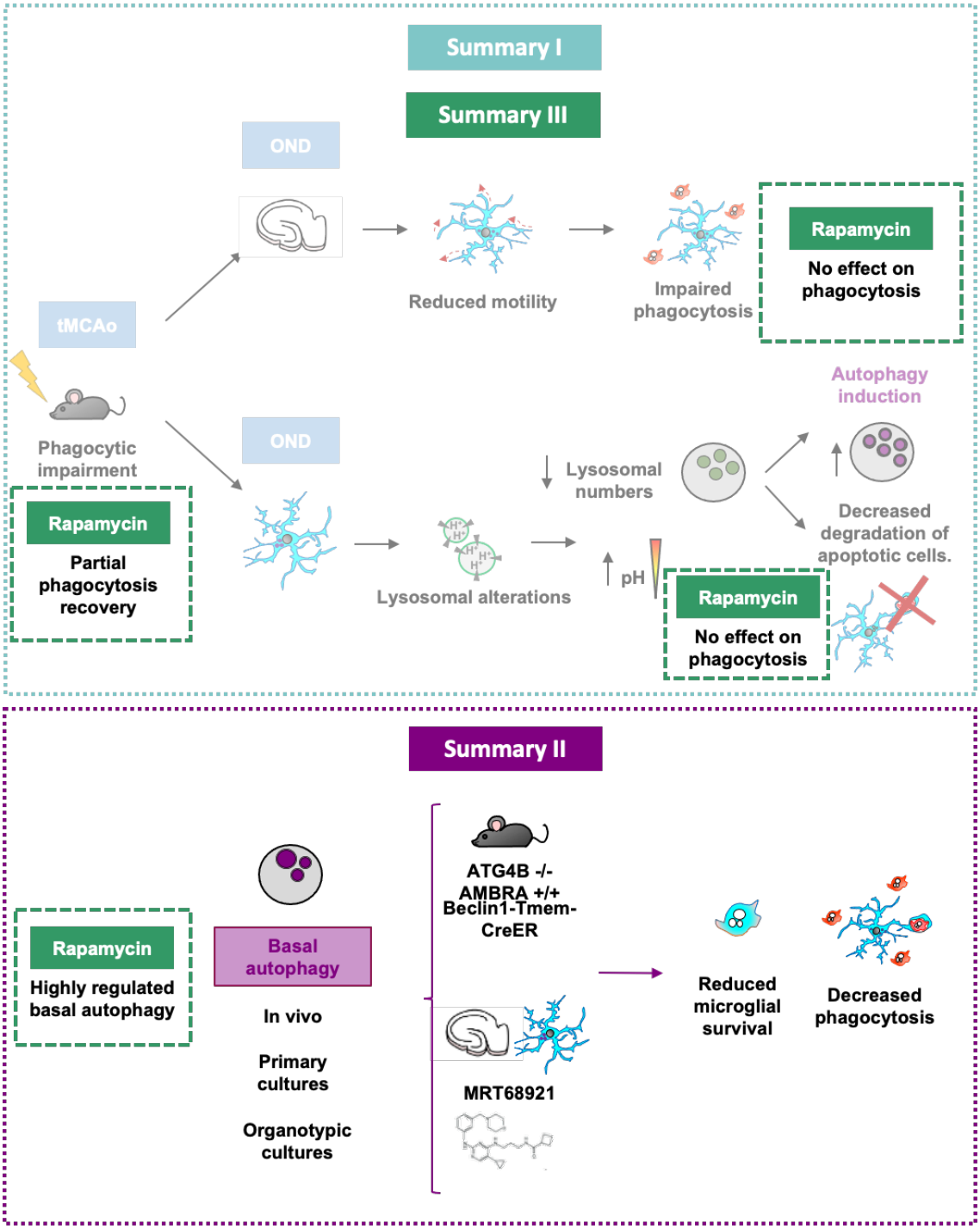

Figure 38. Summary II. *Major findings on the modulation of autophagy and phagocytosis with rapamycin.*

In the following section we will extend our analysis of LC3 western blot data to study autophagy. It will be divided in three major blocks: First, we will describe a two-step model to analyse LC3 data; second, we will describe several simulated scenarios; and, finally, we will test our model in different context of autophagy status.

6.6 ASSESING AUTOPHAGY IN MICROGLIA: FORMATION, DEGRADATION AND NET TURNOVER

In the previous sections, we discussed that the LC3 western blot assay was not sensitive enough to detect changes in autophagy, at least in our hands, compared to other techniques such as confocal imaging of the tandem GFP-RFP-LC3 or TEM. For this reason, we further explored in more detail the amount of information that could be obtained from LC3 western blotting under OND, MRT and rapamycin treatments. We propose a two-step method to describe the two major steps of autophagy: formation and degradation of the autophagosomes, using LC3 western blot data.

[This section has been published in Plaza-Zabala A, Sierra-Torre v, Sierra A. Assessing Autophagy in Microglia: A Two-Step Model to Determine Autophagosome Formation, Degradation, and Net Turnover. Frontiers in Immunology 2021.]

6.6.1 A two-step model to analyse western blot

Autophagy is a complex multistep process that encompass the formation, maturation and final degradation of the autophagosomes (Yu et al., 2018). The current guidelines suggest the use of several complementary techniques to analyse the full process (Klionsky et al., 2021); however, the gold standard method remains the analysis of the autophagy flux using LC3. Traditionally, the autophagy flux is calculated as the differential amount of LC3-II in the presence/absence of lysosomal inhibitors, such as bafilomycin A1 or chloroquine. As the lysosomal degradation is inhibited, autophagosomes accumulate and, thus, the LC3-II bound to the membrane of the non-degraded autophagosomes gives an idea of the amount of autophagic vesicles that would have been degraded. The autophagy flux is then a measure of autophagosome degradation, but we will show here that LC3-II western blot raw data contains information of both autophagosome formation and degradation (**Figure 39**).

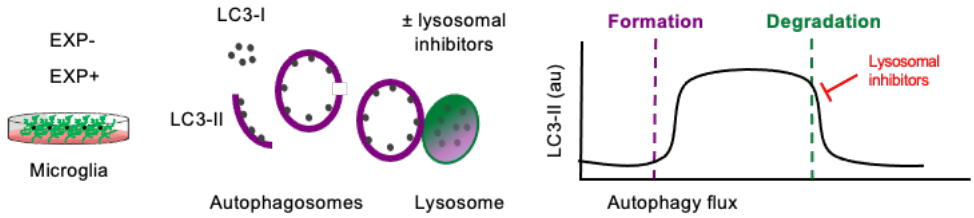

Figure 39. Estimation of autophagy flux variations using LC3 turnover assay. ***[A]*** *Total protein homogenates obtained from microglia under control (EXP^-) and experimental conditions (EXP^+) are analyzed by Western Blot to evaluate LC3 levels in the presence and absence of lysosomal inhibitors. When autophagy is activated, LC3-I (soluble form) is lipidated to the phophatidylethanolamine of the nascent phagophore forming LC3-II (membrane-bound form). LC3-II accumulates along the extension of the autophagic vacuoles as it closes and is used as an estimate of the number of autophagosomes. Upon fusion with lysosomes, LC3-II levels decrease due to the degradation of the inner autophagosomal membrane simultaneously with the luminal cargo. In the presence of lysosomal inhibitors, no degradation occurs, and LC3-II levels are maintained. The subtraction of LC3-II quantities in the presence and absence of lysosomal inhibitors provides an estimate of the autophagosomes that have been degraded during the experimental period of time.*

To discriminate between autophagosome formation and degradation we propose that the net number of autophagosomes (i.e., the autophagosome pool) at any given time is treated as a black box with an input (autophagosome formation) and an output (autophagosome degradation) (**Figure 40A**). The formation phase is defined as the phagophore formation, cargo sequestration and autophagosome closure, and the degradation step refers to the fusion with late endosomes and lysosomes followed by the enzymatic degradation of the enclosed cargo. These steps can be modelled by a simple equation in which the size of the autophagosome (APh) population in a given time point depends on the number of autophagosomes in the steady state (ss), equivalent to the basal pool, plus the number of newly formed autophagosomes minus the degraded autophagosomes in a certain period of time:

$$APh_t = APh_{ss} + \text{APh Formation} - \text{APh Degradation}$$

The ratio between degradation and formation is defined as the net autophagic turnover, which is a measure of the relative velocity of autophagosome formation versus degradation. There are certain stimuli that can act proportionally both on formation and degradation, maintaining the size of the APh pool and resulting in a constant net turnover ratio (**Figure 40A1**). However, other stimuli act differentially on formation and degradation leading to a dissociation of the two processes: an increased degradation would decrease the APh pool and increase the net turnover

ratio (**Figure 40A2**); and on the contrary, an increased formation would increase the size of the APh pool and reduce the net ratio (**Figure 40A3**). Thus, to fully understand the biology behind the autophagosome turnover we need to analyse separately formation and degradation and extract from them the net autophagic turnover.

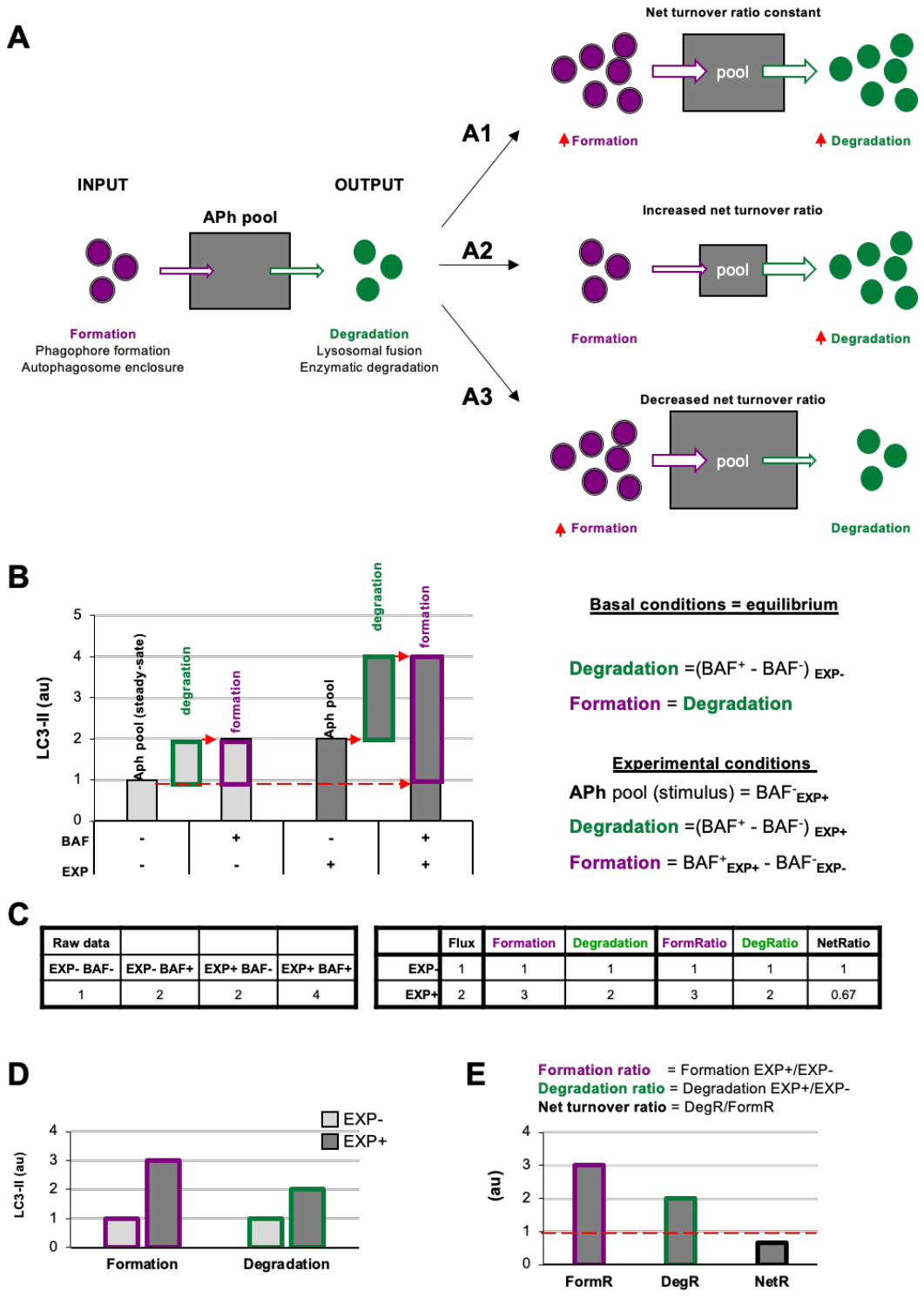

Figure 40. A two-step model of autophagy to analyze formation and degradation of autophagosomes. ***[A]*** *The model represents the autophagosomes as a box with an input (autophagosome formation, purple dots) and an output (autophagosome degradation, green dots) that determines the autophagosome net*

turnover. ***[A1-A3]*** *represent different possible scenarios with no changes* ***[A]****, an increase* ***[A2]*** *and a decrease* ***[A3]*** *in the autophagosome net turnover.* ***[B]*** *Graph representing the amount of LC3-II (au, arbitrary units) in two experimental conditions representing (EXP$^-$ and EXP$^+$) in the presence or absence of the lysosomal inhibitor bafilomycin (BAF$^-$ and BAF$^+$), and the formulas used to calculate formation, degradation, and net turnover. The dotted red arrows mark the LC3-II raw data values used to calculate the formation and degradation rates and ratios.* ***[C]*** *Simulated raw LC3-II data (au) (left) used to calculate the formation and degradation rates and ratios (right) used in the graphs shown in* ***[B, D, E] [D, E].*** *Graphs representing the rate of change of formation, degradation and net turnover between the two experimental conditions.*

This analysis is conceived to be used in conventional LC3 assays by western blot. Commonly, this approach consists of two experimental conditions: EXP$^-$ (control) and EXP$^+$ (experimental stimulus) incubated in the presence or absence of lysosomal inhibitors such as bafilomycin A1 (BAF$^-$ and BAF$^+$) for an established period of time. The extracted protein from these groups is analysed by Western blot and normalized to reference proteins such as actin (Klionsky et al., 2021).

In the control condition (EXP$^-$), the amount of LC3-II without lysosomal inhibitors (BAF$^-$) represents the APh pool in the steady state (**Figure 40B**). The difference between the amount of LC3-II in the presence and absence of lysosomal inhibitors (BAF$^+$-BAF$^-$) in control conditions represent the quantity of lysosomes that have disappeared, the degradation phase or conventionally, the autophagy flux. To calculate the autophagosomes that have formed, our model is funded in the assumption that in control or basal conditions formation and degradation occur at the same speed, thus, autophagy is in equilibrium:

Basal condition

APh Formation = APh Degradation

$APh_{equilibrium} = APh_{ss}$

Hence, in the basal condition (EXP$^-$), the autophagosomes that have been formed are identical to the autophagosomes that have been degraded, represented as the amount of LC3-II with and without lysosomal inhibitors (BAF$^+$-BAF$^-$) (**Figure 40B**, **C**).

In the experimental condition (EXP$^+$), the amount of LC3-II in the absence of lysosomal inhibitors (BAF$^-$ in EXP$^+$) represents the size of the APh pool under the stimulus. As a reminder, degradation

is calculated as the difference in LC3-II with and without lysosomal inhibitors, in this case under the stimulus [$(BAF^{+}\text{-}BAF^{-})_{EXP+}$] (**Figure 40B**). Formation can be calculated as the difference between the amount of LC3-II in the presence of lysosomal inhibitors minus the size of the initial APh pool in steady-state [$(BAF^{+})_{EXP+}$- $(BAF^{-})_{EXP}$-] (**Figure 40B**). This method allows us to calculate degradation and formation both in control and experimental conditions. To determine if the stimulus acts proportionally in both formation and degradation, we can calculate the ratio between experimental and control conditions (EXP^{+}/EXP^{-}) for formation and degradation (**Figure 40C**, **D**). Last, to assess the magnitude of degradation compared to formation we can calculate the ratio between both of them (degradation/formation) as the net turnover ratio (**Figure 40E**), which has a value of one in basal condition, as formation and degradation occur at the same rate. Then we can compare how autophagosome net turnover ratio increases or decreases when facing a stimulus compared to the control condition. That formation and degradation occur at the same rate, is the first assumption that we considered to develop this model (**Figure 40E**, red dotted line).

6.6.2 Dissecting out autophagosome formation and degradation

This model allowed us to discriminate and quantify different potential biological scenarios that may affect autophagosome formation, degradation, or both. For instance, a typical autophagic stimulus would be expected to proportionally increase autophagosome formation and degradation, maintaining a balanced autophagy (**Figure 41A1**). An example of this scenario is the activation of the Transcription Factor-EB (TFEB) (Settembre et al., 2011), which co-ordinately regulates the biogenesis of autophagosomes and lysosomes, maintaining the equilibrium between formation and degradation.

To exemplify this scenario, we simulated raw LC3-II western blot data from a canonical autophagy stimulus (**Figure 41A2**) and, from here, we calculated the classic autophagy flux, showing the expected increase (**Figure 41A3**). We then applied our model to the raw data and observed that the canonical autophagic stimulus increased both formation and degradation (**Figure 41A4**). Importantly, both formation and degradation ratios were similar and, as a result, the net autophagy ratio was constant (**Figure 41A5**), implying a maintenance of the net autophagic turnover but at a higher rate/velocity, that could be possibly maintained in the long term.

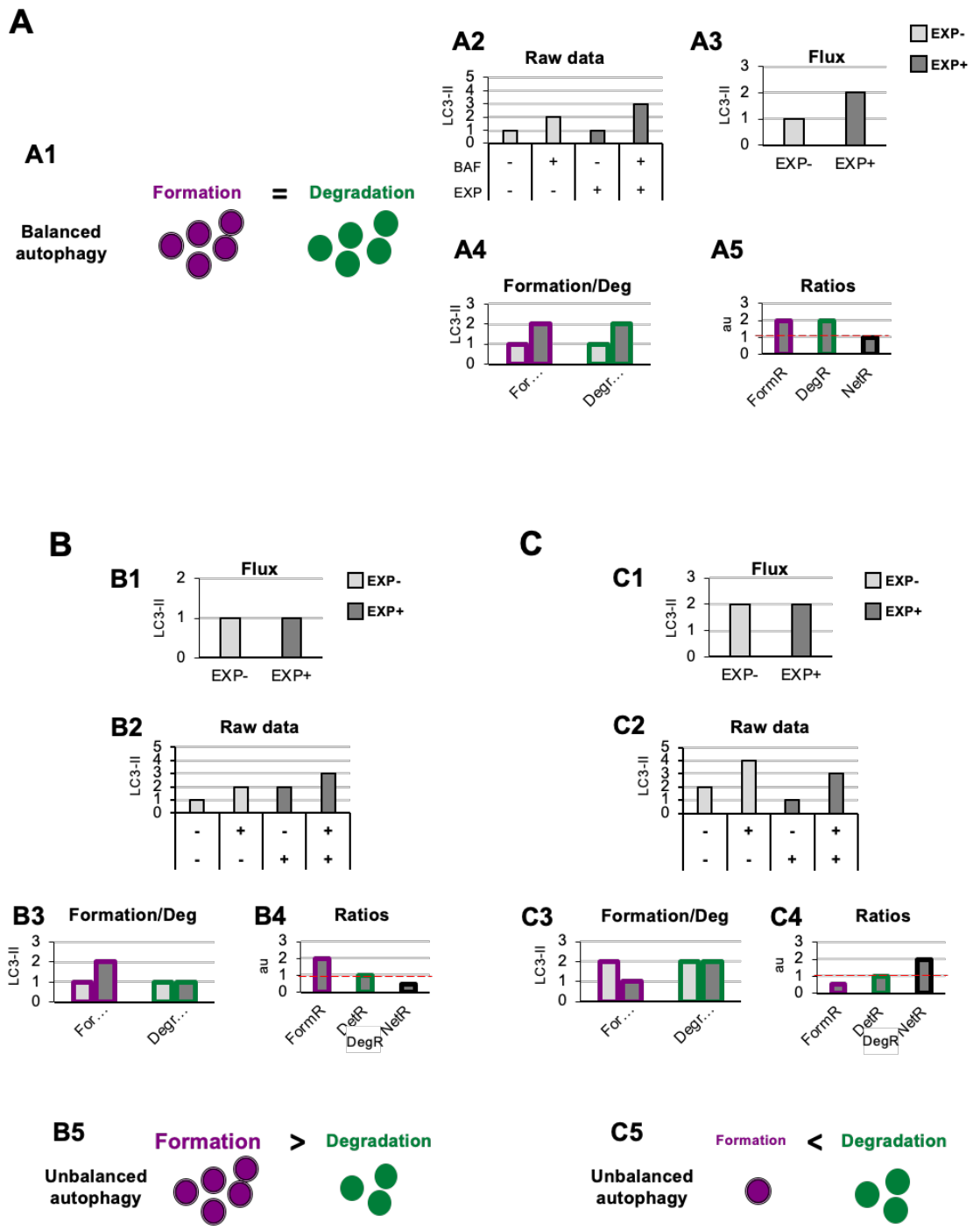

Figure 41. Theoretical examples of variations in the formation of autophagosomes that lead to balanced or unbalanced autophagy. ***[A]*** *Example of a balanced flux with proportional increase in autophagosome formation and degradation. The model of balanced flux with equal formation (purple dots) and degradation (green dots)* ***[A1]****, the raw LC3-II/actin Western blot data* ***[A2]****, the conventional autophagy flux* ***[A3]****, the formation and degradation rates* ***[A4]****, and the formation, degradation, and net ratios* ***[A5]*** *are shown. The red dotted line represents the threshold of one to determine a significant change (over 1, basal conditions) in the formation, degradation and net turnover ratios.* ***[B, C]*** *Show examples with similar conventional flux* ***[B1, C1]****, which are in fact derived from dissimilar raw LC3-II/actin Western blot data* ***[B2, C2]****. In* ***[B]*** *our model would reveal increased autophagosome formation rate and no changes in*

*degradation rate **[B3]** leading to an increased formation ratio and reduced net ratio **[B4]**, and an unbalanced autophagy **[B5]**. In contrast, in **[C]** our model would reveal decreased autophagosome formation rate and no changes in degradation rate **[C3]**, leading to an increased formation ratio and reduced net ratio **[C4]**, and an unbalanced autophagy **[C5]**.*

In contrast, there are other biological scenarios that are not so easily discriminated using the conventional calculation of the autophagy flux (**Figure 41B, C**). Examples of these scenarios are situations in which autophagosome formation is increased (**Figure 41B**) or decreased (**Figure 41C**), without concomitantly affecting degradation. For instance, overexpression of ATG proteins or accumulation of intracellular debris would lead to increased autophagosome formation. But if lysosomal efficiency (i.e., degradation) is not proportionally increased, autophagosomes will stall in the lysosomes without degrading the autophagic cargo, leading to a decreased net turnover ratio and increased autophagosome pool. This effect has been for example observed in cells that overexpress Atg5 but whose lysosomal function is compromised (Pyo et al., 2013). In this case, calculation of the autophagy flux would not reveal any changes (**Figure 41B1, C1**), although the raw LC3-II data is evidently different (**Figure 41B2, C2**). Our model would help to quantify the specific effect on degradation (**Figure 41B3, C3**), and the alteration of the net autophagy ratio (**Figure 41B4, C4**), revealing an unbalanced autophagy (**Figure 41B5, C5**), and a potentially catastrophic situation for the cell that could not possibly be maintained over time.

Other biological scenarios that cannot be discriminated using conventional analysis of the autophagy flux are shown in **Figures 42-43**. Some stimuli may selectively increase autophagosome degradation without affecting their formation co-ordinately (**Figure 42A**), or even reducing it (**Figure 42B**). For example, enhanced lysosomal biogenesis or lysosomal enzymes efficiency might lead to increased autophagosome degradation, resulting in an increased net turnover ratio and reduced autophagosome pool size. This imbalance has been reported in mice genetically deficient for the cathepsin inhibitor cystatin B, which exhibit enhanced lysosomal proteolysis (Yang et al., 2011). Whereas in this case the calculation of the autophagy flux would suggest an enhanced autophagy, our model would reveal the imbalance between formation and degradation, suggesting that in fact cellular debris would not be removed any faster from the cytoplasm.

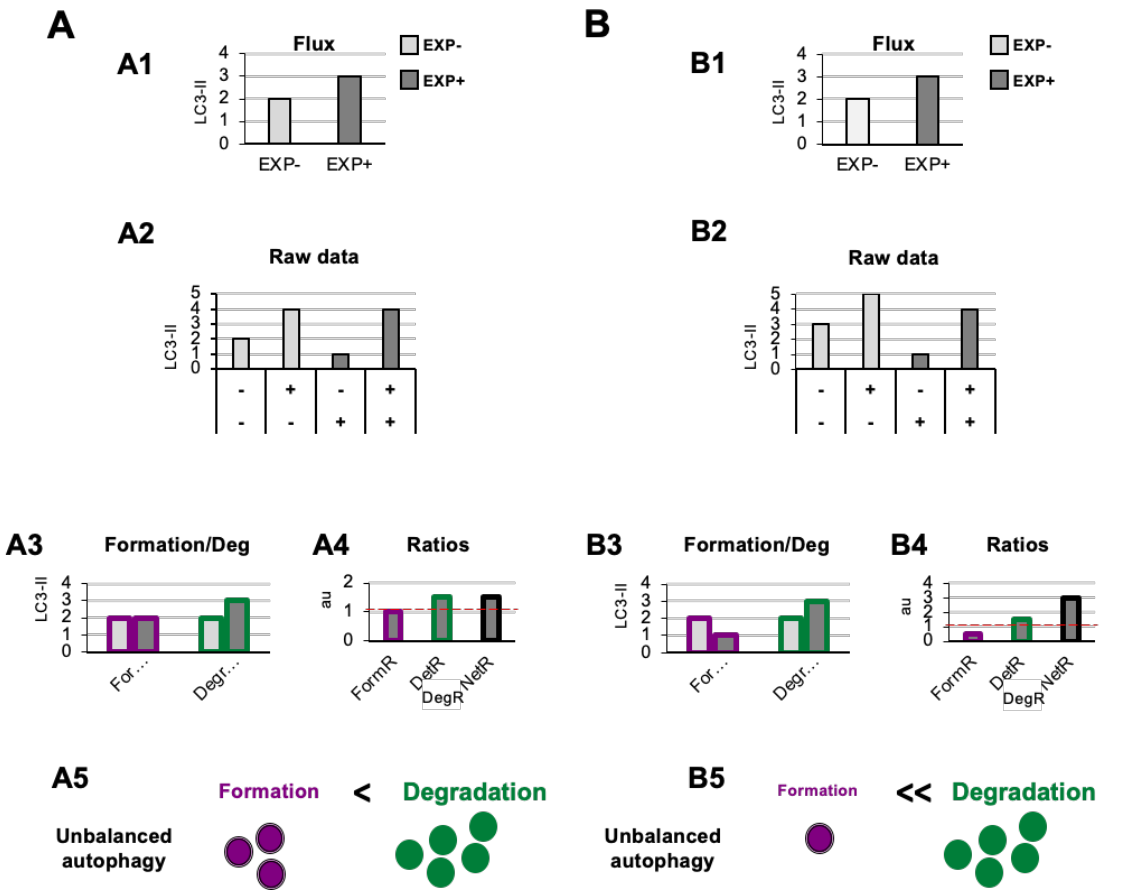

Figure 42. Theoretical examples of increased autophagosome degradation that lead to unbalanced autophagy. ***[A, B]*** *show examples with similar conventional flux* ***[A1, B1]****, derived from apparently similar raw LC3-II/actin Western blot data* ***[A2, B2]****. In* ***[A]*** *our model would reveal an increased autophagosome degradation rate and no changes in the formation rate* ***[A3]****, leading to an increased degradation ratio and net ratio* ***[A4]****, and an unbalanced autophagy* ***[A5]****. In contrast, in* ***[B]*** *our model would reveal decreased autophagosome formation rate but increased degradation* ***[B3]****, leading to decreased formation ratio, increased degradation ratio, and a strong increase in the net ratio* ***[C4]****, ultimately resulting in a highly unbalanced autophagy****[B5]****.*

Another scenario in which our model may prove useful is a where autophagosome degradation is reduced but formation is maintained (**Figure 43A**) or even increased (**Figure 43B**). An example of this scenario is a pathological condition where dysfunctional organelles accumulate and the cell tries to enclose them in autophagosomes, but lysosomal functionality is compromised, for instance because lysosomes are defective or engaged in other degradation pathways such as phagocytosis or endocytosis. This effect could be observed in Parkinson's disease (PD) dopaminergic neurons, which contain LC3-positive Lewy bodies, and have stalled autophagosomes and lysosomal depletion (Dehay et al., 2010). This complex effect cannot be

fully understood by simply analysing the reduction in the autophagy flux but would be instead clearly described by our two-step model.

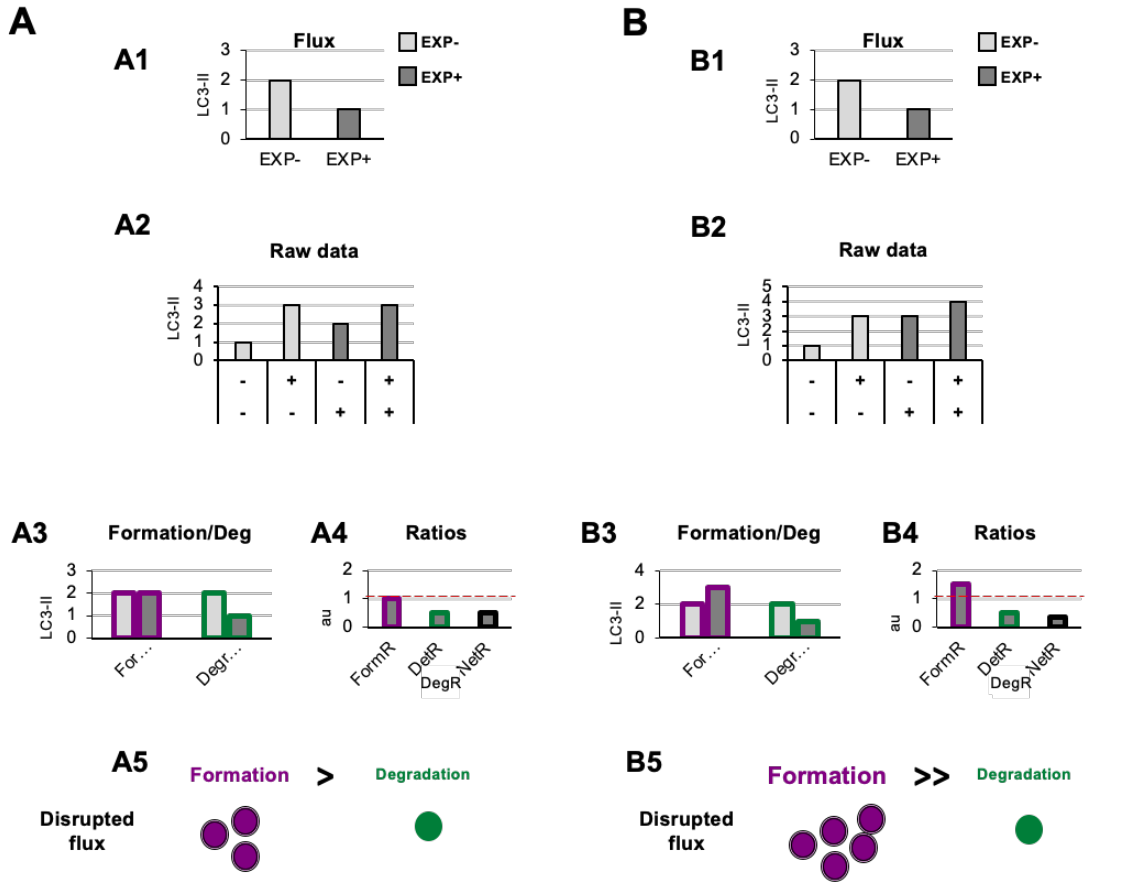

Figure 42. Theoretical examples of decreased autophagosome degradation that lead to unbalanced autophagy. ***[A, B]*** show examples with similar conventional flux ***[A1, B1]***, derived from apparently similar raw LC3-II/actin Western blot data ***[A2, B2]***. In (A) our model would reveal a decreased autophagosome degradation rate and no changes in the formation rate ***[A3]***, leading to a reduced degradation ratio and net ratio ***[A4]***, and an unbalanced autophagy ***[A5]***. In contrast, in ***[B]*** our model would reveal increased autophagosome formation rate but decreased degradation ***[B3]***, leading to increased formation ratio, reduced degradation ratio, and a strong reduction in the net ratio ***[C4]***, ultimately resulting in a highly unbalanced autophagy ***[B5]***.

6.6.3 Testing the model in vitro

To validate our model, we analysed autophagy data in the context of autophagy induction, using rapamycin, and in the context of autophagy inhibition, using MRT. Rapamycin and MRT target autophagy at early states of the cascade; hence, they can be considered as early checkpoints of canonical autophagy: mTORC1 transduces signals from energy and damage sensors and is inhibited under stressful situations, releasing ULK1/2 (unc-51-like kinase 1/2) by a series of phosphorylation and dephosphorylation events to initiate the autophagy cascade (Morel et al.,

2017) (Petherick et al., 2015). As a cell model, we used cultures of microglia (BV2 cells or primary cultures) and analysed the amount of LC3-II by western blot as a measurement of the size of the autophagosome pool. (The following data are an extension of the already shown results in **Figures 22**, **27**, and **28**).

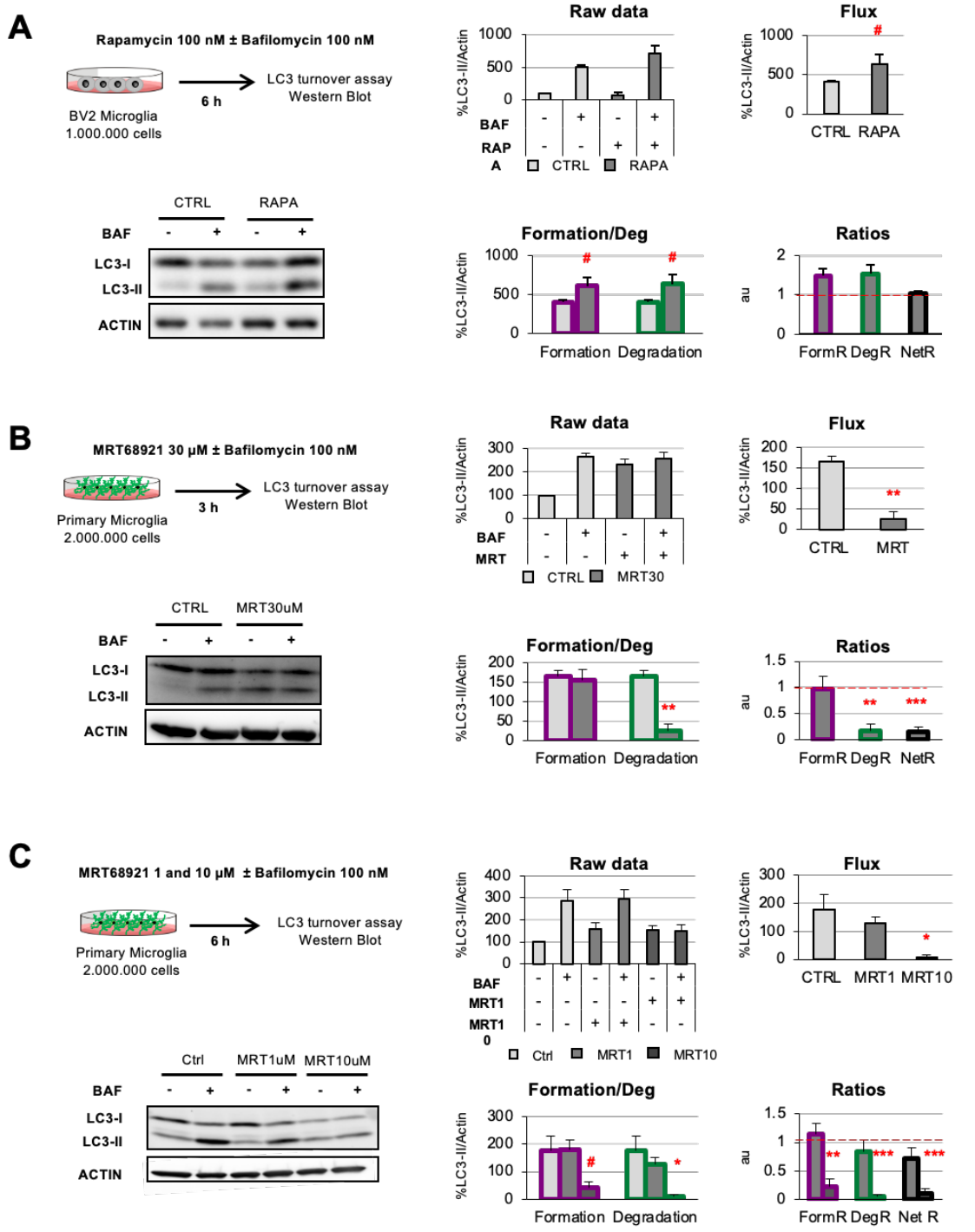

Figure 44. Validation of the two-step model with autophagy modulating compounds. ***[A]*** *Autophagy induction assessed after treatment with rapamycin (100 nM, 6 h) in the presence and absence of Bafilomycin (100 nM) in the BV2 microglia cell line. A representative blot, the raw data obtained, and the calculations of flux, autophagosome formation and degradation, and net turnover ratios are shown. Data*

is presented as % over control (LC3-II/actin). ***[B, C]*** *Autophagy inhibition assessed after treatment with MRT68921 (30 mM, 3 h in* ***[B]****; 1 and 10 mM, 6 h in* ***[C]*** *in the presence and absence of Bafilomycin (100 nM) in mouse primary microglia. A representative blot, the raw data obtained, and the calculations of flux, autophagosome formation and degradation, and net turnover ratios are shown. Data is presented as % over control (LC3-II/actin). Data represent mean ± SEM of 3 independent experiments.* $^{\#}$*represents p < 0.1, *represents p < 0.05 and ** represents p < 0.01 by one tailed Student t-test (A, B), or Holm-Sidak after a significant effect of the treatment was found with 1-way ANOVA* ***[C]****.*

In BV2 microglia rapamycin (6h, 100nM) showed the expected response and a trend to increased LC3-II flux (**Figure 44A**). In addition, our model uncovered a parallel increase in formation and degradation of autophagosomes, resulting in a constant size of the APh pool and no changes in the net autophagosome turnover. Thus, rapamycin allowed the maintenance of the equilibrium between formation and degradation (**Figure 44A**), indicating a sustained autophagy that the cell can maintain over time.

On the other hand, MRT (3h, 30μM) resulted in the expected decrease in the LC3-II flux in primary microglia (**Figure 44B**), which we already described (**Figure 27**). However, analysis with our model revealed that only degradation was reduced whereas autophagosome formation remained constant (**Figure 44B**). This data is in apparent contradiction with the described role of MRT in blocking the autophagy pre-initiation complex (Morel et al., 2017; Petherick et al., 2015). To address this discrepancy, we used the second paradigm of MRT with a longer treatment and lower dosage (6h, 1-10μM; **Figure 44C**), and observed that the upstream effect of inhibition of autophagosome formation with MRT 10μM translated into a similar decrease in degradation (**Figure 44C**), previously described (**Figure 28**). Therefore, our model proves useful to discriminate the effect of experimental manipulations on the formation and/or degradation of autophagosomes.

We further extended the applicability of our two-step model to the western blot data obtained after 3h of OND (**Figure 44**) and compared it with the TEM results and the imaging data of transfected BV2 cells with the tandem GFP-RFP-LC3 (**Figure 10D, E**). After OND, we were not able to detect the subtle changes in the autophagy flux that we did observe using TEM and the tandem GFP-RFP-LC3; hence, we determined that the western blot technique had not enough sensitivity to detect subtle changes in the autophagy flux in OND experiments. However, to fully characterize the status of the autophagy cascade after OND by western blot we applied our 2-step model to discriminate between the formation and degradation steps (**Figure 45**) in OND

treated microglia for 3 hours (**Figure 45A**, **B**). The LC3-II/actin ratio or raw data (**Figure 31C**) remained at control levels, as previously described (**Figure 22**), apparently suggesting no changes after OND and, moreover, the dissection of the formation and degradation steps (**Figure 45D-F**) did not reveal any changes in autophagy dynamics. These results confirm that, despite being an accurate tool for the analysis of western blot data, the two-step model did not uncover the effects of OND in microglia, hence confirming the low sensitivity of western blot to assess small changes. On the other hand, by TEM we were able to assess the increase in autophagy vesicles after 3 hours of OND (**Figure 45**). In addition, analysing the tandem GFP-RFP-LC3 by confocal microscopy we could determine the induction of autophagy after OND directly visualizing the autophagosomes according to the fluorescence expression of the transfected tandem (**Figure 10D, E**). The results obtained from TEM and confocal imaging strengthen the hypothesis that the western blot technique has low sensitivity to detect small changes in LC3 that could be functionally relevant for the cell physiology.

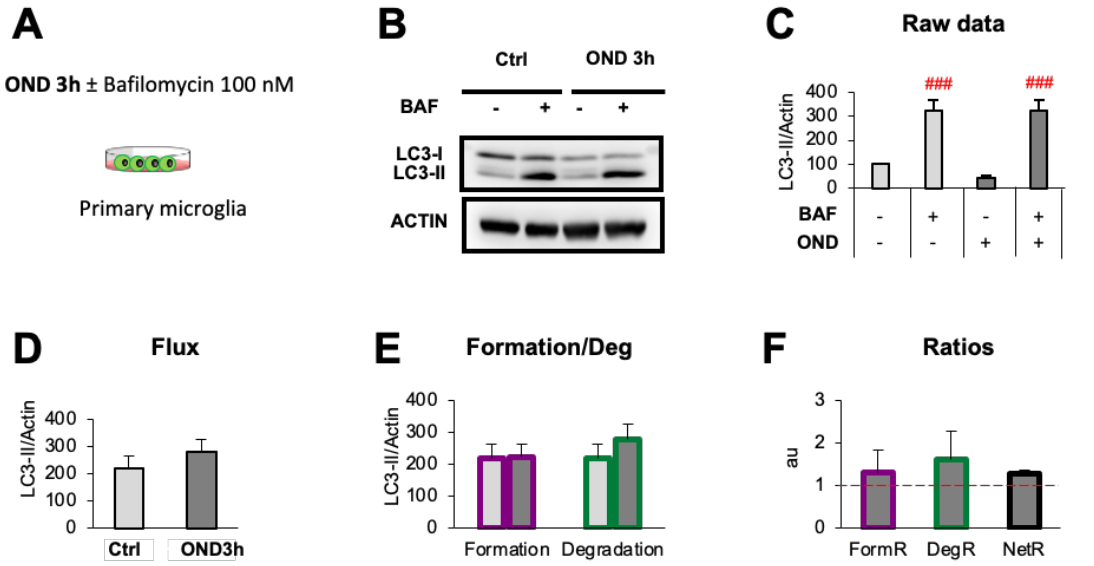

Figure 45. Validation of the two-step model with the OND model. ***[A]*** *Primary microglia were exposed to OND for 3 hours in the presence and absence of bafilomycin-A1 (BAF, 100 nM, 3 hours) to assess autophagy flux by LC3 turnover assay. Delipidated (~1 KDa) and lipidated (~17 KDa) LC3 levels were analyzed by western blot. Beta-actin (~42 KDa) was used as a loading control.* ***[B]*** *Representative blots showing LC3-I, LC3-II and actin bands,* ***[C]*** *LC3-II levels normalized to actin* ***[D]*** *autophagy flux* ***[E]*** *autophagosome formation and degradation,* ***[F]*** *net turnover ratios. Bars show mean ± SEM. n=4 independent experiments. Data is presented as % over control (LC3-II/actin). Data represent mean ± SEM of 3 independent experiments.* $^{\#}$*represents p < 0.01 by Holm-Sidak after a significant effect of the treatment was found with 1-way ANOVA* ***[C]****.*

In the final section, we will describe the functional effects on phagocytosis of the deficiency of the lysosomal protein cystatin B (CSTB), further extending the relationship between phagocytosis and the lysosomal compartment.

6.7 MICROGLIAL PHAGOCYTOSIS DYSFUNCTION IN THE DENTATE GYRUS IS RELATED TO LOCAL NEURONAL ACTIVITY IN A GENETIC MODEL OF EPILEPSY

Here, we further extended our studies on the effects of lysosomal alterations on microglial phagocytosis using a genetic model of epilepsy, progressive myoclonus epilepsy 1 (EPM1) or Unverricht-Lundborg disease (Joensuu et al., 2008; Lalioti et al., 1997; Pennacchio et al., 1996). This disease is characterized by loss-of-function mutations in the cystatin B gene (*CSTB*), which encodes cystatin B, a protease inhibitor that regulates and limits the activity of lysosomal, nuclear and cytoplasmic cysteine proteases known as cathepsins (Koskenkorva et al., 2012; Riccio et al., 2001). The loss of function of cystatin B and the dysregulation of the cathepsin activity could lead to alterations in microglial phagocytosis, as the lysosome is the ending point to recycle the phagocytosed cargo.

Previous data from our laboratory (PhD Thesis Ohiane Abiega, 2017) demonstrated that microglial phagocytosis was impaired in a mouse model of EPM1: *Cstb* KO mice. This phagocytosis deficiency in epilepsy was also described by our laboratory in a model of mesial temporal lobe epilepsy (MTLE), where microglia were “blinded” by the massive release of ATP during seizures (Abiega et al., 2016). In the EPM1 model, the analysis was performed in P30 *Cstb* KO mice, which are considered clinically symptomatic, as they develop visible seizures along with cortical and cerebellar atrophy. Here, we studied the mechanism underlying the phagocytosis impairment in *Cstb* KO mice. First, we studied cell-autonomous effects due to microglial Cstb deficiency using an acute model of Cstb deletion in the microglial cell line BV2. And second, we studied the role of seizures by analysing microglial phagocytosis in P14 *Cstb* KO mice, prior to the seizure onset.

[This section has been published in Sierra-Torre V et al., in Epilepsia: Microglial phagocytosis dysfunction in the dentate gyrus is related to local neuronal activity in a genetic model of epilepsy. 2020]

6.7.1 Cstb knock-down in microglia does not alter phagocytosis in vitro

To determine a possible cell-autonomous effect of *Cstb* on microglial phagocytosis we first addressed whether microglia expressed *Cstb in vivo*. For this purpose, we FACS-sorted microglia from P30 fms-EGFP hippocampi (**Figure 46A**), where microglia constitutively express the EGFP protein (Sasmono et al., 2003; Sierra et al., 2007), allowing the discrimination of microglia from other cell types. We analysed the mRNA expression of *Cstb* as well as downstream *cathepsins B, L* and *S* by RT-qPCR, because *Cstb* mutations are related to increased cysteine protease expression (Lieuallen et al., 2001). We found that *Cstb* and *cathepsins B* and *L* were expressed by both microglia and non-microglia cells, whereas *cathepsin S* was solely expressed by microglia (**Figure 46B**). While *Cstb* was not enriched in microglia compared to other cell types, its robust expression suggested that the phagocytosis impairment could be the direct consequence of microglia lacking *Cstb* per se.

To directly assess the effect of microglial *Cstb* on phagocytosis, we set up an in vitro model of *Cstb* knock-down in the microglial cell line BV2 (**Figure 46C-I**). We transfected BV2 microglia with 6-carboxyfluorescein (FAM)-labelled siRNAs against *Cstb* or a scrambled siRNA as a control (**Figure 46C**). We obtained a high transfection efficiency through a time course of 6, 24 and 48h (**Figure 46D**) and validated the transcription down-regulation of the *Cstb* gene by RT-qPCR through the time course. We observed that the expression of *Cstb* was greatly reduced up to 48 hours (**Figure 46E**), whereas the expression of the related cathepsins was not affected by *Cstb* siRNA treatment (**Figure 46F**). Control and *Cstb* KO microglia were then fed with apoptotic SHSY5Y-vampire neurons for 1 and 4h, in which apoptosis was previously induced (staurosporine 3µM, 4 hours) (Abiega et al., 2016; Diaz-Aparicio et al., 2020) (**Figure 46G**). Microglia were stained with CD11b, apoptotic neurons constitutively expressed the red fluorescent protein and nuclei were stained with DAPI (**Figure 46H**). We found no differences in phagocytosis in microglia treated with either scrambled or *Cstb* siRNA (**Figure 46I**). Our in vitro model, nonetheless, does not fully recapitulate the *in vivo* situation, because *Cstb* KO mice have *Cstb* chronic depletion in all cell types that is accompanied by modulation of cathepsin activity and/or expression (Kaur et al., 2010; Lieuallen et al., 2001; Rinne et al., 2002), whereas in our in vitro model cathepsin levels remained unaffected despite the *Cstb* deletion. Nonetheless, these results suggest that the cell autonomous acute *Cstb* deficiency in microglia is not sufficient to induce the phagocytosis impairment observed *in vivo*. We, therefore, searched for alternative mechanisms to explain the reduced phagocytosis in *Cstb* KO mice. As we had previously shown that seizures interfere with phagocytosis in MTLE (Abiega et al., 2016), our next step was to determine if the phagocytosis blockage was related to seizures by analysing an early developmental stage, P14, when seizures have not yet appeared.

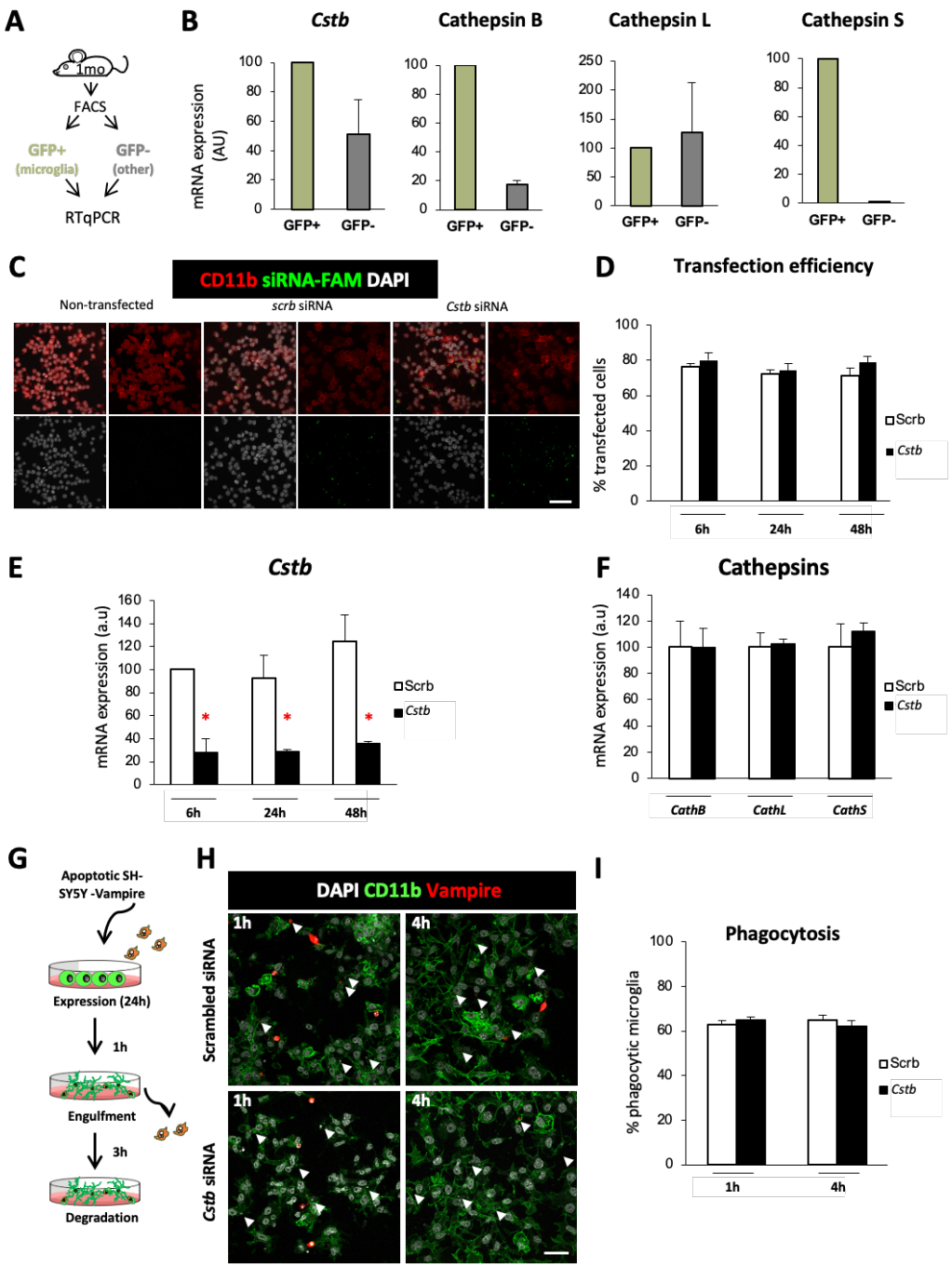

Figure 46. Cstb knockdown in microglia does not alter phagocytosis in vitro. ***[A]*** *Experimental design used to isolate microglia (GFP+) from non-microglial cells (GFP-) for the hippocampi of 1-month-old mice using flow cytometry and RT-qPCR for gene expression analysis.* ***[B]*** *Expression of CSTB gene and cathepsins B, L and S in microglia (GFP+) versus non-microglial cells (GFP-) in FACS sorted cells from EGFP-fms mice hippocampi. OAZ1 (ornithine decarboxylase antizyme 1) was selected as a reference gene.* ***[C]*** *Representative confocal images of non-transfected (left panels) and scrambled/Cstb siRNA transfected BV2 microglia (middle and right panels). Nuclei are stained with DAPI (white), BV2 microglia were stained for CD11b (red) and siRNA transfection was assessed by FAM (green) labeling.* ***[D]*** *Percentage of scrambled/Cstb siRNA transfected cells along a time course (6, 24 and 48 hours).* ***[E]*** *RT-qPCR Cstb gene*

expression in BV2 cells after Cstb siRNA silencing through a time course (6, 24 and 48 hours), using OAZ1 as a reference gene. ***[F]*** *RT-qPCR cathepsins B, L, S gene expression in BV2 cells 24 hours after siRNA Cstb silencing, using OAZ1 as a reference gene.* ***[G]*** *Experimental design of the phagocytosis assay performed 24 hours after BV2 siRNA transfection. Knockdown BV2 cells are fed for 1 and 4 hours with apoptotic SH-SY5Y vampire neurons.* ***[H]*** *Representative confocal images of scrambled and Cstb siRNA transfected BV2 cells (CD11b staining, green) fed with apoptotic SH-SY5Y vampire neurons (red) for 1 and 4 hours. Arrowheads show phagocytosed SH-SY5Y vampire fragments or full cells.* ***[I]*** *Percentage of phagocytic BV2 cells after 1 and 4 hours of phagocytosis. Only particles fully enclosed by BV2 pouches were identified as phagocytosis. Bars represent the mean ± SEM. * indicates $p < 0.05$, *** indicates $p < 0.001$ by two-way ANOVA. Scale bars= 60 µm* ***[C]****, 40 µm* ***[H]****.*

6.7.2 Phagocytosis impairment is specific of the GL in Cstb KO mice at P14

At P14, *Cstb* KO mice are asymptomatic and do not have seizures (Tegelberg et al., 2012) and, in agreement, we did not observe any changes in the number of active neurons, labelled with the immediate early gene cFos, whose expression is rapidly induced upon depolarization (Verma & Sassone-Corsi, 1987) (**Figure 47A-C**). $cFos^+$ neurons (magenta) were found at similar numbers in both WT and *Cstb* KO mice at P14 and they were located exclusively in the granular cell layer (GL) and not in the subgranular zone (SGZ), where radial neural stem cells and their immature progeny reside (**Figure 47A, C**). However, we did notice that whereas in WT mice most apoptotic cells were found in the SGZ, in *Cstb* KO mice apoptotic cells were found mostly in the GL and in very close proximity to $cFos^+$ neurons (**Figure 47B**), prompting us to analyse separately GL and SGZ apoptosis and phagocytosis.

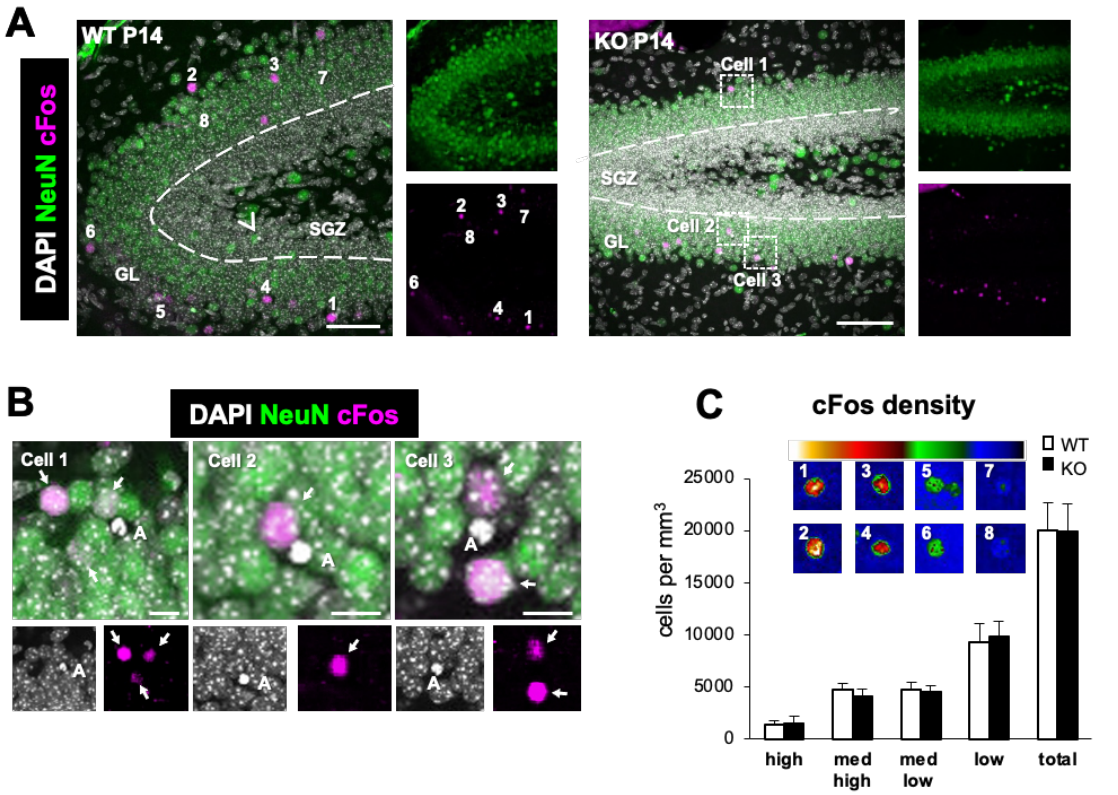

Figure 47. cFos+ cells in the DG of WT and Cstb KO P14 mice. ***[A]*** *Representative confocal images of the DG of WT and Cstb KO mice. Healthy or apoptotic (pyknotic/karyorrhectic) nuclear morphology was visualized with DAPI (white), neurons were identified with the neuronal marker NeuN (green) and activated neurons were stained for the early expression gene cFos (magenta). Arrowhead points to an apoptotic cell in the SGZ in WT mice; framed apoptotic cells in Cstb KO mice are shown in* ***B****. Numbered cFos⁺ cells are shown in* ***C****, as cells with high (1,2), medium high (3, 4), medium low (5, 6) and low (7,8) cFos intensity.* ***[B]*** *High magnification examples showing the close proximity between apoptotic cells (DAPI, white) and cFos+ neurons (magenta) in Cstb KO mice. Granular neurons are stained with NeuN (green). Arrows point to cFos+ neurons.* ***[C]*** *Distribution of cFos⁺ cells in WT and Cstb KO mice (per mm³). The color code indicates the classification criteria of the cFos⁺ cells based on their intensity (high, medium high, medium low, low). A total of 1046 cells for WT P14 mice and 713 cells for Cstb KO mice were quantified and classified according to their cFos expression. No significant differences were found. Scale bars= 50µm* ***[A]****, 10µm* ***[B]****; z=28 µm* ***[A****, WT****]****, 17.5 µm* ***[A****, KO****]***

In the SGZ, we did not observe any significant difference in apoptosis nor phagocytosis between WT and *Cstb* KO mice at P14 (**Figure 48A-F**). In contrast, in the GL there were few apoptotic cells in WT mice and a 10-fold increase in *Cstb* KO mice (**Figure 48D, E**). Most of these GL apoptotic cells were not phagocytosed, resulting in a reduced GL Ph index in *Cstb* KO mice compared to WT mice, at P14 (**Figure 48F**). Similar to the global effect we had observed before in the whole dentate gyrus at P30, we found that GL microglia increased their Ph capacity in *Cstb* KO mice

compared to WT mice although this effect was insufficient to cope with the increased number of apoptotic cells (**Figure 48G, H**). In this early stage, we found no obvious morphological changes nor increases in microglial numbers (**Figure 48I**). Overall, we found that the increase in apoptotic cells was not compensated by a sufficient increase in phagocytosis, resulting in an uncoupling between apoptosis and phagocytosis (**Figure 48J)**. Altogether, these results demonstrate that the microglial phagocytosis impairment was specific of the GL and preceded seizure development in *Cstb* KO mice at P14. This data suggested that there could be functional differences between GL and SGZ that could explain the GL-specific increase in apoptosis and microglial phagocytosis impairment.

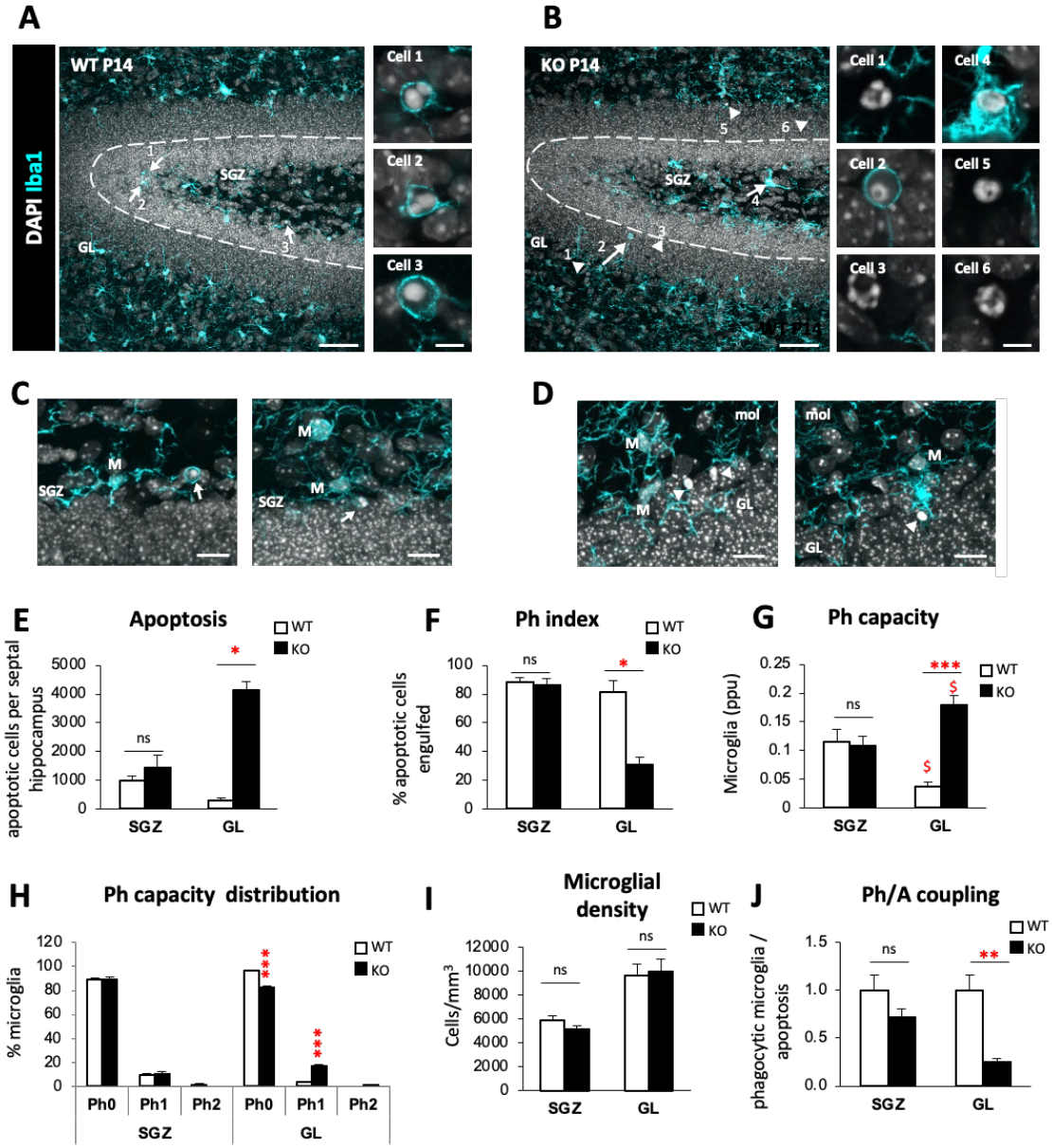

Figure 48. Phagocytosis impairment is specific of the granule cell layer in Cstb KO mice at P14. ***[A, B]*** *DG general view of both WT and Cstb KO P14 mice, nuclei are stained with DAPI (white) and microglia with Iba1 (cyan). Close up images show phagocytosed and non-phagocytosed apoptotic cells in WT and Cstb KO P14 mice.* ***[C, D]*** *Representative images of apoptotic cells (condensed DAPI) engulfed by microglia (M, cyan) in the SGZ of WT P14 mice* ***[C]*** *and non-phagocytosed cells in the GL of Cstb KO P14 mice* ***[D]****. Arrows point at phagocytosed apoptotic cells and arrow heads to non-phagocytosed apoptotic cells* ***[A-D]****.* ***[E]*** *Number of apoptotic cells (pyknotic/karyorrhectic) both in the SGZ and GL, per septal hippocampus (n = 12 animal for each condition).* ***[F]*** *Phagocytic index (in % of apoptotic cells being engulfed by microglia) in the SGZ and GL of the septal hippocampus in WT and Cstb KO P14 mice.* ***[G]*** *Histogram showing the Ph capacity distribution of DG microglia (in % of microglial cells) in the SGZ and GL.* ***[H]*** *Microglial density (cells/mm^3) per septal hippocampus both in WT and Cstb KO P14 mice, distinguishing between SGZ and GL.* ***[I]*** *Weighted Ph capacity of DG microglia (in ppu).* ***(J)*** *Ph/A (in fold change) in the SGZ and GL of the septal hippocampus in WT and Cstb KO P14 mice. Bars represent the mean ± SEM. * indicates p < 0.05, ** indicates p < 0.01, *** indicates p < 0.001 by Student´s t-Test comparing WT vs KO. Scale bars= 50µm* ***[A, B]****, 5µm (inserts in* ***[A, B]****), 30µm* ***[C, D]****; z=18.9 µm* ***[A, B]****, 9.8 µm* ***[C left]****, 16.1* ***[C right]****, 11.2 µm* ***[D left]****, 12.6 µm* ***[D right]****.*

6.7.3 Apoptotic cells are in close proximity to active cFos+ neurons

The close vicinity of apoptotic cells to GL cFos$^+$ neurons in P14 mice (**Figure 47B**), suggested that the phagocytosis efficiency of GL microglia could be related to neuronal activity, as neuronal hyperactivity during seizures prevents microglia from targeting apoptotic cells (Abiega et al., 2016). To address whether the proximity of cFos$^+$ neurons had an impact on apoptosis and phagocytosis, we directly estimated the distance to each phagocytosed and non-phagocytosed cell to the closest cFos$^+$ neuron (nearest neighbour, NN) (**Figure 49A**). Because of the limitations limitation imposed by the relatively small thickness of our z-stacks (border effect; see Materials and Methods for more detail), we only had a sufficient number of apoptotic cells in KO mice (n=15 phagocytosed and n=5 non-phagocytosed apoptotic cells from n=9 mice, from an initial set of 295 cells).

In *Cstb* KO mice, both phagocytosed and non-phagocytosed cells were found very close to the cFos$^+$ NN (3.0 ± 0.5 and 3.0 ± 0.6µm, respectively; non-significant difference; **Figure 49B**). To determine whether this short distance would be expected if cells were homogenously distributed through the thickness of our z-stacks, we calculate that 50% of the cells should be located at ¼ distance to either z-border (green-shaded area in **Figure 50B**), that is, at 5.9 ± 0.2 and 6.0 ± 0.1µm to the cFos$^+$ NN for phagocytosed and non-phagocytosed cells, respectively (**Figure 50C)**. Thus, both phagocytosed and non-phagocytosed apoptotic cells in *Cstb* KO mice

seem to be much closer (3µm) to active neurons than would be expected. Although we could not detect significant differences between phagocytosed and non-phagocytosed cells in *Cstb* KO mice, these results do suggest an unexpected relationship between neuronal activity and apoptosis.

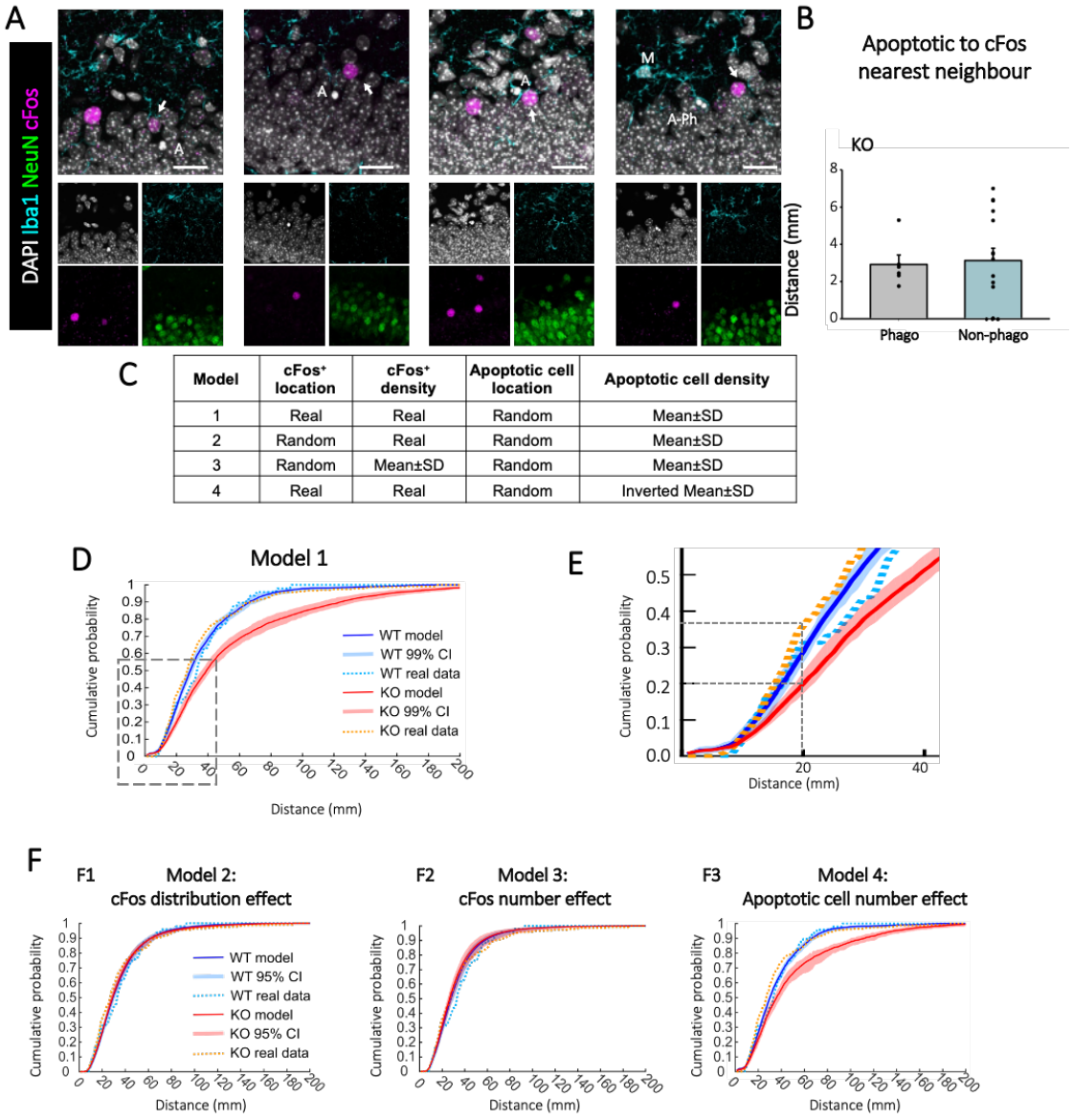

Model	cFos⁺ location	cFos⁺ density	Apoptotic cell location	Apoptotic cell density
1	Real	Real	Random	Mean±SD
2	Random	Real	Random	Mean±SD
3	Random	Mean±SD	Random	Mean±SD
4	Real	Real	Random	Inverted Mean±SD

Figure 49. Proximal relationship between apoptotic cells and cFos+ neurons in the granule cell layer of Cstb KO mice. ***[A]*** *Representative confocal images of the GL of Cstb KO mice. Healthy or apoptotic (pyknotic/karyorrhectic) nuclear morphology was visualized with DAPI (white), neurons were identified with the neuronal marker NeuN (green), microglia with Iba1 (cyan) and activated neurons were stained for the early expression gene cFos (magenta). Both phagocytosed (A-Ph) and non-phagocytosed apoptotic cells (A) were close to cFos⁺ neurons (arrows).* ***[B]*** *Quantification of distance from phagocytosed and non-phagocytosed apoptotic cells to the cFos+ NN, for those cells that met the inclusion criteria (see Methods).* ***[C]****. Summary of the different simulation models based on the location and density of cFos⁺ and apoptotic*

cells. ***[D]*** *Cumulative probability of the distances between apoptotic cells and NN cFos⁺ neurons for WT (blue) and Cstb KO mice (red), resulting from 10,000 simulations of a virtual 3D model, indicating the 99% confidence interval (CI). The cumulative probability for real (measured) data is shown for WT (light blue) and Cstb KO (orange).* ***[E]*** *Amplification of the area showed in C.* ***[F]*** *Cumulative probabilities of the distances between apoptotic cells and NN cFos⁺ neurons for WT (blue) and Cstb KO mice (red), resulting from 10,000 simulations of the indicated virtual 3D model. Scale bars indicate 20µm. z= 9.1 µm, 7.7 µm, 16.8 µm, 9.1 µm* ***[A****, from left to right****]****.*

To strengthen the analysis of distance between apoptotic cells and NN cFos⁺ neurons in both WT and KO mice and overcome the limitation of analyzing only 20 cells, we developed a mathematical model (see Methods for details). We created a virtual 3D model of the GL based on the spatial distribution and density of neurons, cFos⁺ neurons and apoptotic cells (**Figure 50D**). In this model we reproduced the same experimental limitations imposed by the limited thickness of the z-stacks (see Methods) compared the size of the (XY) field of view and therefore no cells were discarded due to the border effect. Using this virtual 3D model, we compared the entire experimental distribution of NN distance between cFos⁺ and apoptotic cells to the distribution generated by the 10,000 simulations. Specifically, we developed four different models (**Figure 49**).

In the first model cFos⁺ neurons were located in their original position (in the z-stack) and the position of the apoptotic cells was randomized, and their numbers were extrapolated from the experimental cell density (**Figure 49A**). For each apoptotic cell we performed 10,000 randomizations and calculated the distance to the NN cFos⁺ cell. Finally, the cumulative probability to encounter a cFos⁺ cell within a given distance from an apoptotic cell was computed with its 99% confidence interval both in the WT- and KO-derived v3D grids (**Figure 49B, C**). In WT mice, the measured apoptotic-cFos⁺ NN distance was within the modeled confidence interval up to a distance of 22 µm, which matches the average z-stack thickness (24.2 ±0.4 µm) and validates that our model is isotropic, i.e., does not depend on the orientation and therefore is within the range of the z-stack thickness. In contrast, in *Cstb* KO mice the measured percentage of NN cFos⁺-apoptotic cells between 17 and 24 µm was significantly higher than what we observed both in the WT and *Cstb* KO models. For instance, in the *Cstb* KO model 20% of the apoptotic cells are found at less than 20 µm distance from the cFos⁺ NN, whereas in the real data from *Cstb* KO mice, 20% of the apoptotic cells were found at less than 16µm and 35% of the apoptotic cells are found at less than 20 µm (**Figure 49C**). This data suggested that as in our direct

quantifications (**Figure 49B**), apoptotic cells were closer than expected to active cFos⁺ neurons in *Cstb* KO mice.

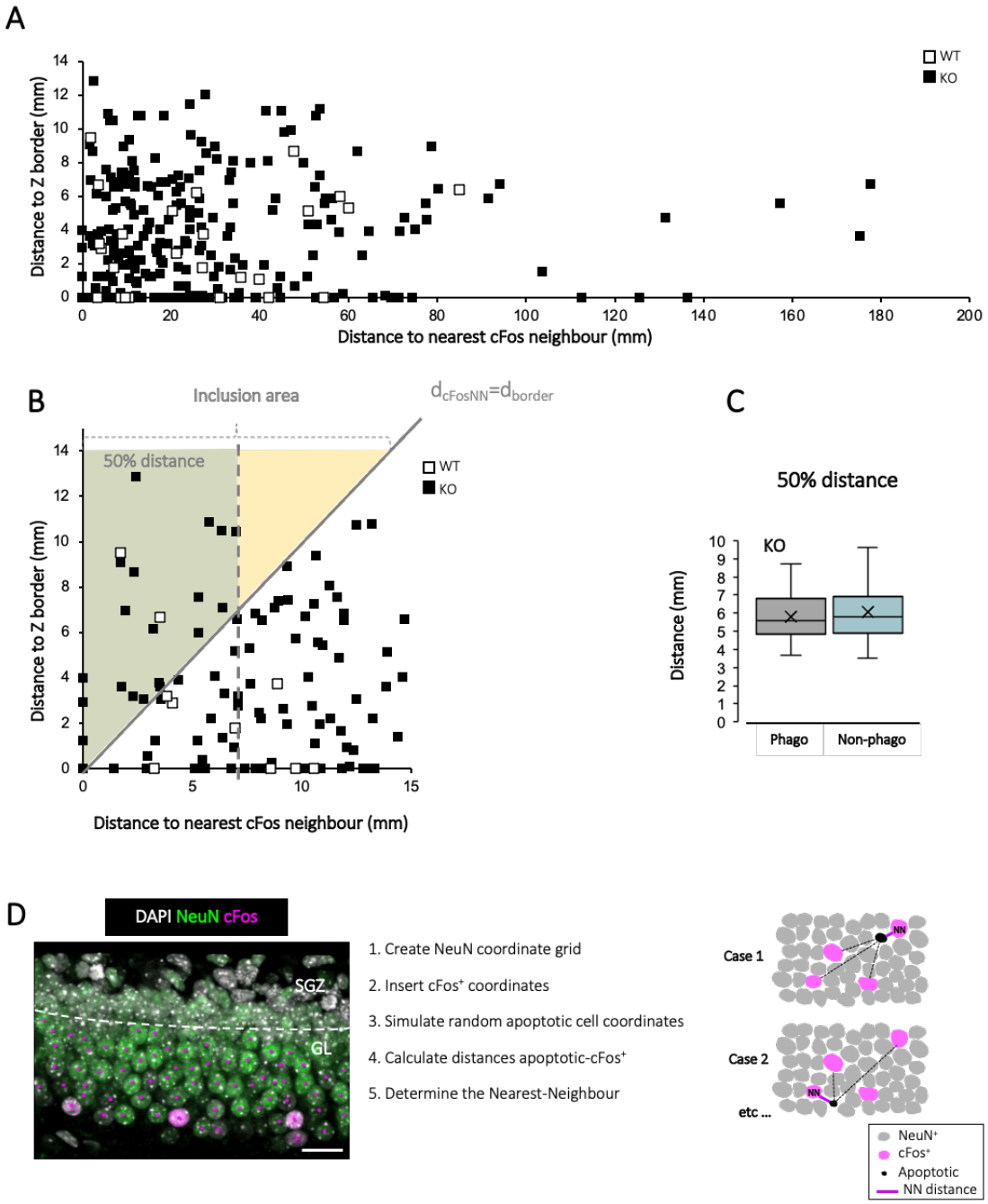

Figure 50. Physical constraints in estimating cFos+ to apoptotic cell NN distances. ***[A]*** *NN distances for WT (white squares) and Cstb KO (black squares) in the 25 and 253 apoptotic cells collected from 2 series of sections from the GL of wild-type (WT) and KO mice, compared to the distance of each cell to the closest z-border of the corresponding z-stack.* ***[B]*** *Higher magnification of the first 15mm shown in* ***[A].*** *The grey line marks the inclusion criteria for the study, where only the cells whose NN distance was smaller to the distance to the nearest z-border were included. Within the inclusion area (dotted line), 50% of the cells would be expected to be found within a distance of 50% the thickness of the z-stack (green-shaded area), i.e., at 25% distance to either the upper or the lower z-stack border, although in fact all cells were found*

within this region. ***[C]****. In Cstb KO mice the 50% distance was similar between phagocytosed and non-phagocytosed apoptotic cells.* ***[D]****), Virtual model for NN distances. First, a grid was created based on the position of NeuN$^+$ neurons in the GL (left panel). On this grid, we positioned cFos$^+$ neurons and apoptotic cells in four different models (****Figure 49C****) and calculated the distances of each apoptotic cells to all the cFos$^+$ neurons on the grid, to determine the NN. Scale bar= 20 µm* ***[D]****).*

Nonetheless, the modelled distance was significantly larger in KO than in WT mice (**Figure 49C**). To further understand the role of other parameters, such as cell number or location, on the model, we used other three different models (**Figure 49A**): Model 2 to test the impact of cFos$^+$ cell location, Model 3 to test cFos$^+$ cell density, and Model 4 to test apoptotic cell density. We first tested the effect of cFos$^+$ cell location (Model 2), by randomly positioning both cFos$^+$ neurons and apoptotic cells (**Figure 49F1**). In this model, there were no differences between the modelled NN distances between WT and KO. Importantly, in KO mice the difference between the measured and modelled apoptotic-cFos$^+$ NN distance was strongly reduced although it was still significant with a maximum around 20µm. The reduced difference between the measured and modelled NN distance in KO mice in model 2 suggest that the differences between the modelled NN distances in Model 1 originated from a differential distribution of cFos$^+$ cells between WT and KO.

We then tested the effect of cFos$^+$ density by creating a Model 3 in which cFos$^+$ cells were positioned randomly in the v3D grid, and their number was estimated from the experimentally measured cFos density rescaled by the number of cells in the grid, whereas apoptotic cells were modelled randomly as above (**Figure 49F2**). The results of Model 3 were similar to Model 2, with no differences between modelled and measured NN distances for WT and KO, suggesting that the number of cFos$^+$ cells was not related to the differential effect found in Model 1. Finally, we tested the effect of different density of apoptotic cells in the WT and KO modelled distances in Model 4. For this, we went back to use the real distribution of cFos+ cells (as in Model 1) and positioned the apoptotic cells randomly but with an inverted density: WT model using KO apoptotic cell density and vice versa (**Figure 49F3**). The results of Model 4 were similar to Model 1: the modeled NN distance was larger in KO than in WT, and apoptotic cells were found closer to active neurons than expected in KO mice. Overall, this data suggests that while *Cstb* KO mice have similar cFos$^+$ density and intensity at P14 (**Figure 49C**) and do not have yet seizures (Tegelberg et al., 2012), they have an abnormal distribution of cFos$^+$ active neurons that results in a closer distance to apoptotic cells (**Figure 49B, 49C**). These results suggest a very close relationship between abnormal neuronal activity in *Cstb* KO mice and apoptotic cells. Indirectly,

they also suggest a relationship with the phagocytosis impairment found in *Cstb* KO mice, because the number of apoptotic cells observed is the net result between apoptosis induction and phagocytosis removal.

In summary, we determined that microglial phagocytosis impairment in the hippocampus is an early feature in the genetic model of EPM1 by *Cstb* deficiency. We also provide an unexpected link between phagocytosis impairment, accumulation of apoptotic cells and local neuronal activity in these mice that further supports the suggestion that both abnormal local neuronal activity (in pre-symptomatic *Cstb* KO mice) and network hyperactivity (in MTLE mice) regulate the efficiency of microglial phagocytosis.

Discussion

7. Discussion

In this PhD Thesis we have explored the functional relationship between autophagy and phagocytosis, two essential processes for the maintenance of the cell and tissue homeostasis. Whilst through autophagy own components are recycled, through phagocytosis extracellular debris is degraded. Autophagy and phagocytosis are part of the endosomal pathway, that converges in the lysosome, and share many similarities at the intracellular level. Some of the autophagy machinery, like Atg proteins or LC3, are derived to the phagosome to enhance phagocytosis.

To test the interaction between phagocytosis, autophagy and lysosomal pathways we have focused on two disease models in which we have recently demonstrated microglial phagocytosis dysfunction: 1, a model of transient ischemia (tMCAo) and a model of genetic epilepsy (EPM1). In the first part of this PhD Thesis we have focused on the role of autophagy in the microglial phagocytosis impairment induced by MCAO, using in vitro models of oxygen and nutrient deprivation (OND). As we had encountered some difficulties in analyzing autophagy induction using the classic LC3 western blot assay, in the second part we focused on exploring this analysis by developing a two-step model. Finally, in the third part, we studied the involvement of lysosomal dysfunction on the microglial phagocytosis impairment induced by Cstb deficiency. In summary, in this section we will discuss the following findings:

First, we have revealed some of the underlying cellular mechanisms that affect both engulfment and degradation of apoptotic cells, including reduced microglial process motility and lysosomal alterations. Then we have showed that the energy depletion associated with stroke leads to increased autophagy, whose basal levels are essential for microglial survival and function both in vivo and in vitro. Overall, we have shed light onto two unappreciated microglial activities with key roles during stroke and high therapeutic potential: autophagy, responsible for intracellular recycling, and the cell´s well-being and function; and phagocytosis, responsible for extracellular laundering and controlling inflammatory responses.

Second, we have proposed and alternative method to assess the different steps of autophagy, formation and degradation, using the classical LC3 assay by western blot. The proposed method

consists of a simple set of equations to dissect formation and degradation that are applicable to a wide set of simulated scenarios and that have proved useful in the analysis of experimental data. This method also the discrimination the effect of a tested drug differentially on formation and degradation, rendering extra information to the classical analysis of the autophagy flux, which only contemplated the degradation step of autophay.

Last, we have provided evidence on the possible mechanisms that underlie the phagocytic disruption associated with CSTB deficiency, based on the following findings: first, the cell-autonomous lack of *Cstb* in microglia did not drive phagocytosis impairment, since *Cstb* down-regulation in pure microglial cultures did not alter phagocytosis efficiency. Second, microglial phagocytosis impairment was already present in the hippocampus of *Cstb* KO mice at P14, prior to the onset of seizures, suggesting that microglial phagocytosis impairment appears at early stages of disease and independent of seizures. Third, the impairment was specific for the GL, whereas the neurogenic niche of the SGZ was spared. Forth, a virtual 3D model of the hippocampal GL in young CSTB KO mice (P14) predicted an aberrant distribution of cFos active neurons that results in a closer distance to apoptotic cells. These results suggest that local neuronal activity may alter apoptosis dynamics in *Cstb* KO mice, which may explain, at least in part, the reported impairment on microglial phagocytosis associated with CSTB deficiency.

7.1 MICROGLIAL PHAGOCYTOSIS IMPAIRMENT IN TWO IN VITRO MODELS OF STROKE IS DRIVEN BY ENERGY DEPLETION AND INDUCTION OF AUTOPHAGY.

7.1.1 Exploiting microglial phagocytosis as a future therapeutic target

The profits of microglial phagocytosis for the diseased brain are evident: prevention of intracellular content spillover and immunomodulatory effects (Morioka et al., 2019). However, its therapeutic potential in brain diseases has been largely unappreciated, likely because phagocytosis was presumed to occur rather than directly assessed (Diaz-Aparicio et al., 2016). Here we have used a quantitative approach that has allowed us to discover microglial phagocytosis dysfunction in stroke in mice and monkeys, similar to what we had observed in mouse and human epilepsy (Abiega et al., 2016; Sierra-Torre et al., 2020). In these diseases, it is necessary not only to prevent neuronal death, but also to accelerate the removal of neuronal debris by developing new strategies to harness phagocytosis.

Pioneer work in cancer has catapulted macrophage phagocytosis as a consolidated target with several ongoing clinical trials (Chen et al., 2021). Here, deficient phagocytosis is due to tumor

cells escaping recognition by macrophages. As such, most efforts have been put into developing opsonizing antibodies to coat the tumor cells and facilitate their interaction with macrophages (Scott et al., 2012). Another rising idea is to interfere with phagocytosis checkpoints such as CD47, a “don´t-eat-me” signal that interacts with SIRPalpha receptors on the macrophage (Matlung et al., 2017). In the brain, however, CD47 expressed by healthy synapses prevents their excessive phagocytosis by microglia, at least during development (Lehrman et al., 2018). Unhinged phagocytosis could lead to phagoptosis, i.e., the engulfment of stressed but viable cells (Brown & Neher, 2014), responsible for delayed neuronal death in stroke models (Neher et al., 2013). These examples highlight that translating cancer-based approaches into effective brain therapies may not be straightforward and requires a deeper understanding of the mechanisms operating on microglial phagocytosis dysfunction, as we will discuss next.

7.1.2 Impairment of microglial phagocytosis during stroke

One key difference between cancer and the diseased brain is that in the first case, tumor cells are the ones to blame for deficient phagocytosis, as they develop mechanisms to escape engulfment. In contrast, in stroke the problem does not seem to lie on the target cells but on the phagocytes, as microglia is severely compromised due to the energy depletion. We found that the lack of oxygen and nutrients reduced the motility of microglial processes and interfered with the engulfment phase of phagocytosis. It also altered the microglial lysosomal number, pH, and the cell´s degrading capacity, which was likely related to reduced apoptotic cell degradation. Finally, it induced autophagy, a cell process that we found necessary for microglial survival and phagocytosis. In addition, environmental-related factors are also likely to play a role on microglial phagocytosis dysfunction. An example is extracellular ATP, one of the major “find-me” signals from apoptotic cells sensed by purinergic receptors on microglia (Calovi et al., 2019). However, ATP is also a neurotransmitter, widely released during pathological conditions such as epilepsy and ischemia (Dale & Frenguelli, 2009). These two sources of ATP put microglia in conflict and disrupt their targeting of apoptotic cells, resulting in impaired phagocytosis during epilepsy (Abiega et al., 2016) and possibly during stroke. Inhibitors of the purinergic receptor P2Y12, such as clopidogrel, are currently used to prevent platelet aggregation in several cardiovascular diseases (Ha et al., 2021), but a side effect not considered is their inhibitory action on microglial phagocytosis (Diaz-Aparicio et al., 2016). In sum, this trio of mechanisms that relate to the target, the phagocyte, and/or the environment should be considered when designing effective therapies to recover or potentiate phagocytosis.

Here, we have used rapamycin to modulate phagocytosis during stroke. The autophagy inducer rapamycin has become an increasingly popular drug since its discovery in the early nineties in soil samples from Easter Island ("A long and winding sTORy," 2017). Due to its immunosuppressant properties, rapamycin (sirolimus) is currently used to prevent kidney transplant rejection and to treat certain lung diseases, and several clinical trials are testing its efficiency in pathologies such as Alzheimer´s disease and aging (Clinical Trials NCT04629495, NCT04488601). In stroke, rapamycin prevents neuronal cell death (Hadley et al., 2019; Li & Huang, 2020a; Wu et al., 2018) and here we have observed a neuroprotective effect on apoptosis induced by OND at 24h, but not at earlier time points either after OND or in the in vivo models of tMCAo. We have also shown that rapamycin did not recover the phagocytosis impairment in vitro in the OND model, contrary to the partial recovery our laboratory observed in vivo (**Figure 15**). We speculate that, in vivo, rapamycin may have indirectly improved microglial phagocytosis by reducing the tMCAo-induced ischemic damage, possibly by acting on the neurovascular unit and facilitating reperfusion (Hadley et al., 2019). While rapamycin may not be the optimal drug to target microglia, these results suggest that preventing phagocytosis impairment in stroke models in vivo is possible.

Microglial autophagy is indeed a challenging target. We achieved autophagy inhibition using pharmacological blocking of Ulk1 or by genetic manipulation of ATG4 and Beclin1, demonstrating that basal autophagy was essential to sustain microglial survival and phagocytosis of apoptotic cells. In agreement with our results, disruption of basal autophagy has been involved in the phagocytosis of myelin (Berglund et al., 2020) and beta amyloid deposits (Lucin et al., 2013), in mice deficient in ATG7 and Beclin1, respectively. However, we found no significant effects in AMBRA1 heterozygous mice, suggesting that microglial autophagy may have a unique set of regulators compared to other cell types (Corona Velazquez & Jackson, 2018). Inhibition of the protective autophagy response mounted after OND was also detrimental for microglial survival. Unexpectedly, promoting this response with rapamycin not only did not recover phagocytosis but even had a deleterious effect on the survival of phagocytic microglia during OND. These results point to the complex regulation of autophagy in microglia, whose beneficial or detrimental effects may depend on the timing and the amount of autophagy. Nonetheless, microglial autophagy is a promising target to be explored. Autophagy controls the microglial inflammatory response in rodent stroke models (He et al., 2020; Yang et al., 2015) through Annexin 1, which activates the inflammatory transcription factor NF-□B by directing its inhibitor IKK to autophagosomes for degradation (Li et al., 2021). Future research will identify the target organelles or subcellular substrates that need to be recycled in microglia to maintain

its health status, and whether microglial autophagy can be therapeutically exploited to support phagocytosis.

7.1.3 Microglia beyond the inflammatory paradigm

For too long, the field of stroke has focused on microglial inflammatory responses with little attention to their other functions. The field is still categorizing pro- or anti-inflammatory microglia using outdated terms (Paolicelli et al., 2022; Ransohoff, 2016), such as M1 and M2 to define presumed beneficial or detrimental subtypes (He et al., 2020; Jiang et al., 2020; Lauro & Limatola, 2020; Li et al., 2021; Ma et al., 2017). In contrast, both bulk and single cell RNA-Seq studies have clearly shown that microglia do not polarize to either of these categories in rodent stroke models (Androvic et al., 2020; Beuker et al., 2022; K. Guo et al., 2021; Rajan et al., 2019; Zheng et al., 2022). This stagnation has led to a shortage of microglial targets for clinical trials, which are to this day still largely focused on inflammation. In addition, studies in stroke patients have also oversimplified the role of human microglia by studying its "activation" in imaging studies, whereas functional studies are largely missing (Ma et al., 2017). Our results demonstrate that microglial phagocytosis is a promising new target in stroke, with a solid therapeutic potential of microglial phagocytosis to restore brain homeostasis that grants further exploration.

7.2 A TWO-STEP MODEL TO DETERMINE AUTOPHAGOSOME FORMATION, DEGRADATION AND NET TURNOVER.

Autophagy is a complex multi-step phenomenon and its assessment is a complicated task that requires using complimentary methods, as most current guidelines recommend (Higo, 2021; Zheng et al., 2022). Visualization of double-membrane autophagosomes by transmission electron microscopy, live imaging of LC3 acidification using ratiometric analysis of fluorophores, or analysis of substrate degradation should corroborate the data obtained by analysis of LC3-II expression as a proxy for autophagosome formation and degradation. It is also important to note that autophagy is a time-dependent process and, as such, its dynamics should be assessed over time (Martin et al., 2013). In addition, LC3-II immunoblotting assays have several limitations, such as the reference protein used to normalize LC3-II values, the timing and concentration of the lysosomal inhibitor used, or the intrinsic nonlinear detection of proteins by enhanced chemiluminescence (ECL) (Rubinsztein et al., 2009). The most widely used method to assess autophagy is, nonetheless, the analysis of the LC3-II flux in the presence of lysosomal inhibitors. However, the complexities associated to interpreting LC3-II flux have been thoroughly pointed out before, in the quest for an optimal "autophagomometer" (Rubinsztein et al., 2009).

One of the key points is that autophagosomes formation and degradation are spatially and temporally dissociated (Börlin et al., 2014) and that therefore they need to be assessed independently.

To address this issue, we have here proposed a simple conceptual frame to help interpreting LC3-II flux experiments. Our two-step model conceives the steady-state levels of LC3-II as an indirect measure of the pool of autophagosomes present when the snapshot is taken. Assuming that in the basal condition the cells or tissue of interest are in some sort of equilibrium, the amount of autophagosomes formed and degraded should be roughly the same. Thus, the autophagosome pool can be treated as a black box to which the input (formation) and output (degradation) are identical and can be estimated as the difference between LC3-II levels in the presence and absence of lysosomal inhibitors. In the experimental condition, degradation can be similarly calculated as the difference between LC3-II levels in the presence and absence of lysosomal inhibitors (i.e., the conventional LC3-II flux). In addition, we proposed that the formation of autophagosomes in the experimental condition can be estimated by subtracting the steady state autophagosome pool to the autophagosomes that have accumulated in the presence of lysosomal inhibitors. This model allows us to dissect out the effects of the experimental conditions to autophagosome formation and degradation. In addition, it also allows us to understand the net changes in the size of the autophagosomal pool that are the result of maintaining (or not) the net turnover ratio at equilibrium.

We have tested the two-step model using pharmacological autophagy modulators such as the autophagy inducer rapamycin and the autophagy inhibitor MRT68921 in microglia. As expected, rapamycin enhanced autophagy flux increasing both autophagosome formation and degradation at the concentration (100 nM) and time point (6 h) tested. However, the autophagy inhibitor MRT68921 exhibited concentration and time-dependent differential effects. At a medium concentration (10 µM) and long time-point (6 h), MRT68921 decreased both autophagosome formation and degradation, in line with the inhibitory effects described over ULK1/2 kinase activity, while no effect was observed at a lower concentration (1 µM). Nevertheless, at high concentration (30 µM) and short time-point (3h), MRT68921 selectively decreased autophagosome degradation while maintaining their formation. This was an unexpected result since MRT68921 inhibits ULK1/2 kinase, a protein mainly known for its role in autophagy initiation (Wong et al., 2013). However, ULK1/2 kinase also regulates the recruitment of other autophagy-related proteins for the productive formation of autophagosomes (Petherick et al., 2015; Turco et al., 2020). Thus, inhibition of ULK1/2 kinase activity at high concentrations and short time-points could preferentially affect autophagosome degradation activity,

maintaining residual autophagy initiation activities, leading to the formation of LC3-II positive stalled phagophores and LC3-II accumulation after inhibitor treatment (Petherick et al., 2015). Overall, using pharmacological modulators of autophagy, we demonstrate that our two-step model is able to accurately measure the selective changes that may occur in autophagosome formation and/or degradation in microglia after exposure of autophagy modulating stimuli.

Nonetheless, our two-step model has several limitations that should be considered. The most important one is the assumption that autophagy (formation and degradation) are at equilibrium in the basal condition. This equilibrium implies coordinated control mechanisms that would be necessary to maintain autophagy in the long term (Shen & Mizushima, 2014), but each cell type may have different regulation mechanisms under different metabolic constraints (Nwadike et al., 2018), and would depend on experimental conditions such as cell density. Another important point is that autophagosome formation and degradation are not independent phenomena, as assumed in our model. For instance, it is obvious that if the lysosomal pool is not a limiting factor, the degradation will directly depend on the formation. In addition, feed-back mechanisms may link excessive lysosomal degradation with a subsequent reduction in autophagosome formation (Yu et al., 2010). In spite of these limitations, our model can provide a more expanded insight into the complexity of the autophagy process than simply analyzing the autophagic flux. In summary, we here show that using the LC3 turnover assay, our two-step model helps to systematically determine changes in autophagosome formation vs degradation, the net turnover and the size of the autophagosome pool to obtain a more comprehensive understanding of autophagy.

Due to the universal nature of LC3 turnover assays, our two-step model is useful to estimate changes in autophagosome formation and degradation in virtually all mammalian cell types, including microglia. As autophagy has emerged as a regulator of a plethora of microglial functions (Plaza-Zabala et al., 2017) related to regulation of metabolic status, inflammation, and phagocytosis (Berglund et al., 2020; Heckmann et al., 2019; Ulland et al., 2017), our two-step model may provide a simple framework to understand the basic dynamics of microglial autophagy in health and disease.

7.3 MICROGLIAL PHAGOCYTOSIS DYSFUNCTION IN THE DENATTE GYRUS IS RELATED TO LOCAL NEURONAL ACTIVITY IN A GENTIC MODEL OF EPILEPSY.

We will first discuss the pathological effects of *Cstb* deficiency in the hippocampus, including atrophy, apoptosis and phagocytosis impairment. Then, we will speculate on the impact of the

microglial phagocytosis deficiency for the pathology of epilepsy. Finally, we will examine possible mechanisms underlying this impairment, including a cell-autonomous effect of *Cstb* on microglia and environment-related factors such as seizures and local neuronal activity.

7.3.1 Early symptomatic Cstb KO mice exhibit slight atrophy of the hippocampus

EPM1 is the most common type of progressive myoclonus epilepsy, a heterogeneous group of inherited diseases that concur with myoclonus, epilepsy, and progressive neuronal degeneration (Arielle et al., 2016). Most EPM1 patients are homozygous for a promoter region repeat expansion mutation resulting in significantly reduced CSTB expression and approximately 10% of CSTB expression left in their cells (Joensuu et al., 2007). Patients with total lack of CSTB display an early infantile onset rapidly progressing encephalopathy(Mancini et al., 2016; O'Brien et al., 2017). Progressive loss of brain volume affecting cerebellum, cortex and hippocampus has been reported in patients with CSTB mutations (Koskenkorva et al., 2009; Koskenkorva et al., 2012; Mascalchi et al., 2002; O'Brien et al., 2017) as well as in *Cstb* KO mice (Manninen et al., 2014; Pennacchio et al., 1996; Shannon et al., 2002; Tegelberg et al., 2012). Accordingly, EPM1 patients have progressive motor deficits and mild cognitive impairment (Lehesjoki & Gardiner, 2012).

We previously showed earlier effects in hippocampal atrophy than previously described starting at 2 months of age using magnetic resonance imaging (MRI) (Manninen et al., 2014). We previously found that at 1 month (P30), *Cstb* KO mice already contained fewer hippocampal granule cells and a tendency to atrophy in the septal hippocampus, with no changes in the temporal region. Furthermore, we did not find increased granule neuron apoptosis as early as P14. These developmental defects suggest that damage associated to CSTB mutations starts earlier than previously suggested, with atrophy developing from 1 to 6 months in cerebellum, cortex and hippocampus in *Cstb* KO mice (Manninen et al., 2014). However, more subtle effects are found as early as P7, when the cerebellum begins to show decreased inhibition and enhanced excitation (Joensuu et al., 2014).Therefore, it is possible that, like the hippocampus, cerebellum and cortex also experience pathophysiological changes such as apoptosis and microglial phagocytosis impairment in the first postnatal days.

7.3.2 Microglial phagocytosis of apoptotic cells is impaired in early symptomatic Cstb KO mice

In addition to the neuronal damage, other cell types have also been involved in the pathology of EPM1. Some of the earliest changes pointed towards an altered inflammatory response by microglia, the brain resident macrophages (Okuneva et al., 2015; Tegelberg et al., 2012). Here we focused on another aspect of microglia: their phagocytic function. Microglia are very efficient phagocytes in the adult hippocampus in physiological conditions, where unchallenged microglia rapidly clears the excess newborn cells produced in the neurogenic niche(Sierra et al., 2010), actively participating in the regulation of neurogenesis (Diaz-Aparicio et al., 2020). After stressful stimuli such as inflammation and excitotoxicity, microglia use different strategies to enhance phagocytosis and match the increased apoptosis levels (Abiega et al., 2016): recruiting more cells to become phagocytic (theoretically, up to 100%), increasing the phagocytic capacity of each microglia (at least up to seven pouches per cell), and proliferating. Combined, these strategies make microglia a very powerful phagocyte.

However, the phagocytic potential of microglia was not fully summoned in the hippocampus of young adult *Cstb* KO mice, at the age when they start to manifest clinical myoclonus (P30). Although microglia tried to compensate for increased apoptosis by 1) increasing the number of apoptotic cells cleared by each microglial cell, and 2) increasing their numbers through proliferation, net phagocytosis did not match increased apoptosis in *Cstb* KO mice. These results are in line with previous mouse and human data of MTLE, where microglial phagocytosis was blocked, leading to accumulation of apoptotic cells in the hippocampus (Abiega et al., 2016). Accumulation of apoptotic cells has also been observed in the cerebellum as early as 2mo (Pennacchio et al., 1998). As an efficient phagocytosis involves rapid clearance of apoptotic cells (around 90min in the hippocampus) (Sierra et al., 2010), this data indirectly suggests microglial phagocytosis dysfunction in the cerebellum of *Cstb* KO mice, a hypothesis that needs to be tested.

7.3.3 Phagocytosis dysfunction in epilepsy

What are the consequences of impaired phagocytosis? The most obvious one is the accumulation of apoptotic cells. As executor caspases are activated in their cytoplasm, when not removed through phagocytosis apoptotic cells evolve into secondary necrotic cells (Savill et al., 2002). Their permeable membrane allows the release of toxic intracellular contents and contributes to further damaging healthy surrounding neurons, which may further contribute to alter the hippocampal connectivity and cognitive impairment. In addition, phagocytosis is immunomodulatory (Abiega et al., 2016) and in a mouse model of MTLE, phagocytosis impairment correlates with the development of an inflammatory response (Abiega et al., 2016).

In *Cstb* KO mice, microglia exhibited a hypertrophic morphology and multinuclearity, suggestive of microglial dysfunction and inflammation (Abiega et al., 2016; Hornik et al., 2014). These results are also in agreement with the early abnormal morphology and expression of the inflammatory protein F4/80 in microglia prior to gross neurodegeneration in *Cstb* KO mice (Tegelberg et al., 2012), although, the inflammatory profile of non-phagocytic microglia needs to be directly determined. Inflammation is a common feature of many types of epilepsies and epilepsy models, including *Cstb* KO mice (Joensuu et al., 2014; Korber et al., 2016; Okuneva et al., 2015). In agreement, inflammatory mediators such as interleukin 1 beta potentiate seizures (Iori et al., 2017; Vezzani & Viviani, 2015). Our results suggest that in both MTLE (Abiega et al., 2016) and EPM1 (here), microglial inflammation may arise at least in part due to the lack of control missing from dysfunctional phagocytosis. Therefore, developing novel tools to manipulate microglial phagocytosis may serve to control secondary neuronal damage, inflammation, and their impact on seizures in epilepsy patients.

7.3.4 Microglial phagocytosis disruption is not due to the cell autonomous lack of CSTB

The microglial phagocytosis impairment could be mechanistically related to the lack of *Cstb* in microglia and/or in other brain cell types. Indeed, we here show that *Cstb* expression was not restricted to microglia in the brain, suggesting that cell autonomous (lack of *Cstb* in microglia) or environment-driven (lack of *Cstb* in other cell types) mechanisms could underlie the phagocytosis impairment. However, we observed no alterations in an *in vitro* model of phagocytosis using siRNA to deplete microglial *Cstb*. Nonetheless, this *in vitro* model does not fully recapitulate the full extent of CSTB deficiency in EPM1 patients, which includes a complex modulation of activity and mRNA expression of target cathepsins of CSTB (Manninen et al., 2014; Rinne et al., 2002). Neither does it fully mimic the complexity of in vivo recognition and engulfment of apoptotic cells, which requires the release of “find-me” signals from apoptotic cells and microglial process motility to engulf the cells (whereas *in vitro* apoptotic cells are simply dumped on top of microglia) (Beccari et al., 2018b). Despite its limitations this data suggests that the lack of *Cstb* in microglia *per se* does not impact the clearance of apoptotic cells and suggests that the phagocytosis impairment could be related to environmental factors associated with the lack of *Cstb*, including its main pathological feature, seizures.

7.3.5 Microglial phagocytosis impairment is independent of seizure-activity

Neuronal hyperactivity during seizures alters the microglial phagocytic response to apoptotic cells. For example, seizure-induced widespread release of ATP in MTLE masks the microgradients of the "find-me" signal ATP used by microglia to find apoptotic cells (Abiega et al., 2016). To analyze the impact of seizures in microglial phagocytosis, we took advantage of young *Cstb* KO mice (P14), which do not present clinical seizures. Using cFos as a marker of neuronal depolarization (Verma & Sassone-Corsi, 1987) we did not find significant changes in the number of $cFos^+$ neurons but, nonetheless, our virtual 3D model indirectly suggested that they were abnormally distributed in *Cstb* KO mice at P14, which is likely reflected in the seizures that appear at later stages. In addition, it is possible that more subtle alterations in the hippocampal circuit are already present at P14. Interestingly, cFos active neurons, increased numbers of apoptotic cells, and microglial phagocytosis impairment were selectively observed in the GL of the hippocampus and spared the SGZ, illuminating an unexpected relationship between neuronal activity, cell death and microglial phagocytosis.

7.3.6 Local neuronal activity in the GL may contribute to the microglial phagocytosis impairment

In the GL, apoptotic cells were frequently positioned near active neurons labeled with cFos in *Cstb* KO mice, at an average distance of 3µm. In agreement, our virtual 3D model suggested that apoptotic cells were located closer to the active neurons than would be expected based on their relative cell densities. The number of apoptotic cells in a given time point is the net result between apoptosis induction (input) minus phagocytosis (output), and thus these results indirectly suggest that local neuronal activity in the GL could alter apoptosis and phagocytosis dynamics in *Cstb* KO mice. Indeed, neuronal activity dependent molecules such as ATP, exert their functions locally due to limited diffusion to short distances in the tortuous brain parenchyma (Wolak & Thorne, 2013). For instance, the effective diffusivity of a small molecule such as sucrose (0.342KDa, close to the 0.551KDa of ATP) is 310µm/s, whereas that of larger molecules such as NGF (nerve growth factor, 26.5KDa) is 2.95µm/s. Therefore, the average 3µm distance between apoptotic cells and active cFos neurons found in *Cstb* KO mice implies that the dead cells are well within the influence area of the active neurons´ soma. Thus, both the dead cells and the reaching microglial processes could be affected by the somatic release of modulators by granule neurons, or by the perisynaptic release of modulators by incoming fibers from several afferent systems (Leranth & Hajszan, 2007).

The close relationship between apoptotic cells and active neurons in *Cstb* KO mice is supported by both direct measurements and the virtual 3D model but does not provide evidence that this relationship affects phagocytosis. Nonetheless, it is important to note that the net apoptosis observed is in part the result of the phagocytosis dynamics: the number of apoptotic cells at any given time depends as much on the input (apoptosis induction) as on the output (removal by phagocytosis) (Márquez-Ropero et al., 2020). Therefore, our data shows an overall impairment of microglial phagocytosis in the GL of *Cstb* KO mice and suggests a complex scenario in which sub-seizure local neuronal activity may affect the clearance of apoptotic cells by microglia.

In addition, other pathophysiological mechanisms may participate in the phagocytosis impairment observed in *Cstb* KO mice. For instance, one possibility is that intrinsic differences between GL and SGZ microglia explain why the impairment is restricted to the GL. SGZ microglia are likely "trained" for phagocytosis, as they have been exposed to apoptotic cells during the postnatal period, whereas GL microglia is not. This "training" could result in differences in their phagocytosis potential. For instance, SGZ microglia can reach a Ph capacity around 0.8ppu in an LPS model at P30(Sierra et al., 2010). This number is very far from the 0.18ppu of GL microglia in *Cstb* KO mice at P14 reported here. Indeed, microglial supbopulations in the CA region of the hippocampus have been recently observed upon seizures induced by pilocarpine, based on the expression of keratan sulfate polysaccharides (epitope 5D4), whose overexpression is related to a higher ex vivo phagocytosis of zymosan particles possibly related to the engulfment of synapses (Ohgomori & Jinno, 2020). Another potential candidate is the complement system, which is used by microglia to facilitate recognition (opsonization) of apoptotic cells (Diaz-Aparicio & Sierra, 2019a) as well as synapses (Thion & Garel, 2018), and is progressively activated in rodent and human epilepsy (Wyatt et al., 2017; Wyatt-Johnson & Brewster, 2019), including *Cstb* KO mice(Joensuu et al., 2014; Lieuallen et al., 2001). Nonetheless, it is beyond the scope of this paper to test the role of complement or keratan sulfate and future studies will decipher the underlying mechanisms of microglial phagocytosis impairment in *Cstb* KO mice.

In summary, we here extend our initial observations that microglial phagocytosis impairment in the hippocampus is an early feature of mouse and human MTLE and show that it also occurs in a genetic model of EPM1 by *Cstb* deficiency. We also provide an unexpected link between phagocytosis impairment, accumulation of apoptotic cells and local neuronal activity in these mice that further supports the suggestion that both abnormal local neuronal activity (in presymptomatic *Cstb* KO mice) and network hyperactivity (in MTLE mice) regulate the efficiency of microglial phagocytosis. Phagocytosis is an essential component of the brain regenerative

response, as it removes cell debris and is immunomodulatory. Therefore, future therapies for epilepsy patients should be aimed not only at reducing neuronal death but also at harnessing microglial phagocytosis.

Conclusions

8. Conclusions

8.1 MICROGLIAL PHYSIOLOGY AND PHAGOCYTIC FUNCTION ARE ALTERED BY OND

8.1.1 OND reduced microglial motility and phagocytosis in organotypic hippocampal slices

- Microglial phagocytosis is severely impaired after OND, consistent with the in vivo impairment induced by tMCAo.
- The engulfment of apoptotic cells is rapidly restored after reperfusion due to the restoration of the oxygen and nutrient supply.
- The lack of oxygen and nutrients reduces microglial motility and surveillance, likely preventing the engulfment of apoptotic cells.

8.1.2 OND decreases microglial degradation of engulfed apoptotic cells in primary microglial cultures.

- OND induces a significant reduction in the degradative capacity of microglia in vitro.
- The engulfment of apoptotic cells is not affected by OND. This impairment is not related to the apoptotic cell to microglia ratio nor to the engulfment time.

8.1.3 The lack of oxygen and nutrients increases the lysosomal pH and reduces the size of the lysosomal compartment.

- The lysosomal pH is basified after 3 hours of OND but this is not translated into a dysfunctional lysosomal activity.
- OND induces a reduction in the lysosomal numbers accompanied by a reduction in the cytoplasmic area they occupy.
- The reduction in the lysosomal numbers could render fewer available lysosomes to degrade the phagocytosed cargo, thus, explaining the decreased degradation of apoptotic cells.

8.2 THE AUTOPHAGY COMPARTMENT IS REMODELLED BY OND

8.2.1 Autophagy modulation by OND is not detectable by LC3 western blot in primary cultures.

- The autophagy flux, measured by LC3-II western, does not change after 1 and 3 hours of OND either in primary microglia or BV2 cells.
- The amount of LC3-I is significantly reduced after OND in BV2 cells, suggesting the conjugation of the soluble form to the autophagosome membrane and the induction of autophagy.
- LC3 western blot is not sensitive enough to detect the subtle changes induced by OND microglia, compared to the tandem GFP-RFP-LC3

8.2.2 OND triggers the remodelling of the autophagy-like compartment in primary microglia assessed by TEM

- The autophagosome-like compartment increases after OND, in number, and occupied area, but remains constant in size.
- The lysosomal compartment is reduced in number, size and occupied area after OND.
- Consumption of lysosomes related to the induction of autophagy could explain the decreased degradation after OND, as the available lysosomes are recruited for the degradation of autophagosomes and not internalised apoptotic cells.

8.3 MICROGLIAL PHYSIOLOGY IS SUSTAINED BY BASAL AUTOPHAGY IN MICROGLIA

8.3.1 In vivo models of autophagy deficiency suggest its essential role in microglial phagocytosis and survival.

- ATG4B KO mice, with a constitutive deletion of Atg4B in all cell types, exhibit reduced microglial phagocytosis and decreased microglial survival.
- TMEM119-creER-Beclin-1 KO mice, with the specific deletion of Beclin-1 in microglia, only present a small trend to reduced phagocytosis and no alterations in microglial survival.
- AMBRA$^{+/-}$ mice, with constitutive heterozygous deletion of AMBRA1, present a normal microglial function and survival.
- The autophagy KO models prove to be useful tool to study the implications of autophagy on phagocytosis. However, the likely, compensatory mechanisms prevent the development of a severe phenotype related to the autophagy deficiency.

8.3.2 The autophagy inhibitor MRT68921 reduces microglial phagocytosis and survival in primary microglia.

- The selective autophagy inhibitor, MRT68921, effectively blocks autophagy and induces microglial apoptosis in a time and dose-dependent manner.
- The dose 10 µM MRT for 6 hours allows the blockage of autophagy without killing microglia.
- Microglial engulfment is reduced after autophagy inhibition and degradation shows a small trend to be reduced in the presence of MRT.

8.3.3 Microglial phagocytosis is impaired in organotypic hippocampal slices after the addition of MRT68921

- The blockage of microglial autophagy in organotypic hippocampal slices shows a small trend to be reduced in control conditions and worsens microglial death after OND.
- The addition of MRT generates a reduction in microglial phagocytosis in basal conditions.
- Autophagy inhibition after OND has no effect on the already impaired phagocytosis, suggesting a relationship between the two processes, that could be relying on the same cellular substrates

8.4 RAPAMYCIN DOES NOT TRIGGER MICROGLIAL AUTOPHAGY AND DOES NOT RECOVER THE PHAGOCYTIC FUNCTION AFTER OND

8.4.1 Autophagy induction with rapamycin in microglia is not detectable by LC3 western blot in primary cultures.

- The effects of rapamycin in basal conditions and after OND were not detectable by LC3 western blot, likely due to its low sensibility under these conditions.
- The modulation of autophagy in microglia is a complex assignment, as autophagy is possibly already working at its optimum in microglia.

8.4.2 The defects in degradation after OND are not recovered by rapamycin, which shows detrimental effects on microglial survival in primary cultures

- Microglial phagocytosis is not affected by rapamycin in organotypic cultures and primary microglia, in contrast to the partial recovery observed in vivo.
- The degradation defects generated by OND were not recovered by rapamycin in vitro.

- Rapamycin has detrimental effects on microglial survival in the degradation step during OND, likely due to an overstimulation of
-

8.4.3 Microglial phagocytosis in organotypic hippocampal slices is not recovered by rapamycin after OND.

- Rapamycin reduces the overall apoptosis after 24 hours in OND treated hippocampal slices, but this reduction is not specific of microglia.
- The effects of rapamycin are variable concerning the phagocytic capacity and do not recover the uncoupling between phagocytosis and apoptosis.

8.5 A TWO STEP MODEL TO ASSESS AUTOPHAGY BY. WESTERN BLOT

8.5.1 Simple equations to dissect out autophagy.

- Autophagy can be assessed as a two-step process that involves the formation of new autophagosomes and their degradation, contributing to the basal autophagosome pool.
- Formation is calculated as the difference between the untreated control group and the groups treated with lysosomal inhibitors, whereas degradation is calculated as the difference between the non-treated and lysosomal inhibitor treated groups within each experimental condition.
- The net ratio between formation and degradation, equal to 1 in basal conditions, allows to determine if a certain stimulus affects formation and degradation differently and how it affects the autophagosome pool.

8.5.2 Formation and degradation of autophagosomes can be assessed by western blot.

- The two-step model serves as a useful tool to analyse complicated scenarios where the effect of the stimulus affects not only degradation but also formation and even both steps.
- The two-step model allows to understand the net changes in the autophagosome pool after a stimulus as a result of maintain or altering the net turnover ratio.

8.5.3 The two-step model can be applied to experimental data

- The two-step model can be applied to different scenarios of autophagy modulation, proving useful to assess both induction and inhibition as demonstrated after the addition of rapamycin and MRT68921 respectively
- The analysis of the autophagy inhibitor MRT68921 using the two-step model revealed an uncovered effect of the formation step that would have been overlooked using the conventional analysis.

8.6 MICROGLIAL PHAGOCYTOSIS DYSFUNCTION IN THE DENTATE GYRUS IS RELATED TO LOCAL NEURONAL ACTIVITY IN A GENETIC MODEL OF EPILEPSY

8.6.1 Cstb knock-down in microglia does not alter phagocytosis in vitro

- *Cstb* and related cathepsins CTSL and CTSB expression is not exclusive of microglia in vivo, with the exception of CSTS.
- The highest *Cstb* silencing efficiency in BV2 cells is obtained after 24 hours of expression and does not alter the expression of the related cysteine proteases.
- In vitro *Cstb* silencing does not alter the engulfment or degradation of apoptotic bodies by BV2 cells.
- The acute deletion of *Cstb* in microglia is not enough to generate the phagocytic blockage observed in P30 *Cstb* KO mice.

8.6.2 Phagocytosis impairment is specific of the granule cell layer in Cstb KO mice at P14

- P14 *Cstb* KO mice present the same activation levels as their wt littermates.
- The majority of the apoptotic cells in *Cstb* KO mice are found in the granule layer, in opposition to wt mice, where most apoptotic cells are located in the SGZ.
- Microglial phagocytosis is impaired in the granule layer of P14 *Cstb* KO mice resulting in an uncoupling between phagocytosis and apoptosis.
- Microglial phagocytosis is deficient in P14 *Cstb* KO mice prior to the seizure onset.

8.6.3 Apoptotic cells are in close proximity to active cFos+ neurons

- Phagocytosed and non-phagocytosed apoptotic cells are close to $cFos^{+}$ neurons in *Cstb* KO mice.
- The observed phagocytosis impairment could be indirectly related to the local neuronal activity because the number of apoptotic cells observed is the net result between apoptosis induction and phagocytosis removal.

Bibliography

9. Bibliography

A

Abiega, O., Beccari, S., Diaz-Aparicio, I., Nadjar, A., Laye, S., Leyrolle, Q., Gomez-Nicola, D., Domercq, M., Perez-Samartin, A., Sanchez-Zafra, V., Paris, I., Valero, J., Savage, J. C., Hui, C. W., Tremblay, M. E., Deudero, J. J., Brewster, A. L., Anderson, A. E., Zaldumbide, L., Galbarriatu, L., Marinas, A., Vivanco, M., Matute, C., Maletic-Savatic, M., Encinas, J. M., & Sierra, A. (2016, May). Neuronal Hyperactivity Disturbs ATP Microgradients, Impairs Microglial Motility, and Reduces Phagocytic Receptor Expression Triggering Apoptosis/Microglial Phagocytosis Uncoupling. *PLoS Biol, 14*(5), e1002466. https://doi.org/10.1371/journal.pbio.1002466

Aderem, A. (2003, Jun 15). Phagocytosis and the inflammatory response. *J Infect Dis, 187 Suppl 2*, S340-345. https://doi.org/10.1086/374747

Agarraberes, F. A., Terlecky, S. R., & Dice, J. F. (1997, May 19). An intralysosomal hsp70 is required for a selective pathway of lysosomal protein degradation. *J Cell Biol, 137*(4), 825-834. https://doi.org/10.1083/jcb.137.4.825

Ahl, M., Avdic, U., Skoug, C., Ali, I., Chugh, D., Johansson, U. E., & Ekdahl, C. T. (2016, Jun 27). Immune response in the eye following epileptic seizures. *J Neuroinflammation, 13*(1), 155. https://doi.org/10.1186/s12974-016-0618-3

Äikiä, M., Hyppönen, J., Mervaala, E., & Kälviäinen, R. (2021, Sep). Cognitive functioning in progressive myoclonus epilepsy type 1 (Unverricht-Lundborg Disease, EPM1). *Epilepsy Behav, 122*, 108157. https://doi.org/10.1016/j.yebeh.2021.108157

Ali, I., Chugh, D., & Ekdahl, C. T. (2015, Feb). Role of fractalkine-CX3CR1 pathway in seizure-induced microglial activation, neurodegeneration, and neuroblast production in the adult rat brain. *Neurobiol Dis, 74*, 194-203. https://doi.org/10.1016/j.nbd.2014.11.009

Altman, J. (2011). The Discovery of Adult Mammalian Neurogenesis.

An, N., Chen, Y., Wang, C., Yang, C., Wu, Z. H., Xue, J., Ye, L., Wang, S., Liu, H. F., & Pan, Q. (2017). Chloroquine Autophagic Inhibition Rebalances Th17/Treg-Mediated Immunity and Ameliorates Systemic Lupus Erythematosus. *Cell Physiol Biochem, 44*(1), 412-422. https://doi.org/10.1159/000484955

Androvic, P., Kirdajova, D., Tureckova, J., Zucha, D., Rohlova, E., Abaffy, P., Kriska, J., Valny, M., Anderova, M., Kubista, M., & Valihrach, L. (2020, Jun 16). Decoding the Transcriptional Response to Ischemic Stroke in Young and Aged Mouse Brain. *Cell Rep, 31*(11), 107777. https://doi.org/10.1016/j.celrep.2020.107777

Ansari, S., Azari, H., McConnell, D. J., Afzal, A., & Mocco, J. (2011, May 8). Intraluminal middle cerebral artery occlusion (MCAO) model for ischemic stroke with laser doppler flowmetry guidance in mice. *J Vis Exp*(51). https://doi.org/10.3791/2879

Anttila, J. E., Whitaker, K. W., Wires, E. S., Harvey, B. K., & Airavaara, M. (2017, Oct 3). Role of microglia in ischemic focal stroke and recovery: focus on Toll-like receptors. *Prog Neuropsychopharmacol Biol Psychiatry, 79*(Pt A), 3-14. https://doi.org/10.1016/j.pnpbp.2016.07.003

Arai, K., Lok, J., Guo, S., Hayakawa, K., Xing, C., & Lo, E. H. (2011, Sep). Cellular mechanisms of neurovascular damage and repair after stroke. *J Child Neurol, 26*(9), 1193-1198. https://doi.org/10.1177/0883073811408610

Arandjelovic, S., & Ravichandran, K. S. (2015, Sep). Phagocytosis of apoptotic cells in homeostasis. *Nat Immunol, 16*(9), 907-917. https://doi.org/10.1038/ni.3253

Arielle, C., Edoardo, F., Silvana, F., Pierre, G., Riadh, G., Reetta, K., Miikka, K., Maria, K. L., Esa, M., Michele, S., & Annika, V. (2016). Unverricht-Lundborg disease. *Epileptic Disorders, 18*(2), 28-37. https://doi.org/10.1684/epd.2016.0841

Arriola Apelo, S. I., & Lamming, D. W. (2016, Jul). Rapamycin: An InhibiTOR of Aging Emerges From the Soil of Easter Island. *J Gerontol A Biol Sci Med Sci, 71*(7), 841-849. https://doi.org/10.1093/gerona/glw090

Atagi, Y., Liu, C. C., Painter, M. M., Chen, X. F., Verbeeck, C., Zheng, H., Li, X., Rademakers, R., Kang, S. S., Xu, H., Younkin, S., Das, P., Fryer, J. D., & Bu, G. (2015, Oct 23). Apolipoprotein E Is a Ligand for Triggering Receptor Expressed on Myeloid Cells 2 (TREM2). *J Biol Chem, 290*(43), 26043-26050. https://doi.org/10.1074/jbc.M115.679043

Avignone, E., Lepleux, M., Angibaud, J., & Nägerl, U. V. (2015, Nov 4). Altered morphological dynamics of activated microglia after induction of status epilepticus. *J Neuroinflammation, 12*, 202. https://doi.org/10.1186/s12974-015-0421-6

Avignone, E., Ulmann, L., Levavasseur, F., Rassendren, F., & Audinat, E. (2008, Sep 10). Status epilepticus induces a particular microglial activation state characterized by enhanced purinergic signaling. *J Neurosci, 28*(37), 9133-9144. https://doi.org/10.1523/jneurosci.1820-08.2008

B

Bae, E. K., Jung, K. H., Chu, K., Lee, S. T., Kim, J. H., Park, K. I., Kim, M., Chung, C. K., Lee, S. K., & Roh, J. K. (2010, Jun). Neuropathologic and clinical features of human medial temporal lobe epilepsy. *J Clin Neurol, 6*(2), 73-80. https://doi.org/10.3988/jcn.2010.6.2.73

Baldwin, A. C., & Kielian, T. (2004, Jun). Persistent immune activation associated with a mouse model of Staphylococcus aureus-induced experimental brain abscess. *J Neuroimmunol, 151*(1-2), 24-32. https://doi.org/10.1016/j.jneuroim.2004.02.002

Ballabio, A., & Bonifacino, J. S. (2020, Feb). Lysosomes as dynamic regulators of cell and organismal homeostasis. *Nat Rev Mol Cell Biol, 21*(2), 101-118. https://doi.org/10.1038/s41580-019-0185-4

Banerjee, H. N., Bartlett, V., Krauss, C., Aurelius, C., Johnston, K., Hedley, J., & Verma, M. (2021). Efferocytosis and the Story of "Find Me," "Eat Me," and "Don't Eat Me" Signaling in the Tumor Microenvironment. *Adv Exp Med Biol, 1329*, 153-162. https://doi.org/10.1007/978-3-030-73119-9_8

Banerjee, J., Banerjee Dixit, A., Tripathi, M., Sarkar, C., Gupta, Y. K., & Chandra, P. S. (2015, Nov). Enhanced endogenous activation of NMDA receptors in pyramidal neurons of hippocampal tissues from patients with mesial temporal lobe epilepsy: A mechanism of hyper excitation. *Epilepsy Res, 117*, 11-16. https://doi.org/10.1016/j.eplepsyres.2015.08.007

Baroja-Mazo, A., Revilla-Nuin, B., Ramírez, P., & Pons, J. A. (2016, Mar 24). Immunosuppressive potency of mechanistic target of rapamycin inhibitors in solid-organ transplantation. *World J Transplant, 6*(1), 183-192. https://doi.org/10.5500/wjt.v6.i1.183

Barres, B. A., Hart, I. K., Coles, H. S., Burne, J. F., Voyvodic, J. T., Richardson, W. D., & Raff, M. C. (1992, Jul 10). Cell death and control of cell survival in the oligodendrocyte lineage. *Cell, 70*(1), 31-46. https://doi.org/10.1016/0092-8674(92)90531-g

Barth, S., Glick, D., & Macleod, K. F. (2010, Jun). Autophagy: assays and artifacts. *J Pathol, 221*(2), 117-124. https://doi.org/10.1002/path.2694

Beard, D. J., Hadley, G., Thurley, N., Howells, D. W., Sutherland, B. A., & Buchan, A. M. (2019, Feb). The effect of rapamycin treatment on cerebral ischemia: A systematic review and meta-analysis of animal model studies. *Int J Stroke, 14*(2), 137-145. https://doi.org/10.1177/1747493018816503

Beccari, S., Diaz-Aparicio, I., & Sierra, A. (2018a, Aug). Quantifying Microglial Phagocytosis of Apoptotic Cells in the Brain in Health and Disease. *Curr Protoc Immunol, 122*(1), e49. https://doi.org/10.1002/cpim.49

Beccari, S., Diaz-Aparicio, I., & Sierra, A. (2018b). Quantifying Microglial Phagocytosis of Apoptotic Cells in the Brain in Health and Disease. *Curr Protoc Immunol*, e49. https://doi.org/10.1002/cpim.49

Bédard, A., Tremblay, P., Chernomoretz, A., & Vallières, L. (2007, Jun). Identification of genes preferentially expressed by microglia and upregulated during cuprizone-induced inflammation. *Glia, 55*(8), 777-789. https://doi.org/10.1002/glia.20477

Behrens, E. M., Gadue, P., Gong, S. Y., Garrett, S., Stein, P. L., & Cohen, P. L. (2003, Aug). The mer receptor tyrosine kinase: expression and function suggest a role in innate immunity. *Eur J Immunol, 33*(8), 2160-2167. https://doi.org/10.1002/eji.200324076

Ben-Ari, Y., & Cossart, R. (2000, Nov). Kainate, a double agent that generates seizures: two decades of progress. *Trends Neurosci, 23*(11), 580-587. https://doi.org/10.1016/s0166-2236(00)01659-3

Bennett, M. L., Bennett, F. C., Liddelow, S. A., Ajami, B., Zamanian, J. L., Fernhoff, N. B., Mulinyawe, S. B., Bohlen, C. J., Adil, A., Tucker, A., Weissman, I. L., Chang, E. F., Li, G., Grant, G. A., Hayden Gephart, M. G., & Barres, B. A. (2016, Mar 22). New tools for studying microglia in the mouse and human CNS. *Proc Natl Acad Sci U S A, 113*(12), E1738-1746. https://doi.org/10.1073/pnas.1525528113

Berglund, R., Guerreiro-Cacais, A. O., Adzemovic, M. Z., Zeitelhofer, M., Lund, H., Ewing, E., Ruhrmann, S., Nutma, E., Parsa, R., Thessen-Hedreul, M., Amor, S., Harris, R. A., Olsson, T., & Jagodic, M. (2020, Oct 16). Microglial autophagy-associated phagocytosis is essential for recovery from neuroinflammation. *Sci Immunol, 5*(52). https://doi.org/10.1126/sciimmunol.abb5077

Beuker, C., Schafflick, D., Strecker, J. K., Heming, M., Li, X., Wolbert, J., Schmidt-Pogoda, A., Thomas, C., Kuhlmann, T., Aranda-Pardos, I., N, A. G., Kumar, P. A., Werner, Y., Kilic, E., Hermann, D. M., Wiendl, H., Stumm, R., Hörste, G. M. Z., & Minnerup, J. (2022, Feb 17). Stroke induces disease-specific myeloid cells in the brain parenchyma and pia. *Nat Commun, 13*(1), 945. https://doi.org/10.1038/s41467-022-28593-1

Blasi, E., Barluzzi, R., Bocchini, V., Mazzolla, R., & Bistoni, F. (1990, May). Immortalization of murine microglial cells by a v-raf/v-myc carrying retrovirus. *J Neuroimmunol, 27*(2-3), 229-237. https://doi.org/10.1016/0165-5728(90)90073-v

Blasi, E., Mazzolla, R., Barluzzi, R., Mosci, P., Bartoli, A., & Bistoni, F. (1991, Jun). Intracerebral transfer of an in vitro established microglial cell line: local induction of a protective state against lethal challenge with Candida albicans. *J Neuroimmunol, 32*(3), 249-257. https://doi.org/10.1016/0165-5728(91)90195-d

Bonifati, D. M., & Kishore, U. (2007, Feb). Role of complement in neurodegeneration and neuroinflammation. *Mol Immunol, 44*(5), 999-1010. https://doi.org/10.1016/j.molimm.2006.03.007

Bonilla, D. L., Bhattacharya, A., Sha, Y., Xu, Y., Xiang, Q., Kan, A., Jagannath, C., Komatsu, M., & Eissa, N. T. (2013, Sep 19). Autophagy regulates phagocytosis by modulating the expression of scavenger receptors. *Immunity, 39*(3), 537-547. https://doi.org/10.1016/j.immuni.2013.08.026

Borish, L. C., & Steinke, J. W. (2003, Feb). 2. Cytokines and chemokines. *J Allergy Clin Immunol, 111*(2 Suppl), S460-475. https://doi.org/10.1067/mai.2003.108

Börlin, C. S., Lang, V., Hamacher-Brady, A., & Brady, N. R. (2014, Sep 10). Agent-based modeling of autophagy reveals emergent regulatory behavior of spatio-temporal autophagy dynamics. *Cell Commun Signal, 12*, 56. https://doi.org/10.1186/s12964-014-0056-8

Boya, P., Reggiori, F., & Codogno, P. (2013, Jul). Emerging regulation and functions of autophagy. *Nat Cell Biol, 15*(7), 713-720. https://doi.org/10.1038/ncb2788

Brandenburg, S., Müller, A., Turkowski, K., Radev, Y. T., Rot, S., Schmidt, C., Bungert, A. D., Acker, G., Schorr, A., Hippe, A., Miller, K., Heppner, F. L., Homey, B., & Vajkoczy, P. (2016, Mar). Resident microglia rather than peripheral macrophages promote vascularization in brain tumors and are source of alternative pro-angiogenic factors. *Acta Neuropathol, 131*(3), 365-378. https://doi.org/10.1007/s00401-015-1529-6

Brown, G. C., & Neher, J. J. (2014, Apr). Microglial phagocytosis of live neurons. *Nat Rev Neurosci, 15*(4), 209-216. https://doi.org/10.1038/nrn3710

Brown, S., Heinisch, I., Ross, E., Shaw, K., Buckley, C. D., & Savill, J. (2002, Jul 11). Apoptosis disables CD31-mediated cell detachment from phagocytes promoting binding and engulfment. *Nature, 418*(6894), 200-203. https://doi.org/10.1038/nature00811

Broz, P., & Dixit, V. M. (2016, Jul). Inflammasomes: mechanism of assembly, regulation and signalling. *Nat Rev Immunol, 16*(7), 407-420. https://doi.org/10.1038/nri.2016.58

Bucci, C., Parton, R. G., Mather, I. H., Stunnenberg, H., Simons, K., Hoflack, B., & Zerial, M. (1992, Sep 4). The small GTPase rab5 functions as a regulatory factor in the early endocytic pathway. *Cell, 70*(5), 715-728. https://doi.org/10.1016/0092-8674(92)90306-w

Buckley, K. M., Hess, D. L., Sazonova, I. Y., Periyasamy-Thandavan, S., Barrett, J. R., Kirks, R., Grace, H., Kondrikova, G., Johnson, M. H., Hess, D. C., Schoenlein, P. V., Hoda, M. N., & Hill, W. D. (2014). Rapamycin up-regulation of autophagy reduces infarct size and improves outcomes in both permanent MCAL, and embolic MCAO, murine models of stroke. *Exp Transl Stroke Med, 6*, 8. https://doi.org/10.1186/2040-7378-6-8

Burdette, B. E., Esparza, A. N., Zhu, H., & Wang, S. (2021, Sep). Gasdermin D in pyroptosis. *Acta Pharm Sin B, 11*(9), 2768-2782. https://doi.org/10.1016/j.apsb.2021.02.006

Bustin, S. A. (2010, Sep). Developments in real-time PCR research and molecular diagnostics. *Expert Rev Mol Diagn, 10*(6), 713-715. https://doi.org/10.1586/erm.10.65

Butovsky, O., Jedrychowski, M. P., Moore, C. S., Cialic, R., Lanser, A. J., Gabriely, G., Koeglsperger, T., Dake, B., Wu, P. M., Doykan, C. E., Fanek, Z., Liu, L., Chen, Z., Rothstein, J. D., Ransohoff, R. M., Gygi, S. P., Antel, J. P., & Weiner, H. L. (2014, Jan). Identification of a unique TGF-β-dependent molecular and functional signature in microglia. *Nat Neurosci, 17*(1), 131-143. https://doi.org/10.1038/nn.3599

C

Caberoy, N. B., Alvarado, G., Bigcas, J. L., & Li, W. (2012, Feb). Galectin-3 is a new MerTK-specific eat-me signal. *J Cell Physiol, 227*(2), 401-407. https://doi.org/10.1002/jcp.22955

Cabukusta, B., & Neefjes, J. (2018, Oct). Mechanisms of lysosomal positioning and movement. *Traffic, 19*(10), 761-769. https://doi.org/10.1111/tra.12587

Calovi, S., Mut-Arbona, P., & Sperlagh, B. (2019, May 1). Microglia and the Purinergic Signaling System. *Neuroscience, 405*, 137-147. https://doi.org/10.1016/j.neuroscience.2018.12.021

Cámara-Lemarroy, C. R., Guzmán-de la Garza, F. J., & Fernández-Garza, N. E. (2010). Molecular inflammatory mediators in peripheral nerve degeneration and regeneration. *Neuroimmunomodulation, 17*(5), 314-324. https://doi.org/10.1159/000292020

Caviston, J. P., Zajac, A. L., Tokito, M., & Holzbaur, E. L. (2011, Feb 15). Huntingtin coordinates the dynein-mediated dynamic positioning of endosomes and lysosomes. *Mol Biol Cell, 22*(4), 478-492. https://doi.org/10.1091/mbc.E10-03-0233

Cemma, M., Grinstein, S., & Brumell, J. H. (2016, Sep). Autophagy proteins are not universally required for phagosome maturation. *Autophagy, 12*(9), 1440-1446. https://doi.org/10.1080/15548627.2016.1191724

Chapman, R. L., Kane, S. E., & Erickson, A. H. (1997, Mar 28). Abnormal glycosylation of procathepsin L due to N-terminal point mutations correlates with failure to sort to lysosomes. *J Biol Chem, 272*(13), 8808-8816. https://doi.org/10.1074/jbc.272.13.8808

Checchin, D., Sennlaub, F., Levavasseur, E., Leduc, M., & Chemtob, S. (2006, Aug). Potential role of microglia in retinal blood vessel formation. *Invest Ophthalmol Vis Sci, 47*(8), 3595-3602. https://doi.org/10.1167/iovs.05-1522

Chekeni, F. B., Elliott, M. R., Sandilos, J. K., Walk, S. F., Kinchen, J. M., Lazarowski, E. R., Armstrong, A. J., Penuela, S., Laird, D. W., Salvesen, G. S., Isakson, B. E., Bayliss, D. A., & Ravichandran, K. S. (2010, Oct 14). Pannexin 1 channels mediate 'find-me' signal release and membrane permeability during apoptosis. *Nature, 467*(7317), 863-867. https://doi.org/10.1038/nature09413

Chen, C., Leys, D., & Esquenazi, A. (2013, Jan 15). The interaction between neuropsychological and motor deficits in patients after stroke. *Neurology, 80*(3 Suppl 2), S27-34. https://doi.org/10.1212/WNL.0b013e3182762569

Chen, L., Deng, H., Cui, H., Fang, J., Zuo, Z., Deng, J., Li, Y., Wang, X., & Zhao, L. (2018, Jan 23). Inflammatory responses and inflammation-associated diseases in organs. *Oncotarget, 9*(6), 7204-7218. https://doi.org/10.18632/oncotarget.23208

Chen, S., Lai, S. W. T., Brown, C. E., & Feng, M. (2021). Harnessing and Enhancing Macrophage Phagocytosis for Cancer Therapy. *Front Immunol, 12*, 635173. https://doi.org/10.3389/fimmu.2021.635173

Chen, S., Zeng, L., & Hu, Z. (2014, Nov). Progressing haemorrhagic stroke: categories, causes, mechanisms and managements. *J Neurol, 261*(11), 2061-2078. https://doi.org/10.1007/s00415-014-7291-1

Chew, N. K., Mir, P., Edwards, M. J., Cordivari, C., Martino, D., Schneider, S. A., Kim, H. T., Quinn, N. P., & Bhatia, K. P. (2008, Jan). The natural history of Unverricht-Lundborg disease: a report of eight genetically proven cases. *Mov Disord, 23*(1), 107-113. https://doi.org/10.1002/mds.21812

Chistiakov, D. A., Killingsworth, M. C., Myasoedova, V. A., Orekhov, A. N., & Bobryshev, Y. V. (2017, Jan). CD68/macrosialin: not just a histochemical marker. *Lab Invest, 97*(1), 4-13. https://doi.org/10.1038/labinvest.2016.116

Cho, M. H., Cho, K., Kang, H. J., Jeon, E. Y., Kim, H. S., Kwon, H. J., Kim, H. M., Kim, D. H., & Yoon, S. Y. (2014, Oct 1). Autophagy in microglia degrades extracellular β-amyloid fibrils and regulates the NLRP3 inflammasome. *Autophagy, 10*(10), 1761-1775. https://doi.org/10.4161/auto.29647

Choi, I., Zhang, Y., Seegobin, S. P., Pruvost, M., Wang, Q., Purtell, K., Zhang, B., & Yue, Z. (2020, Mar 13). Microglia clear neuron-released α-synuclein via selective autophagy and prevent neurodegeneration. *Nat Commun, 11*(1), 1386. https://doi.org/10.1038/s41467-020-15119-w

Cignarella, F., Filipello, F., Bollman, B., Cantoni, C., Locca, A., Mikesell, R., Manis, M., Ibrahim, A., Deng, L., Benitez, B. A., Cruchaga, C., Licastro, D., Mihindukulasuriya, K., Harari, O., Buckland, M., Holtzman, D. M., Rosenthal, A., Schwabe, T., Tassi, I., & Piccio, L. (2020, Oct). TREM2 activation on microglia promotes myelin debris clearance and remyelination in a model of multiple sclerosis. *Acta Neuropathol, 140*(4), 513-534. https://doi.org/10.1007/s00401-020-02193-z

Cimino, G. (1999). Reticular theory versus neuron theory in the work of Camillo Golgi. *Physis Riv Int Stor Sci, 36*(2), 431-472.

Civiletto, G., Dogan, S. A., Cerutti, R., Fagiolari, G., Moggio, M., Lamperti, C., Beninca, C., Viscomi, C., & Zeviani, M. (2018, Nov). Rapamycin rescues mitochondrial myopathy via coordinated activation of autophagy and lysosomal biogenesis. *EMBO Mol Med, 10*(11). https://doi.org/10.15252/emmm.201708799

Claveau, D., & Riendeau, D. (2001, Feb 23). Mutations of the C-terminal end of cathepsin K affect proenzyme secretion and intracellular maturation. *Biochem Biophys Res Commun, 281*(2), 551-557. https://doi.org/10.1006/bbrc.2001.4394

Cockram, T. O. J., Puigdellívol, M., & Brown, G. C. (2019). Calreticulin and Galectin-3 Opsonise Bacteria for Phagocytosis by Microglia. *Front Immunol, 10*, 2647. https://doi.org/10.3389/fimmu.2019.02647

Corona Velazquez, A. F., & Jackson, W. T. (2018, Nov 1). So Many Roads: the Multifaceted Regulation of Autophagy Induction. *Mol Cell Biol, 38*(21). https://doi.org/10.1128/MCB.00303-18

Coull, J. A., Beggs, S., Boudreau, D., Boivin, D., Tsuda, M., Inoue, K., Gravel, C., Salter, M. W., & De Koninck, Y. (2005, Dec 15). BDNF from microglia causes the shift in neuronal anion gradient underlying neuropathic pain. *Nature, 438*(7070), 1017-1021. https://doi.org/10.1038/nature04223

Császár, E., Lénárt, N., Cserép, C., Környei, Z., Fekete, R., Pósfai, B., Balázsfi, D., Hangya, B., Schwarcz, A. D., Szabadits, E., Szöllősi, D., Szigeti, K., Máthé, D., West, B. L., Sviatkó, K., Brás, A. R., Mariani, J. C., Kliewer, A., Lenkei, Z., Hricisák, L., Benyó, Z., Baranyi, M., Sperlágh, B., Menyhárt, Á., Farkas, E., & Dénes, Á. (2022, Mar 7). Microglia modulate blood flow, neurovascular coupling, and hypoperfusion via purinergic actions. *J Exp Med, 219*(3). https://doi.org/10.1084/jem.20211071

Cuartero, M. I., Ballesteros, I., de la Parra, J., Harkin, A. L., Abautret-Daly, A., Sherwin, E., Fernandez-Salguero, P., Corbi, A. L., Lizasoain, I., & Moro, M. A. (2014, Dec 2). L-kynurenine/aryl hydrocarbon receptor pathway mediates brain damage after experimental stroke. *Circulation, 130*(23), 2040-2051. https://doi.org/10.1161/CIRCULATIONAHA.114.011394

Cumming, T. B., Marshall, R. S., & Lazar, R. M. (2013, Jan). Stroke, cognitive deficits, and rehabilitation: still an incomplete picture. *Int J Stroke, 8*(1), 38-45. https://doi.org/10.1111/j.1747-4949.2012.00972.x

Cunningham, C. L., Martínez-Cerdeño, V., & Noctor, S. C. (2013, Mar 6). Microglia regulate the number of neural precursor cells in the developing cerebral cortex. *J Neurosci, 33*(10), 4216-4233. https://doi.org/10.1523/jneurosci.3441-12.2013

D

D'Arcy, M. S. (2019, Jun). Cell death: a review of the major forms of apoptosis, necrosis and autophagy. *Cell Biol Int, 43*(6), 582-592. https://doi.org/10.1002/cbin.11137

da Silva, R. P., & Gordon, S. (1999, Mar 15). Phagocytosis stimulates alternative glycosylation of macrosialin (mouse CD68), a macrophage-specific endosomal protein. *Biochem J, 338 (Pt 3)*(Pt 3), 687-694.

Dale, N., & Frenguelli, B. G. (2009, Sep). Release of adenosine and ATP during ischemia and epilepsy. *Curr Neuropharmacol, 7*(3), 160-179. https://doi.org/10.2174/157015909789152146

Dalmau, I., Vela, J. M., González, B., Finsen, B., & Castellano, B. (2003, Mar 31). Dynamics of microglia in the developing rat brain. *J Comp Neurol, 458*(2), 144-157. https://doi.org/10.1002/cne.10572

Dando, S. J., Mackay-Sim, A., Norton, R., Currie, B. J., St John, J. A., Ekberg, J. A., Batzloff, M., Ulett, G. C., & Beacham, I. R. (2014, Oct). Pathogens penetrating the central nervous system: infection pathways and the cellular and molecular mechanisms of invasion. *Clin Microbiol Rev, 27*(4), 691-726. https://doi.org/10.1128/cmr.00118-13

Daria, A., Colombo, A., Llovera, G., Hampel, H., Willem, M., Liesz, A., Haass, C., & Tahirovic, S. (2017, Mar 1). Young microglia restore amyloid plaque clearance of aged microglia. *Embo j, 36*(5), 583-603. https://doi.org/10.15252/embj.201694591

Das, A., Kim, S. H., Arifuzzaman, S., Yoon, T., Chai, J. C., Lee, Y. S., Park, K. S., Jung, K. H., & Chai, Y. G. (2016, Jul 11). Transcriptome sequencing reveals that LPS-triggered transcriptional responses in established microglia BV2 cell lines are poorly representative of primary microglia. *J Neuroinflammation, 13*(1), 182. https://doi.org/10.1186/s12974-016-0644-1

Dawson, T. M., Golde, T. E., & Lagier-Tourenne, C. (2018, Oct). Animal models of neurodegenerative diseases. *Nat Neurosci, 21*(10), 1370-1379. https://doi.org/10.1038/s41593-018-0236-8

Dayer, J. M., Oliviero, F., & Punzi, L. (2017). A Brief History of IL-1 and IL-1 Ra in Rheumatology. *Front Pharmacol, 8*, 293. https://doi.org/10.3389/fphar.2017.00293

De Biase, L. M., Schuebel, K. E., Fusfeld, Z. H., Jair, K., Hawes, I. A., Cimbro, R., Zhang, H. Y., Liu, Q. R., Shen, H., Xi, Z. X., Goldman, D., & Bonci, A. (2017, Jul 19). Local Cues Establish and Maintain Region-

Specific Phenotypes of Basal Ganglia Microglia. *Neuron, 95*(2), 341-356.e346. https://doi.org/10.1016/j.neuron.2017.06.020

De Duve, C., & Wattiaux, R. (1966). Functions of lysosomes. *Annu Rev Physiol, 28*, 435-492. https://doi.org/10.1146/annurev.ph.28.030166.002251

de Haas, A. H., Boddeke, H. W., & Biber, K. (2008, Jun). Region-specific expression of immunoregulatory proteins on microglia in the healthy CNS. *Glia, 56*(8), 888-894. https://doi.org/10.1002/glia.20663

de Lanerolle, N. C., Kim, J. H., Williamson, A., Spencer, S. S., Zaveri, H. P., Eid, T., & Spencer, D. D. (2003, May). A retrospective analysis of hippocampal pathology in human temporal lobe epilepsy: evidence for distinctive patient subcategories. *Epilepsia, 44*(5), 677-687. https://doi.org/10.1046/j.1528-1157.2003.32701.x

de Miranda, A. S., Zhang, C. J., Katsumoto, A., & Teixeira, A. L. (2017, Jan 15). Hippocampal adult neurogenesis: Does the immune system matter? *J Neurol Sci, 372*, 482-495. https://doi.org/10.1016/j.jns.2016.10.052

De Simone, R., Ajmone-Cat, M. A., Tirassa, P., & Minghetti, L. (2003, Feb). Apoptotic PC12 cells exposing phosphatidylserine promote the production of anti-inflammatory and neuroprotective molecules by microglial cells. *J Neuropathol Exp Neurol, 62*(2), 208-216. https://doi.org/10.1093/jnen/62.2.208

Decuypere, J. P., Parys, J. B., & Bultynck, G. (2012, Jul 6). Regulation of the autophagic bcl-2/beclin 1 interaction. *Cells, 1*(3), 284-312. https://doi.org/10.3390/cells1030284

Dehay, B., Bové, J., Rodríguez-Muela, N., Perier, C., Recasens, A., Boya, P., & Vila, M. (2010, Sep 15). Pathogenic lysosomal depletion in Parkinson's disease. *J Neurosci, 30*(37), 12535-12544. https://doi.org/10.1523/jneurosci.1920-10.2010

Deitch, E. A. (1998, Jan). Animal models of sepsis and shock: a review and lessons learned. *Shock, 9*(1), 1-11. https://doi.org/10.1097/00024382-199801000-00001

Del Río-Hortega Bereciartu, J. (2020, May). Pío del Río-Hortega: The Revolution of Glia. *Anat Rec (Hoboken), 303*(5), 1232-1241. https://doi.org/10.1002/ar.24266

del Rio-Hortega, P. (1919). *El" Tercer"" elemento" de los centros nerviosos: poder fagocitario y movilidad de la microglia*.

Denes, A., Vidyasagar, R., Feng, J., Narvainen, J., McColl, B. W., Kauppinen, R. A., & Allan, S. M. (2007, Dec). Proliferating resident microglia after focal cerebral ischaemia in mice. *J Cereb Blood Flow Metab, 27*(12), 1941-1953. https://doi.org/10.1038/sj.jcbfm.9600495

Dengjel, J., & Dumit, V. (2012, 2012-March-14). Autophagosomal Protein Dynamics and Influenza Virus Infection [Review]. *Frontiers in Immunology, 3*. https://doi.org/10.3389/fimmu.2012.00043

Dere, E., Dahm, L., Lu, D., Hammerschmidt, K., Ju, A., Tantra, M., Kästner, A., Chowdhury, K., & Ehrenreich, H. (2014, 2014-May-16). Heterozygous Ambra1 Deficiency in Mice: A Genetic Trait with Autism-Like Behavior Restricted to the Female Gender [Original Research]. *Frontiers in Behavioral Neuroscience, 8*. https://doi.org/10.3389/fnbeh.2014.00181

Desjardins, M. (1995, May). Biogenesis of phagolysosomes: the 'kiss and run' hypothesis. *Trends Cell Biol, 5*(5), 183-186. https://doi.org/10.1016/s0962-8924(00)88989-8

Desjardins, M., Huber, L. A., Parton, R. G., & Griffiths, G. (1994, Mar). Biogenesis of phagolysosomes proceeds through a sequential series of interactions with the endocytic apparatus. *J Cell Biol, 124*(5), 677-688. https://doi.org/10.1083/jcb.124.5.677

Devi, L. A. (2000, Sep). G-protein-coupled receptor dimers in the lime light. *Trends Pharmacol Sci, 21*(9), 324-326. https://doi.org/10.1016/s0165-6147(00)01519-4

Diaz-Aparicio, I., Beccari, S., Abiega, O., & Sierra, A. (2016, Oct). Clearing the corpses: regulatory mechanisms, novel tools, and therapeutic potential of harnessing microglial phagocytosis in the diseased brain. *Neural Regen Res, 11*(10), 1533-1539. https://doi.org/10.4103/1673-5374.193220

Diaz-Aparicio, I., Paris, I., Sierra-Torre, V., Plaza-Zabala, A., Rodriguez-Iglesias, N., Marquez-Ropero, M., Beccari, S., Huguet, P., Abiega, O., Alberdi, E., Matute, C., Bernales, I., Schulz, A., Otrokocsi, L., Sperlagh, B., Happonen, K. E., Lemke, G., Maletic-Savatic, M., Valero, J., & Sierra, A. (2020, Feb 12). Microglia Actively Remodel Adult Hippocampal Neurogenesis through the Phagocytosis Secretome. *J Neurosci, 40*(7), 1453-1482. https://doi.org/10.1523/JNEUROSCI.0993-19.2019

Diaz-Aparicio, I., & Sierra, A. (2019a, 05/10). C1q is related to microglial phagocytosis in the hippocampus in physiological conditions. *Matters*. https://doi.org/10.19185/matters.201904000013

Diaz-Aparicio, I., & Sierra, A. (2019b). C1q is related to microglial phagocytosis in the hippocampus in physiological conditions. *Science Matters, 10*.

Dice, J. F. (1982, Dec 25). Altered degradation of proteins microinjected into senescent human fibroblasts. *J Biol Chem, 257*(24), 14624-14627.

Diesselberg, C., Ribes, S., Seele, J., Kaufmann, A., Redlich, S., Bunkowski, S., Hanisch, U. K., Michel, U., Nau, R., & Schütze, S. (2018, Jun 7). Activin A increases phagocytosis of Escherichia coli K1 by primary murine microglial cells activated by toll-like receptor agonists. *J Neuroinflammation, 15*(1), 175. https://doi.org/10.1186/s12974-018-1209-2

Dinarello, C. A. (2000, Aug). Proinflammatory cytokines. *Chest, 118*(2), 503-508. https://doi.org/10.1378/chest.118.2.503

Dirnagl, U., Iadecola, C., & Moskowitz, M. A. (1999, Sep). Pathobiology of ischaemic stroke: an integrated view. *Trends Neurosci, 22*(9), 391-397. https://doi.org/10.1016/s0166-2236(99)01401-0

Domingues, H. S., Portugal, C. C., Socodato, R., & Relvas, J. B. (2016). Oligodendrocyte, Astrocyte, and Microglia Crosstalk in Myelin Development, Damage, and Repair. *Front Cell Dev Biol, 4*, 71. https://doi.org/10.3389/fcell.2016.00071

Dossou, A. S., & Basu, A. (2019, Sep 24). The Emerging Roles of mTORC1 in Macromanaging Autophagy. *Cancers (Basel), 11*(10). https://doi.org/10.3390/cancers11101422

Drobny, A., Prieto Huarcaya, S., Dobert, J., Kluge, A., Bunk, J., Schlothauer, T., & Zunke, F. (2022, Feb 23). The role of lysosomal cathepsins in neurodegeneration: Mechanistic insights, diagnostic potential and therapeutic approaches. *Biochim Biophys Acta Mol Cell Res, 1869*(7), 119243. https://doi.org/10.1016/j.bbamcr.2022.119243

Duclos, S., Diez, R., Garin, J., Papadopoulou, B., Descoteaux, A., Stenmark, H., & Desjardins, M. (2000, Oct). Rab5 regulates the kiss and run fusion between phagosomes and endosomes and the acquisition of phagosome leishmanicidal properties in RAW 264.7 macrophages. *J Cell Sci, 113 Pt 19*, 3531-3541. https://doi.org/10.1242/jcs.113.19.3531

Duveau, V., Pouyatos, B., Bressand, K., Bouyssières, C., Chabrol, T., Roche, Y., Depaulis, A., & Roucard, C. (2016, Jun). Differential Effects of Antiepileptic Drugs on Focal Seizures in the Intrahippocampal Kainate Mouse Model of Mesial Temporal Lobe Epilepsy. *CNS Neurosci Ther, 22*(6), 497-506. https://doi.org/10.1111/cns.12523

E

Ehirchiou, D., Xiong, Y., Xu, G., Chen, W., Shi, Y., & Zhang, L. (2007, Jul 9). CD11b facilitates the development of peripheral tolerance by suppressing Th17 differentiation. *J Exp Med, 204*(7), 1519-1524. https://doi.org/10.1084/jem.20062292

Ekdahl, C. T., Claasen, J. H., Bonde, S., Kokaia, Z., & Lindvall, O. (2003, Nov 11). Inflammation is detrimental for neurogenesis in adult brain. *Proc Natl Acad Sci U S A, 100*(23), 13632-13637. https://doi.org/10.1073/pnas.2234031100

Elliott, M. R., Chekeni, F. B., Trampont, P. C., Lazarowski, E. R., Kadl, A., Walk, S. F., Park, D., Woodson, R. I., Ostankovich, M., Sharma, P., Lysiak, J. J., Harden, T. K., Leitinger, N., & Ravichandran, K. S. (2009, Sep 10). Nucleotides released by apoptotic cells act as a find-me signal to promote phagocytic clearance. *Nature, 461*(7261), 282-286. https://doi.org/10.1038/nature08296

Elmore, M. R., Lee, R. J., West, B. L., & Green, K. N. (2015). Characterizing newly repopulated microglia in the adult mouse: impacts on animal behavior, cell morphology, and neuroinflammation. *PLoS One, 10*(4), e0122912. https://doi.org/10.1371/journal.pone.0122912

Elmore, M. R., Najafi, A. R., Koike, M. A., Dagher, N. N., Spangenberg, E. E., Rice, R. A., Kitazawa, M., Matusow, B., Nguyen, H., West, B. L., & Green, K. N. (2014, Apr 16). Colony-stimulating factor 1 receptor signaling is necessary for microglia viability, unmasking a microglia progenitor cell in the adult brain. *Neuron, 82*(2), 380-397. https://doi.org/10.1016/j.neuron.2014.02.040

Elmore, S. (2007, Jun). Apoptosis: a review of programmed cell death. *Toxicol Pathol, 35*(4), 495-516. https://doi.org/10.1080/01926230701320337

Elward, K., Griffiths, M., Mizuno, M., Harris, C. L., Neal, J. W., Morgan, B. P., & Gasque, P. (2005, Oct 28). CD46 plays a key role in tailoring innate immune recognition of apoptotic and necrotic cells. *J Biol Chem, 280*(43), 36342-36354. https://doi.org/10.1074/jbc.M506579200

Erdman, L. K., Cosio, G., Helmers, A. J., Gowda, D. C., Grinstein, S., & Kain, K. C. (2009, Nov 15). CD36 and TLR interactions in inflammation and phagocytosis: implications for malaria. *J Immunol, 183*(10), 6452-6459. https://doi.org/10.4049/jimmunol.0901374

Erie, C., Sacino, M., Houle, L., Lu, M. L., & Wei, J. (2015, Aug). Altered lysosomal positioning affects lysosomal functions in a cellular model of Huntington's disease. *Eur J Neurosci, 42*(3), 1941-1951. https://doi.org/10.1111/ejn.12957

Eriksson, C., Zou, L. P., Ahlenius, S., Winblad, B., & Schultzberg, M. (2000, Dec 28). Inhibition of kainic acid induced expression of interleukin-1 beta and interleukin-1 receptor antagonist mRNA in the rat brain by NMDA receptor antagonists. *Brain Res Mol Brain Res, 85*(1-2), 103-113. https://doi.org/10.1016/s0169-328x(00)00251-5

Erlich, S., Alexandrovich, A., Shohami, E., & Pinkas-Kramarski, R. (2007, Apr). Rapamycin is a neuroprotective treatment for traumatic brain injury. *Neurobiol Dis, 26*(1), 86-93. https://doi.org/10.1016/j.nbd.2006.12.003

Eskelinen, E. L. (2005, Apr). Maturation of autophagic vacuoles in Mammalian cells. *Autophagy, 1*(1), 1-10. https://doi.org/10.4161/auto.1.1.1270

Eskelinen, E. L., Reggiori, F., Baba, M., Kovács, A. L., & Seglen, P. O. (2011, Sep). Seeing is believing: the impact of electron microscopy on autophagy research. *Autophagy, 7*(9), 935-956. https://doi.org/10.4161/auto.7.9.15760

Eskelinen, E. L., Tanaka, Y., & Saftig, P. (2003, Mar). At the acidic edge: emerging functions for lysosomal membrane proteins. *Trends Cell Biol, 13*(3), 137-145. https://doi.org/10.1016/s0962-8924(03)00005-9

Eyo, U. B., Peng, J., Murugan, M., Mo, M., Lalani, A., Xie, P., Xu, P., Margolis, D. J., & Wu, L. J. (2016, Nov-Dec). Regulation of Physical Microglia-Neuron Interactions by Fractalkine Signaling after Status Epilepticus. *eNeuro, 3*(6). https://doi.org/10.1523/eneuro.0209-16.2016

Eyo, U. B., Peng, J., Swiatkowski, P., Mukherjee, A., Bispo, A., & Wu, L. J. (2014, Aug 6). Neuronal hyperactivity recruits microglial processes via neuronal NMDA receptors and microglial P2Y12 receptors after status epilepticus. *J Neurosci, 34*(32), 10528-10540. https://doi.org/10.1523/jneurosci.0416-14.2014

F

Fadok, V. A., Voelker, D. R., Campbell, P. A., Cohen, J. J., Bratton, D. L., & Henson, P. M. (1992, Apr 1). Exposure of phosphatidylserine on the surface of apoptotic lymphocytes triggers specific recognition and removal by macrophages. *J Immunol, 148*(7), 2207-2216.

Famitafreshi, H., & Karimian, M. (2020). Prostaglandins as the Agents That Modulate the Course of Brain Disorders. *Degener Neurol Neuromuscul Dis, 10*, 1-13. https://doi.org/10.2147/dnnd.S240800

Fang, S. H., Wei, E. Q., Zhou, Y., Wang, M. L., Zhang, W. P., Yu, G. L., Chu, L. S., & Chen, Z. (2006, Jul 7). Increased expression of cysteinyl leukotriene receptor-1 in the brain mediates neuronal damage and astrogliosis after focal cerebral ischemia in rats. *Neuroscience, 140*(3), 969-979. https://doi.org/10.1016/j.neuroscience.2006.02.051

Fang, Y., Tan, J., & Zhang, Q. (2015, Aug). Signaling pathways and mechanisms of hypoxia-induced autophagy in the animal cells. *Cell Biol Int, 39*(8), 891-898. https://doi.org/10.1002/cbin.10463

Fantin, A., Vieira, J. M., Gestri, G., Denti, L., Schwarz, Q., Prykhozhij, S., Peri, F., Wilson, S. W., & Ruhrberg, C. (2010, Aug 5). Tissue macrophages act as cellular chaperones for vascular anastomosis downstream of VEGF-mediated endothelial tip cell induction. *Blood, 116*(5), 829-840. https://doi.org/10.1182/blood-2009-12-257832

Fattorusso, A., Matricardi, S., Mencaroni, E., Dell'Isola, G. B., Di Cara, G., Striano, P., & Verrotti, A. (2021). The Pharmacoresistant Epilepsy: An Overview on Existant and New Emerging Therapies. *Front Neurol, 12*, 674483. https://doi.org/10.3389/fneur.2021.674483

Fazeli, G., & Wehman, A. M. (2017, Oct). Safely removing cell debris with LC3-associated phagocytosis. *Biol Cell, 109*(10), 355-363. https://doi.org/10.1111/boc.201700028

Ferro, J. M., Caeiro, L., & Figueira, M. L. (2016, May). Neuropsychiatric sequelae of stroke. *Nat Rev Neurol, 12*(5), 269-280. https://doi.org/10.1038/nrneurol.2016.46

Fimia, G. M., Stoykova, A., Romagnoli, A., Giunta, L., Di Bartolomeo, S., Nardacci, R., Corazzari, M., Fuoco, C., Ucar, A., Schwartz, P., Gruss, P., Piacentini, M., Chowdhury, K., & Cecconi, F. (2007, Jun 28). Ambra1 regulates autophagy and development of the nervous system. *Nature, 447*(7148), 1121-1125. https://doi.org/10.1038/nature05925

Fisher, R. S., Acevedo, C., Arzimanoglou, A., Bogacz, A., Cross, J. H., Elger, C. E., Engel, J., Jr., Forsgren, L., French, J. A., Glynn, M., Hesdorffer, D. C., Lee, B. I., Mathern, G. W., Moshé, S. L., Perucca, E., Scheffer, I. E., Tomson, T., Watanabe, M., & Wiebe, S. (2014, Apr). ILAE official report: a practical clinical definition of epilepsy. *Epilepsia, 55*(4), 475-482. https://doi.org/10.1111/epi.12550

Fisher, R. S., Cross, J. H., French, J. A., Higurashi, N., Hirsch, E., Jansen, F. E., Lagae, L., Moshé, S. L., Peltola, J., Roulet Perez, E., Scheffer, I. E., & Zuberi, S. M. (2017, Apr). Operational classification of seizure types by the International League Against Epilepsy: Position Paper of the ILAE Commission for Classification and Terminology. *Epilepsia, 58*(4), 522-530. https://doi.org/10.1111/epi.13670

Forsgren, L., Hauser, W. A., Olafsson, E., Sander, J. W., Sillanpää, M., & Tomson, T. (2005). Mortality of epilepsy in developed countries: a review. *Epilepsia, 46 Suppl 11*, 18-27. https://doi.org/10.1111/j.1528-1167.2005.00403.x

Foster, J. R. (2001, Jun). The functions of cytokines and their uses in toxicology. *Int J Exp Pathol, 82*(3), 171-192. https://doi.org/10.1046/j.1365-2613.2001.iep0082-0171-x

Fourgeaud, L., Través, P. G., Tufail, Y., Leal-Bailey, H., Lew, E. D., Burrola, P. G., Callaway, P., Zagórska, A., Rothlin, C. V., Nimmerjahn, A., & Lemke, G. (2016, Apr 14). TAM receptors regulate multiple features of microglial physiology. *Nature, 532*(7598), 240-244. https://doi.org/10.1038/nature17630

Franke, H., Günther, A., Grosche, J., Schmidt, R., Rossner, S., Reinhardt, R., Faber-Zuschratter, H., Schneider, D., & Illes, P. (2004, Jul). P2X7 receptor expression after ischemia in the cerebral cortex of rats. *J Neuropathol Exp Neurol, 63*(7), 686-699. https://doi.org/10.1093/jnen/63.7.686

Fraser, D. A., Pisalyaput, K., & Tenner, A. J. (2010, Feb). C1q enhances microglial clearance of apoptotic neurons and neuronal blebs, and modulates subsequent inflammatory cytokine production. *J Neurochem, 112*(3), 733-743. https://doi.org/10.1111/j.1471-4159.2009.06494.x

Friedman, B. A., Srinivasan, K., Ayalon, G., Meilandt, W. J., Lin, H., Huntley, M. A., Cao, Y., Lee, S. H., Haddick, P. C. G., Ngu, H., Modrusan, Z., Larson, J. L., Kaminker, J. S., van der Brug, M. P., & Hansen, D. V. (2018, Jan 16). Diverse Brain Myeloid Expression Profiles Reveal Distinct Microglial Activation States and Aspects of Alzheimer's Disease Not Evident in Mouse Models. *Cell Rep, 22*(3), 832-847. https://doi.org/10.1016/j.celrep.2017.12.066

Fritsch, B., Reis, J., Gasior, M., Kaminski, R. M., & Rogawski, M. A. (2014, Apr 23). Role of GluK1 kainate receptors in seizures, epileptic discharges, and epileptogenesis. *J Neurosci, 34*(17), 5765-5775. https://doi.org/10.1523/jneurosci.5307-13.2014

Fuchs, Y., & Steller, H. (2015, Jun). Live to die another way: modes of programmed cell death and the signals emanating from dying cells. *Nat Rev Mol Cell Biol, 16*(6), 329-344. https://doi.org/10.1038/nrm3999

Fujita, N., Hayashi-Nishino, M., Fukumoto, H., Omori, H., Yamamoto, A., Noda, T., & Yoshimori, T. (2008, Nov). An Atg4B mutant hampers the lipidation of LC3 paralogues and causes defects in autophagosome closure. *Mol Biol Cell, 19*(11), 4651-4659. https://doi.org/10.1091/mbc.e08-03-0312

Fujita, S., & Kitamura, T. (1975). Origin of brain macrophages and the nature of the so-called microglia. *Acta Neuropathol Suppl, Suppl 6*, 291-296. https://doi.org/10.1007/978-3-662-08456-4_51

Fumagalli, S., Fiordaliso, F., Perego, C., Corbelli, A., Mariani, A., De Paola, M., & De Simoni, M. G. (2019, Jan 16). The phagocytic state of brain myeloid cells after ischemia revealed by superresolution structured illumination microscopy. *J Neuroinflammation, 16*(1), 9. https://doi.org/10.1186/s12974-019-1401-z

Funk, C. D. (2001, Nov 30). Prostaglandins and leukotrienes: advances in eicosanoid biology. *Science, 294*(5548), 1871-1875. https://doi.org/10.1126/science.294.5548.1871

Futai, M., Sun-Wada, G. H., Wada, Y., Matsumoto, N., & Nakanishi-Matsui, M. (2019). Vacuolar-type ATPase: A proton pump to lysosomal trafficking. *Proc Jpn Acad Ser B Phys Biol Sci, 95*(6), 261-277. https://doi.org/10.2183/pjab.95.018

G

Gagliardi, S., Rees, M., & Farina, C. (1999, Dec). Chemistry and structure activity relationships of bafilomycin A1, a potent and selective inhibitor of the vacuolar H+-ATPase. *Curr Med Chem, 6*(12), 1197-1212. https://www.ncbi.nlm.nih.gov/pubmed/10519916

Gähwiler, B. H., Capogna, M., Debanne, D., McKinney, R. A., & Thompson, S. M. (1997, Oct). Organotypic slice cultures: a technique has come of age. *Trends Neurosci, 20*(10), 471-477. https://doi.org/10.1016/s0166-2236(97)01122-3

Gaitatzis, A., & Sander, J. W. (2004, Mar). The mortality of epilepsy revisited. *Epileptic Disord, 6*(1), 3-13.

Galluzzi, L., Bravo-San Pedro, J. M., Blomgren, K., & Kroemer, G. (2016, Aug). Autophagy in acute brain injury. *Nat Rev Neurosci, 17*(8), 467-484. https://doi.org/10.1038/nrn.2016.51

Garbayo, E., Raval, A. P., Curtis, K. M., Della-Morte, D., Gomez, L. A., D'Ippolito, G., Reiner, T., Perez-Stable, C., Howard, G. A., Perez-Pinzon, M. A., Montero-Menei, C. N., & Schiller, P. C. (2011, Dec). Neuroprotective properties of marrow-isolated adult multilineage-inducible cells in rat hippocampus following global cerebral ischemia are enhanced when complexed to biomimetic microcarriers. *J Neurochem, 119*(5), 972-988. https://doi.org/10.1111/j.1471-4159.2011.07272.x

Gardai, S. J., Bratton, D. L., Ogden, C. A., & Henson, P. M. (2006, May). Recognition ligands on apoptotic cells: a perspective. *J Leukoc Biol, 79*(5), 896-903. https://doi.org/10.1189/jlb.1005550

Gardai, S. J., McPhillips, K. A., Frasch, S. C., Janssen, W. J., Starefeldt, A., Murphy-Ullrich, J. E., Bratton, D. L., Oldenborg, P. A., Michalak, M., & Henson, P. M. (2005, Oct 21). Cell-surface calreticulin initiates clearance of viable or apoptotic cells through trans-activation of LRP on the phagocyte. *Cell, 123*(2), 321-334. https://doi.org/10.1016/j.cell.2005.08.032

Gatica, D., Lahiri, V., & Klionsky, D. J. (2018, Mar). Cargo recognition and degradation by selective autophagy. *Nat Cell Biol, 20*(3), 233-242. https://doi.org/10.1038/s41556-018-0037-z

Gerace, E., Cialdai, F., Sereni, E., Lana, D., Nosi, D., Giovannini, M. G., Monici, M., & Mannaioni, G. (2021, Oct). NIR Laser Photobiomodulation Induces Neuroprotection in an In Vitro Model of Cerebral Hypoxia/Ischemia. *Mol Neurobiol, 58*(10), 5383-5395. https://doi.org/10.1007/s12035-021-02496-6

Ginhoux, F., Greter, M., Leboeuf, M., Nandi, S., See, P., Gokhan, S., Mehler, M. F., Conway, S. J., Ng, L. G., Stanley, E. R., Samokhvalov, I. M., & Merad, M. (2010, Nov 5). Fate mapping analysis reveals that

adult microglia derive from primitive macrophages. *Science, 330*(6005), 841-845. https://doi.org/10.1126/science.1194637

Ginhoux, F., & Guilliams, M. (2016, Mar 15). Tissue-Resident Macrophage Ontogeny and Homeostasis. *Immunity, 44*(3), 439-449. https://doi.org/10.1016/j.immuni.2016.02.024

Ginhoux, F., Lim, S., Hoeffel, G., Low, D., & Huber, T. (2013). Origin and differentiation of microglia. *Front Cell Neurosci, 7*, 45. https://doi.org/10.3389/fncel.2013.00045

Giulian, D., & Baker, T. J. (1986, Aug). Characterization of ameboid microglia isolated from developing mammalian brain. *J Neurosci, 6*(8), 2163-2178. https://doi.org/10.1523/jneurosci.06-08-02163.1986

Global, regional, and national burden of stroke, 1990-2016: a systematic analysis for the Global Burden of Disease Study 2016. (2019, May). *Lancet Neurol, 18*(5), 439-458. https://doi.org/10.1016/s1474-4422(19)30034-1

Goldmann, T., Wieghofer, P., Jordão, M. J., Prutek, F., Hagemeyer, N., Frenzel, K., Amann, L., Staszewski, O., Kierdorf, K., Krueger, M., Locatelli, G., Hochgerner, H., Zeiser, R., Epelman, S., Geissmann, F., Priller, J., Rossi, F. M., Bechmann, I., Kerschensteiner, M., Linnarsson, S., Jung, S., & Prinz, M. (2016, Jul). Origin, fate and dynamics of macrophages at central nervous system interfaces. *Nat Immunol, 17*(7), 797-805. https://doi.org/10.1038/ni.3423

Gomez Perdiguero, E., Klapproth, K., Schulz, C., Busch, K., Azzoni, E., Crozet, L., Garner, H., Trouillet, C., de Bruijn, M. F., Geissmann, F., & Rodewald, H. R. (2015, Feb 26). Tissue-resident macrophages originate from yolk-sac-derived erythro-myeloid progenitors. *Nature, 518*(7540), 547-551. https://doi.org/10.1038/nature13989

Gomez-Nicola, D., & Perry, V. H. (2015, Apr). Microglial dynamics and role in the healthy and diseased brain: a paradigm of functional plasticity. *Neuroscientist, 21*(2), 169-184. https://doi.org/10.1177/1073858414530512

Gonçalves, J. T., Schafer, S. T., & Gage, F. H. (2016, Nov 3). Adult Neurogenesis in the Hippocampus: From Stem Cells to Behavior. *Cell, 167*(4), 897-914. https://doi.org/10.1016/j.cell.2016.10.021

Gordon, S., & Plüddemann, A. (2018). Macrophage Clearance of Apoptotic Cells: A Critical Assessment. *Front Immunol, 9*, 127. https://doi.org/10.3389/fimmu.2018.00127

Grathwohl, S. A., Kälin, R. E., Bolmont, T., Prokop, S., Winkelmann, G., Kaeser, S. A., Odenthal, J., Radde, R., Eldh, T., Gandy, S., Aguzzi, A., Staufenbiel, M., Mathews, P. M., Wolburg, H., Heppner, F. L., & Jucker, M. (2009, Nov). Formation and maintenance of Alzheimer's disease beta-amyloid plaques in the absence of microglia. *Nat Neurosci, 12*(11), 1361-1363. https://doi.org/10.1038/nn.2432

Green, D. R., Oguin, T. H., & Martinez, J. (2016, Jun). The clearance of dying cells: table for two. *Cell Death Differ, 23*(6), 915-926. https://doi.org/10.1038/cdd.2015.172

Griffiths, M. R., Gasque, P., & Neal, J. W. (2009, Mar). The multiple roles of the innate immune system in the regulation of apoptosis and inflammation in the brain. *J Neuropathol Exp Neurol, 68*(3), 217-226. https://doi.org/10.1097/NEN.0b013e3181996688

Gubas, A., & Dikic, I. (2022, Jan). A guide to the regulation of selective autophagy receptors. *Febs j, 289*(1), 75-89. https://doi.org/10.1111/febs.15824

Gude, D. R., Alvarez, S. E., Paugh, S. W., Mitra, P., Yu, J., Griffiths, R., Barbour, S. E., Milstien, S., & Spiegel, S. (2008, Aug). Apoptosis induces expression of sphingosine kinase 1 to release sphingosine-1-phosphate as a "come-and-get-me" signal. *Faseb j, 22*(8), 2629-2638. https://doi.org/10.1096/fj.08-107169

Guerrero, B. L., & Sicotte, N. L. (2020, 2020-March-20). Microglia in Multiple Sclerosis: Friend or Foe? [Review]. *Frontiers in Immunology, 11*. https://doi.org/10.3389/fimmu.2020.00374

Guo, H., Callaway, J. B., & Ting, J. P. (2015, Jul). Inflammasomes: mechanism of action, role in disease, and therapeutics. *Nat Med, 21*(7), 677-687. https://doi.org/10.1038/nm.3893

Guo, K., Luo, J., Feng, D., Wu, L., Wang, X., Xia, L., Tao, K., Wu, X., Cui, W., He, Y., Wang, B., Zhao, Z., & Zhang, Z. (2021). Single-Cell RNA Sequencing With Combined Use of Bulk RNA Sequencing to Reveal Cell Heterogeneity and Molecular Changes at Acute Stage of Ischemic Stroke in Mouse Cortex Penumbra Area. *Front Cell Dev Biol, 9*, 624711. https://doi.org/10.3389/fcell.2021.624711

Guo, K., Luo, J., Feng, D., Wu, L., Wang, X., Xia, L., Tao, K., Wu, X., Cui, W., He, Y., Wang, B., Zhao, Z., & Zhang, Z. (2021, 2021-February-22). Single-Cell RNA Sequencing With Combined Use of Bulk RNA Sequencing to Reveal Cell Heterogeneity and Molecular Changes at Acute Stage of Ischemic Stroke in Mouse Cortex Penumbra Area [Original Research]. *Frontiers in Cell and Developmental Biology, 9*. https://doi.org/10.3389/fcell.2021.624711

Guo, S., Wang, H., & Yin, Y. (2022). Microglia Polarization From M1 to M2 in Neurodegenerative Diseases. *Front Aging Neurosci, 14*, 815347. https://doi.org/10.3389/fnagi.2022.815347

H

Ha, A. C. T., Bhatt, D. L., Rutka, J. T., Johnston, S. C., Mazer, C. D., & Verma, S. (2021, Sep 28). Intracranial Hemorrhage During Dual Antiplatelet Therapy: JACC Review Topic of the Week. *J Am Coll Cardiol, 78*(13), 1372-1384. https://doi.org/10.1016/j.jacc.2021.07.048

Hadley, G., Beard, D. J., Couch, Y., Neuhaus, A. A., Adriaanse, B. A., DeLuca, G. C., Sutherland, B. A., & Buchan, A. M. (2019, Jan). Rapamycin in ischemic stroke: Old drug, new tricks? *J Cereb Blood Flow Metab, 39*(1), 20-35. https://doi.org/10.1177/0271678X18807309

Hall, C. N., Reynell, C., Gesslein, B., Hamilton, N. B., Mishra, A., Sutherland, B. A., O'Farrell, F. M., Buchan, A. M., Lauritzen, M., & Attwell, D. (2014, Apr 3). Capillary pericytes regulate cerebral blood flow in health and disease. *Nature, 508*(7494), 55-60. https://doi.org/10.1038/nature13165

Hamley, I. W. (2012, Oct 10). The amyloid beta peptide: a chemist's perspective. Role in Alzheimer's and fibrillization. *Chem Rev, 112*(10), 5147-5192. https://doi.org/10.1021/cr3000994

Hammond, T. R., Dufort, C., Dissing-Olesen, L., Giera, S., Young, A., Wysoker, A., Walker, A. J., Gergits, F., Segel, M., Nemesh, J., Marsh, S. E., Saunders, A., Macosko, E., Ginhoux, F., Chen, J., Franklin, R. J. M., Piao, X., McCarroll, S. A., & Stevens, B. (2019, Jan 15). Single-Cell RNA Sequencing of Microglia throughout the Mouse Lifespan and in the Injured Brain Reveals Complex Cell-State Changes. *Immunity, 50*(1), 253-271.e256. https://doi.org/10.1016/j.immuni.2018.11.004

Hanayama, R., Tanaka, M., Miwa, K., Shinohara, A., Iwamatsu, A., & Nagata, S. (2002, May 9). Identification of a factor that links apoptotic cells to phagocytes. *Nature, 417*(6885), 182-187. https://doi.org/10.1038/417182a

Hara, T., Nakamura, K., Matsui, M., Yamamoto, A., Nakahara, Y., Suzuki-Migishima, R., Yokoyama, M., Mishima, K., Saito, I., Okano, H., & Mizushima, N. (2006, Jun 15). Suppression of basal autophagy in neural cells causes neurodegenerative disease in mice. *Nature, 441*(7095), 885-889. https://doi.org/10.1038/nature04724

Harrison, R. E., Bucci, C., Vieira, O. V., Schroer, T. A., & Grinstein, S. (2003, Sep). Phagosomes fuse with late endosomes and/or lysosomes by extension of membrane protrusions along microtubules: role of Rab7 and RILP. *Mol Cell Biol, 23*(18), 6494-6506. https://doi.org/10.1128/mcb.23.18.6494-6506.2003

Hashimoto, D., Chow, A., Noizat, C., Teo, P., Beasley, M. B., Leboeuf, M., Becker, C. D., See, P., Price, J., Lucas, D., Greter, M., Mortha, A., Boyer, S. W., Forsberg, E. C., Tanaka, M., van Rooijen, N., García-Sastre, A., Stanley, E. R., Ginhoux, F., Frenette, P. S., & Merad, M. (2013, Apr 18). Tissue-resident macrophages self-maintain locally throughout adult life with minimal contribution from circulating monocytes. *Immunity, 38*(4), 792-804. https://doi.org/10.1016/j.immuni.2013.04.004

Hasilik, A. (1992, Feb 15). The early and late processing of lysosomal enzymes: proteolysis and compartmentation. *Experientia, 48*(2), 130-151. https://doi.org/10.1007/bf01923507

Hasselmann, J., & Blurton-Jones, M. (2020, Apr). Human iPSC-derived microglia: A growing toolset to study the brain's innate immune cells. *Glia, 68*(4), 721-739. https://doi.org/10.1002/glia.23781

Haynes, S. E., Hollopeter, G., Yang, G., Kurpius, D., Dailey, M. E., Gan, W. B., & Julius, D. (2006, Dec). The P2Y12 receptor regulates microglial activation by extracellular nucleotides. *Nat Neurosci, 9*(12), 1512-1519. https://doi.org/10.1038/nn1805

He, T., Li, W., Song, Y., Li, Z., Tang, Y., Zhang, Z., & Yang, G. Y. (2020, Nov 5). Sestrin2 regulates microglia polarization through mTOR-mediated autophagic flux to attenuate inflammation during experimental brain ischemia. *J Neuroinflammation, 17*(1), 329. https://doi.org/10.1186/s12974-020-01987-y

He, Y., Yao, X., Taylor, N., Bai, Y., Lovenberg, T., & Bhattacharya, A. (2018, May 22). RNA sequencing analysis reveals quiescent microglia isolation methods from postnatal mouse brains and

limitations of BV2 cells. *J Neuroinflammation, 15*(1), 153. https://doi.org/10.1186/s12974-018-1195-4

Healy, L. M., Perron, G., Won, S. Y., Rao, V. T. S., Guiot, M. C., Moore, C., Bar-Or, A., & Antel, J. P. (2018, Apr). Differential transcriptional response profiles in human myeloid cell populations. *Clin Immunol, 189*, 63-74. https://doi.org/10.1016/j.clim.2016.04.006

Heckmann, B. L., Teubner, B. J. W., Tummers, B., Boada-Romero, E., Harris, L., Yang, M., Guy, C. S., Zakharenko, S. S., & Green, D. R. (2019, Jul 25). LC3-Associated Endocytosis Facilitates β-Amyloid Clearance and Mitigates Neurodegeneration in Murine Alzheimer's Disease. *Cell, 178*(3), 536-551.e514. https://doi.org/10.1016/j.cell.2019.05.056

Heldmann, U., Mine, Y., Kokaia, Z., Ekdahl, C. T., & Lindvall, O. (2011, Jun). Selective depletion of Mac-1-expressing microglia in rat subventricular zone does not alter neurogenic response early after stroke. *Exp Neurol, 229*(2), 391-398. https://doi.org/10.1016/j.expneurol.2011.03.005

Hellwig, S., Masuch, A., Nestel, S., Katzmarski, N., Meyer-Luehmann, M., & Biber, K. (2015, Sep 29). Forebrain microglia from wild-type but not adult 5xFAD mice prevent amyloid-β plaque formation in organotypic hippocampal slice cultures. *Sci Rep, 5*, 14624. https://doi.org/10.1038/srep14624

Heneka, M. T., Kummer, M. P., Stutz, A., Delekate, A., Schwartz, S., Vieira-Saecker, A., Griep, A., Axt, D., Remus, A., Tzeng, T. C., Gelpi, E., Halle, A., Korte, M., Latz, E., & Golenbock, D. T. (2013, Jan 31). NLRP3 is activated in Alzheimer's disease and contributes to pathology in APP/PS1 mice. *Nature, 493*(7434), 674-678. https://doi.org/10.1038/nature11729

Henson, P. M., & Hume, D. A. (2006, May). Apoptotic cell removal in development and tissue homeostasis. *Trends Immunol, 27*(5), 244-250. https://doi.org/10.1016/j.it.2006.03.005

Hickman, S., Izzy, S., Sen, P., Morsett, L., & El Khoury, J. (2018, Oct). Microglia in neurodegeneration. *Nat Neurosci, 21*(10), 1359-1369. https://doi.org/10.1038/s41593-018-0242-x

Hickman, S. E., Kingery, N. D., Ohsumi, T. K., Borowsky, M. L., Wang, L. C., Means, T. K., & El Khoury, J. (2013, Dec). The microglial sensome revealed by direct RNA sequencing. *Nat Neurosci, 16*(12), 1896-1905. https://doi.org/10.1038/nn.3554

Higo, N. (2021). Non-human Primate Models to Explore the Adaptive Mechanisms After Stroke. *Front Syst Neurosci, 15*, 760311. https://doi.org/10.3389/fnsys.2021.760311

Hijioka, M., Futokoro, R., Ohto-Nakanishi, T., Nakanishi, H., Katsuki, H., & Kitamura, Y. (2020, Aug). Microglia-released leukotriene B(4) promotes neutrophil infiltration and microglial activation following intracerebral hemorrhage. *Int Immunopharmacol, 85*, 106678. https://doi.org/10.1016/j.intimp.2020.106678

Hilverling, A., Szegö, E. M., Dinter, E., Cozma, D., Saridaki, T., & Falkenburger, B. H. (2022, Jan). Maturing Autophagosomes are Transported Towards the Cell Periphery. *Cell Mol Neurobiol, 42*(1), 155-171. https://doi.org/10.1007/s10571-021-01116-0

Hipolito, V. E. B., Ospina-Escobar, E., & Botelho, R. J. (2018, Apr). Lysosome remodelling and adaptation during phagocyte activation. *Cell Microbiol, 20*(4). https://doi.org/10.1111/cmi.12824

Hirota, Y., Masuyama, N., Kuronita, T., Fujita, H., Himeno, M., & Tanaka, Y. (2004, Feb 6). Analysis of post-lysosomal compartments. *Biochem Biophys Res Commun, 314*(2), 306-312. https://doi.org/10.1016/j.bbrc.2003.12.092

Hoeffel, G., & Ginhoux, F. (2018, Aug). Fetal monocytes and the origins of tissue-resident macrophages. *Cell Immunol, 330*, 5-15. https://doi.org/10.1016/j.cellimm.2018.01.001

Holland, L. K. K., Nielsen, I., Maeda, K., & Jäättelä, M. (2020, Apr 30). SnapShot: Lysosomal Functions. *Cell, 181*(3), 748-748.e741. https://doi.org/10.1016/j.cell.2020.03.043

Holmes, G. L. (2015, Jun). Cognitive impairment in epilepsy: the role of network abnormalities. *Epileptic Disord, 17*(2), 101-116. https://doi.org/10.1684/epd.2015.0739

Hong, S., Dissing-Olesen, L., & Stevens, B. (2016, Feb). New insights on the role of microglia in synaptic pruning in health and disease. *Curr Opin Neurobiol, 36*, 128-134. https://doi.org/10.1016/j.conb.2015.12.004

Hornik, T. C., Neniskyte, U., & Brown, G. C. (2014). Inflammation induces multinucleation of Microglia via PKC inhibition of cytokinesis, generating highly phagocytic multinucleated giant cells. *Journal of Neurochemistry, 128*(5), 650-661. https://doi.org/10.1111/jnc.12477

Hoshiko, M., Arnoux, I., Avignone, E., Yamamoto, N., & Audinat, E. (2012, Oct 24). Deficiency of the microglial receptor CX3CR1 impairs postnatal functional development of thalamocortical synapses in the barrel cortex. *J Neurosci, 32*(43), 15106-15111. https://doi.org/10.1523/jneurosci.1167-12.2012

Hosmane, S., Tegenge, M. A., Rajbhandari, L., Uapinyoying, P., Ganesh Kumar, N., Thakor, N., & Venkatesan, A. (2012, May 30). Toll/interleukin-1 receptor domain-containing adapter inducing interferon-β mediates microglial phagocytosis of degenerating axons. *J Neurosci, 32*(22), 7745-7757. https://doi.org/10.1523/jneurosci.0203-12.2012

Hou, L., Qu, X., Qiu, X., Huang, R., Zhao, X., & Wang, Q. (2020, May 6). Integrin CD11b mediates locus coeruleus noradrenergic neurodegeneration in a mouse Parkinson's disease model. *J Neuroinflammation, 17*(1), 148. https://doi.org/10.1186/s12974-020-01823-3

Houtman, J., Freitag, K., Gimber, N., Schmoranzer, J., Heppner, F. L., & Jendrach, M. (2019, Feb 15). Beclin1-driven autophagy modulates the inflammatory response of microglia via NLRP3. *Embo j, 38*(4). https://doi.org/10.15252/embj.201899430

Hsieh, C. L., Koike, M., Spusta, S. C., Niemi, E. C., Yenari, M., Nakamura, M. C., & Seaman, W. E. (2009, May). A role for TREM2 ligands in the phagocytosis of apoptotic neuronal cells by microglia. *J Neurochem, 109*(4), 1144-1156. https://doi.org/10.1111/j.1471-4159.2009.06042.x

Hu, H., Chen, G., Zhang, J. M., Zhang, W. P., Zhang, L., Ge, Q. F., Yao, H. T., Ding, W., Chen, Z., & Wei, E. Q. (2005, Jun). Distribution of cysteinyl leukotriene receptor 2 in human traumatic brain injury and brain tumors. *Acta Pharmacol Sin, 26*(6), 685-690. https://doi.org/10.1111/j.1745-7254.2005.00092.x

Hu, X., Li, P., Guo, Y., Wang, H., Leak, R. K., Chen, S., Gao, Y., & Chen, J. (2012, Nov). Microglia/macrophage polarization dynamics reveal novel mechanism of injury expansion after focal cerebral ischemia. *Stroke, 43*(11), 3063-3070. https://doi.org/10.1161/strokeaha.112.659656

Hua, J. Y., & Smith, S. J. (2004, Apr). Neural activity and the dynamics of central nervous system development. *Nat Neurosci, 7*(4), 327-332. https://doi.org/10.1038/nn1218

Huang, T., Lin, Y., Pang, Q., Shen, W., Chen, X., & Tu, F. (2021). The Synergistic Effect of TRPV1 on Oxidative Stress-Induced Autophagy and Apoptosis in Microglia. *Anal Cell Pathol (Amst), 2021*, 7955791. https://doi.org/10.1155/2021/7955791

Huang, Y., Happonen, K. E., Burrola, P. G., O'Connor, C., Hah, N., Huang, L., Nimmerjahn, A., & Lemke, G. (2021, May). Microglia use TAM receptors to detect and engulf amyloid β plaques. *Nat Immunol, 22*(5), 586-594. https://doi.org/10.1038/s41590-021-00913-5

Hughes, C. E., & Nibbs, R. J. B. (2018, Aug). A guide to chemokines and their receptors. *Febs j, 285*(16), 2944-2971. https://doi.org/10.1111/febs.14466

Hughes, P. M., Botham, M. S., Frentzel, S., Mir, A., & Perry, V. H. (2002, Mar 15). Expression of fractalkine (CX3CL1) and its receptor, CX3CR1, during acute and chronic inflammation in the rodent CNS. *Glia, 37*(4), 314-327.

Humphries, W. H. t., & Payne, C. K. (2012, May 15). Imaging lysosomal enzyme activity in live cells using self-quenched substrates. *Anal Biochem, 424*(2), 178-183. https://doi.org/10.1016/j.ab.2012.02.033

Humphries, W. H. t., Szymanski, C. J., & Payne, C. K. (2011). Endo-lysosomal vesicles positive for Rab7 and LAMP1 are terminal vesicles for the transport of dextran. *PLoS One, 6*(10), e26626. https://doi.org/10.1371/journal.pone.0026626

Hurbain, I., Romao, M., Bergam, P., Heiligenstein, X., & Raposo, G. (2017). Analyzing Lysosome-Related Organelles by Electron Microscopy. *Methods Mol Biol, 1594*, 43-71. https://doi.org/10.1007/978-1-4939-6934-0_4

Hwang, D. Y., Eom, J. I., Jang, J. E., Jeung, H. K., Chung, H., Kim, J. S., Cheong, J. W., & Min, Y. H. (2020, May 11). ULK1 inhibition as a targeted therapeutic strategy for FLT3-ITD-mutated acute myeloid leukemia. *J Exp Clin Cancer Res, 39*(1), 85. https://doi.org/10.1186/s13046-020-01580-4

Hyttinen, J. M., Niittykoski, M., Salminen, A., & Kaarniranta, K. (2013, Mar). Maturation of autophagosomes and endosomes: a key role for Rab7. *Biochim Biophys Acta, 1833*(3), 503-510. https://doi.org/10.1016/j.bbamcr.2012.11.018

I

Iadecola, C., & Anrather, J. (2011, Jul 7). The immunology of stroke: from mechanisms to translation. *Nat Med, 17*(7), 796-808. https://doi.org/10.1038/nm.2399

Igney, F. H., & Krammer, P. H. (2002, Apr). Death and anti-death: tumour resistance to apoptosis. *Nat Rev Cancer, 2*(4), 277-288. https://doi.org/10.1038/nrc776

Iori, V., Iyer, A. M., Ravizza, T., Beltrame, L., Paracchini, L., Marchini, S., Cerovic, M., Hill, C., Ferrari, M., Zucchetti, M., Molteni, M., Rossetti, C., Brambilla, R., Steve White, H., D'Incalci, M., Aronica, E., & Vezzani, A. (2017). Blockade of the IL-1R1/TLR4 pathway mediates disease-modification therapeutic effects in a model of acquired epilepsy. *Neurobiol Dis, 99*, 12-23. https://doi.org/10.1016/j.nbd.2016.12.007

Isailovic, N., Daigo, K., Mantovani, A., & Selmi, C. (2015, Jun). Interleukin-17 and innate immunity in infections and chronic inflammation. *J Autoimmun, 60*, 1-11. https://doi.org/10.1016/j.jaut.2015.04.006

Ito, D., Tanaka, K., Suzuki, S., Dembo, T., & Fukuuchi, Y. (2001, May). Enhanced expression of Iba1, ionized calcium-binding adapter molecule 1, after transient focal cerebral ischemia in rat brain. *Stroke, 32*(5), 1208-1215. https://doi.org/10.1161/01.str.32.5.1208

J

Jeong, H. K., Ji, K., Min, K., & Joe, E. H. (2013, Jun). Brain inflammation and microglia: facts and misconceptions. *Exp Neurobiol, 22*(2), 59-67. https://doi.org/10.5607/en.2013.22.2.59

Jeong, J. H., Yu, K. S., Bak, D. H., Lee, J. H., Lee, N. S., Jeong, Y. G., Kim, D. K., Kim, J. J., & Han, S. Y. (2016, Nov). Intermittent fasting is neuroprotective in focal cerebral ischemia by minimizing autophagic flux disturbance and inhibiting apoptosis. *Exp Ther Med, 12*(5), 3021-3028. https://doi.org/10.3892/etm.2016.3852

Ji, X., Trandafir, C. C., Wang, A., & Kurahashi, K. (2013, Nov). Effects of the experimental subarachnoid hemorrhage on the eicosanoid receptors in nicotine-induced contraction of the rat basilar artery. *J Stroke Cerebrovasc Dis, 22*(8), 1258-1262. https://doi.org/10.1016/j.jstrokecerebrovasdis.2012.07.007

Jiang, C. T., Wu, W. F., Deng, Y. H., & Ge, J. W. (2020, May). Modulators of microglia activation and polarization in ischemic stroke (Review). *Mol Med Rep, 21*(5), 2006-2018. https://doi.org/10.3892/mmr.2020.11003

Jin, M., Liu, X., & Klionsky, D. J. (2013, Jan 17). SnapShot: Selective autophagy. *Cell, 152*(1-2), 368-368.e362. https://doi.org/10.1016/j.cell.2013.01.004

Jin, T., Xu, X., & Hereld, D. (2008, Oct). Chemotaxis, chemokine receptors and human disease. *Cytokine, 44*(1), 1-8. https://doi.org/10.1016/j.cyto.2008.06.017

Joensuu, T., Kuronen, M., Alakurtti, K., Tegelberg, S., Hakala, P., Aalto, A., Huopaniemi, L., Aula, N., Michellucci, R., Eriksson, K., & Lehesjoki, A. E. (2007). Cystatin B: mutation detection, alternative splicing and expression in progressive myclonus epilepsy of Unverricht-Lundborg type (EPM1) patients. *Eur J Hum Genet, 15*(2), 185-193. https://doi.org/10.1038/sj.ejhg.5201723

Joensuu, T., Lehesjoki, A. E., & Kopra, O. (2008). Molecular background of EPM1-Unverricht-Lundborg disease. *Epilepsia, 49*(4), 557-563. https://doi.org/10.1111/j.1528-1167.2007.01422.x

Joensuu, T., Tegelberg, S., Reinmaa, E., Segerstrale, M., Hakala, P., Pehkonen, H., Korpi, E. R., Tyynela, J., Taira, T., Hovatta, I., Kopra, O., & Lehesjoki, A. E. (2014). Gene expression alterations in the cerebellum and granule neurons of Cstb(-/-) mouse are associated with early synaptic changes and inflammation. *PLoS One, 9*(2), e89321. https://doi.org/10.1371/journal.pone.0089321

Johansen, T., & Lamark, T. (2020, Jan 3). Selective Autophagy: ATG8 Family Proteins, LIR Motifs and Cargo Receptors. *J Mol Biol, 432*(1), 80-103. https://doi.org/10.1016/j.jmb.2019.07.016

Jones, E. G. (1999, Aug). Colgi, Cajal and the Neuron Doctrine. *J Hist Neurosci, 8*(2), 170-178. https://doi.org/10.1076/jhin.8.2.170.1838

Jongsma, M. L., Berlin, I., Wijdeven, R. H., Janssen, L., Janssen, G. M., Garstka, M. A., Janssen, H., Mensink, M., van Veelen, P. A., Spaapen, R. M., & Neefjes, J. (2016, Jun 30). An ER-Associated Pathway Defines Endosomal Architecture for Controlled Cargo Transport. *Cell, 166*(1), 152-166. https://doi.org/10.1016/j.cell.2016.05.078

Joshi, P., Riffel, F., Kumar, S., Villacampa, N., Theil, S., Parhizkar, S., Haass, C., Colonna, M., Heneka, M. T., Arzberger, T., Herms, J., & Walter, J. (2021, Oct 18). TREM2 modulates differential deposition of modified and non-modified Aβ species in extracellular plaques and intraneuronal deposits. *Acta Neuropathol Commun, 9*(1), 168. https://doi.org/10.1186/s40478-021-01263-x

Jung, M., Choi, H., & Mun, J. Y. (2019, 2019/11/06). The autophagy research in electron microscopy. *Applied Microscopy, 49*(1), 11. https://doi.org/10.1186/s42649-019-0012-6

Jung, S., Aliberti, J., Graemmel, P., Sunshine, M. J., Kreutzberg, G. W., Sher, A., & Littman, D. R. (2000, Jun). Analysis of fractalkine receptor CX(3)CR1 function by targeted deletion and green fluorescent protein reporter gene insertion. *Mol Cell Biol, 20*(11), 4106-4114. https://doi.org/10.1128/MCB.20.11.4106-4114.2000

K

Kabeya, Y., Mizushima, N., Ueno, T., Yamamoto, A., Kirisako, T., Noda, T., Kominami, E., Ohsumi, Y., & Yoshimori, T. (2000, Nov 1). LC3, a mammalian homologue of yeast Apg8p, is localized in autophagosome membranes after processing. *Embo j, 19*(21), 5720-5728. https://doi.org/10.1093/emboj/19.21.5720

Kandratavicius, L., Balista, P. A., Lopes-Aguiar, C., Ruggiero, R. N., Umeoka, E. H., Garcia-Cairasco, N., Bueno-Junior, L. S., & Leite, J. P. (2014). Animal models of epilepsy: use and limitations. *Neuropsychiatr Dis Treat, 10*, 1693-1705. https://doi.org/10.2147/ndt.S50371

Karim, M. R., Kanazawa, T., Daigaku, Y., Fujimura, S., Miotto, G., & Kadowaki, M. (2007, Nov-Dec). Cytosolic LC3 ratio as a sensitive index of macroautophagy in isolated rat hepatocytes and H4-II-E cells. *Autophagy, 3*(6), 553-560. https://doi.org/10.4161/auto.4615

Kaur, G., Mohan, P., Pawlik, M., DeRosa, S., Fajiculay, J., Che, S., Grubb, A., Ginsberg, S. D., Nixon, R. A., & Levy, E. (2010). Cystatin C Rescues Degenerating Neurons in a Cystatin B-Knockout Mouse Model of Progressive Myoclonus Epilepsy. *The American Journal of Pathology, 177*(5), 2256-2267. https://doi.org/https://doi.org/10.2353/ajpath.2010.100461

Kaur, J., & Debnath, J. (2015, Aug). Autophagy at the crossroads of catabolism and anabolism. *Nat Rev Mol Cell Biol, 16*(8), 461-472. https://doi.org/10.1038/nrm4024

Kaushik, S., & Cuervo, A. M. (2018, Jun). The coming of age of chaperone-mediated autophagy. *Nat Rev Mol Cell Biol, 19*(6), 365-381. https://doi.org/10.1038/s41580-018-0001-6

Kempermann, G., Jessberger, S., Steiner, B., & Kronenberg, G. (2004, Aug). Milestones of neuronal development in the adult hippocampus. *Trends Neurosci, 27*(8), 447-452. https://doi.org/10.1016/j.tins.2004.05.013

Kettenmann, H. (2007, Apr 26). Neuroscience: the brain's garbage men. *Nature, 446*(7139), 987-989. https://doi.org/10.1038/nature05713

Kettenmann, H., Hanisch, U. K., Noda, M., & Verkhratsky, A. (2011, Apr). Physiology of microglia. *Physiol Rev, 91*(2), 461-553. https://doi.org/10.1152/physrev.00011.2010

Khaminets, A., Behl, C., & Dikic, I. (2016, Jan). Ubiquitin-Dependent And Independent Signals In Selective Autophagy. *Trends Cell Biol, 26*(1), 6-16. https://doi.org/10.1016/j.tcb.2015.08.010

Kim, H. J., Cho, M. H., Shim, W. H., Kim, J. K., Jeon, E. Y., Kim, D. H., & Yoon, S. Y. (2017, Nov). Deficient autophagy in microglia impairs synaptic pruning and causes social behavioral defects. *Mol Psychiatry, 22*(11), 1576-1584. https://doi.org/10.1038/mp.2016.103

Kim, J. S., Lee, J. Y., Yang, J. W., Lee, K. H., Effenberger, M., Szpirt, W., Kronbichler, A., & Shin, J. I. (2021). Immunopathogenesis and treatment of cytokine storm in COVID-19. *Theranostics, 11*(1), 316-329. https://doi.org/10.7150/thno.49713

Kim, J. Y., Kawabori, M., & Yenari, M. A. (2014). Innate inflammatory responses in stroke: mechanisms and potential therapeutic targets. *Curr Med Chem, 21*(18), 2076-2097. https://doi.org/10.2174/09298673216661312282051 46

Kimura, S., Noda, T., & Yoshimori, T. (2007, Sep-Oct). Dissection of the autophagosome maturation process by a novel reporter protein, tandem fluorescent-tagged LC3. *Autophagy, 3*(5), 452-460. https://doi.org/10.4161/auto.4451

Kinchen, J. M., Doukoumetzidis, K., Almendinger, J., Stergiou, L., Tosello-Trampont, A., Sifri, C. D., Hengartner, M. O., & Ravichandran, K. S. (2008, May). A pathway for phagosome maturation during engulfment of apoptotic cells. *Nat Cell Biol, 10*(5), 556-566. https://doi.org/10.1038/ncb1718

Kinchen, J. M., & Ravichandran, K. S. (2008, Oct). Phagosome maturation: going through the acid test. *Nat Rev Mol Cell Biol, 9*(10), 781-795. https://doi.org/10.1038/nrm2515

Kleinschnitz, C., Braeuninger, S., Pham, M., Austinat, M., Nölte, I., Renné, T., Nieswandt, B., Bendszus, M., & Stoll, G. (2008, Apr). Blocking of platelets or intrinsic coagulation pathway-driven thrombosis does not prevent cerebral infarctions induced by photothrombosis. *Stroke, 39*(4), 1262-1268. https://doi.org/10.1161/strokeaha.107.496448

Klionsky, D. J., …& Tong, C. K. (2021, Jan). Guidelines for the use and interpretation of assays for monitoring autophagy (4th edition)(1). *Autophagy, 17*(1), 1-382. https://doi.org/10.1080/15548627.2020.1797280

Knight-Greenfield, A., Nario, J. J. Q., & Gupta, A. (2019, Nov). Causes of Acute Stroke: A Patterned Approach. *Radiol Clin North Am, 57*(6), 1093-1108. https://doi.org/10.1016/j.rcl.2019.07.007

Kochan, T., Singla, A., Tosi, J., & Kumar, A. (2012, Jun). Toll-like receptor 2 ligand pretreatment attenuates retinal microglial inflammatory response but enhances phagocytic activity toward Staphylococcus aureus. *Infect Immun, 80*(6), 2076-2088. https://doi.org/10.1128/iai.00149-12

Koizumi, J.-i., Yoshida, Y., Nakazawa, T., & Ooneda, G. (1986). Experimental studies of ischemic brain edema

1. A new experimental model of cerebral embolism in rats in which recirculation can be introduced in the ischemic area. *Nosotchu, 8*(1), 1-8. https://doi.org/10.3995/jstroke.8.1

Koizumi, S., Ohsawa, K., Inoue, K., & Kohsaka, S. (2013). Purinergic receptors in microglia: functional modal shifts of microglia mediated by P2 and P1 receptors. *Glia, 61*(1), 47-54. https://doi.org/10.1002/glia.22358

Komatsu, M., Waguri, S., Chiba, T., Murata, S., Iwata, J., Tanida, I., Ueno, T., Koike, M., Uchiyama, Y., Kominami, E., & Tanaka, K. (2006, Jun 15). Loss of autophagy in the central nervous system causes neurodegeneration in mice. *Nature, 441*(7095), 880-884. https://doi.org/10.1038/nature04723

Korber, I., Katayama, S., Einarsdottir, E., Krjutskov, K., Hakala, P., Kere, J., Lehesjoki, A. E., & Joensuu, T. (2016). Gene-Expression Profiling Suggests Impaired Signaling via the Interferon Pathway in Cstb-/- Microglia. *PLoS One, 11*(6), e0158195. https://doi.org/10.1371/journal.pone.0158195

Koskenkorva, P., Khyuppenen, J., Niskanen, E., Könönen, M., Bendel, P., Mervaala, E., Lehesjoki, A. E., Kälviäinen, R., & Vanninen, R. (2009). Motor cortex and thalamic atrophy in Unverricht–Lundborg disease. *Voxel-based morphometric study, 73*(8), 606-611. https://doi.org/10.1212/WNL.0b013e3181b3888b

Koskenkorva, P., Niskanen, E., Hyppönen, J., Könönen, M., Mervaala, E., Soininen, H., Kälviäinen, R., & Vanninen, R. (2012). Sensorimotor, Visual, and Auditory Cortical Atrophy in Unverricht-Lundborg Disease Mapped with Cortical Thickness Analysis. *American Journal of Neuroradiology, 33*(5), 878-883. https://doi.org/10.3174/ajnr.A2882

Kourtzelis, I., Hajishengallis, G., & Chavakis, T. (2020, 2020-March-31). Phagocytosis of Apoptotic Cells in Resolution of Inflammation [Mini Review]. *Frontiers in Immunology, 11*. https://doi.org/10.3389/fimmu.2020.00553

Kovács, A. L., László, L., Fellinger, E., Jakab, A., Orosz, A., Réz, G., & Kovács, J. (1989). Combined effects of fasting and vinblastine treatment on serum insulin level, the size of autophagic-lysosomal compartment, protein content and lysosomal enzyme activities of liver and exocrine pancreatic cells of the mouse. *Comp Biochem Physiol B, 94*(3), 505-510. https://doi.org/10.1016/0305-0491(89)90189-2

Krabbe, G., Halle, A., Matyash, V., Rinnenthal, J. L., Eom, G. D., Bernhardt, U., Miller, K. R., Prokop, S., Kettenmann, H., & Heppner, F. L. (2013). Functional impairment of microglia coincides with Beta-amyloid deposition in mice with Alzheimer-like pathology. *PLoS One, 8*(4), e60921. https://doi.org/10.1371/journal.pone.0060921

Krafft, P. R., Bailey, E. L., Lekic, T., Rolland, W. B., Altay, O., Tang, J., Wardlaw, J. M., Zhang, J. H., & Sudlow, C. L. (2012, Jul). Etiology of stroke and choice of models. *Int J Stroke, 7*(5), 398-406. https://doi.org/10.1111/j.1747-4949.2012.00838.x

Kubota, Y., Takubo, K., Shimizu, T., Ohno, H., Kishi, K., Shibuya, M., Saya, H., & Suda, T. (2009, May 11). M-CSF inhibition selectively targets pathological angiogenesis and lymphangiogenesis. *J Exp Med, 206*(5), 1089-1102. https://doi.org/10.1084/jem.20081605

Kuehl, F. A., Jr., & Egan, R. W. (1980, Nov 28). Prostaglandins, arachidonic acid, and inflammation. *Science, 210*(4473), 978-984. https://doi.org/10.1126/science.6254151

Kwon, M. J., Oh, E., Lee, S., Roh, M. R., Kim, S. E., Lee, Y., Choi, Y. L., In, Y. H., Park, T., Koh, S. S., & Shin, Y. K. (2009, Jul 7). Identification of novel reference genes using multiplatform expression data and their validation for quantitative gene expression analysis. *PLoS One, 4*(7), e6162. https://doi.org/10.1371/journal.pone.0006162

L

Lai, A. Y., & Todd, K. G. (2006, Jan). Microglia in cerebral ischemia: molecular actions and interactions. *Can J Physiol Pharmacol, 84*(1), 49-59. https://doi.org/10.1139/y05-143

Lalancette-Hébert, M., Gowing, G., Simard, A., Weng, Y. C., & Kriz, J. (2007, Mar 7). Selective ablation of proliferating microglial cells exacerbates ischemic injury in the brain. *J Neurosci, 27*(10), 2596-2605. https://doi.org/10.1523/jneurosci.5360-06.2007

Lalioti, M. D., Scott, H. S., Buresi, C., Rossier, C., Bottani, A., Morris, M. A., Malafosse, A., & Antonarakis, S. E. (1997). Dodecamer repeat expansion in cystatin B gene in progressive myoclonus epilepsy. *Nature, 386*(6627), 847-851. https://doi.org/10.1038/386847a0

Lambertsen, K. L., Clausen, B. H., Babcock, A. A., Gregersen, R., Fenger, C., Nielsen, H. H., Haugaard, L. S., Wirenfeldt, M., Nielsen, M., Dagnaes-Hansen, F., Bluethmann, H., Faergeman, N. J., Meldgaard, M., Deierborg, T., & Finsen, B. (2009, Feb 4). Microglia protect neurons against ischemia by synthesis of tumor necrosis factor. *J Neurosci, 29*(5), 1319-1330. https://doi.org/10.1523/jneurosci.5505-08.2009

Lampron, A., Larochelle, A., Laflamme, N., Préfontaine, P., Plante, M. M., Sánchez, M. G., Yong, V. W., Stys, P. K., Tremblay, M., & Rivest, S. (2015, Apr 6). Inefficient clearance of myelin debris by microglia impairs remyelinating processes. *J Exp Med, 212*(4), 481-495. https://doi.org/10.1084/jem.20141656

Lan, X., Han, X., Li, Q., Yang, Q. W., & Wang, J. (2017, Jul). Modulators of microglial activation and polarization after intracerebral haemorrhage. *Nat Rev Neurol, 13*(7), 420-433. https://doi.org/10.1038/nrneurol.2017.69

Lauber, K., Blumenthal, S. G., Waibel, M., & Wesselborg, S. (2004, May 7). Clearance of apoptotic cells: getting rid of the corpses. *Mol Cell, 14*(3), 277-287. https://doi.org/10.1016/s1097-2765(04)00237-0

Lauber, K., Bohn, E., Kröber, S. M., Xiao, Y. J., Blumenthal, S. G., Lindemann, R. K., Marini, P., Wiedig, C., Zobywalski, A., Baksh, S., Xu, Y., Autenrieth, I. B., Schulze-Osthoff, K., Belka, C., Stuhler, G., & Wesselborg, S. (2003, Jun 13). Apoptotic cells induce migration of phagocytes via caspase-3-mediated release of a lipid attraction signal. *Cell, 113*(6), 717-730. https://doi.org/10.1016/s0092-8674(03)00422-7

Lauro, C., & Limatola, C. (2020). Metabolic Reprograming of Microglia in the Regulation of the Innate Inflammatory Response. *Front Immunol, 11*, 493. https://doi.org/10.3389/fimmu.2020.00493

Lee, H. J., Woo, Y., Hahn, T. W., Jung, Y. M., & Jung, Y. J. (2020, Aug 25). Formation and Maturation of the Phagosome: A Key Mechanism in Innate Immunity against Intracellular Bacterial Infection. *Microorganisms, 8*(9). https://doi.org/10.3390/microorganisms8091298

Lee, J. M., Zipfel, G. J., & Choi, D. W. (1999, Jun 24). The changing landscape of ischaemic brain injury mechanisms. *Nature, 399*(6738 Suppl), A7-14. https://doi.org/10.1038/399a007

Lee, J. W., Nam, H., Kim, L. E., Jeon, Y., Min, H., Ha, S., Lee, Y., Kim, S. Y., Lee, S. J., Kim, E. K., & Yu, S. W. (2019, May). TLR4 (toll-like receptor 4) activation suppresses autophagy through inhibition of FOXO3 and impairs phagocytic capacity of microglia. *Autophagy, 15*(5), 753-770. https://doi.org/10.1080/15548627.2018.1556946

Legler, D. F., Bruckner, M., Uetz-von Allmen, E., & Krause, P. (2010, Feb). Prostaglandin E2 at new glance: novel insights in functional diversity offer therapeutic chances. *Int J Biochem Cell Biol, 42*(2), 198-201. https://doi.org/10.1016/j.biocel.2009.09.015

Lehesjoki, A. E., & Gardiner, M. (2012). Progressive myoclonus epilepsy: Unverricht-Lundborg disease and Neuronal ceroid lipofuscinoses. In th, J. L. Noebels, M. Avoli, M. A. Rogawski, R. W. Olsen, & A. V. Delgado-Escueta (Eds.), *Jasper's Basic Mechanisms of the Epilepsies*. http://www.ncbi.nlm.nih.gov/pubmed/22787658

Lehesjoki, A. E., & Kälviäinen, R. (1993). Progressive Myoclonic Epilepsy Type 1. In M. P. Adam, H. H. Ardinger, R. A. Pagon, S. E. Wallace, L. J. H. Bean, K. W. Gripp, G. M. Mirzaa, & A. Amemiya (Eds.), *GeneReviews(®)*. University of Washington, Seattle

Lehrman, E. K., Wilton, D. K., Litvina, E. Y., Welsh, C. A., Chang, S. T., Frouin, A., Walker, A. J., Heller, M. D., Umemori, H., Chen, C., & Stevens, B. (2018, Oct 10). CD47 Protects Synapses from Excess Microglia-Mediated Pruning during Development. *Neuron, 100*(1), 120-134 e126. https://doi.org/10.1016/j.neuron.2018.09.017

Lehtinen, M. K., Tegelberg, S., Schipper, H., Su, H., Zukor, H., Manninen, O., Kopra, O., Joensuu, T., Hakala, P., Bonni, A., & Lehesjoki, A. E. (2009, May 6). Cystatin B deficiency sensitizes neurons to oxidative stress in progressive myoclonus epilepsy, EPM1. *J Neurosci, 29*(18), 5910-5915. https://doi.org/10.1523/jneurosci.0682-09.2009

Lemke, G. (2013, Nov 1). Biology of the TAM receptors. *Cold Spring Harb Perspect Biol, 5*(11), a009076. https://doi.org/10.1101/cshperspect.a009076

Leranth, C., & Hajszan, T. (2007). Extrinsic afferent systems to the dentate gyrus. *Prog Brain Res, 163*, 63-84. https://doi.org/10.1016/S0079-6123(07)63004-0

Lévesque, M., & Avoli, M. (2013, Dec). The kainic acid model of temporal lobe epilepsy. *Neurosci Biobehav Rev, 37*(10 Pt 2), 2887-2899. https://doi.org/10.1016/j.neubiorev.2013.10.011

Lévesque, M., Avoli, M., & Bernard, C. (2016, Feb 15). Animal models of temporal lobe epilepsy following systemic chemoconvulsant administration. *J Neurosci Methods, 260*, 45-52. https://doi.org/10.1016/j.jneumeth.2015.03.009

Levin, R., Grinstein, S., & Canton, J. (2016, Sep). The life cycle of phagosomes: formation, maturation, and resolution. *Immunol Rev, 273*(1), 156-179. https://doi.org/10.1111/imr.12439

Levine, B., & Kroemer, G. (2019, Jan 10). Biological Functions of Autophagy Genes: A Disease Perspective. *Cell, 176*(1-2), 11-42. https://doi.org/10.1016/j.cell.2018.09.048

Li, J., Kim, S. G., & Blenis, J. (2014, Mar 4). Rapamycin: one drug, many effects. *Cell Metab, 19*(3), 373-379. https://doi.org/10.1016/j.cmet.2014.01.001

Li, L., & Huang, J. (2020a, Jul-Sep). Rapamycin Pretreatment Alleviates Cerebral Ischemia/Reperfusion Injury in Dose-Response Manner Through Inhibition of the Autophagy and NFkappaB Pathways in Rats. *Dose Response, 18*(3), 1559325820946194. https://doi.org/10.1177/1559325820946194

Li, L., & Huang, J. (2020b, Jul-Sep). Rapamycin Pretreatment Alleviates Cerebral Ischemia/Reperfusion Injury in Dose-Response Manner Through Inhibition of the Autophagy and NFκB Pathways in Rats. *Dose Response, 18*(3), 1559325820946194. https://doi.org/10.1177/1559325820946194

Li, T., Pang, S., Yu, Y., Wu, X., Guo, J., & Zhang, S. (2013, Dec). Proliferation of parenchymal microglia is the main source of microgliosis after ischaemic stroke. *Brain, 136*(Pt 12), 3578-3588. https://doi.org/10.1093/brain/awt287

Li, W. (2012, Apr). Eat-me signals: keys to molecular phagocyte biology and "appetite" control. *J Cell Physiol, 227*(4), 1291-1297. https://doi.org/10.1002/jcp.22815

Li, W. W., Li, J., & Bao, J. K. (2012, Apr). Microautophagy: lesser-known self-eating. *Cell Mol Life Sci, 69*(7), 1125-1136. https://doi.org/10.1007/s00018-011-0865-5

Li, X., He, S., & Ma, B. (2020, Jan 22). Autophagy and autophagy-related proteins in cancer. *Mol Cancer, 19*(1), 12. https://doi.org/10.1186/s12943-020-1138-4

Li, X., Xia, Q., Mao, M., Zhou, H., Zheng, L., Wang, Y., Zeng, Z., Yan, L., Zhao, Y., & Shi, J. (2021, Jan). Annexin-A1 SUMOylation regulates microglial polarization after cerebral ischemia by modulating IKKalpha stability via selective autophagy. *Sci Adv, 7*(4). https://doi.org/10.1126/sciadv.abc5539

Lieuallen, K., Pennacchio, L. A., Park, M., Myers, R. M., & Lennon, G. G. (2001). Cystatin B-deficient mice have increased expression of apoptosis and glial activation genes. *Hum Mol Genet, 10*(18), 1867-1871. https://doi.org/10.1093/hmg/10.18.1867

Lim, T. K., & Ruthazer, E. S. (2021, Mar 16). Microglial trogocytosis and the complement system regulate axonal pruning in vivo. *Elife, 10*. https://doi.org/10.7554/eLife.62167

Lima, J. G., de Freitas Vinhas, C., Gomes, I. N., Azevedo, C. M., dos Santos, R. R., Vannier-Santos, M. A., & Veras, P. S. (2011, Feb 25). Phagocytosis is inhibited by autophagic induction in murine macrophages. *Biochem Biophys Res Commun, 405*(4), 604-609. https://doi.org/10.1016/j.bbrc.2011.01.076

Lin, Y., Huang, T., Shen, W., Pang, Q., Xie, Q., Chen, X., & Tu, F. (2022, 2022/01/18). TRPV1 Suppressed NLRP3 Through Regulating Autophagy in Microglia After Ischemia-Reperfusion Injury. *Journal of Molecular Neuroscience*. https://doi.org/10.1007/s12031-021-01935-2

Lindner, B., Burkard, T., & Schuler, M. (2020, May). Phagocytosis assays with different pH-sensitive fluorescent particles and various readouts. *Biotechniques, 68*(5), 245-250. https://doi.org/10.2144/btn-2020-0003

Lindsay, M. P., Norrving, B., Sacco, R. L., Brainin, M., Hacke, W., Martins, S., Pandian, J., & Feigin, V. (2019, Oct). World Stroke Organization (WSO): Global Stroke Fact Sheet 2019. *Int J Stroke, 14*(8), 806-817. https://doi.org/10.1177/1747493019881353

Ling, M., & Murali, M. (2019, Dec). Analysis of the Complement System in the Clinical Immunology Laboratory. *Clin Lab Med, 39*(4), 579-590. https://doi.org/10.1016/j.cll.2019.07.006

Linnartz, B., Kopatz, J., Tenner, A. J., & Neumann, H. (2012, Jan 18). Sialic acid on the neuronal glycocalyx prevents complement C1 binding and complement receptor-3-mediated removal by microglia. *J Neurosci, 32*(3), 946-952. https://doi.org/10.1523/jneurosci.3830-11.2012

Lionakis, M. S., Lim, J. K., Lee, C. C., & Murphy, P. M. (2011). Organ-specific innate immune responses in a mouse model of invasive candidiasis. *J Innate Immun, 3*(2), 180-199. https://doi.org/10.1159/000321157

Liu, T., van Rooijen, N., & Tracey, D. J. (2000, May). Depletion of macrophages reduces axonal degeneration and hyperalgesia following nerve injury. *Pain, 86*(1-2), 25-32. https://doi.org/10.1016/s0304-3959(99)00306-1

Liu, Y., Hao, W., Letiembre, M., Walter, S., Kulanga, M., Neumann, H., & Fassbender, K. (2006, Dec 13). Suppression of microglial inflammatory activity by myelin phagocytosis: role of p47-PHOX-mediated generation of reactive oxygen species. *J Neurosci, 26*(50), 12904-12913. https://doi.org/10.1523/jneurosci.2531-06.2006

Loftis, J. M., Huckans, M., & Morasco, B. J. (2010, Mar). Neuroimmune mechanisms of cytokine-induced depression: current theories and novel treatment strategies. *Neurobiol Dis, 37*(3), 519-533. https://doi.org/10.1016/j.nbd.2009.11.015

A long and winding sTORy. (2017, Sep 28). *Nat Cell Biol, 19*(10), 1131. https://doi.org/10.1038/ncb3624

Longa, E. Z., Weinstein, P. R., Carlson, S., & Cummins, R. (1989, Jan). Reversible middle cerebral artery occlusion without craniectomy in rats. *Stroke, 20*(1), 84-91. https://doi.org/10.1161/01.str.20.1.84

Lopez, A., Fleming, A., & Rubinsztein, D. C. (2018, Oct 24). Seeing is believing: methods to monitor vertebrate autophagy in vivo. *Open Biol, 8*(10). https://doi.org/10.1098/rsob.180106

Lopez, M. S., & Vemuganti, R. (2018). Modeling Transient Focal Ischemic Stroke in Rodents by Intraluminal Filament Method of Middle Cerebral Artery Occlusion. *Methods Mol Biol, 1717*, 101-113. https://doi.org/10.1007/978-1-4939-7526-6_9

López-Muñoz, F., Boya, J., & Alamo, C. (2006, Oct 16). Neuron theory, the cornerstone of neuroscience, on the centenary of the Nobel Prize award to Santiago Ramón y Cajal. *Brain Res Bull, 70*(4-6), 391-405. https://doi.org/10.1016/j.brainresbull.2006.07.010

Lőrincz, P., & Juhász, G. (2020, Apr 3). Autophagosome-Lysosome Fusion. *J Mol Biol, 432*(8), 2462-2482. https://doi.org/10.1016/j.jmb.2019.10.028

Lucas, S. M., Rothwell, N. J., & Gibson, R. M. (2006, Jan). The role of inflammation in CNS injury and disease. *Br J Pharmacol, 147 Suppl 1*(Suppl 1), S232-240. https://doi.org/10.1038/sj.bjp.0706400

Lucin, K. M., O'Brien, C. E., Bieri, G., Czirr, E., Mosher, K. I., Abbey, R. J., Mastroeni, D. F., Rogers, J., Spencer, B., Masliah, E., & Wyss-Coray, T. (2013, Sep 4). Microglial beclin 1 regulates retromer trafficking and phagocytosis and is impaired in Alzheimer's disease. *Neuron, 79*(5), 873-886. https://doi.org/10.1016/j.neuron.2013.06.046

Lucocq, J. M., & Hacker, C. (2013, Sep). Cutting a fine figure: On the use of thin sections in electron microscopy to quantify autophagy. *Autophagy, 9*(9), 1443-1448. https://doi.org/10.4161/auto.25570

Luzio, J. P., Hackmann, Y., Dieckmann, N. M., & Griffiths, G. M. (2014, Sep 2). The biogenesis of lysosomes and lysosome-related organelles. *Cold Spring Harb Perspect Biol, 6*(9), a016840. https://doi.org/10.1101/cshperspect.a016840

M

Ma, Y., Wang, J., Wang, Y., & Yang, G. Y. (2017, Oct). The biphasic function of microglia in ischemic stroke. *Prog Neurobiol, 157*, 247-272. https://doi.org/10.1016/j.pneurobio.2016.01.005

Madden, S. D., & Cotter, T. G. (2008, Feb). Cell death in brain development and degeneration: control of caspase expression may be key! *Mol Neurobiol, 37*(1), 1-6. https://doi.org/10.1007/s12035-008-8021-4

Magaudda, A., Ferlazzo, E., Nguyen, V. H., & Genton, P. (2006, May). Unverricht-Lundborg disease, a condition with self-limited progression: long-term follow-up of 20 patients. *Epilepsia, 47*(5), 860-866. https://doi.org/10.1111/j.1528-1167.2006.00553.x

Magnus, T., Chan, A., Grauer, O., Toyka, K. V., & Gold, R. (2001, Nov 1). Microglial phagocytosis of apoptotic inflammatory T cells leads to down-regulation of microglial immune activation. *J Immunol, 167*(9), 5004-5010. https://doi.org/10.4049/jimmunol.167.9.5004

Mahapatra, K. K., Mishra, S. R., Behera, B. P., Patil, S., Gewirtz, D. A., & Bhutia, S. K. (2021, Dec). The lysosome as an imperative regulator of autophagy and cell death. *Cell Mol Life Sci, 78*(23), 7435-7449. https://doi.org/10.1007/s00018-021-03988-3

Maher, K., Jeric Kokelj, B., Butinar, M., Mikhaylov, G., Mancek-Keber, M., Stoka, V., Vasiljeva, O., Turk, B., Grigoryev, S. A., & Kopitar-Jerala, N. (2014). A role for stefin B (cystatin B) in inflammation and endotoxemia. *J Biol Chem, 289*(46), 31736-31750. https://doi.org/10.1074/jbc.M114.609396

Majumdar, A., Chung, H., Dolios, G., Wang, R., Asamoah, N., Lobel, P., & Maxfield, F. R. (2008, May). Degradation of fibrillar forms of Alzheimer's amyloid beta-peptide by macrophages. *Neurobiol Aging, 29*(5), 707-715. https://doi.org/10.1016/j.neurobiolaging.2006.12.001

Majumdar, A., Cruz, D., Asamoah, N., Buxbaum, A., Sohar, I., Lobel, P., & Maxfield, F. R. (2007, Apr). Activation of microglia acidifies lysosomes and leads to degradation of Alzheimer amyloid fibrils. *Mol Biol Cell, 18*(4), 1490-1496. https://doi.org/10.1091/mbc.e06-10-0975

Makide, K., Uwamizu, A., Shinjo, Y., Ishiguro, J., Okutani, M., Inoue, A., & Aoki, J. (2014, Oct). Novel lysophosphoplipid receptors: their structure and function. *J Lipid Res, 55*(10), 1986-1995. https://doi.org/10.1194/jlr.R046920

Malik, A., & Kanneganti, T. D. (2017, Dec 1). Inflammasome activation and assembly at a glance. *J Cell Sci, 130*(23), 3955-3963. https://doi.org/10.1242/jcs.207365

Mancini, G. M., Schot, R., de Wit, M. C., de Coo, R. F., Oostenbrink, R., Bindels-de Heus, K., Berger, L. P., Lequin, M. H., de Vries, F. A., Wilke, M., & van Slegtenhorst, M. A. (2016). CSTB null mutation associated with microcephaly, early developmental delay, and severe dyskinesia. *Neurology, 86*(9), 877-878. https://doi.org/10.1212/WNL.0000000000002422

Mandrekar, S., Jiang, Q., Lee, C. Y., Koenigsknecht-Talboo, J., Holtzman, D. M., & Landreth, G. E. (2009, Apr 1). Microglia mediate the clearance of soluble Abeta through fluid phase macropinocytosis. *J Neurosci, 29*(13), 4252-4262. https://doi.org/10.1523/jneurosci.5572-08.2009

Manninen, O., Koskenkorva, P., Lehtimaki, K. K., Hypponen, J., Kononen, M., Laitinen, T., Kalimo, H., Kopra, O., Kalviainen, R., Grohn, O., Lehesjoki, A. E., & Vanninen, R. (2013). White matter degeneration with Unverricht-Lundborg progressive myoclonus epilepsy: a translational diffusion-tensor imaging study in patients and cystatin B-deficient mice. *Radiology, 269*(1), 232-239. https://doi.org/10.1148/radiol.13122458

Manninen, O., Laitinen, T., Lehtimäki, K. K., Tegelberg, S., Lehesjoki, A.-E., Gröhn, O., & Kopra, O. (2014). Progressive Volume Loss and White Matter Degeneration in Cstb-Deficient Mice: A Diffusion Tensor and Longitudinal Volumetry MRI Study. *PLoS One, 9*(3), e90709. https://doi.org/10.1371/journal.pone.0090709

Marino, G., Fernandez, A. F., Cabrera, S., Lundberg, Y. W., Cabanillas, R., Rodriguez, F., Salvador-Montoliu, N., Vega, J. A., Germana, A., Fueyo, A., Freije, J. M., & Lopez-Otin, C. (2010, Jul). Autophagy is essential for mouse sense of balance. *J Clin Invest, 120*(7), 2331-2344. https://doi.org/10.1172/JCI42601

Mariño, G., Uría, J. A., Puente, X. S., Quesada, V., Bordallo, J., & López-Otín, C. (2003, Feb 7). Human autophagins, a family of cysteine proteinases potentially implicated in cell degradation by autophagy. *J Biol Chem, 278*(6), 3671-3678. https://doi.org/10.1074/jbc.M208247200

Márquez-Ropero, M., Benito, E., Plaza-Zabala, A., & Sierra, A. (2020). Microglial Corpse Clearance: Lessons From Macrophages [Review]. *Frontiers in Immunology, 11*(506). https://doi.org/10.3389/fimmu.2020.00506

Martin, K. R., Barua, D., Kauffman, A. L., Westrate, L. M., Posner, R. G., Hlavacek, W. S., & Mackeigan, J. P. (2013, Jan). Computational model for autophagic vesicle dynamics in single cells. *Autophagy, 9*(1), 74-92. https://doi.org/10.4161/auto.22532

Martina, J. A., Chen, Y., Gucek, M., & Puertollano, R. (2012, Jun). MTORC1 functions as a transcriptional regulator of autophagy by preventing nuclear transport of TFEB. *Autophagy, 8*(6), 903-914. https://doi.org/10.4161/auto.19653

Martinet, W., Schrijvers, D. M., Timmermans, J. P., Herman, A. G., & De Meyer, G. R. (2009, Apr). Phagocytosis of bacteria is enhanced in macrophages undergoing nutrient deprivation. *Febs j, 276*(8), 2227-2240. https://doi.org/10.1111/j.1742-4658.2009.06951.x

Martinez, J., Almendinger, J., Oberst, A., Ness, R., Dillon, C. P., Fitzgerald, P., Hengartner, M. O., & Green, D. R. (2011, Oct 18). Microtubule-associated protein 1 light chain 3 alpha (LC3)-associated phagocytosis is required for the efficient clearance of dead cells. *Proc Natl Acad Sci U S A, 108*(42), 17396-17401. https://doi.org/10.1073/pnas.1113421108

Martinez, J., Cunha, L. D., Park, S., Yang, M., Lu, Q., Orchard, R., Li, Q. Z., Yan, M., Janke, L., Guy, C., Linkermann, A., Virgin, H. W., & Green, D. R. (2016, May 5). Noncanonical autophagy inhibits the autoinflammatory, lupus-like response to dying cells. *Nature, 533*(7601), 115-119. https://doi.org/10.1038/nature17950

Mascalchi, M., Michelucci, R., Cosottini, M., Tessa, C., Lolli, F., Riguzzi, P., Lehesjoki, A. E., Tosetti, M., Villari, N., & Tassinari, C. A. (2002). Brainstem involvement in Unverricht-Lundborg disease (EPM1): An MRI and (1)H MRS study. *Neurology, 58*(11), 1686-1689. https://doi.org/10.1212/wnl.58.11.1686

Mathon, B., Bédos Ulvin, L., Adam, C., Baulac, M., Dupont, S., Navarro, V., Cornu, P., & Clemenceau, S. (2015, Mar). Surgical treatment for mesial temporal lobe epilepsy associated with hippocampal sclerosis. *Rev Neurol (Paris), 171*(3), 315-325. https://doi.org/10.1016/j.neurol.2015.01.561

Matlung, H. L., Szilagyi, K., Barclay, N. A., & van den Berg, T. K. (2017, Mar). The CD47-SIRPalpha signaling axis as an innate immune checkpoint in cancer. *Immunol Rev, 276*(1), 145-164. https://doi.org/10.1111/imr.12527

Mauthe, M., Orhon, I., Rocchi, C., Zhou, X., Luhr, M., Hijlkema, K. J., Coppes, R. P., Engedal, N., Mari, M., & Reggiori, F. (2018). Chloroquine inhibits autophagic flux by decreasing autophagosome-lysosome fusion. *Autophagy, 14*(8), 1435-1455. https://doi.org/10.1080/15548627.2018.1474314

Mauvezin, C., & Neufeld, T. P. (2015). Bafilomycin A1 disrupts autophagic flux by inhibiting both V-ATPase-dependent acidification and Ca-P60A/SERCA-dependent autophagosome-lysosome fusion. *Autophagy, 11*(8), 1437-1438. https://doi.org/10.1080/15548627.2015.1066957

Mawuenyega, K. G., Sigurdson, W., Ovod, V., Munsell, L., Kasten, T., Morris, J. C., Yarasheski, K. E., & Bateman, R. J. (2010, Dec 24). Decreased clearance of CNS beta-amyloid in Alzheimer's disease. *Science, 330*(6012), 1774. https://doi.org/10.1126/science.1197623

McComb, S., Thiriot, A., Akache, B., Krishnan, L., & Stark, F. (2019). Introduction to the Immune System. *Methods Mol Biol, 2024*, 1-24. https://doi.org/10.1007/978-1-4939-9597-4_1

McGonigal, R., Cunningham, M. E., Yao, D., Barrie, J. A., Sankaranarayanan, S., Fewou, S. N., Furukawa, K., Yednock, T. A., & Willison, H. J. (2016, Mar 2). C1q-targeted inhibition of the classical complement pathway prevents injury in a novel mouse model of acute motor axonal neuropathy. *Acta Neuropathol Commun, 4*, 23. https://doi.org/10.1186/s40478-016-0291-x

McGrath, M. E. (1999). The lysosomal cysteine proteases. *Annu Rev Biophys Biomol Struct, 28*, 181-204. https://doi.org/10.1146/annurev.biophys.28.1.181

Mehta, P., Henault, J., Kolbeck, R., & Sanjuan, M. A. (2014, Feb). Noncanonical autophagy: one small step for LC3, one giant leap for immunity. *Curr Opin Immunol, 26*, 69-75. https://doi.org/10.1016/j.coi.2013.10.012

Melani, A., Amadio, S., Gianfriddo, M., Vannucchi, M. G., Volontè, C., Bernardi, G., Pedata, F., & Sancesario, G. (2006, Jul). P2X7 receptor modulation on microglial cells and reduction of brain infarct caused by middle cerebral artery occlusion in rat. *J Cereb Blood Flow Metab, 26*(7), 974-982. https://doi.org/10.1038/sj.jcbfm.9600250

Menassa, D. A., & Gomez-Nicola, D. (2018). Microglial Dynamics During Human Brain Development. *Front Immunol, 9*, 1014. https://doi.org/10.3389/fimmu.2018.01014

Mennicken, F., Maki, R., de Souza, E. B., & Quirion, R. (1999, Feb). Chemokines and chemokine receptors in the CNS: a possible role in neuroinflammation and patterning. *Trends Pharmacol Sci, 20*(2), 73-78. https://doi.org/10.1016/s0165-6147(99)01308-5

Mercer, T. J., Gubas, A., & Tooze, S. A. (2018, Apr 13). A molecular perspective of mammalian autophagosome biogenesis. *J Biol Chem, 293*(15), 5386-5395. https://doi.org/10.1074/jbc.R117.810366

Michael, J., Unger, M. S., Poupardin, R., Schernthaner, P., Mrowetz, H., Attems, J., & Aigner, L. (2020, Aug 8). Microglia depletion diminishes key elements of the leukotriene pathway in the brain of Alzheimer's Disease mice. *Acta Neuropathol Commun, 8*(1), 129. https://doi.org/10.1186/s40478-020-00989-4

Michelozzi, C., & Cognard, C. (2019, Jun). [The role of interventional neuroradiology in treatment of hemorrhagic stroke]. *Presse Med, 48*(6), 684-695. https://doi.org/10.1016/j.lpm.2019.05.002 (Rôle de la neuroradiologie interventionnelle dans la prise en charge de l'accident vasculaire cérébral hémorragique.)

Mijaljica, D., Prescott, M., & Devenish, R. J. (2011, Jul). Microautophagy in mammalian cells: revisiting a 40-year-old conundrum. *Autophagy, 7*(7), 673-682. https://doi.org/10.4161/auto.7.7.14733

Mindell, J. A. (2012). Lysosomal acidification mechanisms. *Annu Rev Physiol, 74*, 69-86. https://doi.org/10.1146/annurev-physiol-012110-142317

Mizushima, N. (2011). Autophagy in protein and organelle turnover. *Cold Spring Harb Symp Quant Biol, 76*, 397-402. https://doi.org/10.1101/sqb.2011.76.011023

Mizushima, N., & Komatsu, M. (2011, Nov 11). Autophagy: renovation of cells and tissues. *Cell, 147*(4), 728-741. https://doi.org/10.1016/j.cell.2011.10.026

Mizutani, M., Pino, P. A., Saederup, N., Charo, I. F., Ransohoff, R. M., & Cardona, A. E. (2012, Jan 1). The fractalkine receptor but not CCR2 is present on microglia from embryonic development throughout adulthood. *J Immunol, 188*(1), 29-36. https://doi.org/10.4049/jimmunol.1100421

Monier, A., Adle-Biassette, H., Delezoide, A. L., Evrard, P., Gressens, P., & Verney, C. (2007, May). Entry and distribution of microglial cells in human embryonic and fetal cerebral cortex. *J Neuropathol Exp Neurol, 66*(5), 372-382. https://doi.org/10.1097/nen.0b013e3180517b46

Monje, M. L., Toda, H., & Palmer, T. D. (2003, Dec 5). Inflammatory blockade restores adult hippocampal neurogenesis. *Science, 302*(5651), 1760-1765. https://doi.org/10.1126/science.1088417

Moraga, A., Pradillo, J. M., García-Culebras, A., Palma-Tortosa, S., Ballesteros, I., Hernández-Jiménez, M., Moro, M. A., & Lizasoain, I. (2015, May 10). Aging increases microglial proliferation, delays cell migration, and decreases cortical neurogenesis after focal cerebral ischemia. *J Neuroinflammation, 12*, 87. https://doi.org/10.1186/s12974-015-0314-8

Morel, E., Mehrpour, M., Botti, J., Dupont, N., Hamaï, A., Nascimbeni, A. C., & Codogno, P. (2017, Jan 6). Autophagy: A Druggable Process. *Annu Rev Pharmacol Toxicol, 57*, 375-398. https://doi.org/10.1146/annurev-pharmtox-010716-104936

Morgan, B. P., & Harris, C. L. (2015, Dec). Complement, a target for therapy in inflammatory and degenerative diseases. *Nat Rev Drug Discov, 14*(12), 857-877. https://doi.org/10.1038/nrd4657

Morin-Brureau, M., Milior, G., Royer, J., Chali, F., Le Duigou, C., Savary, E., Blugeon, C., Jourdren, L., Akbar, D., Dupont, S., Navarro, V., Baulac, M., Bielle, F., Mathon, B., Clemenceau, S., & Miles, R. (2018, Dec 1). Microglial phenotypes in the human epileptic temporal lobe. *Brain, 141*(12), 3343-3360. https://doi.org/10.1093/brain/awy276

Morioka, S., Maueroder, C., & Ravichandran, K. S. (2019). Living on the Edge: Efferocytosis at the Interface of Homeostasis and Pathology. *Immunity, 50*(5), 1149-1162. https://doi.org/10.1016/j.immuni.2019.04.018

Morotti, A., & Goldstein, J. N. (2016, Nov). Diagnosis and Management of Acute Intracerebral Hemorrhage. *Emerg Med Clin North Am, 34*(4), 883-899. https://doi.org/10.1016/j.emc.2016.06.010

Morris, G. P., Wright, A. L., Tan, R. P., Gladbach, A., Ittner, L. M., & Vissel, B. (2016). A Comparative Study of Variables Influencing Ischemic Injury in the Longa and Koizumi Methods of Intraluminal Filament Middle Cerebral Artery Occlusion in Mice. *PLoS One, 11*(2), e0148503. https://doi.org/10.1371/journal.pone.0148503

Morrison, H. W., & Filosa, J. A. (2013, Jan 11). A quantitative spatiotemporal analysis of microglia morphology during ischemic stroke and reperfusion. *J Neuroinflammation, 10*, 4. https://doi.org/10.1186/1742-2094-10-4

Moskowitz, M. A., Lo, E. H., & Iadecola, C. (2010, Jul 29). The science of stroke: mechanisms in search of treatments. *Neuron, 67*(2), 181-198. https://doi.org/10.1016/j.neuron.2010.07.002

Mozaffarian, D., Benjamin, E. J., Go, A. S., Arnett, D. K., Blaha, M. J., Cushman, M., Das, S. R., de Ferranti, S., Després, J. P., Fullerton, H. J., Howard, V. J., Huffman, M. D., Isasi, C. R., Jiménez, M. C., Judd, S. E., Kissela, B. M., Lichtman, J. H., Lisabeth, L. D., Liu, S., Mackey, R. H., Magid, D. J., McGuire, D. K., Mohler, E. R., 3rd, Moy, C. S., Muntner, P., Mussolino, M. E., Nasir, K., Neumar, R. W., Nichol, G., Palaniappan, L., Pandey, D. K., Reeves, M. J., Rodriguez, C. J., Rosamond, W., Sorlie, P. D., Stein, J., Towfighi, A., Turan, T. N., Virani, S. S., Woo, D., Yeh, R. W., & Turner, M. B. (2016, Jan 26). Heart Disease and Stroke Statistics-2016 Update: A Report From the American Heart Association. *Circulation, 133*(4), e38-360. https://doi.org/10.1161/cir.0000000000000350

Mueller, M., Leonhard, C., Wacker, K., Ringelstein, E. B., Okabe, M., Hickey, W. F., & Kiefer, R. (2003, Feb). Macrophage response to peripheral nerve injury: the quantitative contribution of resident and hematogenous macrophages. *Lab Invest, 83*(2), 175-185. https://doi.org/10.1097/01.lab.0000056993.28149.bf

Mueller, M., Wacker, K., Ringelstein, E. B., Hickey, W. F., Imai, Y., & Kiefer, R. (2001, Dec). Rapid response of identified resident endoneurial macrophages to nerve injury. *Am J Pathol, 159*(6), 2187-2197. https://doi.org/10.1016/s0002-9440(10)63070-2

Mukherjee, S., Ghosh, R. N., & Maxfield, F. R. (1997, Jul). Endocytosis. *Physiol Rev, 77*(3), 759-803. https://doi.org/10.1152/physrev.1997.77.3.759

Mukhopadhyay, S., Frias, M. A., Chatterjee, A., Yellen, P., & Foster, D. A. (2016, Mar). The Enigma of Rapamycin Dosage. *Mol Cancer Ther, 15*(3), 347-353. https://doi.org/10.1158/1535-7163.Mct-15-0720

Münz, C. (2016, Jul). Autophagy proteins in antigen processing for presentation on MHC molecules. *Immunol Rev, 272*(1), 17-27. https://doi.org/10.1111/imr.12422

N

Naeini, M. B., Bianconi, V., Pirro, M., & Sahebkar, A. (2020). The role of phosphatidylserine recognition receptors in multiple biological functions. *Cell Mol Biol Lett, 25*, 23. https://doi.org/10.1186/s11658-020-00214-z

Nagata, K., Ohashi, K., Nakano, T., Arita, H., Zong, C., Hanafusa, H., & Mizuno, K. (1996, Nov 22). Identification of the product of growth arrest-specific gene 6 as a common ligand for Axl, Sky, and Mer receptor tyrosine kinases. *J Biol Chem, 271*(47), 30022-30027. https://doi.org/10.1074/jbc.271.47.30022

Nagata, S., Hanayama, R., & Kawane, K. (2010, Mar 5). Autoimmunity and the clearance of dead cells. *Cell, 140*(5), 619-630. https://doi.org/10.1016/j.cell.2010.02.014

Nakamura, S., & Yoshimori, T. (2017, Apr 1). New insights into autophagosome-lysosome fusion. *J Cell Sci, 130*(7), 1209-1216. https://doi.org/10.1242/jcs.196352

Nakanishi, H. (2003, Oct). Neuronal and microglial cathepsins in aging and age-related diseases. *Ageing Res Rev, 2*(4), 367-381. https://doi.org/10.1016/s1568-1637(03)00027-8

Nakanishi, H. (2020, Sep). Cathepsin regulation on microglial function. *Biochim Biophys Acta Proteins Proteom, 1868*(9), 140465. https://doi.org/10.1016/j.bbapap.2020.140465

Navarro-Orozco, D., & Sánchez-Manso, J. C. (2022). Neuroanatomy, Middle Cerebral Artery. In *StatPearls*. StatPearls Publishing

Nayak, D., Roth, T. L., & McGavern, D. B. (2014). Microglia development and function. *Annu Rev Immunol, 32*, 367-402. https://doi.org/10.1146/annurev-immunol-032713-120240

Neher, J. J., Emmrich, J. V., Fricker, M., Mander, P. K., Thery, C., & Brown, G. C. (2013, Oct 22). Phagocytosis executes delayed neuronal death after focal brain ischemia. *Proc Natl Acad Sci U S A, 110*(43), E4098-4107. https://doi.org/10.1073/pnas.1308679110

Netea-Maier, R. T., Plantinga, T. S., van de Veerdonk, F. L., Smit, J. W., & Netea, M. G. (2016). Modulation of inflammation by autophagy: Consequences for human disease. *Autophagy, 12*(2), 245-260. https://doi.org/10.1080/15548627.2015.1071759

Neumann, H., & Takahashi, K. (2007, Mar). Essential role of the microglial triggering receptor expressed on myeloid cells-2 (TREM2) for central nervous tissue immune homeostasis. *J Neuroimmunol, 184*(1-2), 92-99. https://doi.org/10.1016/j.jneuroim.2006.11.032

Neumann, J., Henneberg, S., von Kenne, S., Nolte, N., Müller, A. J., Schraven, B., Görtler, M. W., Reymann, K. G., Gunzer, M., & Riek-Burchardt, M. (2018). Beware the intruder: Real time observation of infiltrated neutrophils and neutrophil-Microglia interaction during stroke in vivo. *PLoS One, 13*(3), e0193970. https://doi.org/10.1371/journal.pone.0193970

Niessen, F., Hilger, T., Hoehn, M., & Hossmann, K. A. (2003, Aug). Differences in clot preparation determine outcome of recombinant tissue plasminogen activator treatment in experimental thromboembolic stroke. *Stroke, 34*(8), 2019-2024. https://doi.org/10.1161/01.Str.0000080941.73934.30

Nimmerjahn, A., Kirchhoff, F., & Helmchen, F. (2005, May 27). Resting microglial cells are highly dynamic surveillants of brain parenchyma in vivo. *Science, 308*(5726), 1314-1318. https://doi.org/10.1126/science.1110647

Nixon, R. A., & Cataldo, A. M. (2006). Lysosomal system pathways: genes to neurodegeneration in Alzheimer's disease. *J Alzheimers Dis, 9*(3 Suppl), 277-289. https://doi.org/10.3233/jad-2006-9s331

Noda, N. N., & Inagaki, F. (2015). Mechanisms of Autophagy. *Annu Rev Biophys, 44*, 101-122. https://doi.org/10.1146/annurev-biophys-060414-034248

Nwadike, C., Williamson, L. E., Gallagher, L. E., Guan, J. L., & Chan, E. Y. W. (2018, May 15). AMPK Inhibits ULK1-Dependent Autophagosome Formation and Lysosomal Acidification via Distinct Mechanisms. *Mol Cell Biol, 38*(10). https://doi.org/10.1128/mcb.00023-18

O

O'Brien, A., Marshall, C. R., Blaser, S., Ray, P. N., & Yoon, G. (2017). Severe neurodegeneration, progressive cerebral volume loss and diffuse hypomyelination associated with a homozygous frameshift mutation in CSTB. *European Journal of Human Genetics, 25*(6), 775-778. https://doi.org/10.1038/ejhg.2017.39

O'Sullivan, S. A., O'Sullivan, C., Healy, L. M., Dev, K. K., & Sheridan, G. K. (2018, Mar). Sphingosine 1-phosphate receptors regulate TLR4-induced CXCL5 release from astrocytes and microglia. *J Neurochem, 144*(6), 736-747. https://doi.org/10.1111/jnc.14313

Obernier, K., & Alvarez-Buylla, A. (2019, Feb 18). Neural stem cells: origin, heterogeneity and regulation in the adult mammalian brain. *Development, 146*(4). https://doi.org/10.1242/dev.156059

Ohgomori, T., & Jinno, S. (2020). The expression of keratan sulfate reveals a unique subset of microglia in the mouse hippocampus after pilocarpine-induced status epileptics. *J Comp Neurol, 528*(1), 14-31. https://doi.org/10.1002/cne.24734

Oku, M., & Sakai, Y. (2018, Jun). Three Distinct Types of Microautophagy Based on Membrane Dynamics and Molecular Machineries. *Bioessays, 40*(6), e1800008. https://doi.org/10.1002/bies.201800008

Okuneva, O., Korber, I., Li, Z., Tian, L., Joensuu, T., Kopra, O., & Lehesjoki, A. E. (2015). Abnormal microglial activation in the Cstb(-/-) mouse, a model for progressive myoclonus epilepsy, EPM1. *Glia, 63*(3), 400-411. https://doi.org/10.1002/glia.22760

Opal, S. M., & DePalo, V. A. (2000, Apr). Anti-inflammatory cytokines. *Chest, 117*(4), 1162-1172. https://doi.org/10.1378/chest.117.4.1162

Otxoa-de-Amezaga, A., Miró-Mur, F., Pedragosa, J., Gallizioli, M., Justicia, C., Gaja-Capdevila, N., Ruíz-Jaen, F., Salas-Perdomo, A., Bosch, A., Calvo, M., Márquez-Kisinousky, L., Denes, A., Gunzer, M., & Planas, A. M. (2019, Feb). Microglial cell loss after ischemic stroke favors brain neutrophil accumulation. *Acta Neuropathol, 137*(2), 321-341. https://doi.org/10.1007/s00401-018-1954-4

P

Paloneva, J., Manninen, T., Christman, G., Hovanes, K., Mandelin, J., Adolfsson, R., Bianchin, M., Bird, T., Miranda, R., Salmaggi, A., Tranebjaerg, L., Konttinen, Y., & Peltonen, L. (2002, Sep). Mutations in two genes encoding different subunits of a receptor signaling complex result in an identical disease phenotype. *Am J Hum Genet, 71*(3), 656-662. https://doi.org/10.1086/342259

Pang, Y., Fan, L. W., Tien, L. T., Dai, X., Zheng, B., Cai, Z., Lin, R. C., & Bhatt, A. (2013, Sep). Differential roles of astrocyte and microglia in supporting oligodendrocyte development and myelination in vitro. *Brain Behav, 3*(5), 503-514. https://doi.org/10.1002/brb3.152

Pang, Y., Yamamoto, H., Sakamoto, H., Oku, M., Mutungi, J. K., Sahani, M. H., Kurikawa, Y., Kita, K., Noda, N. N., Sakai, Y., Jia, H., & Mizushima, N. (2019, Apr). Evolution from covalent conjugation to non-covalent interaction in the ubiquitin-like ATG12 system. *Nat Struct Mol Biol, 26*(4), 289-296. https://doi.org/10.1038/s41594-019-0204-3

Paolicelli, R., Sierra-Torre, V., Stevens, B., & Tremblay, M. E. (2022). Defining microglial states and nomenclature: a roadmap to 2030. *SneakPeek (under review in Cell)*. https://papers.ssrn.com/sol3/papers.cfm?abstract_id=4065080

Paolicelli, R. C., Bolasco, G., Pagani, F., Maggi, L., Scianni, M., Panzanelli, P., Giustetto, M., Ferreira, T. A., Guiducci, E., Dumas, L., Ragozzino, D., & Gross, C. T. (2011, Sep 9). Synaptic pruning by microglia is necessary for normal brain development. *Science, 333*(6048), 1456-1458. https://doi.org/10.1126/science.1202529

Pardridge, W. M. (2005, Jan). The blood-brain barrier: bottleneck in brain drug development. *NeuroRx, 2*(1), 3-14. https://doi.org/10.1602/neurorx.2.1.3

Parhizkar, S., Arzberger, T., Brendel, M., Kleinberger, G., Deussing, M., Focke, C., Nuscher, B., Xiong, M., Ghasemigharagoz, A., Katzmarski, N., Krasemann, S., Lichtenthaler, S. F., Müller, S. A., Colombo, A., Monasor, L. S., Tahirovic, S., Herms, J., Willem, M., Pettkus, N., Butovsky, O., Bartenstein, P., Edbauer, D., Rominger, A., Ertürk, A., Grathwohl, S. A., Neher, J. J., Holtzman, D. M., Meyer-Luehmann, M., & Haass, C. (2019, Feb). Loss of TREM2 function increases amyloid seeding but reduces plaque-associated ApoE. *Nat Neurosci, 22*(2), 191-204. https://doi.org/10.1038/s41593-018-0296-9

Park, D., Han, C. Z., Elliott, M. R., Kinchen, J. M., Trampont, P. C., Das, S., Collins, S., Lysiak, J. J., Hoehn, K. L., & Ravichandran, K. S. (2011, Aug 21). Continued clearance of apoptotic cells critically depends on the phagocyte Ucp2 protein. *Nature, 477*(7363), 220-224. https://doi.org/10.1038/nature10340

Park, S. Y., Jung, M. Y., Lee, S. J., Kang, K. B., Gratchev, A., Riabov, V., Kzhyshkowska, J., & Kim, I. S. (2009, Sep 15). Stabilin-1 mediates phosphatidylserine-dependent clearance of cell corpses in alternatively activated macrophages. *J Cell Sci, 122*(Pt 18), 3365-3373. https://doi.org/10.1242/jcs.049569

Park, S. Y., & Kim, I. S. (2017, May 12). Engulfment signals and the phagocytic machinery for apoptotic cell clearance. *Exp Mol Med, 49*(5), e331. https://doi.org/10.1038/emm.2017.52

Parkhurst, C. N., Yang, G., Ninan, I., Savas, J. N., Yates, J. R., 3rd, Lafaille, J. J., Hempstead, B. L., Littman, D. R., & Gan, W. B. (2013, Dec 19). Microglia promote learning-dependent synapse formation through brain-derived neurotrophic factor. *Cell, 155*(7), 1596-1609. https://doi.org/10.1016/j.cell.2013.11.030

Parkin, J., & Cohen, B. (2001, Jun 2). An overview of the immune system. *Lancet, 357*(9270), 1777-1789. https://doi.org/10.1016/s0140-6736(00)04904-7

Parzych, K. R., & Klionsky, D. J. (2014, Jan 20). An overview of autophagy: morphology, mechanism, and regulation. *Antioxid Redox Signal, 20*(3), 460-473. https://doi.org/10.1089/ars.2013.5371

Pellon, A., Ramirez-Garcia, A., Guruceaga, X., Zabala, A., Buldain, I., Antoran, A., Anguita, J., Rementeria, A., Matute, C., & Hernando, F. L. (2018, Aug). Microglial immune response is impaired against the neurotropic fungus Lomentospora prolificans. *Cell Microbiol, 20*(8), e12847. https://doi.org/10.1111/cmi.12847

Pennacchio, L. A., Bouley, D. M., Higgins, K. M., Scott, M. P., Noebels, J. L., & Myers, R. M. (1998). Progressive ataxia, myoclonic epilepsy and cerebellar apoptosis in cystatin B-deficient mice. *Nat Genet, 20*(3), 251-258. https://doi.org/10.1038/3059

Pennacchio, L. A., Lehesjoki, A.-E., Stone, N. E., Willour, V. L., Virtaneva, K., Miao, J., D'Amato, E., Ramirez, L., Faham, M., Koskiniemi, M., Warrington, J. A., Norio, R., de la Chapelle, A., Cox, D. R., & Myers, R. M. (1996). Mutations in the Gene Encoding Cystatin B in Progressive Myoclonus Epilepsy (EPM1). *Science, 271*(5256), 1731-1734. https://doi.org/10.1126/science.271.5256.1731

Perera, R. M., & Zoncu, R. (2016, Oct 6). The Lysosome as a Regulatory Hub. *Annu Rev Cell Dev Biol, 32*, 223-253. https://doi.org/10.1146/annurev-cellbio-111315-125125

Perez-Pouchoulen, M., VanRyzin, J. W., & McCarthy, M. M. (2015, Jul-Aug). Morphological and Phagocytic Profile of Microglia in the Developing Rat Cerebellum. *eNeuro, 2*(4). https://doi.org/10.1523/eneuro.0036-15.2015

Peter, C., Waibel, M., Radu, C. G., Yang, L. V., Witte, O. N., Schulze-Osthoff, K., Wesselborg, S., & Lauber, K. (2008, Feb 29). Migration to apoptotic "find-me" signals is mediated via the phagocyte receptor G2A. *J Biol Chem, 283*(9), 5296-5305. https://doi.org/10.1074/jbc.M706586200

Peter, C., Wesselborg, S., & Lauber, K. (2010, Apr). Molecular suicide notes: last call from apoptosing cells. *J Mol Cell Biol, 2*(2), 78-80. https://doi.org/10.1093/jmcb/mjp045

Peters-Golden, M., & Henderson, W. R., Jr. (2007, Nov 1). Leukotrienes. *N Engl J Med, 357*(18), 1841-1854. https://doi.org/10.1056/NEJMra071371

Petherick, K. J., Conway, O. J., Mpamhanga, C., Osborne, S. A., Kamal, A., Saxty, B., & Ganley, I. G. (2015, Nov 27). Pharmacological inhibition of ULK1 kinase blocks mammalian target of rapamycin (mTOR)-dependent autophagy. *J Biol Chem, 290*(48), 28726. https://doi.org/10.1074/jbc.A114.627778

Plaza-Zabala, A., Sierra-Torre, V., & Sierra, A. (2017, Mar 9). Autophagy and Microglia: Novel Partners in Neurodegeneration and Aging. *Int J Mol Sci, 18*(3). https://doi.org/10.3390/ijms18030598

Poon, I. K., Chiu, Y. H., Armstrong, A. J., Kinchen, J. M., Juncadella, I. J., Bayliss, D. A., & Ravichandran, K. S. (2014, Mar 20). Unexpected link between an antibiotic, pannexin channels and apoptosis. *Nature, 507*(7492), 329-334. https://doi.org/10.1038/nature13147

Powers, W. J., Rabinstein, A. A., Ackerson, T., Adeoye, O. M., Bambakidis, N. C., Becker, K., Biller, J., Brown, M., Demaerschalk, B. M., Hoh, B., Jauch, E. C., Kidwell, C. S., Leslie-Mazwi, T. M., Ovbiagele, B., Scott, P. A., Sheth, K. N., Southerland, A. M., Summers, D. V., & Tirschwell, D. L. (2019, Dec). Guidelines for the Early Management of Patients With Acute Ischemic Stroke: 2019 Update to the 2018 Guidelines for the Early Management of Acute Ischemic Stroke: A Guideline for Healthcare Professionals From the American Heart Association/American Stroke Association. *Stroke, 50*(12), e344-e418. https://doi.org/10.1161/str.0000000000000211

Preissler, J., Grosche, A., Lede, V., Le Duc, D., Krügel, K., Matyash, V., Szulzewsky, F., Kallendrusch, S., Immig, K., Kettenmann, H., Bechmann, I., Schöneberg, T., & Schulz, A. (2015, Feb). Altered microglial phagocytosis in GPR34-deficient mice. *Glia, 63*(2), 206-215. https://doi.org/10.1002/glia.22744

Prinz, M., Jung, S., & Priller, J. (2019, Oct 3). Microglia Biology: One Century of Evolving Concepts. *Cell, 179*(2), 292-311. https://doi.org/10.1016/j.cell.2019.08.053

Pu, J., Guardia, C. M., Keren-Kaplan, T., & Bonifacino, J. S. (2016, Dec 1). Mechanisms and functions of lysosome positioning. *J Cell Sci, 129*(23), 4329-4339. https://doi.org/10.1242/jcs.196287

Pyo, J. O., Yoo, S. M., Ahn, H. H., Nah, J., Hong, S. H., Kam, T. I., Jung, S., & Jung, Y. K. (2013). Overexpression of Atg5 in mice activates autophagy and extends lifespan. *Nat Commun, 4*, 2300. https://doi.org/10.1038/ncomms3300

Q

Qin, Y., Qiu, J., Wang, P., Liu, J., Zhao, Y., Jiang, F., & Lou, H. (2021, Jan). Impaired autophagy in microglia aggravates dopaminergic neurodegeneration by regulating NLRP3 inflammasome activation in experimental models of Parkinson's disease. *Brain Behav Immun, 91*, 324-338. https://doi.org/10.1016/j.bbi.2020.10.010

Quintas, R., Raggi, A., Giovannetti, A. M., Pagani, M., Sabariego, C., Cieza, A., & Leonardi, M. (2012, Sep). Psychosocial difficulties in people with epilepsy: a systematic review of literature from 2005 until 2010. *Epilepsy Behav, 25*(1), 60-67. https://doi.org/10.1016/j.yebeh.2012.05.016

R

Rabinstein, A. A. (2020, Apr). Update on Treatment of Acute Ischemic Stroke. *Continuum (Minneap Minn), 26*(2), 268-286. https://doi.org/10.1212/con.0000000000000840

Rajan, W. D., Wojtas, B., Gielniewski, B., Gieryng, A., Zawadzka, M., & Kaminska, B. (2019, Feb). Dissecting functional phenotypes of microglia and macrophages in the rat brain after transient cerebral ischemia. *Glia, 67*(2), 232-245. https://doi.org/10.1002/glia.23536

Rakic, P. (1972, May). Mode of cell migration to the superficial layers of fetal monkey neocortex. *J Comp Neurol, 145*(1), 61-83. https://doi.org/10.1002/cne.901450105

Ramakers, C., Ruijter, J. M., Deprez, R. H., & Moorman, A. F. (2003, Mar 13). Assumption-free analysis of quantitative real-time polymerase chain reaction (PCR) data. *Neurosci Lett, 339*(1), 62-66. https://doi.org/10.1016/s0304-3940(02)01423-4

Ransohoff, R. M. (2016, Jul 26). A polarizing question: do M1 and M2 microglia exist? *Nat Neurosci, 19*(8), 987-991. https://doi.org/10.1038/nn.4338

Rappold, P. M., Lynd-Balta, E., & Joseph, S. A. (2006, May 17). P2X7 receptor immunoreactive profile confined to resting and activated microglia in the epileptic brain. *Brain Res, 1089*(1), 171-178. https://doi.org/10.1016/j.brainres.2006.03.040

Ravichandran, K. S., & Lorenz, U. (2007, Dec). Engulfment of apoptotic cells: signals for a good meal. *Nat Rev Immunol, 7*(12), 964-974. https://doi.org/10.1038/nri2214

Read, R., Savelieva, K., Baker, K., Hansen, G., & Vogel, P. (2011, Mar). Histopathological and neurological features of Atg4b knockout mice. *Vet Pathol, 48*(2), 486-494. https://doi.org/10.1177/0300985810375810

Reggiori, F., Komatsu, M., Finley, K., & Simonsen, A. (2012, 2012/05/15). Autophagy: More Than a Nonselective Pathway. *International Journal of Cell Biology, 2012*, 219625. https://doi.org/10.1155/2012/219625

Riccio, M., Di Giaimo, R., Pianetti, S., Palmieri, P. P., Melli, M., & Santi, S. (2001). Nuclear localization of cystatin B, the cathepsin inhibitor implicated in myoclonus epilepsy (EPM1). *Exp Cell Res, 262*(2), 84-94. https://doi.org/10.1006/excr.2000.5085

Ricklin, D., Hajishengallis, G., Yang, K., & Lambris, J. D. (2010, Sep). Complement: a key system for immune surveillance and homeostasis. *Nat Immunol, 11*(9), 785-797. https://doi.org/10.1038/ni.1923

Rinne, R., Saukko, P., Jarvinen, M., & Lehesjoki, A. E. (2002). Reduced cystatin B activity correlates with enhanced cathepsin activity in progressive myoclonus epilepsy. *Ann Med, 34*(5), 380-385. http://www.ncbi.nlm.nih.gov/pubmed/12452481

Ritzel, R. M., Patel, A. R., Grenier, J. M., Crapser, J., Verma, R., Jellison, E. R., & McCullough, L. D. (2015, May 29). Functional differences between microglia and monocytes after ischemic stroke. *J Neuroinflammation, 12*, 106. https://doi.org/10.1186/s12974-015-0329-1

Rocha, N. P., Teixeira, A. L., Coelho, F. M., Caramelli, P., Guimarães, H. C., Barbosa, I. G., da Silva, T. A., Mukhamedyarov, M. A., Zefirov, A. L., Rizvanov, A. A., Kiyasov, A. P., Vieira, L. B., Janka, Z., Palotás, A., & Reis, H. J. (2012, Jan). Peripheral blood mono-nuclear cells derived from Alzheimer's disease patients show elevated baseline levels of secreted cytokines but resist stimulation with β-amyloid peptide. *Mol Cell Neurosci, 49*(1), 77-84. https://doi.org/10.1016/j.mcn.2011.09.005

Romao, S., Gasser, N., Becker, A. C., Guhl, B., Bajagic, M., Vanoaica, D., Ziegler, U., Roesler, J., Dengjel, J., Reichenbach, J., & Münz, C. (2013, Dec 9). Autophagy proteins stabilize pathogen-containing

phagosomes for prolonged MHC II antigen processing. *J Cell Biol, 203*(5), 757-766. https://doi.org/10.1083/jcb.201308173

Ross, C., & Boroviak, T. E. (2020, Jul 28). Origin and function of the yolk sac in primate embryogenesis. *Nat Commun, 11*(1), 3760. https://doi.org/10.1038/s41467-020-17575-w

Roth, S., Cao, J., Singh, V., Tiedt, S., Hundeshagen, G., Li, T., Boehme, J. D., Chauhan, D., Zhu, J., Ricci, A., Gorka, O., Asare, Y., Yang, J., Lopez, M. S., Rehberg, M., Bruder, D., Zhang, S., Groß, O., Dichgans, M., Hornung, V., & Liesz, A. (2021, Apr 13). Post-injury immunosuppression and secondary infections are caused by an AIM2 inflammasome-driven signaling cascade. *Immunity, 54*(4), 648-659.e648. https://doi.org/10.1016/j.immuni.2021.02.004

Roumier, A., Béchade, C., Poncer, J. C., Smalla, K. H., Tomasello, E., Vivier, E., Gundelfinger, E. D., Triller, A., & Bessis, A. (2004, Dec 15). Impaired synaptic function in the microglial KARAP/DAP12-deficient mouse. *J Neurosci, 24*(50), 11421-11428. https://doi.org/10.1523/jneurosci.2251-04.2004

Rubinsztein, D. C., Cuervo, A. M., Ravikumar, B., Sarkar, S., Korolchuk, V., Kaushik, S., & Klionsky, D. J. (2009, Jul). In search of an "autophagomometer". *Autophagy, 5*(5), 585-589. https://doi.org/10.4161/auto.5.5.8823

Runwal, G., Stamatakou, E., Siddiqi, F. H., Puri, C., Zhu, Y., & Rubinsztein, D. C. (2019, Jul 12). LC3-positive structures are prominent in autophagy-deficient cells. *Sci Rep, 9*(1), 10147. https://doi.org/10.1038/s41598-019-46657-z

S

Saftig, P., & Klumperman, J. (2009, Sep). Lysosome biogenesis and lysosomal membrane proteins: trafficking meets function. *Nat Rev Mol Cell Biol, 10*(9), 623-635. https://doi.org/10.1038/nrm2745

Sanchez-Garrido, J., & Shenoy, A. R. (2021, Jul). Regulation and repurposing of nutrient sensing and autophagy in innate immunity. *Autophagy, 17*(7), 1571-1591. https://doi.org/10.1080/15548627.2020.1783119

Sanjuan, M. A., Dillon, C. P., Tait, S. W., Moshiach, S., Dorsey, F., Connell, S., Komatsu, M., Tanaka, K., Cleveland, J. L., Withoff, S., & Green, D. R. (2007, Dec 20). Toll-like receptor signalling in macrophages links the autophagy pathway to phagocytosis. *Nature, 450*(7173), 1253-1257. https://doi.org/10.1038/nature06421

Santavanond, J. P., Rutter, S. F., Atkin-Smith, G. K., & Poon, I. K. H. (2021). Apoptotic Bodies: Mechanism of Formation, Isolation and Functional Relevance. *Subcell Biochem, 97*, 61-88. https://doi.org/10.1007/978-3-030-67171-6_4

Sardiello, M., & Ballabio, A. (2009, Dec 15). Lysosomal enhancement: a CLEAR answer to cellular degradative needs. *Cell Cycle, 8*(24), 4021-4022. https://doi.org/10.4161/cc.8.24.10263

Sarkar, S. (2013, Oct). Regulation of autophagy by mTOR-dependent and mTOR-independent pathways: autophagy dysfunction in neurodegenerative diseases and therapeutic application of autophagy enhancers. *Biochem Soc Trans, 41*(5), 1103-1130. https://doi.org/10.1042/bst20130134

Sarma, J. V., & Ward, P. A. (2011, Jan). The complement system. *Cell Tissue Res, 343*(1), 227-235. https://doi.org/10.1007/s00441-010-1034-0

Sasmono, R. T., Oceandy, D., Pollard, J. W., Tong, W., Pavli, P., Wainwright, B. J., Ostrowski, M. C., Himes, S. R., & Hume, D. A. (2003, Feb 1). A macrophage colony-stimulating factor receptor-green fluorescent protein transgene is expressed throughout the mononuclear phagocyte system of the mouse. *Blood, 101*(3), 1155-1163. https://doi.org/10.1182/blood-2002-02-0569

Sastre, M., Klockgether, T., & Heneka, M. T. (2006, Apr-May). Contribution of inflammatory processes to Alzheimer's disease: molecular mechanisms. *Int J Dev Neurosci, 24*(2-3), 167-176. https://doi.org/10.1016/j.ijdevneu.2005.11.014

Satoh, J., Kino, Y., Asahina, N., Takitani, M., Miyoshi, J., Ishida, T., & Saito, Y. (2016, Feb). TMEM119 marks a subset of microglia in the human brain. *Neuropathology, 36*(1), 39-49. https://doi.org/10.1111/neup.12235

Savage, N. (2014, Jul 10). Epidemiology: The complexities of epilepsy. *Nature, 511*(7508), S2-3. https://doi.org/10.1038/511s2a

Savarin-Vuaillat, C., & Ransohoff, R. M. (2007, Oct). Chemokines and chemokine receptors in neurological disease: raise, retain, or reduce? *Neurotherapeutics, 4*(4), 590-601. https://doi.org/10.1016/j.nurt.2007.07.004

Savill, J., Dransfield, I., Gregory, C., & Haslett, C. (2002). A blast from the past: clearance of apoptotic cells regulates immune responses. *Nat Rev Immunol, 2*(12), 965-975. https://doi.org/10.1038/nri957

Schafer, D. P., Lehrman, E. K., Kautzman, A. G., Koyama, R., Mardinly, A. R., Yamasaki, R., Ransohoff, R. M., Greenberg, M. E., Barres, B. A., & Stevens, B. (2012, May 24). Microglia sculpt postnatal neural circuits in an activity and complement-dependent manner. *Neuron, 74*(4), 691-705. https://doi.org/10.1016/j.neuron.2012.03.026

Schilling, M., Besselmann, M., Leonhard, C., Mueller, M., Ringelstein, E. B., & Kiefer, R. (2003, Sep). Microglial activation precedes and predominates over macrophage infiltration in transient focal cerebral ischemia: a study in green fluorescent protein transgenic bone marrow chimeric mice. *Exp Neurol, 183*(1), 25-33. https://doi.org/10.1016/s0014-4886(03)00082-7

Schneider, C. A., Rasband, W. S., & Eliceiri, K. W. (2012, Jul). NIH Image to ImageJ: 25 years of image analysis. *Nat Methods, 9*(7), 671-675. https://doi.org/10.1038/nmeth.2089

Schöneberg, T., Meister, J., Knierim, A. B., & Schulz, A. (2018, Sep). The G protein-coupled receptor GPR34 - The past 20 years of a grownup. *Pharmacol Ther, 189*, 71-88. https://doi.org/10.1016/j.pharmthera.2018.04.008

Schulz, C., Gomez Perdiguero, E., Chorro, L., Szabo-Rogers, H., Cagnard, N., Kierdorf, K., Prinz, M., Wu, B., Jacobsen, S. E., Pollard, J. W., Frampton, J., Liu, K. J., & Geissmann, F. (2012, Apr 6). A lineage of myeloid cells independent of Myb and hematopoietic stem cells. *Science, 336*(6077), 86-90. https://doi.org/10.1126/science.1219179

Schwartzkroin, P. A. (1986). Hippocampal slices in experimental and human epilepsy. *Adv Neurol, 44*, 991-1010.

Schwarz, J. M., Sholar, P. W., & Bilbo, S. D. (2012, Mar). Sex differences in microglial colonization of the developing rat brain. *J Neurochem, 120*(6), 948-963. https://doi.org/10.1111/j.1471-4159.2011.07630.x

Scott, A. M., Wolchok, J. D., & Old, L. J. (2012, Mar 22). Antibody therapy of cancer. *Nat Rev Cancer, 12*(4), 278-287. https://doi.org/10.1038/nrc3236

Segawa, K., Kurata, S., Yanagihashi, Y., Brummelkamp, T. R., Matsuda, F., & Nagata, S. (2014, Jun 6). Caspase-mediated cleavage of phospholipid flippase for apoptotic phosphatidylserine exposure. *Science, 344*(6188), 1164-1168. https://doi.org/10.1126/science.1252809

Sehgal, S. N. (2003, May). Sirolimus: its discovery, biological properties, and mechanism of action. *Transplant Proc, 35*(3 Suppl), 7S-14S. https://doi.org/10.1016/s0041-1345(03)00211-2

Selkoe, D. J., & Hardy, J. (2016, Jun). The amyloid hypothesis of Alzheimer's disease at 25 years. *EMBO Mol Med, 8*(6), 595-608. https://doi.org/10.15252/emmm.201606210

Settembre, C., Di Malta, C., Polito, V. A., Garcia Arencibia, M., Vetrini, F., Erdin, S., Erdin, S. U., Huynh, T., Medina, D., Colella, P., Sardiello, M., Rubinsztein, D. C., & Ballabio, A. (2011, Jun 17). TFEB links autophagy to lysosomal biogenesis. *Science, 332*(6036), 1429-1433. https://doi.org/10.1126/science.1204592

Settembre, C., Fraldi, A., Medina, D. L., & Ballabio, A. (2013, May). Signals from the lysosome: a control centre for cellular clearance and energy metabolism. *Nat Rev Mol Cell Biol, 14*(5), 283-296. https://doi.org/10.1038/nrm3565

Shannon, P., Pennacchio, L. A., Houseweart, M. K., Minassian, B. A., & Myers, R. M. (2002). Neuropathological changes in a mouse model of progressive myoclonus epilepsy: cystatin B deficiency and Unverricht-Lundborg disease. *J Neuropathol Exp Neurol, 61*(12), 1085-1091. https://doi.org/10.1093/jnen/61.12.1085

Sharma, A. K., Reams, R. Y., Jordan, W. H., Miller, M. A., Thacker, H. L., & Snyder, P. W. (2007, Dec). Mesial temporal lobe epilepsy: pathogenesis, induced rodent models and lesions. *Toxicol Pathol, 35*(7), 984-999. https://doi.org/10.1080/01926230701748305

Shen, H. M., & Mizushima, N. (2014, Feb). At the end of the autophagic road: an emerging understanding of lysosomal functions in autophagy. *Trends Biochem Sci, 39*(2), 61-71. https://doi.org/10.1016/j.tibs.2013.12.001

Sieger, D., Moritz, C., Ziegenhals, T., Prykhozhij, S., & Peri, F. (2012, Jun 12). Long-range Ca2+ waves transmit brain-damage signals to microglia. *Dev Cell, 22*(6), 1138-1148. https://doi.org/10.1016/j.devcel.2012.04.012

Sierra, A., Abiega, O., Shahraz, A., & Neumann, H. (2013). Janus-faced microglia: beneficial and detrimental consequences of microglial phagocytosis. *Front Cell Neurosci, 7*, 6. https://doi.org/10.3389/fncel.2013.00006

Sierra, A., Beccari, S., Diaz-Aparicio, I., Encinas, J. M., Comeau, S., & Tremblay, M. E. (2014). Surveillance, phagocytosis, and inflammation: how never-resting microglia influence adult hippocampal neurogenesis. *Neural Plast, 2014*, 610343. https://doi.org/10.1155/2014/610343

Sierra, A., de Castro, F., Del Río-Hortega, J., Rafael Iglesias-Rozas, J., Garrosa, M., & Kettenmann, H. (2016, Nov). The "Big-Bang" for modern glial biology: Translation and comments on Pío del Río-Hortega 1919 series of papers on microglia. *Glia, 64*(11), 1801-1840. https://doi.org/10.1002/glia.23046

Sierra, A., Encinas, J. M., Deudero, J. J., Chancey, J. H., Enikolopov, G., Overstreet-Wadiche, L. S., Tsirka, S. E., & Maletic-Savatic, M. (2010, Oct 8). Microglia shape adult hippocampal neurogenesis through apoptosis-coupled phagocytosis. *Cell Stem Cell, 7*(4), 483-495. https://doi.org/10.1016/j.stem.2010.08.014

Sierra, A., Gottfried-Blackmore, A. C., McEwen, B. S., & Bulloch, K. (2007, Mar). Microglia derived from aging mice exhibit an altered inflammatory profile. *Glia, 55*(4), 412-424. https://doi.org/10.1002/glia.20468

Sierra, A., Martín-Suárez, S., Valcárcel-Martín, R., Pascual-Brazo, J., Aelvoet, S. A., Abiega, O., Deudero, J. J., Brewster, A. L., Bernales, I., Anderson, A. E., Baekelandt, V., Maletić-Savatić, M., & Encinas, J. M. (2015, May 7). Neuronal hyperactivity accelerates depletion of neural stem cells and impairs hippocampal neurogenesis. *Cell Stem Cell, 16*(5), 488-503. https://doi.org/10.1016/j.stem.2015.04.003

Sierra, A., Paolicelli, R. C., & Kettenmann, H. (2019, Nov). Cien Años de Microglía: Milestones in a Century of Microglial Research. *Trends Neurosci, 42*(11), 778-792. https://doi.org/10.1016/j.tins.2019.09.004

Sierra-Torre, V., Plaza-Zabala, A., Bonifazi, P., Abiega, O., Díaz-Aparicio, I., Tegelberg, S., Lehesjoki, A. E., Valero, J., & Sierra, A. (2020, Nov). Microglial phagocytosis dysfunction in the dentate gyrus is related to local neuronal activity in a genetic model of epilepsy. *Epilepsia, 61*(11), 2593-2608. https://doi.org/10.1111/epi.16692

Sinkovits, G., Mező, B., Réti, M., Müller, V., Iványi, Z., Gál, J., Gopcsa, L., Reményi, P., Szathmáry, B., Lakatos, B., Szlávik, J., Bobek, I., Prohászka, Z. Z., Förhécz, Z., Csuka, D., Hurler, L., Kajdácsi, E., Cervenak, L., Kiszel, P., Masszi, T., Vályi-Nagy, I., & Prohászka, Z. (2021, 2021-March-25). Complement Overactivation and Consumption Predicts In-Hospital Mortality in SARS-CoV-2 Infection [Original Research]. *Frontiers in Immunology, 12*. https://doi.org/10.3389/fimmu.2021.663187

Smith, J. A., Das, A., Ray, S. K., & Banik, N. L. (2012, Jan 4). Role of pro-inflammatory cytokines released from microglia in neurodegenerative diseases. *Brain Res Bull, 87*(1), 10-20. https://doi.org/10.1016/j.brainresbull.2011.10.004

Smolders, S. M., Kessels, S., Vangansewinkel, T., Rigo, J. M., Legendre, P., & Brône, B. (2019, Jul). Microglia: Brain cells on the move. *Prog Neurobiol, 178*, 101612. https://doi.org/10.1016/j.pneurobio.2019.04.001

Sokolowski, J. D., Chabanon-Hicks, C. N., Han, C. Z., Heffron, D. S., & Mandell, J. W. (2014). Fractalkine is a "find-me" signal released by neurons undergoing ethanol-induced apoptosis. *Front Cell Neurosci, 8*, 360. https://doi.org/10.3389/fncel.2014.00360

Spangenberg, E. E., & Green, K. N. (2017, Mar). Inflammation in Alzheimer's disease: Lessons learned from microglia-depletion models. *Brain Behav Immun, 61*, 1-11. https://doi.org/10.1016/j.bbi.2016.07.003

Stern, M., Savill, J., & Haslett, C. (1996, Sep). Human monocyte-derived macrophage phagocytosis of senescent eosinophils undergoing apoptosis. Mediation by alpha v beta 3/CD36/thrombospondin recognition mechanism and lack of phlogistic response. *Am J Pathol, 149*(3), 911-921.

Stevens, B., Allen, N. J., Vazquez, L. E., Howell, G. R., Christopherson, K. S., Nouri, N., Micheva, K. D., Mehalow, A. K., Huberman, A. D., Stafford, B., Sher, A., Litke, A. M., Lambris, J. D., Smith, S. J., John, S. W., & Barres, B. A. (2007, Dec 14). The classical complement cascade mediates CNS synapse elimination. *Cell, 131*(6), 1164-1178. https://doi.org/10.1016/j.cell.2007.10.036

Stoka, V., Turk, V., & Turk, B. (2016, Dec). Lysosomal cathepsins and their regulation in aging and neurodegeneration. *Ageing Res Rev, 32*, 22-37. https://doi.org/10.1016/j.arr.2016.04.010

Stowell, R. D., Wong, E. L., Batchelor, H. N., Mendes, M. S., Lamantia, C. E., Whitelaw, B. S., & Majewska, A. K. (2018, Jun). Cerebellar microglia are dynamically unique and survey Purkinje neurons in vivo. *Dev Neurobiol, 78*(6), 627-644. https://doi.org/10.1002/dneu.22572

Su, F., Bai, F., & Zhang, Z. (2016, Oct). Inflammatory Cytokines and Alzheimer's Disease: A Review from the Perspective of Genetic Polymorphisms. *Neurosci Bull, 32*(5), 469-480. https://doi.org/10.1007/s12264-016-0055-4

Su, P., Zhang, J., Wang, D., Zhao, F., Cao, Z., Aschner, M., & Luo, W. (2016, Apr 5). The role of autophagy in modulation of neuroinflammation in microglia. *Neuroscience, 319*, 155-167. https://doi.org/10.1016/j.neuroscience.2016.01.035

Sugimoto, K., Nishioka, R., Ikeda, A., Mise, A., Takahashi, H., Yano, H., Kumon, Y., Ohnishi, T., & Tanaka, J. (2014, Feb). Activated microglia in a rat stroke model express NG2 proteoglycan in peri-infarct tissue through the involvement of TGF-β1. *Glia, 62*(2), 185-198. https://doi.org/10.1002/glia.22598

Suzuki, H., Osawa, T., Fujioka, Y., & Noda, N. N. (2017, Apr). Structural biology of the core autophagy machinery. *Curr Opin Struct Biol, 43*, 10-17. https://doi.org/10.1016/j.sbi.2016.09.010

Suzuki, J., Imanishi, E., & Nagata, S. (2016, Aug 23). Xkr8 phospholipid scrambling complex in apoptotic phosphatidylserine exposure. *Proc Natl Acad Sci U S A, 113*(34), 9509-9514. https://doi.org/10.1073/pnas.1610403113

T

Takeuchi, O., & Akira, S. (2010, Mar 19). Pattern recognition receptors and inflammation. *Cell, 140*(6), 805-820. https://doi.org/10.1016/j.cell.2010.01.022

Tamura, A., Graham, D. I., McCulloch, J., & Teasdale, G. M. (1981). Focal cerebral ischaemia in the rat: 1. Description of technique and early neuropathological consequences following middle cerebral artery occlusion. *J Cereb Blood Flow Metab, 1*(1), 53-60. https://doi.org/10.1038/jcbfm.1981.6

Tan, Y. L., Yuan, Y., & Tian, L. (2020, Feb). Microglial regional heterogeneity and its role in the brain. *Mol Psychiatry, 25*(2), 351-367. https://doi.org/10.1038/s41380-019-0609-8

Tanaka, T., Ueno, M., & Yamashita, T. (2009, Aug 7). Engulfment of axon debris by microglia requires p38 MAPK activity. *J Biol Chem, 284*(32), 21626-21636. https://doi.org/10.1074/jbc.M109.005603

Tang, Y., Liu, J., Wang, Y., Yang, L., Han, B., Zhang, Y., Bai, Y., Shen, L., Li, M., Jiang, T., Ye, Q., Yu, X., Huang, R., Zhang, Z., Xu, Y., & Yao, H. (2021, Oct). PARP14 inhibits microglial activation via LPAR5 to promote post-stroke functional recovery. *Autophagy, 17*(10), 2905-2922. https://doi.org/10.1080/15548627.2020.1847799

Tanida, I., Ueno, T., & Kominami, E. (2008). LC3 and Autophagy. *Methods Mol Biol, 445*, 77-88. https://doi.org/10.1007/978-1-59745-157-4_4

Tarozzo, G., Campanella, M., Ghiani, M., Bulfone, A., & Beltramo, M. (2002, May). Expression of fractalkine and its receptor, CX3CR1, in response to ischaemia-reperfusion brain injury in the rat. *Eur J Neurosci, 15*(10), 1663-1668. https://doi.org/10.1046/j.1460-9568.2002.02007.x

Tatum, W. O. t. (2012, Oct). Mesial temporal lobe epilepsy. *J Clin Neurophysiol, 29*(5), 356-365. https://doi.org/10.1097/WNP.0b013e31826b3ab7

Tay, T. L., Savage, J. C., Hui, C. W., Bisht, K., & Tremblay, M. (2017, Mar 15). Microglia across the lifespan: from origin to function in brain development, plasticity and cognition. *J Physiol, 595*(6), 1929-1945. https://doi.org/10.1113/jp272134

Tegelberg, S., Kopra, O., Joensuu, T., Cooper, J. D., & Lehesjoki, A. E. (2012). Early microglial activation precedes neuronal loss in the brain of the Cstb-/- mouse model of progressive myoclonus epilepsy, EPM1. *J Neuropathol Exp Neurol, 71*(1), 40-53. https://doi.org/10.1097/NEN.0b013e31823e68e1

Temkin, N. R. (2009, Feb). Preventing and treating posttraumatic seizures: the human experience. *Epilepsia, 50 Suppl 2*, 10-13. https://doi.org/10.1111/j.1528-1167.2008.02005.x

Thion, M. S., & Garel, S. (2018). Microglia Under the Spotlight: Activity and Complement-Dependent Engulfment of Synapses. *Trends Neurosci, 41*(6), 332-334. https://doi.org/10.1016/j.tins.2018.03.017

Thored, P., Heldmann, U., Gomes-Leal, W., Gisler, R., Darsalia, V., Taneera, J., Nygren, J. M., Jacobsen, S. E., Ekdahl, C. T., Kokaia, Z., & Lindvall, O. (2009, Jun). Long-term accumulation of microglia with proneurogenic phenotype concomitant with persistent neurogenesis in adult subventricular zone after stroke. *Glia, 57*(8), 835-849. https://doi.org/10.1002/glia.20810

Thrash, J. C., Torbett, B. E., & Carson, M. J. (2009, Jan). Developmental regulation of TREM2 and DAP12 expression in the murine CNS: implications for Nasu-Hakola disease. *Neurochem Res, 34*(1), 38-45. https://doi.org/10.1007/s11064-008-9657-1

Thurman, D. J., Beghi, E., Begley, C. E., Berg, A. T., Buchhalter, J. R., Ding, D., Hesdorffer, D. C., Hauser, W. A., Kazis, L., Kobau, R., Kroner, B., Labiner, D., Liow, K., Logroscino, G., Medina, M. T., Newton, C. R., Parko, K., Paschal, A., Preux, P. M., Sander, J. W., Selassie, A., Theodore, W., Tomson, T., & Wiebe, S. (2011, Sep). Standards for epidemiologic studies and surveillance of epilepsy. *Epilepsia, 52 Suppl 7*, 2-26. https://doi.org/10.1111/j.1528-1167.2011.03121.x

Timmerman, R., Burm, S. M., & Bajramovic, J. J. (2018). An Overview of in vitro Methods to Study Microglia. *Front Cell Neurosci, 12*, 242. https://doi.org/10.3389/fncel.2018.00242

Tong, C. K., & Vidyadaran, S. (2016, Sep). Role of microglia in embryonic neurogenesis. *Exp Biol Med (Maywood), 241*(15), 1669-1675. https://doi.org/10.1177/1535370216664430

Traystman, R. J. (2003). Animal models of focal and global cerebral ischemia. *Ilar j, 44*(2), 85-95. https://doi.org/10.1093/ilar.44.2.85

Tremblay, M., Lecours, C., Samson, L., Sánchez-Zafra, V., & Sierra, A. (2015). From the Cajal alumni Achúcarro and Río-Hortega to the rediscovery of never-resting microglia. *Front Neuroanat, 9*, 45. https://doi.org/10.3389/fnana.2015.00045

Tremblay, M., Lowery, R. L., & Majewska, A. K. (2010, Nov 2). Microglial interactions with synapses are modulated by visual experience. *PLoS Biol, 8*(11), e1000527. https://doi.org/10.1371/journal.pbio.1000527

Trotman-Lucas, M., & Gibson, C. L. (2021). A review of experimental models of focal cerebral ischemia focusing on the middle cerebral artery occlusion model. *F1000Res, 10*, 242. https://doi.org/10.12688/f1000research.51752.2

Trouw, L. A., Blom, A. M., & Gasque, P. (2008, Mar). Role of complement and complement regulators in the removal of apoptotic cells. *Mol Immunol, 45*(5), 1199-1207. https://doi.org/10.1016/j.molimm.2007.09.008

Truman, L. A., Ford, C. A., Pasikowska, M., Pound, J. D., Wilkinson, S. J., Dumitriu, I. E., Melville, L., Melrose, L. A., Ogden, C. A., Nibbs, R., Graham, G., Combadiere, C., & Gregory, C. D. (2008, Dec 15).

CX3CL1/fractalkine is released from apoptotic lymphocytes to stimulate macrophage chemotaxis. *Blood, 112*(13), 5026-5036. https://doi.org/10.1182/blood-2008-06-162404

Tsai, R. K., & Discher, D. E. (2008, Mar 10). Inhibition of "self" engulfment through deactivation of myosin-II at the phagocytic synapse between human cells. *J Cell Biol, 180*(5), 989-1003. https://doi.org/10.1083/jcb.200708043

Turco, E., Fracchiolla, D., & Martens, S. (2020, Jan 3). Recruitment and Activation of the ULK1/Atg1 Kinase Complex in Selective Autophagy. *J Mol Biol, 432*(1), 123-134. https://doi.org/10.1016/j.jmb.2019.07.027

U

Ubogu, E. E., Cossoy, M. B., & Ransohoff, R. M. (2006, Jan). The expression and function of chemokines involved in CNS inflammation. *Trends Pharmacol Sci, 27*(1), 48-55. https://doi.org/10.1016/j.tips.2005.11.002

Ulland, T. K., Song, W. M., Huang, S. C., Ulrich, J. D., Sergushichev, A., Beatty, W. L., Loboda, A. A., Zhou, Y., Cairns, N. J., Kambal, A., Loginicheva, E., Gilfillan, S., Cella, M., Virgin, H. W., Unanue, E. R., Wang, Y., Artyomov, M. N., Holtzman, D. M., & Colonna, M. (2017, Aug 10). TREM2 Maintains Microglial Metabolic Fitness in Alzheimer's Disease. *Cell, 170*(4), 649-663.e613. https://doi.org/10.1016/j.cell.2017.07.023

Unnithan, A. K. A., & Mehta, P. (2022). Hemorrhagic Stroke. In *StatPearls*. StatPearls Publishing

Uribe-Querol, E., & Rosales, C. (2020). Phagocytosis: Our Current Understanding of a Universal Biological Process. *Front Immunol, 11*, 1066. https://doi.org/10.3389/fimmu.2020.01066

V

van de Moosdijk, A. A., & van Amerongen, R. (2016, Oct 18). Identification of reliable reference genes for qRT-PCR studies of the developing mouse mammary gland. *Sci Rep, 6*, 35595. https://doi.org/10.1038/srep35595

Verkhratsky, A., Sun, D., & Tanaka, J. (2021, Mar). Snapshot of microglial physiological functions. *Neurochem Int, 144*, 104960. https://doi.org/10.1016/j.neuint.2021.104960

Verma, I. M., & Sassone-Corsi, P. (1987). Proto-oncogene fos: complex but versatile regulation. *Cell, 51*(4), 513-514. https://doi.org/10.1016/0092-8674(87)90115-2

Verney, C., Monier, A., Fallet-Bianco, C., & Gressens, P. (2010, Oct). Early microglial colonization of the human forebrain and possible involvement in periventricular white-matter injury of preterm infants. *J Anat, 217*(4), 436-448. https://doi.org/10.1111/j.1469-7580.2010.01245.x

Vezzani, A. (2009, Sep-Oct). Pilocarpine-induced seizures revisited: what does the model mimic? *Epilepsy Curr, 9*(5), 146-148. https://doi.org/10.1111/j.1535-7511.2009.01323.x

Vezzani, A., Friedman, A., & Dingledine, R. J. (2013, Jun). The role of inflammation in epileptogenesis. *Neuropharmacology, 69*, 16-24. https://doi.org/10.1016/j.neuropharm.2012.04.004

Vezzani, A., & Viviani, B. (2015). Neuromodulatory properties of inflammatory cytokines and their impact on neuronal excitability. *Neuropharmacology, 96*(Pt A), 70-82. https://doi.org/10.1016/j.neuropharm.2014.10.027

Vilalta, A., & Brown, G. C. (2018, Oct). Neurophagy, the phagocytosis of live neurons and synapses by glia, contributes to brain development and disease. *Febs j, 285*(19), 3566-3575. https://doi.org/10.1111/febs.14323

Vivier, E., Tomasello, E., Baratin, M., Walzer, T., & Ugolini, S. (2008, May). Functions of natural killer cells. *Nat Immunol, 9*(5), 503-510. https://doi.org/10.1038/ni1582

Voet, S., Prinz, M., & van Loo, G. (2019, Feb). Microglia in Central Nervous System Inflammation and Multiple Sclerosis Pathology. *Trends Mol Med, 25*(2), 112-123. https://doi.org/10.1016/j.molmed.2018.11.005

Voll, R. E., Herrmann, M., Roth, E. A., Stach, C., Kalden, J. R., & Girkontaite, I. (1997, Nov 27). Immunosuppressive effects of apoptotic cells. *Nature, 390*(6658), 350-351. https://doi.org/10.1038/37022

Vorup-Jensen, T., & Jensen, R. K. (2018). Structural Immunology of Complement Receptors 3 and 4. *Front Immunol, 9*, 2716. https://doi.org/10.3389/fimmu.2018.02716

Voss, A. K., & Strasser, A. (2020). The essentials of developmental apoptosis. *F1000Res, 9*. https://doi.org/10.12688/f1000research.21571.1

W

Wake, H., Moorhouse, A. J., Jinno, S., Kohsaka, S., & Nabekura, J. (2009, Apr 1). Resting microglia directly monitor the functional state of synapses in vivo and determine the fate of ischemic terminals. *J Neurosci, 29*(13), 3974-3980. https://doi.org/10.1523/jneurosci.4363-08.2009

Wang, W., Jia, W. D., Xu, G. L., Wang, Z. H., Li, J. S., Ma, J. L., Ge, Y. S., Xie, S. X., & Yu, J. H. (2009, Oct). Antitumoral activity of rapamycin mediated through inhibition of HIF-1alpha and VEGF in hepatocellular carcinoma. *Dig Dis Sci, 54*(10), 2128-2136. https://doi.org/10.1007/s10620-008-0605-3

Wei, Y., Liu, M., Li, X., Liu, J., & Li, H. (2018). Origin of the Autophagosome Membrane in Mammals. *Biomed Res Int, 2018*, 1012789. https://doi.org/10.1155/2018/1012789

Weinhard, L., di Bartolomei, G., Bolasco, G., Machado, P., Schieber, N. L., Neniskyte, U., Exiga, M., Vadisiute, A., Raggioli, A., Schertel, A., Schwab, Y., & Gross, C. T. (2018, Mar 26). Microglia remodel synapses by presynaptic trogocytosis and spine head filopodia induction. *Nat Commun, 9*(1), 1228. https://doi.org/10.1038/s41467-018-03566-5

Wen, Y. D., Sheng, R., Zhang, L. S., Han, R., Zhang, X., Zhang, X. D., Han, F., Fukunaga, K., & Qin, Z. H. (2008, Aug). Neuronal injury in rat model of permanent focal cerebral ischemia is associated with activation of autophagic and lysosomal pathways. *Autophagy, 4*(6), 762-769. https://doi.org/10.4161/auto.6412

Westman, J., Grinstein, S., & Marques, P. E. (2020, 2020-January-09). Phagocytosis of Necrotic Debris at Sites of Injury and Inflammation [Review]. *Frontiers in Immunology, 10*. https://doi.org/10.3389/fimmu.2019.03030

Wijeyesakere, S. J., Bedi, S. K., Huynh, D., & Raghavan, M. (2016, May 1). The C-Terminal Acidic Region of Calreticulin Mediates Phosphatidylserine Binding and Apoptotic Cell Phagocytosis. *J Immunol, 196*(9), 3896-3909. https://doi.org/10.4049/jimmunol.1502122

Williams, P. A., Tribble, J. R., Pepper, K. W., Cross, S. D., Morgan, B. P., Morgan, J. E., John, S. W., & Howell, G. R. (2016, Apr 6). Inhibition of the classical pathway of the complement cascade prevents early dendritic and synaptic degeneration in glaucoma. *Mol Neurodegener, 11*, 26. https://doi.org/10.1186/s13024-016-0091-6

Wolak, D. J., & Thorne, R. G. (2013). Diffusion of macromolecules in the brain: implications for drug delivery. *Mol Pharm, 10*(5), 1492-1504. https://doi.org/10.1021/mp300495e

Wolf, S. A., Boddeke, H. W., & Kettenmann, H. (2017, Feb 10). Microglia in Physiology and Disease. *Annu Rev Physiol, 79*, 619-643. https://doi.org/10.1146/annurev-physiol-022516-034406

Wolf, Y., Yona, S., Kim, K. W., & Jung, S. (2013). Microglia, seen from the CX3CR1 angle. *Front Cell Neurosci, 7*, 26. https://doi.org/10.3389/fncel.2013.00026

Wong, P. M., Puente, C., Ganley, I. G., & Jiang, X. (2013, Feb 1). The ULK1 complex: sensing nutrient signals for autophagy activation. *Autophagy, 9*(2), 124-137. https://doi.org/10.4161/auto.23323

Wu, M., Zhang, H., Kai, J., Zhu, F., Dong, J., Xu, Z., Wong, M., & Zeng, L. H. (2018, Feb). Rapamycin prevents cerebral stroke by modulating apoptosis and autophagy in penumbra in rats. *Ann Clin Transl Neurol, 5*(2), 138-146. https://doi.org/10.1002/acn3.507

Wu, Y., Singh, S., Georgescu, M. M., & Birge, R. B. (2005, Feb 1). A role for Mer tyrosine kinase in alphavbeta5 integrin-mediated phagocytosis of apoptotic cells. *J Cell Sci, 118*(Pt 3), 539-553. https://doi.org/10.1242/jcs.01632

Wurm, J., Konttinen, H., Andressen, C., Malm, T., & Spittau, B. (2021, Mar 17). Microglia Development and Maturation and Its Implications for Induction of Microglia-Like Cells from Human iPSCs. *Int J Mol Sci, 22*(6). https://doi.org/10.3390/ijms22063088

Wyatt, S. K., Witt, T., Barbaro, N. M., Cohen-Gadol, A. A., & Brewster, A. L. (2017). Enhanced classical complement pathway activation and altered phagocytosis signaling molecules in human epilepsy. *Experimental Neurology, 295*, 184-193. https://doi.org/https://doi.org/10.1016/j.expneurol.2017.06.009

Wyatt-Johnson, S. K., & Brewster, A. L. (2019). Emerging Roles for Microglial Phagocytic Signaling in Epilepsy. *Epilepsy Currents, 20*(1), 33-38. https://doi.org/10.1177/1535759719890336

X

Xie, L., Sun, F., Wang, J., Mao, X., Xie, L., Yang, S. H., Su, D. M., Simpkins, J. W., Greenberg, D. A., & Jin, K. (2014, Jun 15). mTOR signaling inhibition modulates macrophage/microglia-mediated neuroinflammation and secondary injury via regulatory T cells after focal ischemia. *J Immunol, 192*(12), 6009-6019. https://doi.org/10.4049/jimmunol.1303492

Xu, J., Yu, T., Pietronigro, E. C., Yuan, J., Arioli, J., Pei, Y., Luo, X., Ye, J., Constantin, G., Mao, C., & Xiao, Y. (2020, Oct). Peli1 impairs microglial Aβ phagocytosis through promoting C/EBPβ degradation. *PLoS Biol, 18*(10), e3000837. https://doi.org/10.1371/journal.pbio.3000837

Xu, X., Lai, Y., & Hua, Z.-C. (2019). Apoptosis and apoptotic body: disease message and therapeutic target potentials. *Bioscience Reports, 39*(1). https://doi.org/10.1042/bsr20180992

Xu, Y., Hu, W., Liu, Y., Xu, P., Li, Z., Wu, R., Shi, X., & Tang, Y. (2016, Aug). P2Y6 Receptor-Mediated Microglial Phagocytosis in Radiation-Induced Brain Injury. *Mol Neurobiol, 53*(6), 3552-3564. https://doi.org/10.1007/s12035-015-9282-3

Xu, Y., Propson, N. E., Du, S., Xiong, W., & Zheng, H. (2021, Jul 6). Autophagy deficiency modulates microglial lipid homeostasis and aggravates tau pathology and spreading. *Proc Natl Acad Sci U S A, 118*(27). https://doi.org/10.1073/pnas.2023418118

Y

Yamamoto, A., Tagawa, Y., Yoshimori, T., Moriyama, Y., Masaki, R., & Tashiro, Y. (1998, Feb). Bafilomycin A1 prevents maturation of autophagic vacuoles by inhibiting fusion between autophagosomes and lysosomes in rat hepatoma cell line, H-4-II-E cells. *Cell Struct Funct, 23*(1), 33-42. https://doi.org/10.1247/csf.23.33

Yamamoto, Y. H., & Noda, T. (2020, Oct 22). Autophagosome formation in relation to the endoplasmic reticulum. *J Biomed Sci, 27*(1), 97. https://doi.org/10.1186/s12929-020-00691-6

Yang, C., & Wang, X. (2021, Jun 7). Lysosome biogenesis: Regulation and functions. *J Cell Biol, 220*(6). https://doi.org/10.1083/jcb.202102001

Yang, C. S., Lee, H. M., Lee, J. Y., Kim, J. A., Lee, S. J., Shin, D. M., Lee, Y. H., Lee, D. S., El-Benna, J., & Jo, E. K. (2007, Nov 26). Reactive oxygen species and p47phox activation are essential for the Mycobacterium tuberculosis-induced pro-inflammatory response in murine microglia. *J Neuroinflammation, 4*, 27. https://doi.org/10.1186/1742-2094-4-27

Yang, D. S., Lee, J. H., & Nixon, R. A. (2009). Monitoring autophagy in Alzheimer's disease and related neurodegenerative diseases. *Methods Enzymol, 453*, 111-144. https://doi.org/10.1016/s0076-6879(08)04006-8

Yang, D. S., Stavrides, P., Mohan, P. S., Kaushik, S., Kumar, A., Ohno, M., Schmidt, S. D., Wesson, D., Bandyopadhyay, U., Jiang, Y., Pawlik, M., Peterhoff, C. M., Yang, A. J., Wilson, D. A., St George-Hyslop, P., Westaway, D., Mathews, P. M., Levy, E., Cuervo, A. M., & Nixon, R. A. (2011, Jan). Reversal of autophagy dysfunction in the TgCRND8 mouse model of Alzheimer's disease ameliorates amyloid pathologies and memory deficits. *Brain, 134*(Pt 1), 258-277. https://doi.org/10.1093/brain/awq341

Yang, G., Li, Y., Zhao, Y., Ouyang, L., Chen, Y., Liu, B., & Liu, J. (2021, Jan 1). Targeting Atg4B for cancer therapy: Chemical mediators. *Eur J Med Chem, 209*, 112917. https://doi.org/10.1016/j.ejmech.2020.112917

Yang, Y. P., Hu, L. F., Zheng, H. F., Mao, C. J., Hu, W. D., Xiong, K. P., Wang, F., & Liu, C. F. (2013, May). Application and interpretation of current autophagy inhibitors and activators. *Acta Pharmacol Sin, 34*(5), 625-635. https://doi.org/10.1038/aps.2013.5

Yang, Z., Zhong, L., Zhong, S., Xian, R., & Yuan, B. (2015, Apr). Hypoxia induces microglia autophagy and neural inflammation injury in focal cerebral ischemia model. *Exp Mol Pathol, 98*(2), 219-224. https://doi.org/10.1016/j.yexmp.2015.02.003

Yatim, K. M., & Lakkis, F. G. (2015, Jul 7). A brief journey through the immune system. *Clin J Am Soc Nephrol, 10*(7), 1274-1281. https://doi.org/10.2215/cjn.10031014

Yim, W. W., & Mizushima, N. (2020). Lysosome biology in autophagy. *Cell Discov, 6*, 6. https://doi.org/10.1038/s41421-020-0141-7

Yokota, S., Himeno, M., & Kato, K. (1989, Apr). Immunocytochemical localization of acid phosphatase in rat liver. *Cell Struct Funct, 14*(2), 163-171. https://doi.org/10.1247/csf.14.163

Yona, S., Kim, K. W., Wolf, Y., Mildner, A., Varol, D., Breker, M., Strauss-Ayali, D., Viukov, S., Guilliams, M., Misharin, A., Hume, D. A., Perlman, H., Malissen, B., Zelzer, E., & Jung, S. (2013, Jan 24). Fate mapping reveals origins and dynamics of monocytes and tissue macrophages under homeostasis. *Immunity, 38*(1), 79-91. https://doi.org/10.1016/j.immuni.2012.12.001

Yu, L., Chen, Y., & Tooze, S. A. (2018). Autophagy pathway: Cellular and molecular mechanisms. *Autophagy, 14*(2), 207-215. https://doi.org/10.1080/15548627.2017.1378838

Yu, L., McPhee, C. K., Zheng, L., Mardones, G. A., Rong, Y., Peng, J., Mi, N., Zhao, Y., Liu, Z., Wan, F., Hailey, D. W., Oorschot, V., Klumperman, J., Baehrecke, E. H., & Lenardo, M. J. (2010, Jun 17).

Termination of autophagy and reformation of lysosomes regulated by mTOR. *Nature, 465*(7300), 942-946. https://doi.org/10.1038/nature09076

Yue, Z., Jin, S., Yang, C., Levine, A. J., & Heintz, N. (2003). Beclin 1, an autophagy gene essential for early embryonic development, is a haploinsufficient tumor suppressor. *Proceedings of the National Academy of Sciences, 100*(25), 15077-15082. https://doi.org/doi:10.1073/pnas.2436255100

Z

Zachari, M., & Ganley, I. G. (2017, Dec 12). The mammalian ULK1 complex and autophagy initiation. *Essays Biochem, 61*(6), 585-596. https://doi.org/10.1042/ebc20170021

Zachari, M., Longo, M., & Ganley, I. G. (2020, Dec). Aberrant autophagosome formation occurs upon small molecule inhibition of ULK1 kinase activity. *Life Sci Alliance, 3*(12). https://doi.org/10.26508/lsa.202000815

Zaman, S., Wang, R., & Gandhi, V. (2014, Sep). Targeting the apoptosis pathway in hematologic malignancies. *Leuk Lymphoma, 55*(9), 1980-1992. https://doi.org/10.3109/10428194.2013.855307

Zhang, J., Xiao, X., Liu, W., Demirci, G., & Li, X. C. (2009, Dec). Inhibitory receptors of the immune system: functions and therapeutic implications. *Cell Mol Immunol, 6*(6), 407-414. https://doi.org/10.1038/cmi.2009.52

Zhang, J. M., & An, J. (2007, Spring). Cytokines, inflammation, and pain. *Int Anesthesiol Clin, 45*(2), 27-37. https://doi.org/10.1097/AIA.0b013e318034194e

Zhang, W. P., Hu, H., Zhang, L., Ding, W., Yao, H. T., Chen, K. D., Sheng, W. W., Chen, Z., & Wei, E. Q. (2004, Jun 17). Expression of cysteinyl leukotriene receptor 1 in human traumatic brain injury and brain tumors. *Neurosci Lett, 363*(3), 247-251. https://doi.org/10.1016/j.neulet.2004.03.088

Zhang, Z., Zhang, Z., Lu, H., Yang, Q., Wu, H., & Wang, J. (2017, Apr). Microglial Polarization and Inflammatory Mediators After Intracerebral Hemorrhage. *Mol Neurobiol, 54*(3), 1874-1886. https://doi.org/10.1007/s12035-016-9785-6

Zhao, C. Z., Zhao, B., Zhang, X. Y., Huang, X. Q., Shi, W. Z., Liu, H. L., Fang, S. H., Lu, Y. B., Zhang, W. P., Tang, F. D., & Wei, E. Q. (2011, Aug 25). Cysteinyl leukotriene receptor 2 is spatiotemporally involved in neuron injury, astrocytosis and microgliosis after focal cerebral ischemia in rats. *Neuroscience, 189*, 1-11. https://doi.org/10.1016/j.neuroscience.2011.05.066

Zhao, R., Hu, W., Tsai, J., Li, W., & Gan, W. B. (2017, Jun 12). Microglia limit the expansion of β-amyloid plaques in a mouse model of Alzheimer's disease. *Mol Neurodegener, 12*(1), 47. https://doi.org/10.1186/s13024-017-0188-6

Zhao, S., Li, X., Wang, j., & Wang, H. (2021, 2021-May-17). The Role of the Effects of Autophagy on NLRP3 Inflammasome in Inflammatory Nervous System Diseases [Review]. *Frontiers in Cell and Developmental Biology, 9*. https://doi.org/10.3389/fcell.2021.657478

Zhao, S. C., Ma, L. S., Chu, Z. H., Xu, H., Wu, W. Q., & Liu, F. (2017, Apr). Regulation of microglial activation in stroke. *Acta Pharmacol Sin, 38*(4), 445-458. https://doi.org/10.1038/aps.2016.162

Zhao, X., Eyo, U. B., Murugan, M., & Wu, L. J. (2018, Jun). Microglial interactions with the neurovascular system in physiology and pathology. *Dev Neurobiol, 78*(6), 604-617. https://doi.org/10.1002/dneu.22576

Zheng, C., Zhou, X. W., & Wang, J. Z. (2016). The dual roles of cytokines in Alzheimer's disease: update on interleukins, TNF-α, TGF-β and IFN-γ. *Transl Neurodegener, 5*, 7. https://doi.org/10.1186/s40035-016-0054-4

Zheng, J., Ru, W., Adolacion, J. R., Spurgat, M. S., Liu, X., Yuan, S., Liang, R. X., Dong, J., Potter, A. S., Potter, S. S., Chen, K., Chen, R., Varadarajan, N., & Tang, S. J. (2021, Mar 19). Single-cell RNA-seq analysis reveals compartment-specific heterogeneity and plasticity of microglia. *iScience, 24*(3), 102186. https://doi.org/10.1016/j.isci.2021.102186

Zheng, K., Lin, L., Jiang, W., Chen, L., Zhang, X., Zhang, Q., Ren, Y., & Hao, J. (2022, Jan). Single-cell RNA-seq reveals the transcriptional landscape in ischemic stroke. *J Cereb Blood Flow Metab, 42*(1), 56-73. https://doi.org/10.1177/0271678x211026770

Zhou, P., Tan, Y. Z., Wang, H. J., Li, T., He, T., Yu, Y., Zhang, J., & Zhang, D. (2016, Nov 1). Cytoprotective effect of autophagy on phagocytosis of apoptotic cells by macrophages. *Exp Cell Res, 348*(2), 165-176. https://doi.org/10.1016/j.yexcr.2016.09.011

Zhou, X., Wahane, S., Friedl, M. S., Kluge, M., Friedel, C. C., Avrampou, K., Zachariou, V., Guo, L., Zhang, B., He, X., Friedel, R. H., & Zou, H. (2020, Mar). Microglia and macrophages promote corralling, wound compaction and recovery after spinal cord injury via Plexin-B2. *Nat Neurosci, 23*(3), 337-350. https://doi.org/10.1038/s41593-020-0597-7

Zhou, X., Zhou, J., Li, X., Guo, C., Fang, T., & Chen, Z. (2011, Jul 29). GSK-3β inhibitors suppressed neuroinflammation in rat cortex by activating autophagy in ischemic brain injury. *Biochem Biophys Res Commun, 411*(2), 271-275. https://doi.org/10.1016/j.bbrc.2011.06.117

Zhou, Z., & Yu, X. (2008, Oct). Phagosome maturation during the removal of apoptotic cells: receptors lead the way. *Trends Cell Biol, 18*(10), 474-485. https://doi.org/10.1016/j.tcb.2008.08.002

Zizzo, G., Hilliard, B. A., Monestier, M., & Cohen, P. L. (2012, Oct 1). Efficient clearance of early apoptotic cells by human macrophages requires M2c polarization and MerTK induction. *J Immunol, 189*(7), 3508-3520. https://doi.org/10.4049/jimmunol.1200662